Peptides as Catalysts for Asymmetric 1,4-Addition Reactions of Aldehydes to Nitroolefins

Inauguraldissertation

zur Erlangung der Würde eines Doktors der Philosophie

vorgelegt der
Philosophisch-Naturwissenschaftlichen Fakultät
der Universität Basel

von

Markus Wiesner

aus Bubendorf (BL)

Basel 2009

creative commons

Namensnennung-Keine kommerzielle Nutzung-Keine Bearbeitung 2.5 Schweiz

---

Sie dürfen:

das Werk vervielfältigen, verbreiten und öffentlich zugänglich machen

Zu den folgenden Bedingungen:

Namensnennung. Sie müssen den Namen des Autors/Rechteinhabers in der von ihm festgelegten Weise nennen (wodurch aber nicht der Eindruck entstehen darf, Sie oder die Nutzung des Werkes durch Sie würden entlohnt).

Keine kommerzielle Nutzung. Dieses Werk darf nicht für kommerzielle Zwecke verwendet werden.

Keine Bearbeitung. Dieses Werk darf nicht bearbeitet oder in anderer Weise verändert werden.

- Im Falle einer Verbreitung müssen Sie anderen die Lizenzbedingungen, unter welche dieses Werk fällt, mitteilen. Am Einfachsten ist es, einen Link auf diese Seite einzubinden.
- Jede der vorgenannten Bedingungen kann aufgehoben werden, sofern Sie die Einwilligung des Rechteinhabers dazu erhalten.
- Diese Lizenz lässt die Urheberpersönlichkeitsrechte unberührt.

Quelle: http://creativecommons.org/licenses/by-nc-nd/2.5/ch/ Datum: 3.4.2009

Genehmigt von der Philosophisch-Naturwissenschaftlichen Fakultät der Universität Basel auf Antrag von:

Prof. Dr. Helma Wennemers

Prof. Dr. Andreas Pfaltz

Basel, den 23. Juni 2009

Prof. Dr. Eberhard Parlow

Dekan

Die vorliegende Arbeit wurde unter Anleitung von Prof. Helma Wennemers in der Zeit von April 2006 bis Juni 2009 am Departement Chemie der Philosophisch-Naturwissenschaftlichen Fakultät der Universität Basel durchgeführt.

Teile dieser Arbeit wurden bereits publiziert:

M. Wiesner, G. Upert, G. Angelici, H. Wennemers, "Enamine Catalysis with Low Catalyst Loadings – High Efficiency via Kinetic Studies", *J. Am. Chem. Soc.* **2009**, *in press.*

M. Wiesner, M. Neuburger, H. Wennemers, "Tripeptides of the Type H-D-Pro-Pro-Xaa-NH_2 as Catalysts for Asymmetric 1,4-Addition Reactions: Structural Requirements for High Catalytic Efficiency", *Chem. Eur. J.* **2009**, 15, 10103-10109.

M. Wiesner, J. D. Revell, S. Tonazzi, H. Wennemers, "Peptide Catalyzed Asymmetric Conjugate Addition Reactions of Aldehydes to Nitroethylene – A Convenient Entry into γ^2-Amino Acids", *J. Am. Chem. Soc.* **2008**, *130*, 5610-5611.

M. Wiesner, J. D. Revell, H. Wennemers, "Tripeptides as Efficient Asymmetric Catalysts for 1,4-Addition Reactions of Aldehydes to Nitroolefins - A Rational Approach", *Angew. Chem. Int. Ed.* **2008**, *47*, 1871-1874.

P. Krattiger, J. D. Revell, M. Wiesner, H. Wennemers, "Peptides as asymmetric catalysts", *Peptide Science* **2006**, *43rd* 333.

Für meine Eltern,
auf deren Unterstützung ich immer zählen kann.

Für Carl,
der mich gelehrt hat ein Ziel nie aus den Augen zu verlieren.

Danksagung

Ich möchte mich bei Prof. Helma Wennemers für die Förderung und Unterstützung während meiner Dissertation herzlich bedanken.

Prof. Andreas Pfaltz danke ich für die Übernahme des Co-Referates.

Bei Dr. Jefferson Revell bedanke ich mich für seine grosse Hilfe und für seine zahlreichen Ratschläge.

Folgende Personen haben am Gelingen dieser Arbeit direkt beigetragen: Dr. Gregory Upert, Dr. Gaetano Angelici, Dr. Daniel Häussinger, Sandro Tonazzi, Markus Neuburger, Robert Kastl, Moritz Stoltz und Wei Liu. Für deren Einsatz bin ich sehr dankbar.

Der gesamten Arbeitsgruppe Wennemers danke ich für die Hilfe und für das angenehme Arbeitsklima.

Allen Mitarbeitern und Mitarbeiterinnen der Werkstatt, der Materialausgabe und des Sekretariats danke ich für ihre Hilfe.

Für die finanzielle Unterstützung danke ich dem Schweizerischen Nationalfonds, der Universität Basel, dem RTN RevCat der Europäischen Union und der Bachem AG.

Ein besonderer Dank geht an meine Familie, an meine Freundin Romina und an alle meine Freunde für ihre grosse Unterstützung.

Contents

I.
Introduction

1. Asymmetric Enamine Catalysis

Organocatalysis is regarded as the application of small organic molecules as catalysts to a variety of organic processes and has recently become very popular for the synthesis of chiral molecules.[1-8] Of particular interest are the high product enantio- and/or diastereoselectivities and reaction yields which can frequently be obtained using organocatalysts. In comparison to other firmly established fields such as enzymatic catalysis and organometallic catalysis, organocatalysis offers several fundamental advantages: In general, organocatalysts can be used in a wider range of solvents and for a broader scope of substrate in comparison to enzymes. In addition, they are typically less toxic and less sensitive towards oxidation and moisture than most organometallic based reagents. However, a major drawback of organocatalysis is their typically low catalytic activity which often requires 10 mol% or more of catalyst for the reaction of interest. Based on a mechanistic classification, organocatalysis can generally be categorised as either Lewis base, Lewis acid, Brønsted base or Brønsted acid mediated.[4] An important class of Lewis base catalysis is asymmetric enamine catalysis which is regarded as the catalysis of electrophilic substitution reactions in the α-position of carbonyl compounds by primary and secondary amines proceeding via enamine intermediates.[9] The versatility of enamines in stochiometric reactions was demonstrated for α-functionalisation of carbonyl compounds by Stork et al. in 1963.[10,11] The first catalytic application of enamines was recorded by Hajos and Parrish[12] and Eder, Sauer and Wiechert[13] in the early 1970's. L-Proline was used to catalyse the asymmetric Robinson annulation of an achiral triketone. The corresponding steroid precursor was obtained in quantitative yield (100 %) and high enantioselectivity (93 % *ee*, Scheme 1.1).

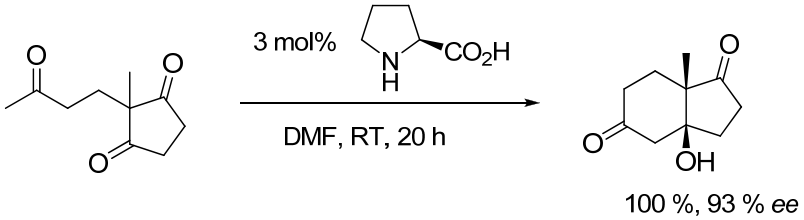

Scheme 1.1. *Proline catalysed Robinson annulation (Hajos-Parrish-Eder-Sauer-Wiechert reaction).*[12,13]

In 2000, List, Lerner and Barbas introduced the proline catalysed intermolecular aldol reaction of ketones and aldehydes (Scheme 1.2a).[14] The use of proline as catalyst for intra- and intermolecular aldolreactions revealed that a small 'rigid' organic molecule could catalyse the same chemical reactions as a much larger enzyme (typ I aldolase) via a similar enamine-type mechanism. Almost simultaneously MacMillan reported iminium-type catalysis of an asymmetric Diels-Alder reaction, catalysed by a chiral imidazolidinone (Scheme 1.2b).[15] These two publications initiated the launch of organocatalyis as a new important research field in asymmetric catalysis.

a)

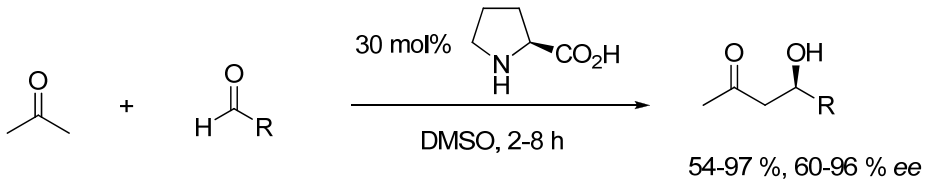

b)

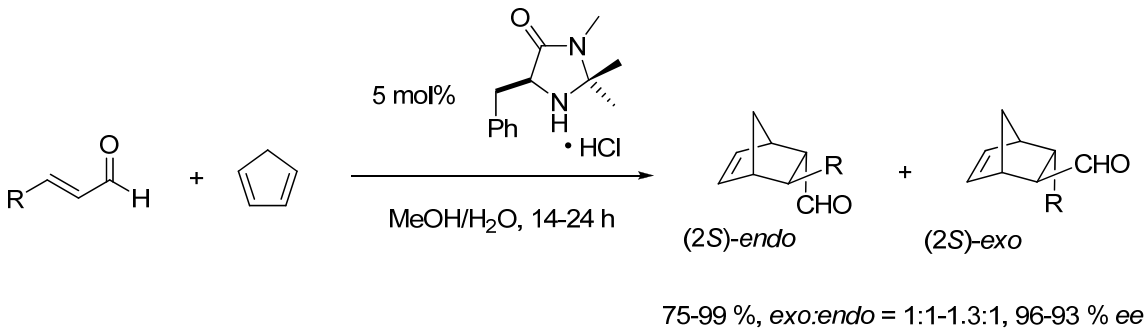

Scheme 1.2. *a) Proline catalysed asymmetric aldol reactions.[14] b) Imidazolidinone catalysed Diels-Alder reactions.[15]*

In enamine catalysis an aldehyde or ketone reacts with the catalyst to form the nucleophilic enamine species with a HOMO of higher energy compared to the respective carbonyl (enol) compound. The enamine can attack an electrophile to form an iminum ion species. Subsequent hydrolysis of this intermediate then releases the corresponding addition product allowing the catalytic cycle to be completed (Scheme 1.3). Examples of organocatalytic reactions proceeding via enamine activation include aldol, Mannich, Michael and hetero Michael reactions as well as α-functionalisations of carbonyl compounds (Scheme 1.4).[9]

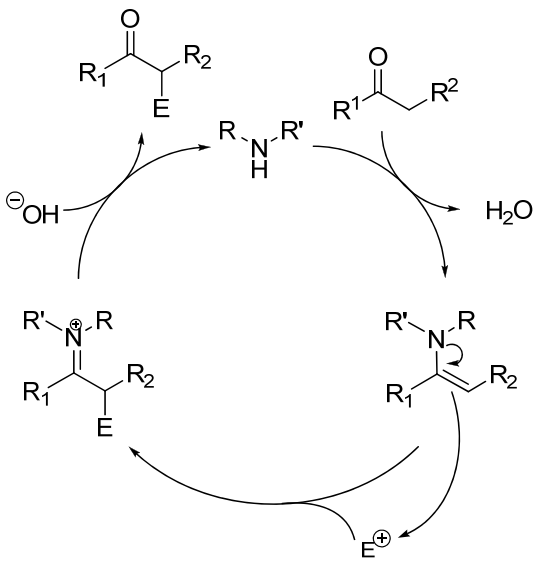

Scheme 1.3. *Enamine activation in secondary amine catalysed reactions.*

a)

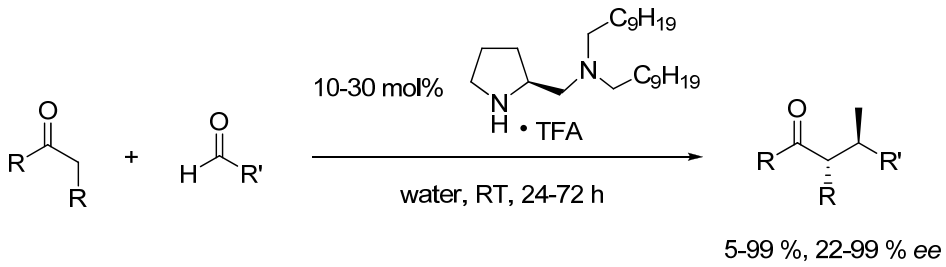

b)

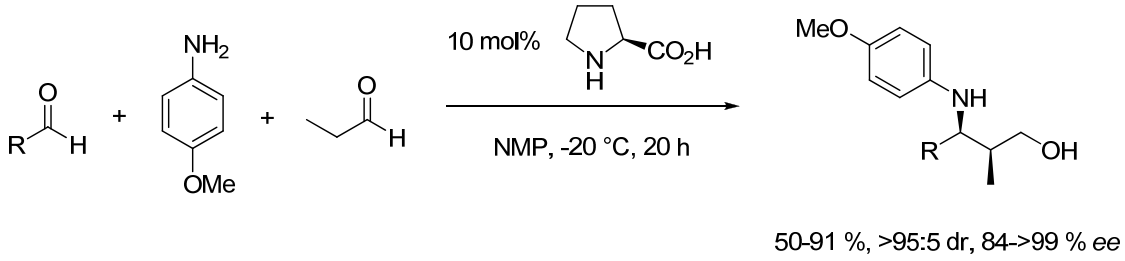

c)

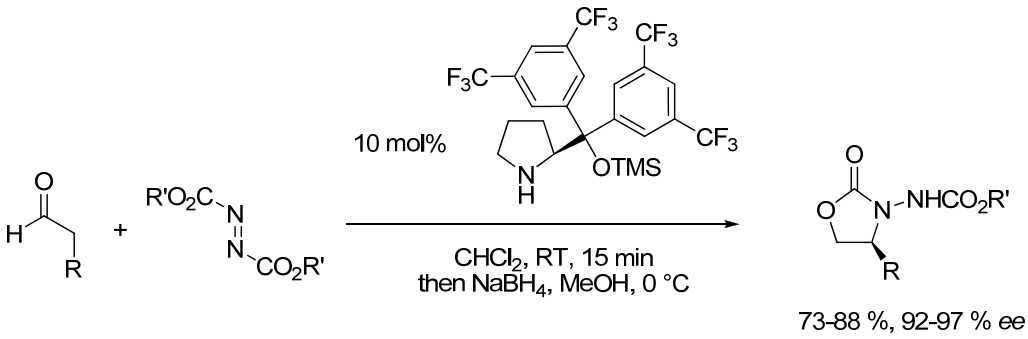

Scheme 1.4. *Examples of asymmetric reactions proceeding via enamine catalysis: a) Diamine catalysed aldol reaction in water.*[16] *b) Proline catalysed three-component Mannich reaction.*[17] *c) Diarylprolinol silyl ether catalysed α-amination of aldehydes.*[18]

1.1 *Enamine Catalysed Conjugate Addition Reactions of Aldehydes and Nitroolefins*

Conjugate addition of nucleophiles to the β-position of α,β-unsaturated compounds are widely used in organic synthesis.[19] In recent years a variety of catalysts and conditions for enamine catalysed conjugate addition reactions between aldehydes or ketones and different Michael acceptors, e.g. nitrostyrenes,[20] enones,[21] vinyl sulfones[22] or alkylidene malonates, [23] have been reported (Scheme 1.5).

a)

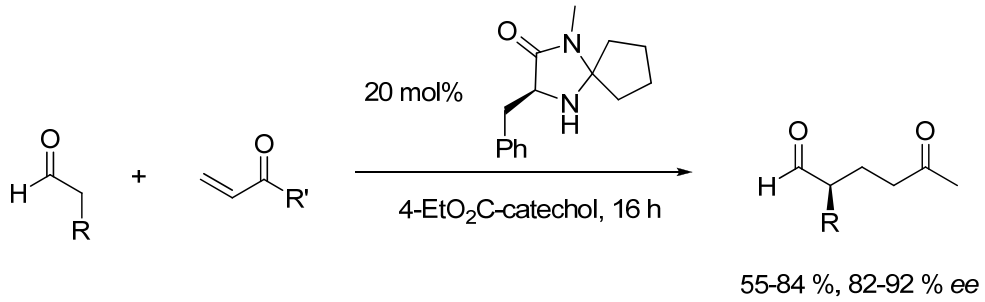

b)

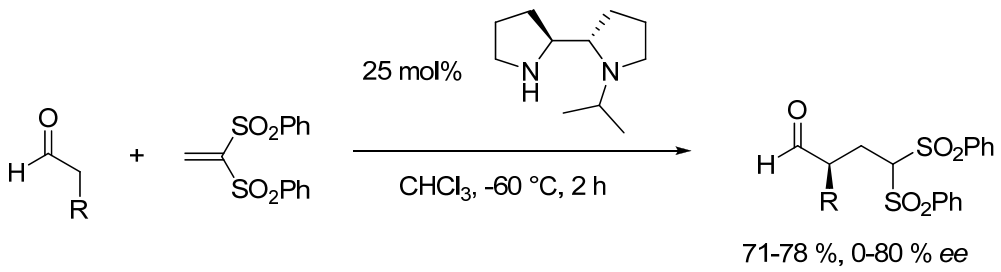

c)

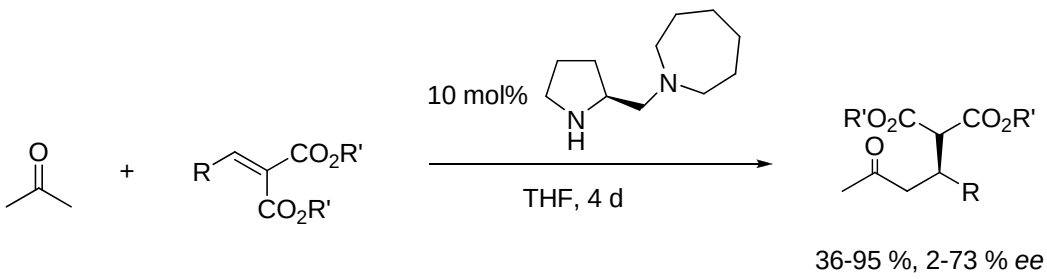

Scheme 1.5. *Examples of enamine catalysed conjugate additions between ketones or aldehydes and different Michael acceptors: a) enones[21] b) vinyl sulfones[22] and c) alkylidene malonate.[23]*

In particular *trans*-β-nitrostyrene can act as a reactive electrophile and is therefore an attractive Michael acceptor. Initial studies of the L-proline catalysed 1,4-addition of cyclohexanone to nitrostyrene revealed that this reaction proceeds smoothly to furnish the Michael adduct in high yield and diastereoselectivity. However, a catalyst loading of 15 mol% was required and the observed enantioselectivity remained low (23 % *ee*, Scheme 1.6).[20] This first example highlighted the need for more optimised catalysts which can address the drawbacks of activity and selectivity of such reactions.

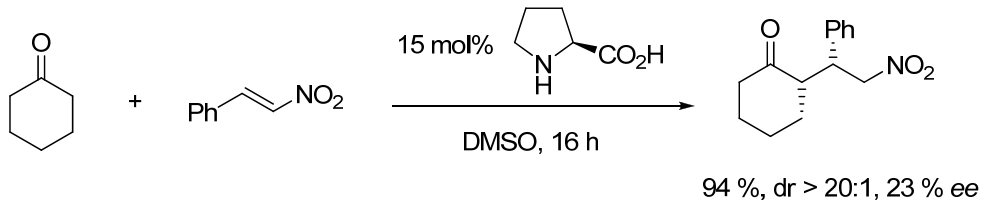

Scheme 1.6. *L-Proline catalysed 1,4-addition reaction of cyclohexanone and nitrostyrene.*[20]

Of perhaps still greater utility than asymmetric addition of ketones to nitroolefins is the corresponding addition of aldehydes, since the resulting chiral γ-nitroaldehydes are versatile building blocks for further transformations into, for example, chiral pyrrolidines,[23-27] γ-butyrolactones,[28] γ-amino acids,[26,29] or tetrahydropyrans.[30] Such addition reactions of aldehydes to nitroolefins have recently become key steps in the development of domino reactions.[31-35] Accordingly, many research groups have focused their efforts on the development of efficient organocatalysts for this reaction. Initial results achieved in 1,4-addition reactions of 'naked' aldehydes to aromatic nitroolefins were published by Barbas in 2001.[24] Enantioselectivities of up to 78 % *ee* were achieved by using a morpholine functionalised pyrrolidine catalyst. To date, a range of different primary and secondary amine based catalysts have been developed (Figure 1.1).[20,36-71] However, drawbacks of low catalytic activity and low substrate scope still remain. Furthermore, the reaction times are long and the reactions typically require a high excess of the aldehyde substrate (up to 10 equivalents) since side reactions as e.g. the formation of homo-aldol product take place.

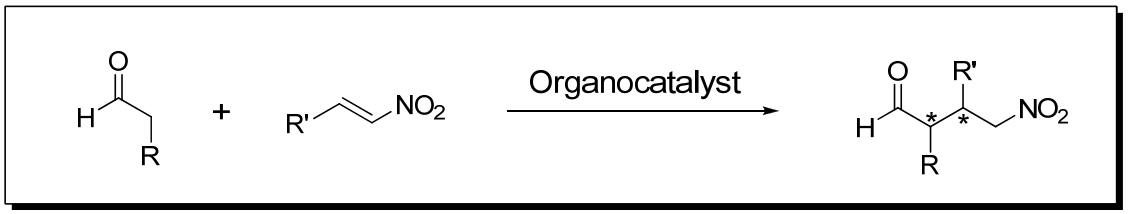

Barbas, **2001**[24]

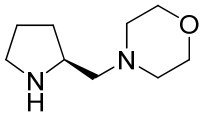

20 mol%
42-96 % yield
dr = 6:1-49:1
56-78 % *ee*

Alexakis **2002**[72]

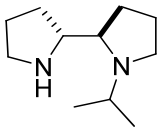

15 mol%
70-99 % yield
dr = 3:1-24:1
61-85 % *ee*

Wang **2005**[54]

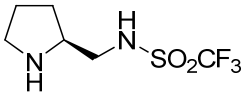

20 mol%
63-99 % yield
dr = 22:1 – 50:1
94-99 % *ee*

Hayashi **2005**[53]

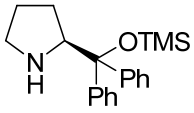

10-20 mol%
52-85 % yield
dr = 5:1-24:1
68-99 % *ee*

Alexakis **2006**[49]

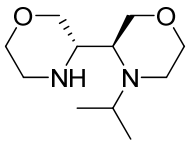

15 mol%
23-90 % yield
dr = 4:1-19:1
74-90 % *ee*

Palomo **2006**[28]

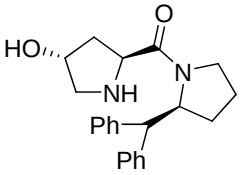

5-10 mol%
67-90 % yield
dr = 9:1->99:1
91->99 % *ee*

Jacobsen **2006**[45]
(α,α-disubst. aldehydes)

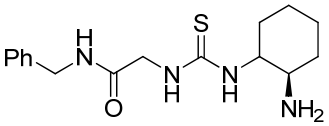

20 mol%
34-98 % yield
dr = 2:1->50:1
94-99 % *ee*

Connon **2007**[41]

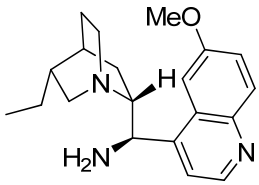

10-20 mol%
76-91 % yield
dr = 7:1-13:1
83-95 % *ee*

Figure 1.1. *Selected examples of organocatalysts developed for conjugate addition reactions of aldehydes to nitroolefins.*

2. Peptides as Asymmetric Catalysts

Short peptides, consisting of fewer than 10 amino acid residues, can be considered in terms of structural complexity, somewhere in between that of small rigid organocatalysts e.g. proline and proline derivatives and highly complex enzymes. The first examples of peptides able to induce high enantioselectivities into organic molecules via asymmetric catalysis were published in the early 1980s. The diketopiperazine cyclo(Phe-His) was found to catalyse the addition of hydrogen cyanide to benzaldehyde,[73] and polymers of leucine and alanine were discovered as asymmetric catalysts for the epoxidation of chalcones[74,75] (Scheme 2.1).

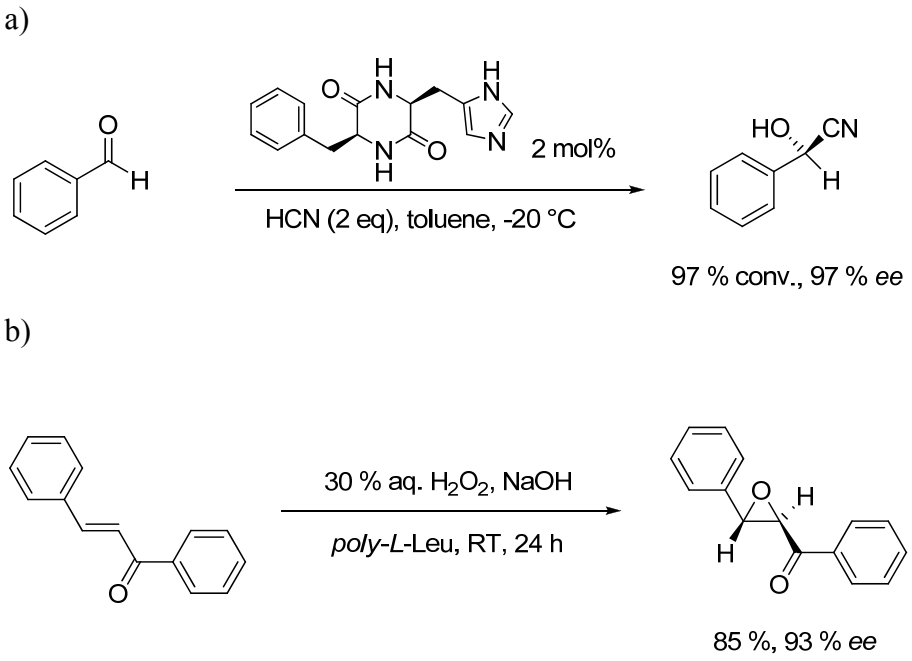

Scheme 2.1. *First examples of peptides as asymmetric catalysts: a) Diketopiperazine catalysed hydrocyanation of benzaldehyde.[73] b) Julià-Colonna epoxidation using poly-L-Leu as catalyst.[74]*

Subsequently, the continued application and development of peptides as catalysts remained dormant for some time until new concepts of combinatorial catalyst discovery were developed. It was recognized that general features such as facile synthesis and modularity, render peptidic catalysts attractive alternatives to metal-based catalysts and other

organocatalysts.[76-78] In recent years, peptides have become increasingly popular as asymmetric catalysts for a range of important organic reactions, often providing the desired products under mild reaction conditions in high yields and selectivities. Important examples of such reactions include the use of peptide based catalysts for selective acylations,[79-81] aldehyde-acylimine cross coupling reactions (Stetter reactions),[82] silylations,[83] phosphorylations,[84] addition reactions of HCN to imines (Strecker reactions),[85] Acyl-Pictet-Spengler reactions,[86] and ester hydrolysis[87] (Scheme 2.2).

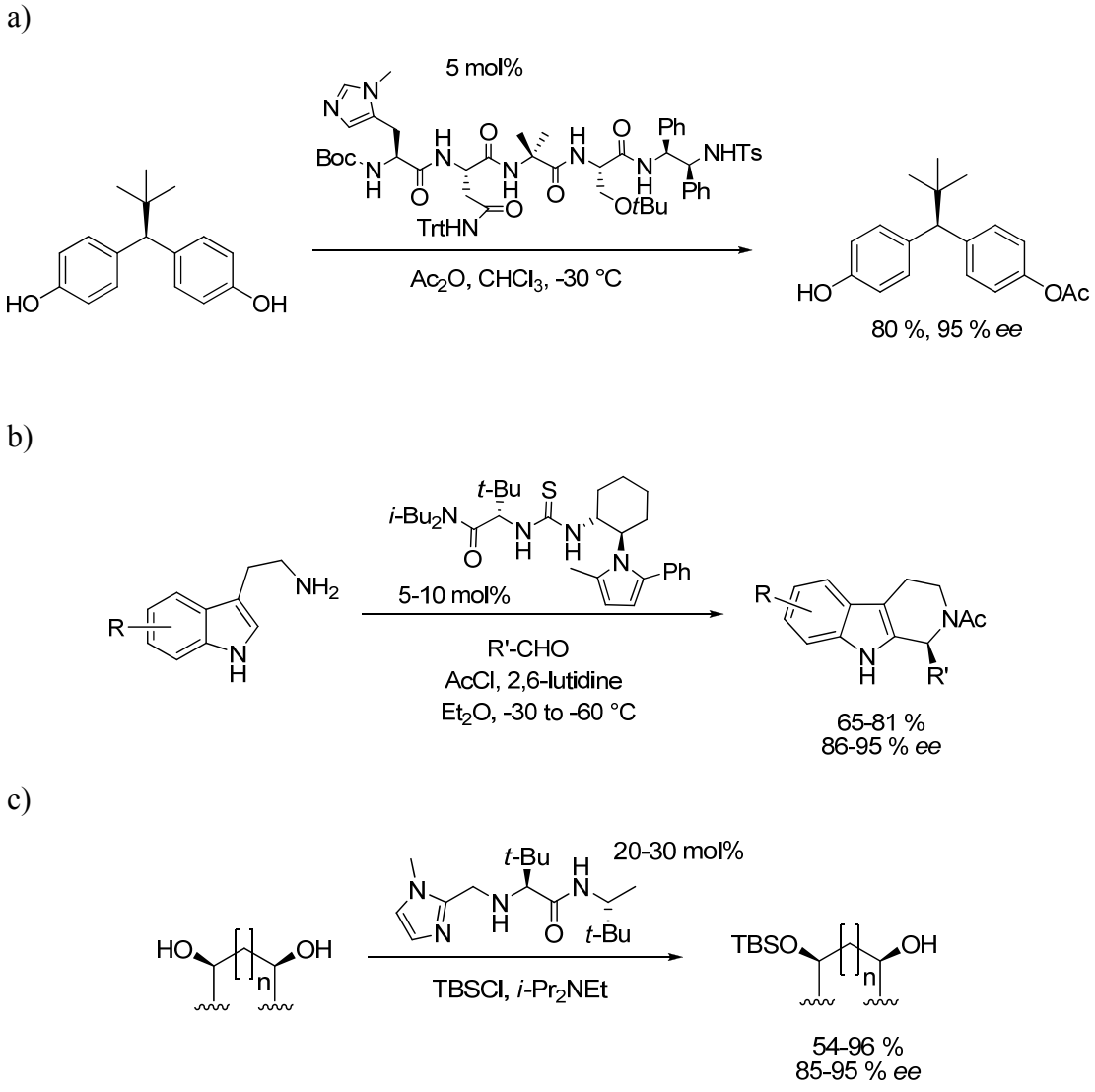

Scheme 2.2. *Examples of important reactions catalysed by peptidic catalysts: a) Peptide catalysed desymmetrization by selective acylation.[81] b) Enantioselective Pictet-Spengler reaction catalysed by thiourea-based catalyst.[86] c) Enantioselective silyl protection of alcohols catalysed by imidazole-based catalyst.[83]*

Beside these illustrations of Brønsted acid and base catalysis, peptides also show a significant potential as Lewis base catalysts. For example, the asymmetric nitro-Henry reactions of cyclohexenone and nitroalkenes catalysed by di- and tripeptides, demonstrates the possible function of peptides as catalysts for reactions relying on iminium catalysis (Scheme 2.3).[88,89] Considering enamine catalysis, a great deal of attention has been paid to peptide catalysed asymmetric aldol reaction, one of the most important carbon-carbon bond forming reactions. Whilst proline and its derivatives can be applied as small and rigid organocatalysts for this transformation (see Chapter 1), nature uses to some extent the metal-free type I aldolase for this task. In both cases, the mechanism is based on intermediate enamine formation.[7] With the aim to combine the best properties of the two systems, many research groups focused their work on the development of peptidic catalysts for asymmetric aldol reactions. Numerous short chained peptides were introduced, containing a secondary amine at the *N*-terminus (Scheme 2.4 a and b).[90-98] Examples are also known for certain aldol reactions catalysed by peptides bearing primary amines at the *N*-terminus (Scheme 2.4 c).[99-101] This work in general reveals that short peptides can indeed function as asymmetric catalysts but the low catalytic activity remains a major issue in most examples.

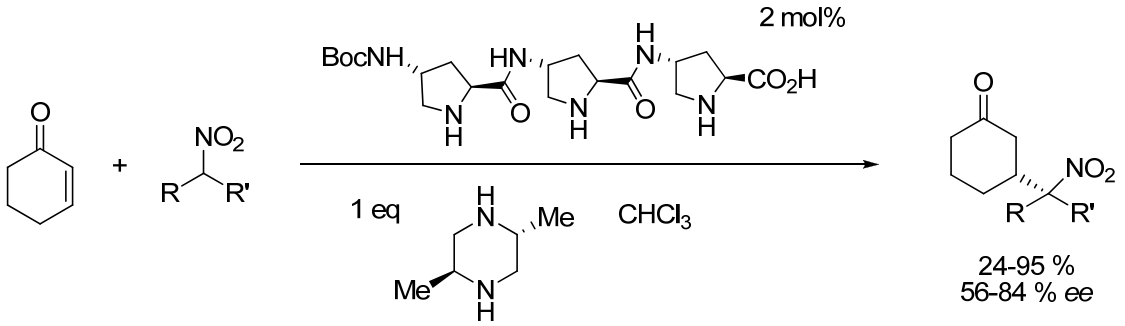

Scheme 2.3. *Example of peptide based iminium catalysis: Asymmetric nitro-Henry reactions of cyclohexenone and nitroalkenes.* [88,89]

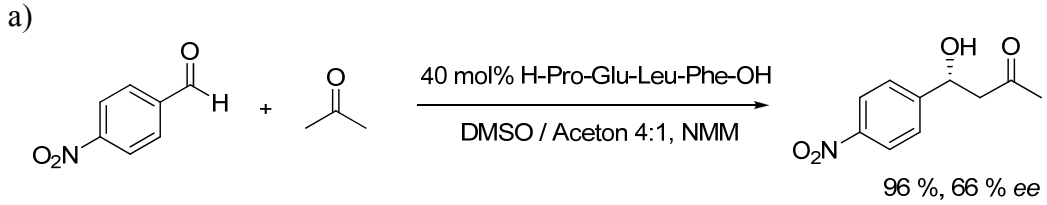

b)

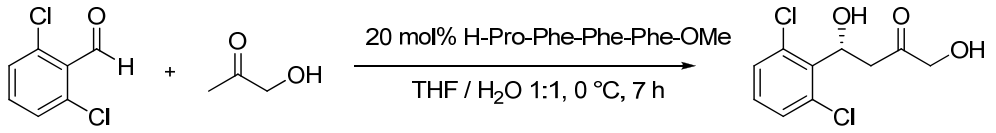

c)

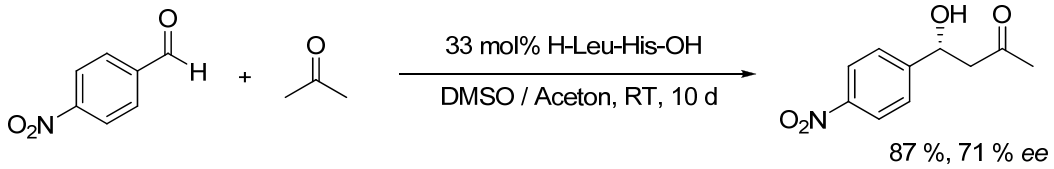

Scheme 2.4. *Specific examples of peptide-catalysed aldol reactions: a) and b) Peptides bearing a secondary amine at the N-terminus.*[90, 91] *c) Peptide with a primary amine at N-terminus.*[100]

2.1 Combinatorial Methods for the Development of Catalytically Active Peptides – The Catalyst Substrate Co-Immobilisation Method

One of the largest challenges to the development of peptidic catalysts is the prediction and incorporation of desirable catalytic properties into a given peptide. This is already a challenge for small rigid catalysts, but even more so for short peptidic catalysts bearing many more degrees of rotational freedom. In nature, the process of catalyst (enzyme) development follows the principles of evolution. Accordingly, combinatorial chemistry is able to deliver an empirical approach, mimicking the natural process of random mutation and selection of the best catalysts among a large molecular diversity. To generate such high molecular diversity, combinatorial libraries which allow investigation of a large number of compounds are assessed for their catalytic properties. Combinatorial methods are particularly suited for the discovery of catalytically active peptides.[77,102,103]

The constitution of individual entities (amino acids) allow the straightforward generation of molecular diversity, because the established protocols in solid phase peptides synthesis are particularly applicable to library synthesis by the split-and-mix method. The protocol for the

generation of such one-bead-one-compound libraries relies on successive cycles of 1. splitting the solid phase resin (beads) into equal portions, 2. subjecting each portion to a different reaction and 3. mixing of the beads. This approach leads to an exponential increase of the different compounds relative to the number of reactions performed. Using this method the molecular diversity achieved is significantly larger in comparison to parallel libraries without the need of automated synthesis.[104-108]

If unbound reaction partners (substrates) as well as possible products are able to freely diffuse in the presence of a combinatorial library bearing potential catalysts, the identification of active library members becomes impossible even when the desired reaction takes place. To solve this issue an intelligent screening method is indispensible. The "catalyst-substrate co-immobilisation method" is a general technique which allows the identification of catalysts for bimolecular reactions.[93,109] The principle of this method relies on the attachment of a library member (= potential catalyst) as well as a reaction partner A on the solid support via a bi-functional linker. The reaction between the immobilised reaction partner A and a dissolved dye- or fluorophore-marked reaction partner B occurs only on those beads bearing active library members which are able to catalyse the reaction. The reaction process results in covalent attachment of the dye or fluorophore on the bead making identification of the catalyst feasible (Figure 2.1).

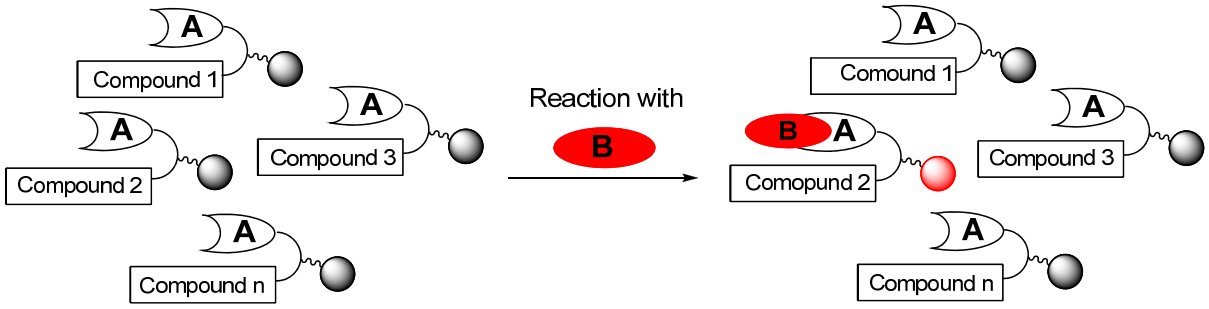

Figure 2.1. *Principle of the "catalyst-substrate co-immobilisation method": Compound 2 catalyses the reaction between A and B resulting in the covalent attachment of the dye on the corresponding bead.*

2.2 *Tripeptides as Catalysts for Asymmetric Aldol Reactions*

Using the concept of catalyst-substrate co-immobilisation (see Chapter 2.1) the Wennemers group achieved the development of reactive peptidic organocatalysts for aldol reactions.[93] Thus, a levulinic acid (ketone) functionalised tripeptide library was incubated with a dye-marked benzaldehyde derivative. After filtration and subsequent washing of the resin approximately 1 % of the beads appeared red. The isolation of the darkest beads and the decoding of the corresponding library members revealed H-Pro-Pro-Asp-NHR and H-Pro-D-Ala-D-Asp-NHR as key sequences. According to these findings, the tripeptides H-Pro-Pro-Asp-NH_2 **1** and H-Pro-D-Ala-D-Asp-NH_2 **2** were synthesised and tested as catalysts for the reaction of acetone and benzaldehyde. Indeed, both peptides proved to be efficient catalysts for this aldol reaction. In comparison to L-proline as organocatalyst, **1** and **2** showed a significantly higher activity. In this respect only 1 mol% of **1** sufficed to catalyse the asymmetric aldol reactions between different aldehydes and acetone in high yields and *ee*'s of up to 90 % (Table 2.1).

Table 2.1. *Aldol reactions of different aldehydes and acetone: Comparison of H-Pro-Pro-Asp-NH_2 **1** with L-proline (30 mol%) as catalyst.*

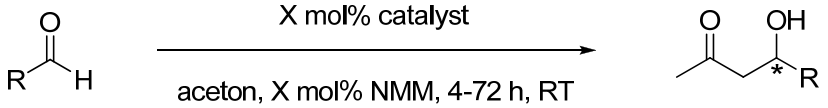

	1 mol% **1**		30 mol% L-proline	
R	yield [%]	*ee* [%]	yield [%]	*ee* [%]
4-NO_2Ph	99	90 (*S*)	68	76 (*R*)
Ph	69	78 (*S*)	62	60 (*R*)
c-Hex	66	82 (*S*)	63	84 (*R*)
i-Pr	79	79 (*S*)	97	96 (*R*)
neo-Pent	28	73 (*R*)	24	22 (*S*)

The results obtained from these studies indicated that an increase in the structural complexity may lead to an enhancement of the catalytic activity. In addition, **1** and **2** showed opposite enantioselectivities, although both peptides bear a *N*-terminal L-proline residues. This demonstrated that different enantiomers are accessible by only small changes in the peptidic primary and thereby secondary structure.

II.
Objective

3. Peptides as Catalysts for Conjugate Addition Reactions of Aldehydes to Nitroolefins?

The successful introduction of H-Pro-Pro-Asp-NH_2 **1** as a catalyst for direct asymmetric aldol reactions led us to further investigate this system. Since studies of closely related peptides demonstrated that the secondary amine at the *N*-terminus, the carboxylic acid in the side chain of the aspartic acid residue, and a well-defined turn conformation are crucial for the high catalytic activity and selectivity of **1**,[110] we assume a mechanism which is closely related to that proposed for proline catalysis.[111-114] This mechanism is reminiscent of that used by natural aldolases typ I involving enamine formation, subsequent reaction with the aldehyde, and proton transfer from the carboxylic acid (Figure 3.1a, see Chapter 1). However, in comparison to L-proline, the distance between the secondary amine and the carboxylic acid within peptide **1** is greater by approximately 3 Å as indicated by molecular modeling studies with Macro Model 8.0 (Figure 3.1).[93] Based on this model we hypothesised, that this extra distance of 3 Å might be spanned by two additional atoms in the structure of the electrophile, allowing catalysis of not only 1,2- but also 1,4-addition reactions. Therefore, H-Pro-Pro-Asp-NH_2 **1** and related peptides might be applicable for Michael addition reactions.

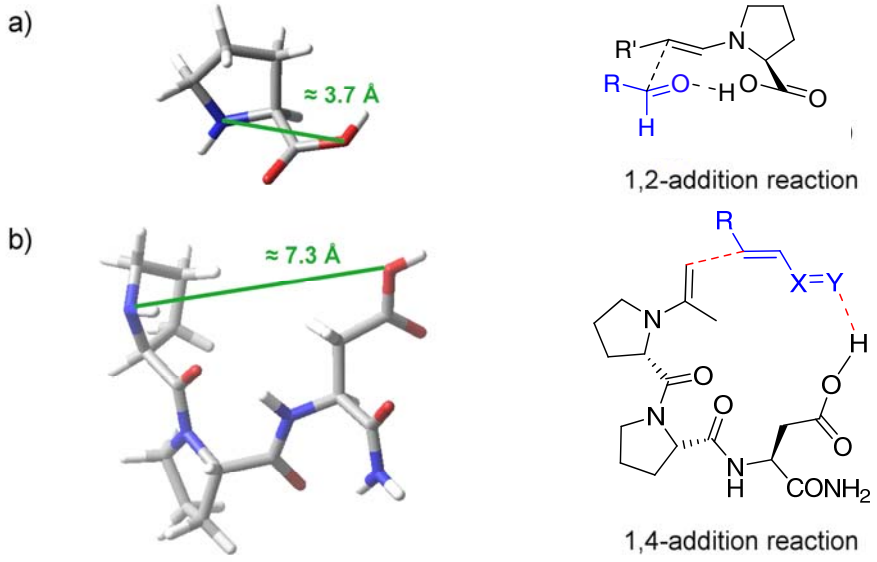

Figure 3.1. *a) Transition state of aldol reaction catalyzed by proline as proposed by Houk and List.*[111-114] *b) Lowest energy conformation of H-Pro-Pro-Asp-NH_2* **1**,[93] *as calculated by MacroModel 8.0 and schematic transition state of conjugate addition reaction.*

Organocatalysed asymmetric conjugate addition reactions of carbon-centered nucleophiles are among the most useful and challenging synthetic tranformations.[6,115-118] Within this family, the addition of aldehydes to nitroolefins is one of most important reactions, because the resulting γ-nitroaldehydes are versatile building blocks for further transformations. As a result, many research groups focused on the development of efficient catalysts for this asymmetric reaction and explored a range of different primary and secondary amine based catalysts (see Chapter 1.1). However, these catalysts typically require a high catalyst loading and a high excess of the aldehyde (up to 10 equivalents). The substrate scope is often limited and reaction times are typically long. Furthermore, the addition of acids and/or bases is often needed. Due to these unsolved problems a more efficient catalytic system is highly desired.

The objective of this thesis was the development and application of peptides as efficient catalysts for asymmetric conjugate addition reactions of aldehydes and nitroolefins. In subsequent studies, conformational characteristics of the catalyst and kinetic properties of the reaction system were further explored to gain insight into a possible mechanism of action and to increase the reaction scope.

III.
Results & Discussions

4. Asymmetric 1,4-Addition Reaction of *n*-Butanal and Nitrostyrene as a Model Reaction

4.1 TFA•H-Pro-Pro-Asp-NH_2 (1) as a Catalyst

4.1.1 Initial Studies

To evaluate the catalytic properties of the tripeptide H-Pro-Pro-Asp-NH_2 **1** (Figure 4.1) in conjugate addition reactions of aldehydes and nitroolefins we used the reaction between *n*-butanal and nitrostyrene as a model reaction.

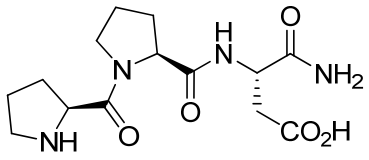

1

Figure 4.1. *H-Pro-Pro-Asp-NH_2*

Peptide **1** was synthesised on a solid support (Rink Amide resin) and cleaved from the resin with TFA. The corresponding TFA-salt of **1** was directly used without further purification. To liberate the secondary amine of the *N*-terminal proline, a base was used in an equivalent amount to the catalyst. In former studies of aldol reactions using TFA•peptide **1** as catalyst, NMM was successfully applied as such a base.[93] Thus, we also used NMM as a base for the initial experiments. *i*-PrOH was used as the solvent since both catalyst and substrates showed good solubility in this media. For the first experiment (Table 4.1, Entry 1) 1 mol% of the TFA•catalyst **1** and 1 mol% of NMM was used for the reaction of 3 equivalents of *n*-butanal and 1 equivalent of nitrostyrene. The concentration with respect to nitrostyrene was 0.4 M. After approximately 3 h more than 90 % conversion to the corresponding γ-nitroaldehyde **3** was observed. The *syn*:*anti* ratio of the resulting product was 10:1 and the enantiomeric excess was 73 %. After obtaining these very promising initial results, we systematically

varied the different reaction parameters of the title reaction. First we changed the catalyst loading and performed the standard reaction under otherwise identical conditions (Table 4.1, Entry 2-4). Even with 0.5 mol% of **1** the reaction went to completion, however, more than 18 h were required whereas the diastereoselectivity (*syn*:*anti* = 11:1) and the enantioselectivity (73 % *ee*) remained unaffected. With 5 mol% or 10 mol% of **1** the reactions showed quantitative conversions within less than 1 h. The enantioselectivity was not influenced when increased quantities of catalyst were used, however, significantly lower *syn*:*anti* ratios were observed (5:1 and 2:1).

Table 4.1. *Initial TFA•H-Pro-Pro-Asp-NH_2* ***1*** *catalysed 1,4-addition reactions between n-butanal and nitrostyrene with the variation of catalyst loading, NMM- and aldehyde addition and concentration of the reaction mixture.* [a]

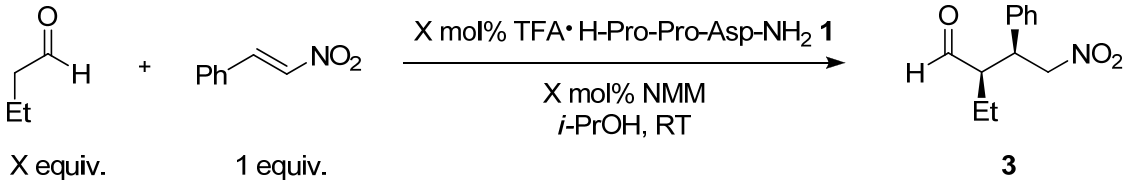

Entry	Cat. [mol%]	NMM [mol%]	Aldehyde [eq]	Conc. [M][b]	Time [h]	Conv. [%][c]	*syn : anti*[d]	*ee (syn)* [%][d]
1	1	1	3	0.40	~3	>90	10 : 1	73
2	0.5	1	3	0.40	~18	>90	11 : 1	73
3	5	1	3	0.40	<1	quant.	5 : 1	72
4	10	1	3	0.40	<1	quant.	2 : 1	73
5	1	none	3	0.40	~24	>90	13 : 1	72
6	1	5	3	0.40	~3	>90	10 : 1	75
7	1	10	3	0.40	~3	>90	11 : 1	74
8	1	20	3	0.40	~18	>90	9 : 1	74
9	1	1	1	0.40	~24	<50	n.d.	n.d.
10	1	1	2	0.40	~3	>90	8 : 1	73
11	1	1	5	0.40	~3	>90	5 : 1	73
12	1	1	3	0.72	~3	>90	11 : 1	74
13	1	1	3	0.28	~5	>90	8 : 1	73
14	1	1	3	0.21	~5	>90	11 : 1	73

[a] Reactions were performed at a 0.45 mmol scale. [b] Concentration with respect to nitrostyrene. [c] Estimated by TLC. [d] Determined by chiral phase HPLC analysis.

The standard reaction without NMM (Table 4.1, Entry 5) proceeded with the same selectivity but much slower (>24 h). A 5 times or even a 10 times excess of NMM (Table 4.1, Entries 6 and 7) neither influenced the reaction progress nor the selectivity, whereas a 20 times excess of NMM slowed down the reaction (18 h, Table 4.1, Entry 8). An excess of *n*-butanal proved to be crucial for efficient catalysis. If the aldehyde was used in an equimolar quantity to the nitrostyrene, the conversion was below 50 % after one day (Table 4.1, Entry 9). The observed conversions and enantioselectivities when using 2 or 5 equivalents of *n*-butanal were comparable with the reaction using 3 equivalents of aldehyde, however, the obtained diastereoselectivity was lower in both cases (*syn:anti* = 8:1 and 5:1, Table 4.1, Entries 10 and 11). Finally, the influence of the overall reaction mixture concentration was tested by performing the reaction at higher concentration (0.72 M, Table 4.1, Entry 12) or lower concentration (0.28 M and 0.21 M, Table 4.1, Entries 13 and 14). The results obtained at higher concentrations were similar to those of the standard reaction and, as expected, the more diluted reactions were slower (~5 h). However, the stereoselectivity remained the same for all reactions. In conclusion, these initial experiments showed that the enantioselectivity of the TFA•H-Pro-Pro-Asp-NH_2 **1** catalysed conjugate addition reaction of *n*-butanal and nitrostyrene remained stable under various conditions. Based on the achieved results we defined the use of a base in a stochiometric amount relative to the catalyst, 1 equivalent of nitrostyrene and 3 equivalents of *n*-butanal with a 0.4 M concentration of the reaction mixture with respect to nitrostryrene as the standard conditions for further studies.

4.1.2 Influence of the Base

Next we tested the influence of the additional base on the reaction of *n*-butanal and nitrostyrene catalysed by TFA•H-Pro-Pro-Asp-NH_2 **1** in *i*-PrOH under the previously defined standard conditions (Table 4.2). With other tertiary amines like DMAP (Table 4.2, Entry 2) and *i*-Pr_2NEt (Table 4.2, Entry 3) results comparable to NMM (Table 4.2, Entry 1) were obtained, whereas the reactivity was significantly reduced when Et_3N (Table 4.2, Entry 4) was used as an additional base. Comparable results to NMM were obtained with *i*-Pr_2NH (Table 4.2, Entry 5). The identical enantiomeric excess suggests that no catalytic competition between the peptide **1** and the additional secondary amine took place. Even $PrNH_2$ and Piperidine (Table 4.2, Entries 6 and 7) could be used as basic additives which lowered the conversion but led to products with similar stereoselectivity. In summary these experiments

indicated, that the influence of the different bases as additives to the TFA salt of catalyst **1** are not important for the stereoselectivity of the corresponding product. For further studies we decided to use NMM as the base of choice.

Table 4.2. *TFA•H-Pro-Pro-Asp-NH_2* ***1*** *catalysed 1,4-addition reactions between n-butanal and nitrostyrene with different bases.*[a]

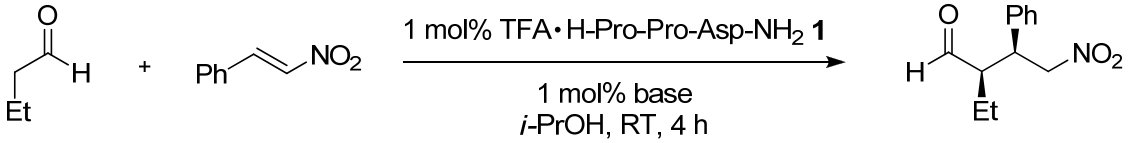

Entry	Base	Conv. [%] [b]	*syn : anti*[c]	*ee* [%][c]
1	NMM	>90	10 : 1	73
2	DMAP	quant.	8 : 1	73
3	*i*-Pr_2NEt	~85	11 : 1	73
4	Et_3N	~50	15 : 1	73
5	*i*-Pr_2NH	~80	10 : 1	73
6	$PrNH_2$	~45	15 : 1	73
7	Piperidine	~60	11 : 1	71

[a] Reactions were performed at a 1.1 mmol scale (0.4 M with respect to nitrostyrene. [b] Estimated by ^1H NMR of the crude material. [c] Determined by chiral-phase HPLC analysis.

4.1.3 Solvent Screening

Various different solvents were then tested for the TFA•H-Pro-Pro-Asp-NH_2 **1** catalysed reaction of *n*-butanal and nitrostyrene under standard conditions (Table 4.3). Whereas the reactions with primary alcohols like *n*-BuOH and EtOH (Table 4.3, Entries 2 and 3) as solvents showed comparable results to the reaction with *i*-PrOH (Table 4.3, Entry 1), the reactions with other solvents proceeded significantly slower. The poor solubility of catalyst **1** in non-polar solvents as for example toluene (Table 4.3, Entry 7) may be the reason for the slow or even missing reaction progress. Higher diastereo- and enantioselectivities compared

to the reaction in *i*-PrOH were obtained in dioxane (Table 4.3, Entry 5), $CHCl_3$ (Table 4.3, Entry 11), CH_2Cl_2 (Table 4.3, Entry 12) and EtOAc (Table 4.3, Entry 13).

Table 4.3. *TFA•H-Pro-Pro-Asp-NH_2* ***1*** *catalysed 1,4-addition reactions between n-butanal and nitrostyrene in different solvents.*[a]

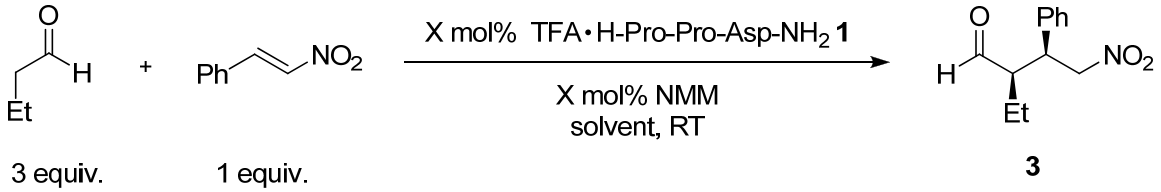

Entry	Solvent	**1** / NMM [mol%]	Time [h]	Conv. [%][b]	*syn : anti*[c]	*ee (syn)* [%][c]
1	*i*-PrOH	1	~3	>90	10 : 1	73
2	*n*-BuOH	1	~3	>90	10 : 1	71
3	EtOH	1	~3	>90	10 : 1	71
4	DMSO	1	~18	>90	6 : 1	57
5	dioxane	1	~24	>90	13 : 1	81
6	THF	1	~24	~40	n.d.	n.d.
7	toluene	1	~24	-	n.d.	n.d.
8	ethylene glycol	1	~24	-	n.d.	n.d.
9	*t*-BuOH	5	~1	>90	5 : 1	73
10	acetonitrile	5	~1	>90	8 : 1	60
11	$CHCl_3$	5	~24	>90	14 : 1	85
12	CH_2Cl_2	5	~24	>90	14 : 1	79
13	EtOAc	5	~24	>90	9 : 1	77
14	THP	5	~48	>90	10 :1	57

[a] Reactions were performed at a 1.1 mmol scale (0.40 M with respect to nitrostyrene). [b] Estimated by TLC. [c] Determined by chiral phase HPLC analysis.

To improve the solubility and therefore the activity of **1** we performed the reactions using mixtures of the solvent providing the most selective reaction ($CHCl_3$) and the solvent that showed the fastest reaction (*i*-PrOH) (see Table 4.4). The best results were obtained in a 9:1 (v/v) mixture of $CHCl_3$ and *i*-PrOH, leading to the corresponding product **3** in only 6 h, with a conversion of >90 % and a *syn:anti* ratio of 10:1 (Table 4.4, Entry 2). Remarkably, the

enantioselectivity remained the same as that obtained in pure $CHCl_3$ (85 % *ee*). Higher diastereoselectivities and slightly higher enantioselectivities were obtained when the reactions were performed in $CHCl_3$/*i*-PrOH 9:1 (v/v) at decreased temperature (0 °C, Table 4.4, Entry 5 and -15 °C, Table 4.4, Entry 6). However, the activity was significantly lower in both cases. The reactions required more than one day, even with the use of 3 mol% of **1**.

Table 4.4. *TFA•H-Pro-Pro-Asp-NH_2* ***1*** *catalysed 1,4-addition reactions between n-butanal and nitrostyrene in different mixtures of $CHCl_3$ and i-PrOH and at different temperatures.*[a]

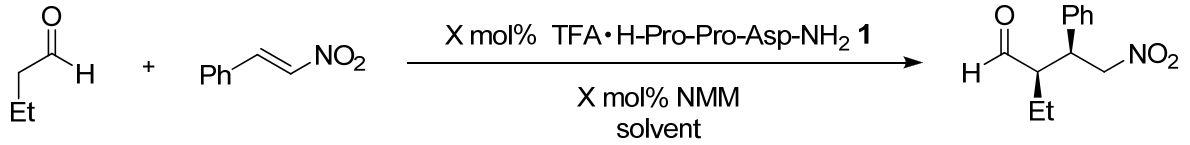

3 equiv. 1 equiv. **3**

Entry	Solvent		Temp.	**1** / NMM [mol%]	Time [h]	Conv. [%][b]	*syn* : *anti*[c]	*ee* [%][c]
1	$CHCl_3$: *i*-PrOH	**8:2**	RT	1	<6	quant.	10 : 1	81
2	$CHCl_3$: *i*-PrOH	**9:1**	RT	1	~6	>90	10 : 1	85
3	$CHCl_3$: *i*-PrOH	**9.5:0.5**	RT	1	~12	>90	12 : 1	85
4	$CHCl_3$: *i*-PrOH	**9.9:0.1**	RT	1	~20	~50	15 : 1	85
5	$CHCl_3$: *i*-PrOH	9:1	**0 °C**	3	<40	>90	20 : 1	86
6	$CHCl_3$: *i*-PrOH	9:1	**-15 °C**	3	~40	~80	19 : 1	86

[a] Reactions were performed at a 1.1 mmol scale (0.40 M with respect to nitrostyrene). [b] Estimated by TLC. [c] Determined by chiral phase HPLC analysis.

4.1.4 Conclusions

In agreement with the rational prediction, it was shown that the tripeptide TFA•H-Pro-Pro-Asp-NH_2 **1** is indeed able to catalyse not only 1,2- but also 1,4-addition reactions. The asymmetric conjugate addition of *n*-butanal to nitrostyrene was chosen as a model reaction. Best results were obtained by using 1 mol% of **1** and NMM as a base, 3 equivalents of *n*-butanal and 1 equivalent of nitrostyrene in a mixture of $CHCl_3$/*i*-PrOH 9:1 (v/v) with a concentration of 0.4 M with respect to nitrostyrene. These conditions were later used for the screening of a range of related peptidic catalysts.

4.2 *Screening of Various Catalysts Containing a N-Terminal Proline Residue and an Acidic Functionality*

Based on the initial lead structure of H-Pro-Pro-Asp-NH_2 **1** we synthesised a large number of related peptides, which contained an *N*-terminal proline residue and an acidic functionality. These peptides were then tested as catalysts for the reaction of *n*-butanal and nitrostyrene under the standard conditions discussed above (Table 4.5). For this initial screening we restricted ourselves to the use of L-amino acid building blocks, however, also non-proteinogenic amino acids like β-homo aspartate, α-methyl proline and Cys(SO_3H) were introduced. Furthermore, we varied the *C*-terminal end groups (carboxylic acids, carboxamides or a methyl ester). L-Proline itself was found to be a rather poor catalyst for the title reaction and under the chosen conditions (Table 4.5, Entry 1). A catalyst loading of 10 mol% L-proline was necessary to obtain the desired product **3** in a yield of 85 % after one day and with a selectivity of *syn:anti* = 8:1 and 39 % *ee*. Significantly better results were obtained with the dipeptide TFA•H-Pro-Pro-OH **4** (Table 4.5, Entry 2). With a catalyst loading of 1 mol% and after 24 h, approximately 50 % conversion and a selectivity of *syn:anti* = 19:1 and 68 % *ee* was observed. In contrast, the dipeptide TFA•H-Pro-Asp-NH_2 **5** (Table 4.5, Entry 3) showed nearly no activity when 1 mol% of **5** was used. Remarkably, the tetrapeptide TFA•H-Pro-Pro-Asp-Pro-NH_2 **6** (Table 4.5, Entry 5), bearing one additional proline residue at the *C*-terminus, showed a lower activity but a significantly higher selectivity in comparison to TFA•H-Pro-Pro-Asp-NH_2 **1** (Table 4.5, Entry 4). Using 1 mol% of **6**, the reaction required 12 h for >90 % conversion while a *syn:anti* ratio of 23:1 and an enantimeric excess of 90 % was obtained. In this case a higher structural complexity led to an increased selectivity. We assume that a stabilising effect of the additional *C*-terminal proline on the catalyst structure, which would lead to a better defined transition state for the 1,4-addition reaction and therefore increase the enantioselectivity, is a possible explanation for the higher *ee* observed with tetrapeptide **6**. In former studies, this peptide **6** was identified as a consensus sequence in a combinatorial experiment where a tetrapeptide split & mix library was screened for intermolecular aldol reactions.[119] For the aldol reaction of benzaldehyde and aceton, catalyst **6** showed an activity comparable to TFA•H-Pro-Pro-Asp-NH_2 **1**, however, the observed enantioselectivity was significantly lower with the tetrapeptide. When the analogous

pentapeptide TFA•H-Pro-Pro-Asp-Pro-Pro-NH_2 **7** was tested as catalyst for the standard 1,4-addition reaction, a beneficial effect on the selectivity was not observed anymore (Table 4.5, Entry 6).

Table 4.5. *Asymmetric 1,4-addition reaction between n-butanal and nitrostyren:. Screening of different peptides containing the H-Pro-Pro motif and an acidic functionality.*[a]

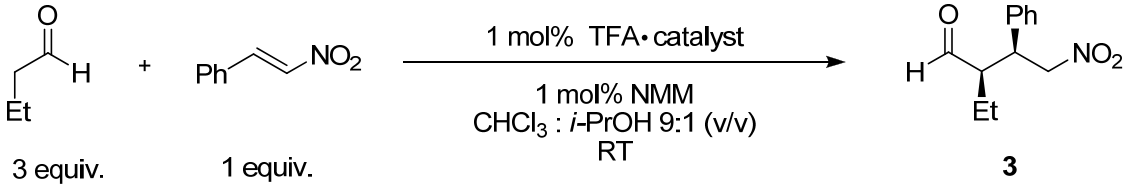

Entry	Catalyst	Time [h]	Conv. [%][b]	*syn : anti*[c]	*ee (syn)* [%][c]
1	H-Pro-OH [d]	24	85[e]	8 : 1	39
2	TFA•H-Pro-Pro-OH **4**	24	~50	19 : 1	68
3	TFA•H-Pro-Asp-NH_2 **5**	15	<10	n.d.	n.d.
4	TFA•H-Pro-Pro-Asp-NH_2 **1**	6	96[e]	10 : 1	85
5	TFA•H-Pro-Pro-Asp-Pro-NH_2 **6**	12	>90	23 : 1	90
6	TFA•H-Pro-Pro-Asp-Pro-Pro-NH_2 **7**	15	>90	15 : 1	85
7	TFA•H-Pro-Pro-Asp-OMe **8**	12	>90	20 : 1	82
8	TFA•H-Pro-Pro-β-homo-Asp-NH_2 **9**	12	>90	9 : 1	83
9	TFA•H-Pro-Pro-β-homo-Asp-OH **10**	12	>90	20 : 1	81
10	TFA•H-Pro-Pro-Asn-OH **11**	12	>90	13 : 1	87
11	TFA•H-Pro-Pro-Ser-OH **12**	5	>90	12 : 1	85
12	TFA•H-Pro-Pro-His-OH **13**	12	>90	6 : 1	84
13	TFA•H-Pro-Pro-Gly-OH **14**	12	>90	10 : 1	76
14	TFA•H-Pro-Pro-Cys(SO_3H)-NH_2 **15**	20	<30	14 : 1	77
15	TFA•H-Pro-MePro-Asp-NH_2 **16**	20	~40	9 : 1	83
16	Me-Pro-Pro-Asp-NH_2 **17** [f]	15	-	n.d.	n.d.
17	Ac-Pro-Pro-Asp-NH_2 **18** [f]	15	-	n.d.	n.d.

[a] Reactions were performed at a 1.1 mmol scale (0.40 M with respect to nitrostyrene). [b] Estimated by TLC. [c] Determined by chiral phase HPLC analysis. [d] 10 mol%. [e] Isolated yield. [f] 10 mol%, no NMM.

With 1 mol% of TFA•H-Pro-Pro-Asp-Pro-Pro-NH_2 **7** an activity comparable to peptide **1** was observed and a selectivity of *syn:anti* = 15:1 and 85 % *ee* was obtained. TFA•H-Pro-Pro-Asp-

OMe **8** (Table 4.5, Entry 7), with a methylester instead of a carboxamide at the *C*-terminus and TFA•H-Pro-Pro-β-homo-Asp-NH_2 **9** (Table 4.5, Entry 8), where the carboxamide is removed from the peptidic backbone by an additional CH_2 group, showed both lower activity (1 mol%, 12 h, >90 % conversion) and lower enantioselectivity in comparison to **1** (82 % *ee* and 83 % *ee,* respectively). Several peptides of the type H-Pro-Pro-Xaa-OH were tested as well (1 mol% each). Thus, the peptides TFA•H-Pro-Pro-Asn-OH **11** (87 % *ee*, Table 4.5, Entry 10), TFA•H-Pro-Pro-Ser-OH **12** (85 % *ee*, Table 4.5, Entry 11) and TFA•H-Pro-Pro-His-OH **13** (84 % *ee*, Table 4.5, Entry 12) showed nearly the same or even better enantioselectivities than **1** whereas TFA•H-Pro-Pro-Gly-OH **14** proved to be less selective (76 % *ee*, Table 4.5, Entry 13). A significantly lower activity and enantioselectivity was observed with the peptide TFA•H-Pro-Pro-Cys(SO_3H)-NH_2 **15** (Table 4.5, Entry 14), bearing a sufonic acid instead of a carboxylic acid in the side chain of the third amino acid residue. The decreased activity of this catalyst **15** (1 mol%, 20 h, <30 %) can be rationalised with the lower pK_a of the acid functionality. The sulfonic acid may protonate the *N*-terminal secondary amine which leads to a deactivation of catalyst **15**. That the *N*-terminal secondary amine is crucial for catalysis was underlined by testing the methylated peptide **17** and the acetylated peptide **18**, which both proved to be inactive as catalysts for the reaction of *n*-butanal and nitrostyrene, even when 10 mol% of the peptides were used.

This initial screening indicated that peptides of the general type H-Pro-Pro-Xaa, containing a free secondary amine at the *N*-terminus and a carboxylic acid either in the side chain of Xaa or at the corresponding *C*-terminus, are good catalysts for the asymmetric conjugate addition reaction of *n*-butanal and nitrostyrene. The original lead structure, H-Pro-Pro-Asp-NH_2 **1**, remained one of the best catalysts in terms of activity and selectivity whereas several peptides of the type H-Pro-Pro-Xaa-OH showed comparable catalytic properties. The highest enantiomeric excess of 90 % was achieved with the tetrapeptide TFA•H-Pro-Pro-Asp-Pro-NH_2 **6**.

4.3 Diastereomeric Tri- and Tetrapeptides

Based on the initial screening of Pro-Pro-Xaa type peptides, we decided to test diastereoisomers of the best catalysts found. First, the four diastereoisomers of the parent TFA•H-Pro-Pro-Asp-NH_2 **1** were synthesised and tested as catalysts for the conjugate addition reaction of *n*-butanal and nitrostyrene under identical conditions as previously applied (Table 4.6). All of the diastereomeric peptides proved to be efficient catalysts, providing the corresponding product **3** in high yields and selectivities within 6 to 20 h using only 1 mol% of catalyst. Furthermore they all showed improved diastereoselectivities *(syn:anti* = 25:1-50:1, Table 4.6, Entries 2-4) in comparison to the parent peptide **1** (*syn:anti* = 10:1, Table 4.6, Entry 1). Whereas TFA•H-Pro-D-Pro-Asp-NH_2 **19** (Table 4.6, Entry 3) and TFA•H-Pro-Pro-D-Asp-NH_2 **20** (Table 4.6, Entry 4) showed slightly lower enantiomeric excesses (81 % *ee* in both cases) than TFA•H-Pro-Pro-Asp-NH_2 **1** (85 % *ee*, Table 4.6, Entry 1), the diastereoisomeric peptide TFA•H-D-Pro-Pro-Asp-NH_2 **21** (Table 4.6, Entry 2) provided the product with a significantly higher enantioselectivity of 95 % *ee*.

Table 4.6. *Asymmetric 1,4-addition reaction between n-butanal and nitrostyrene: Screening of diasteroisomeric peptides of the Pro-Pro-Asp-NH_2 motif.*[a]

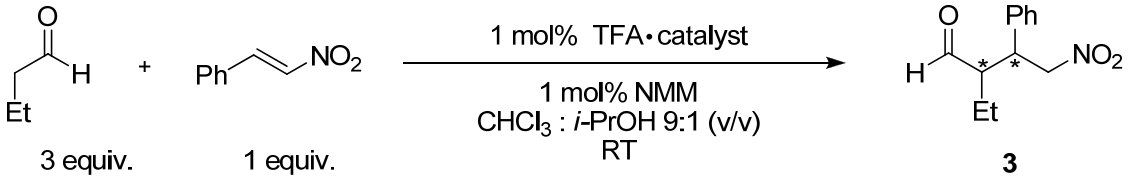

Entry	Catalyst	Time [h]	Yield [%][b]	*syn : anti*[c]	*ee (syn)* [%][c]	Abs. Conf.
1	TFA•H-Pro-Pro-Asp-NH_2 **1**	6	96[d]	10 : 1	85	*(R,S)*
2	TFA•H-**D**-Pro-Pro-Asp-NH_2 **21**	12	93[d]	25 : 1	95	***(S,R)***
3	TFA•H-Pro-**D**-Pro-Asp-NH_2 **19**	20	92[d]	25 : 1	81	*(R,S)*
4	TFA•H-Pro-Pro-**D**-Asp-NH_2 **20**	10	84[d]	50 : 1	81	*(R,S)*

[a] Reactions were performed at a 1.1 mmol scale (0.40 M with respect to nitrostyrene). [b] Isolated yield. [c] Determined by chiral phase HPLC analysis.

Notably, the peptides **1** and **21**, with inverted absolute configurations at the *N*-terminal proline residue, both afforded the *syn* addition reaction products, but with opposite enantioselectivity.

TFA•H-Pro-Pro-Asp-NH_2 **1** afforded the (*R,S*) and TFA•H-D-Pro-Pro-Asp-NH_2 **21** the (*S,R*) product. This result demonstrates that a switch in the stereoselectivity of peptidic catalysts can be easily achieved by seemingly small changes in their primary and thereby secondary structure.

Since the tetrapeptide TFA•H-Pro-Pro-Asp-Pro-NH_2 **6** showed an enantiomeric excess of 90 % in the initial catalyst screening, we also synthesised and tested its eight diastereoisomers for the standard reaction of *n*-butanal and nitrostyrene (Table 4.7). Very similar results were obtained for all catalysts. The peptides were able to catalyse the reactions with a catalyst loading of 1 mol%, providing the product **3** in very high conversions within 10 h. The *syn:anti* ratios were determined within a range of 22:1 to 58:1, and enantiomeric excesses between 86 % and 91 % (TFA•H-Pro-D-Pro-Asp-Pro-NH_2 **25**, Table 4.7, Entry 3). However, the excellent enantioselectivity of 95 % *ee,* achieved with tripeptide TFA•H-D-Pro-Pro-Asp-NH_2 **21**, was not improved upon.

Table 4.7. *Asymmetric 1,4-addition reaction between n-butanal and nitrostyrene: Screening of diasteroisomeric peptides of the Pro-Pro-Asp-Pro-NH_2 motif.*[a]

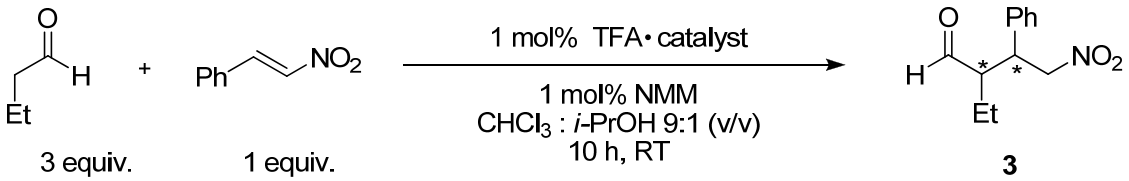

Entry	Catalyst	Conv. [%][b]	*syn : anti*[b]	*ee* [%][c]	Abs. Conf.
1	TFA•H-Pro-Pro-Asp-Pro-NH_2 **6**	89	32 : 1	90	*(R,S)*
2	TFA•H-**D**-Pro-Pro-Asp-Pro-NH_2 **24**	90	56 : 1	90	***(S,R)***
3	TFA•H-Pro-**D**-Pro-Asp-Pro-NH_2 **25**	quant.	43 : 1	91	*(R,S)*
4	TFA•H-Pro-Pro-**D**-Asp-Pro-NH_2 **22**	82	41 : 1	86	*(R,S)*
5	TFA•H-Pro-Pro-Asp-**D**-Pro-NH_2 **26**	quant.	22 : 1	86	*(R,S)*
6	TFA•H-Pro-Pro-**D**-Asp-**D**-Pro-NH_2 **27**	92	41 : 1	86	*(R,S)*
7	TFA•H-Pro-**D**-Pro-Asp-**D**-Pro-NH_2 **23**	93	58 : 1	90	*(R,S)*
8	TFA•H-Pro-**D**-Pro-**D**-Asp-Pro-NH_2 **28**	90	40 : 1	90	*(R,S)*

[a] Reactions were performed at a 1.1 mmol scale (0.40 M with respect to nitrostyrene). [b] Determined by ^{1}H NMR analysis. [c] Determined by chiral phase HPLC analysis.

The previous finding that an exchange of L-proline with D-proline in the first position of the primary catalyst structure also changes the enantioselectivity of the corresponding addition product was underlined: TFA•H-D-Pro-Pro-Asp-Pro-NH_2 **24** provided the (*S,R*)-enantiomer as the only diastereoisomeric catalyst. Finally, the peptides of the type H-Pro-Pro-Xaa-OH, which proved to be good catalysts in the initial peptide screening, were modified by exchanging the L-proline with the D-proline residue in the first positions. These peptides were then tested as catalysts for the standard reaction. Activities and diastereoselectivities of peptides **29**, **30** and **31** (Table 4.8, Entries 1-3) were comparable with the results obtained by TFA•H-D-Pro-Pro-Asp-NH_2 **21** but enantioselectivities were significantly lower in all cases (81-84 % *ee*). TFA•H-D-Pro-Pro-His-OH **32** was not only less selective, but also less active (Table 4.8, Entry 4). Again, in all cases the formation of the (*S,R*)-enantiomer was favoured.

Table 4.8. *Asymmetric 1,4-addition reaction between n-butanal and nitrostyrene: Screening of peptides of the type H-D-Pro-Pro-Xaa-OH.*[a]

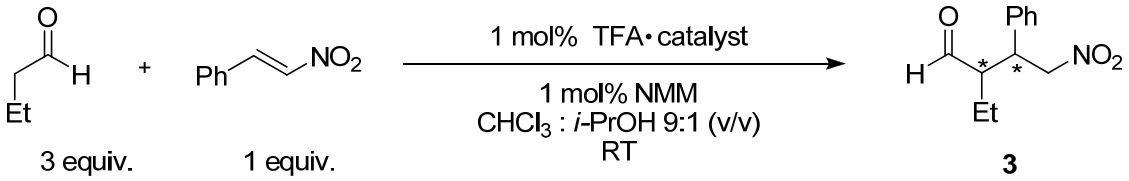

Entry	Catalyst	Time [h]	Conv. [%][b]	*syn : anti*[c]	*ee (syn)* [%][c]	Abs. Conf.
1	TFA•H-**D**-Pro-Pro-Asn-OH **29**	12	>90	21 : 1	84	***(S,R)***
2	TFA•H-**D**-Pro-Pro-**D**-Asn-OH **30**	12	~80	20 : 1	81	***(S,R)***
3	TFA•H-**D**-Pro-Pro-Ser-OH **31**	12	>90	12 : 1	82	***(S,R)***
4	TFA•H-D-Pro-Pro-His-OH **32**	15	~60	10 : 1	72	***(S,R)***

[a] Reactions were performed at a 1.1 mmol scale (0.40 M with respect to nitrostyrene). [b] Estimated by TLC. [c] Determined by chiral phase HPLC analysis.

From all of the tested peptidic catalysts, TFA•H-D-Pro-Pro-Asp-NH_2 **21** clearly showed the highest enantioselectivity. The fact, that only 1 mol% of this catalyst suffices to obtain the desired product **3** after 12 h with an isolated yield of 93 %, a *syn:anti* ratio of 25:1 and an enantiomeric excess of 95 %, makes **21** a very attractive organocatalyst for the reaction of aldehydes to nitroolefins.

5. TFA•H-D-Pro-Pro-Asp-NH_2 (21) as a Catalyst for Asymmetric 1,4-Addition Reactions of Aldehydes to Nitroolefins

To evaluate the substrate scope of TFA•H-D-Pro-Pro-Asp-NH_2 **21** we allowed a range of aldehyde and nitroolefin combinations to react in the presence of 1-5 mol% of **21**. Aldehydes were used in an excess (3 equivalents) and reactions were performed in $CHCl_3$/*i*-PrOH 9:1 (v/v) as solvent with a concentration of 0.4 M with respect to the nitroolefin. To liberate the secondary amine of TFA•catalyst **21**, an equimolar quantity of NMM was added. High to excellent yields (82-99 %) and stereoselectivities (*syn:anti* = 4:1->99:1, 88-98 % *ee*) were obtained for a variety of aldehydes and nitroolefins reacting at RT within 12-24 h (Table 5.1).

Table 5.1. *Asymmetric conjugate addition of aldehydes to nitroolefins catalysed by TFA•H-D-Pro-Pro-Asp-NH_2* ***21***. [a]

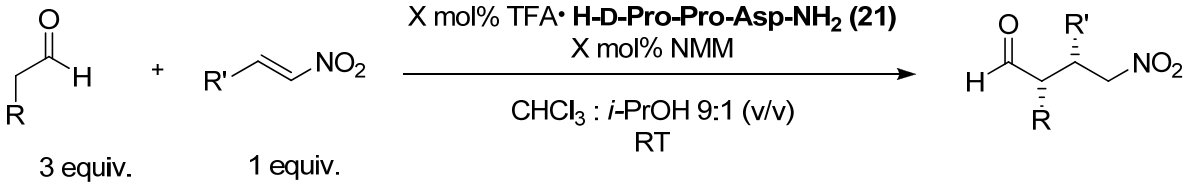

Entry	**21** [mol%]	Product		Temp. [°C]	Time [h]	Yield [%][b]	*syn:anti*[c]	*ee* [%][d]
1	1	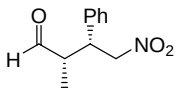	**33**	25	24	98	9:1	91
2	5			-15	48	70	>99:1	97
3	1	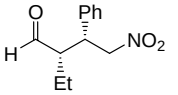	**3**	25	12	93	24:1	95
4	3			-15	48	92	>99:1	97
5	1	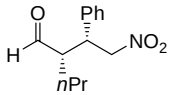	**34**	25	12	94	16:1	92
6	3			-15	48	90	>50:1	96
7	1	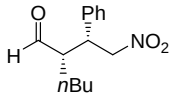	**35**	25	12	99	16:1	92
8	5			-15	48	96	>99:1	96
9	3	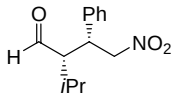	**36**	25	24	88	49:1	92
10	5			-15	48	99	>99:1	96

11	1	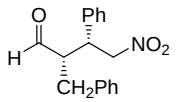		25	12	89	16:1	95
12	3		**37**	-15	48	95	>50:1	98
13	1	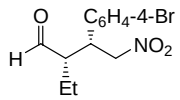		25	12	99	16:1	95
14	5		**38**	-15	48	95	>50:1	97
15	1	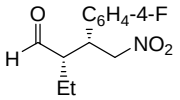		25	12	99	24:1	95
16	5		**39**	-15	48	99	>99:1	97
17	1	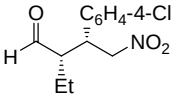		25	12	99	32:1	95
18	3		**40**	-15	48	97	>99:1	97
19	1	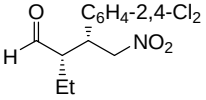		25	24	96	24:1	95
20	3		**41**	-15	48	97	>50:1	97
21	1	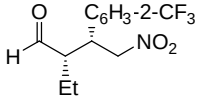		25	12	88	>99:1	98
22	3		**42**	-15	48	95	>99:1	99
23	1	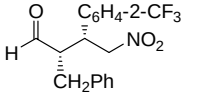		25	12	93	49:1	98
24	1		**43**	0	24	84	>99:1	>99
25	3	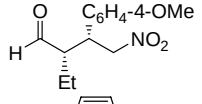		25	12	99	19:1	92
26	5		**44**	-15	48	97	>50:1	94
27	1	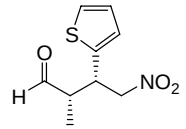		25	24	99	6:1	88
28	3		**45**	-15	48	94	32:1	95
29	3	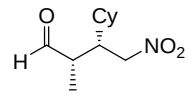		25	36	88	4:1	98
30	5		**46**	-15	48	55	4:1	98
31	3	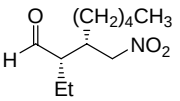		25	12	82	16:1	93
32	5		**47**	-15	48	80	24:1	94

[a] Reactions were performed with 1 eq of the β-nitroolefin and 3 eq of the aldehyde. [b] Isolated yield. [c]Determined by ^{1}H NMR on the crude material. [d] Determined by chiral phase HPLC analysis.

Yet higher stereoselectivities were achieved when reactions were performed at a lower temperature. These conditions required slightly greater amounts of catalyst (3-5 mol%) and longer reaction times, but provided diastereoselectivities of up to more than *syn:anti* = 99:1 and enantioselectivities of up to more than 99 % *ee*. Best results were obtained using a nitroolefin with an electron-poor aromatic substituent (trans-β-2-(trifluoromethyl)styrene: 84-95 % yield, *syn:anti* = 49:1->99:1, 98->99 % *ee*, Table 5.1, Entries 21-24). However, even with the poorest substrate combination (aliphatic nitroolefin and propanal, Table 5.1, Entries 29 and 30) we obtained a diastereoselectivity of *syn:anti* = 4:1 and enantioselectivity of 94 %

ee. Aldehydes bearing branched substituents in the β-position (isovaleraldehyde) were also tolerated but required 3-5 mol% of catalyst to provide the product in a yield greater than 88 % (Table 5.1, Entry 9 and 10). These results demonstrate that peptide **21** is an excellent catalyst for conjugate addition reactions between a broad range of different aldehydes and aromatic as well as aliphatic nitroolefins. 1 mol% of catalyst **21** and 3 equivalents of the aldehyde typically suffice to provide the addition products in high yields and stereoselectivities.

6. Conformational Studies I

6.1 *Lowest Energy Structures of Diastereoisomeric Catalysts and Transition State Model*

To gain insight into a possible mechanism of action of the peptide catalysed 1,4-addition reactions, and in particular to understand the opposite enantioselectivity of the diastereomeric peptides H-Pro-Pro-Asp-NH_2 **1** and H-D-Pro-Pro-Asp-NH_2 **21**, we analysed the conformations of the peptides using molecular modelling. Calculations were performed with MacroModel 8.0[120] using the OPLS-AA force field[121] and the GB/SA model for chloroform.[122] The obtained lowest energy conformations of peptides **1** and **19-21** were compared with each other (Figure 6.1).

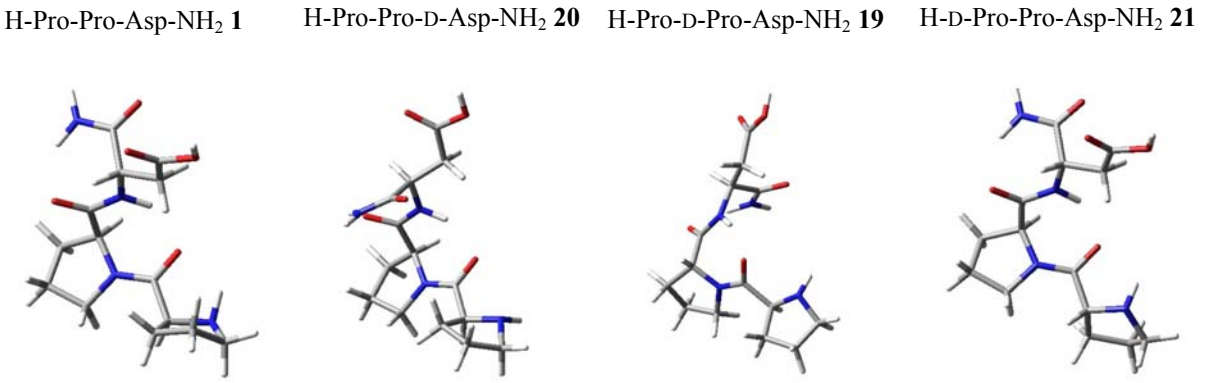

Figure 6.1. *Lowest energy structures of peptides **1** and **19-21**, calculated by MacroModel 8.0.*

In the lowest energy structures all peptides adopt γ-turn conformations. The carboxylic acid functionalities of peptides **19** and **20** are pointing away from the secondary amines of the *N*-terminal proline residues. This is in contrast to peptides **1** and **21**, where the *C*-terminal carboxamides point away from the *N*-termini whereas the carboxylic acids are in close vicinity to the secondary amines. An overlay of the lowest energy structures of peptides H-

Pro-Pro-Asp-NH_2 **1** and H-D-Pro-Pro-Asp-NH_2 **21** illustrates that in the lowest energy structures both peptides adopt turn-like conformations that are identical apart from the *N*-terminal proline residues which point in opposite directions with respect to the turn (Figure 6.2).

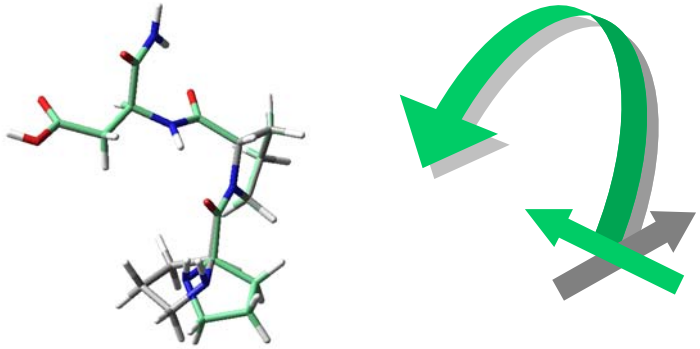

Figure 6.2. *Overlay of the lowest energy structures of H-Pro-Pro-Asp-NH_2* ***1*** *(grey) and H-D-Pro-Pro-Asp-NH_2* ***21*** *(green) and a cartoon of the two structures implicating the differently oriented N-terminal proline residues.*

Under the assumption that a *s-trans* enamine forms upon reaction of **1** and **21**, respectively with the aldehyde, the two transition states of the diastereomeric peptides will behave like pseudo enantiomers, providing *syn* products with opposite absolute configuration (Figure 6.3a). Thus, we assume that the induction of the chiral information occurs via the discrimination of the two enantiotopic faces of the enamine by the interaction between the carboxylic acid of the aspartate and the nitrogroup of the substrate. In both cases the enamine would react with the nitroolefin via a synclinal (gauche) transition state. This is consistent with a topolocical rule proposed by Seebach.[123] The nitroolefin approaches the enamine in such a way that the donor and the acceptor double bond are in a gauche relationship (Figure 6.3b). The nitroolefin is oriented in such a manner, that the sterically demanding β-substituent is *anti* to the enamine double bond and that favourable electrostatic interactions between the nitrogen of the enamine (developing positive charge) and the nitrogroup (developing negative charge) can take place.

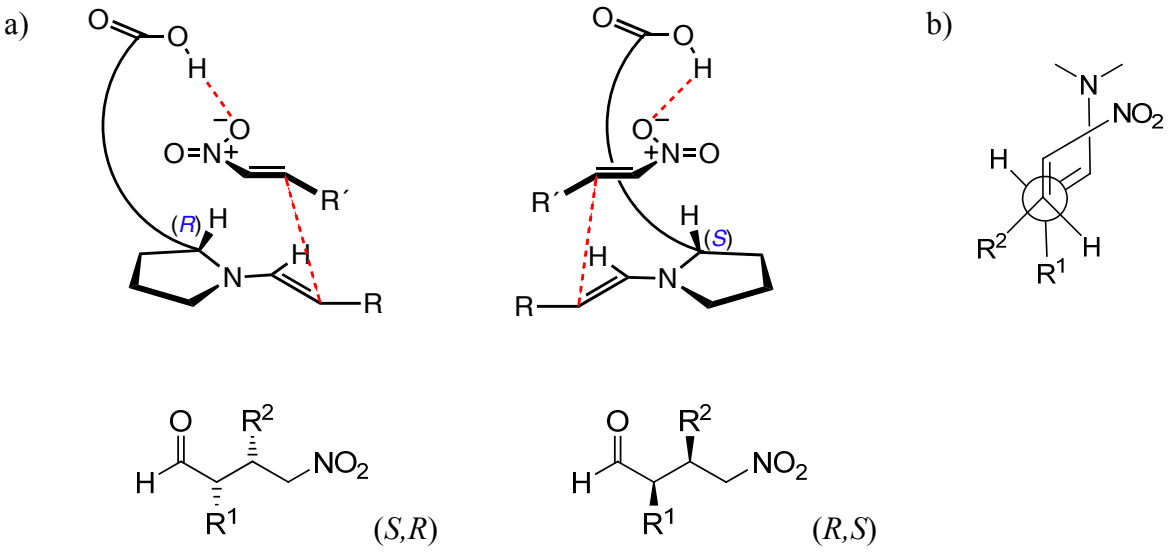

Figure 6.3. *a) Proposed transition state structures for* ***21*** *(left) and* ***1*** *(right) leading to enantiomeric syn products (bottom). b) Newman projection of synclinal transition state according to the topological rule proposed by Seebach.*[123]

6.2 X-Ray Crystal Structure Analysis of Peptidic Catalysts

Crystal structures can provide further important insight into the preferred conformation of catalysts. We were therefore pleased to obtain crystals of the peptides H-Pro-Pro-Asp-NH_2 **1** and H-D-Pro-Pro-Asp-NH_2 **21** that were suitable for x-ray single crystal structure analysis. The crystals were obtained after removal of the TFA by ion exchange chromatography and crystallisation of the "desalted peptides" from a mixture of H_2O/MeOH/THF. In the solid state both peptides adopt β-turn structures as indicated by a hydrogen bond formed between the Pro-Pro/D-Pro-Pro amide bond and the *C*-terminal carboxamide (Figure 6.4).

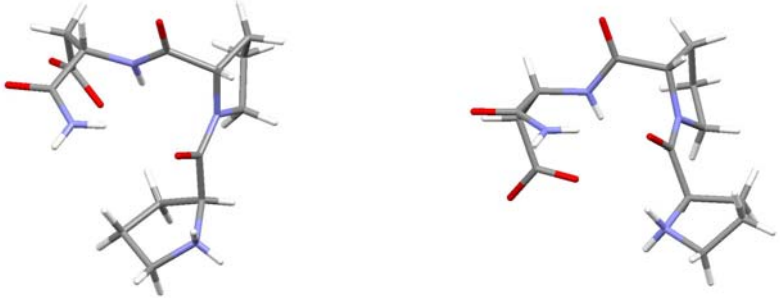

Figure 6.4. *Crystal structures of H-Pro-Pro-Asp-NH_2* ***1*** *(left) and H-D-Pro-Pro-Asp-NH_2* ***21*** *(right).*

In former studies by other groups, similar structures have been observed for internal Pro-Pro/D-Pro-Pro motives within linear and cyclic peptides.[124-127] The obtained β-turn conformations of peptides **1** and **21** in the solid state are in contrast to the γ-turn conformations of the calculated lowest energy structures discussed above (see Chapter 6.1). However, the β-turn conformations within the solid state are rather compact, suggesting that packing effects could favour these structures.

In analogy to the calculated lowest energy structures of H-Pro-Pro-Asp-NH_2 **1** and H-D-Pro-Pro-Asp-NH_2 **21**, an overlay of the two crystal structures demonstrates that the two conformations are identical apart from the *N*-terminal proline residues which point into opposite directions (Figure 6.5).

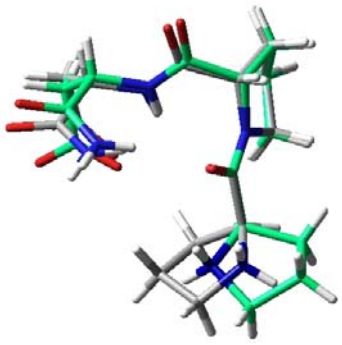

Figure 6.5. *Overlay of crystal structures of peptide* ***1*** *(grey) and peptide* ***21*** *(green).*

This is further evidence that diastereomeric peptides behave like pseudo enantiomers as discussed for the proposed transition state model (see Chapter 6.1).

6.3 Importance of the Turn-Structure and the N-terminal Proline Residue

In previous work by Krattiger et al. the tripeptides H-Pro-Pro-Asp-NH_2 **1** and H-Pro-D-Ala-D-Asp-NH_2 **2** were identified as efficient catalysts for asymmetric aldol reactions (see Chapter 2.2).[93] The use of these peptidic catalysts for aldol reactions between aldehydes and acetone afforded products with opposite absolute configurations. This opposite entantioselectivity was rationalized based on the calculated lowest energy structures of the peptides **1** and **2** using

MacroModel (Figure 6.6). The overlay of the two structures revealed that peptide **1** forms a right-handed turn and peptide **2** a left-handed turn that behave almost like mirror images. These oppositely handed turn-conformations explain the formation of enantiomeric aldol products. However, this is in contrast to the previously discussed overlay of the lowest energy conformations of **1** and **21** where both peptides show right-handed turns and oppositely directed *N*-terminal proline residues (see Chapter 6.1).

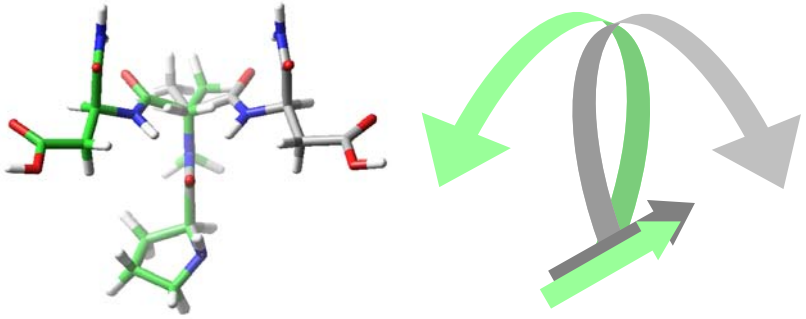

Figure 6.6. *Overlay of the lowest energy structures of H-Pro-D-Ala-D-Asp-NH_2* ***2*** *(grey) and H-Pro-Pro-Asp-NH_2* ***1*** *(green) and a cartoon of the two structures implicating the differently directed turns.*

We tested TFA•H-Pro-D-Ala-D-Asp-NH_2 **2** as catalyst for the asymmetric 1,4-addition reaction of *n*-butanal and nitrostyrene and compared the results with those obtained using TFA•H-Pro-Pro-Asp-NH_2 **1** and TFA•H-D-Pro-Pro-Asp-NH_2 **21** (Table 6.1).

Table 6.1. *Asymmetric 1,4-addition reaction between n-butanal and nitrostyrene: Comparision of peptides* ***1****,* ***2*** *and* ***21****.*[a]

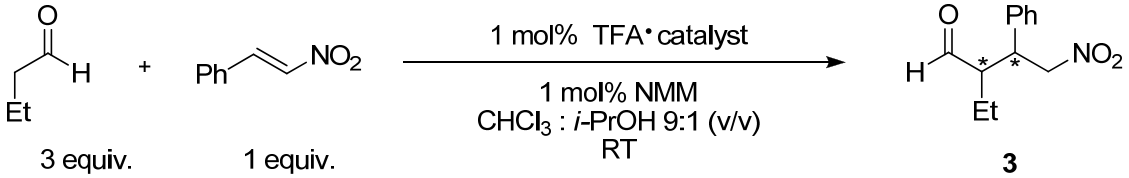

Entry	Catalyst	Time [h]	Conv. [%][b]	*syn* : *anti*[c]	*ee* [%][c]	Abs. Conf.
1	TFA•H-Pro-Pro-Asp-NH_2 **1**	6	96[d]	10 : 1	85	***(R,S)***
2	TFA•H-D-Pro-Pro-Asp-NH_2 **21**	12	93[d]	25 : 1	95	***(S,R)***
3	TFA•H-Pro-D-Ala-D-Asp-NH_2 **2**[e]	15	73	34 : 1	87	***(R,S)***

[a] Reactions were performed at a 1.1 mmol scale (0.40 M with respect to nitrostyrene). [b] Determined by ^1H NMR. [c] Determined by chiral phase HPLC analysis. [d] Isolated yield. [e] 5 mol%.

TFA•H-Pro-D-Ala-D-Asp-NH_2 **2** exhibits a higher diastereoselectivity and enantioselectivity than TFA•H-Pro-Pro-Asp-NH_2 **1** but is significantly less active (Table 6.1, Entry 3). However, in contrast to the aldol reactions, identical absolute configurations were obtained for the 1,4-addition products. CD-spectroscopy provided further evidence for the differently directed turn structures of H-Pro-Pro-Asp-NH_2 **1** and H-Pro-D-Ala-D-Asp-NH_2 **2** (Figure 6.7). Spectra of the peptides were measured in *i*-PrOH at a concentration of ~200 µM. In the range of 260 – 215 nm the peptides **1** and **2** have nearly mirror-like spectra with a maximum for H-Pro-D-Ala-D-Asp-NH_2 **2** and a minimum for H-Pro-Pro-Asp-NH_2 **1** at 223 nm. The spectum of H-D-Pro-Pro-Asp-NH_2 **21** shows a minimum as well, indicating a turn-structure more related to that of H-Pro-Pro-Asp-NH_2 **1**. However, the minimum in the spetrum of **21** is at 204 nm and significantly more intensive then in the spectrum of **1**.

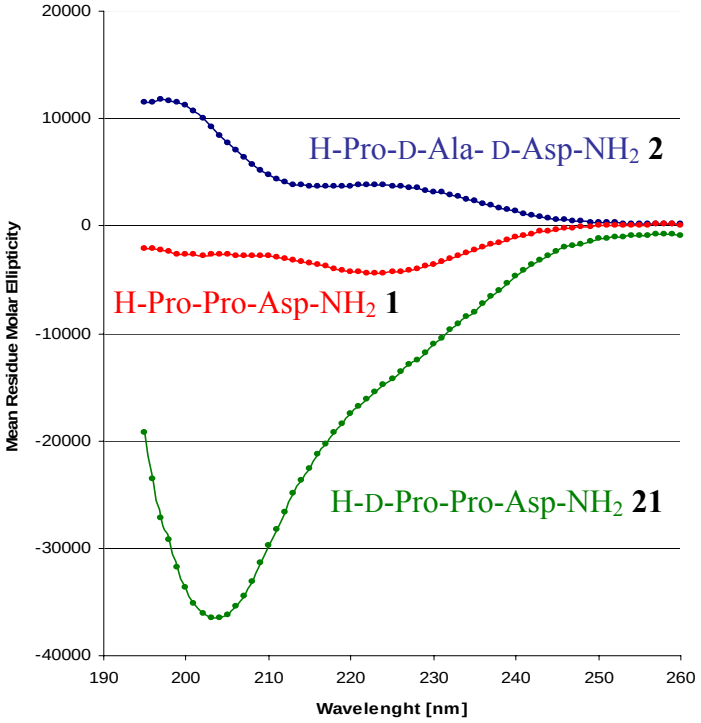

Figure 6.7. *CD-spectra of peptides **1**, **2** and **21**, ~200 µM in i-PrOH.*

The absolute configurations obtained with TFA•H-Pro-Pro-Asp-NH_2 **1** and TFA•H-Pro-D-Ala-D-Asp-NH_2 **2** are opposite for the aldol reaction products but identical for the 1,4-addition reaction products. These findings indicate that not the direction of the turn within the peptide but the configuration of the *N*-terminal proline residue is determining the absolute configuration of the 1,4-addition product.

7. Catalysts of the Type H-D-Pro-Pro-Xaa: Directed Modifications

Based on the conformational studies described in chapter 6 we synthesised a range of peptides in analogy to H-D-Pro-Pro-Asp-NH_2 **21** with the objective to find further support for the proposed transition state model and to discover improved catalytically active peptides. Towards this goal, the importance of the carboxylic acid and the role of the *C*-terminus, as well as the spacer length between the peptidic backbone and the carboxylic acid were investigated.

7.1 Importance of the Carboxylic Acid in the Side Chain

To evaluate the importance of the carboxylic acid within the structure of H-D-Pro-Pro-Asp-NH_2 **21** the analogues H-D-Pro-Pro-Asn-NH_2 **48** and H-D-Pro-Pro-Asp(O*t*Bu)-NH_2 **49** with amide and ester residues, respectively, in place of the carboxylic acid were prepared. Their catalytic properties were then evaluated in the standard reaction of *n*-butanal and nitrostyrene (Table 7.1). Both peptides proved to be significantly poorer catalysts compared to **21**, both with respect to their catalytic activities and stereoselectivies. Even with 3 to 6 times longer reactions, conversions below 44 %, *syn:anti* ratios below 8:1 and entantioselectivities below 72 % *ee* were observed (Table 7.1, Entries 2 and 3). Thus, not only the secondary amine but also the carboxylic acid is important for effective catalysis. This result suggests that the carboxylic acid plays a crucial role in coordinating and thereby orienting the nitroolefin into a position that allows for the excellent stereochemical induction observed for peptidic catalyst **21**. This is in agreement with our transition state model which involves coordination between the carboxylic acid of the peptide and the nitro group of the nitroolefin (see Chapter 6.1). However, the exact nature of their interactions (e.g. hydrogen bond formation between the nitronate and the carboxylic acid in the transition state) is not clear.[128]

Table 7.1. *Asymmetric 1,4-addition reaction between n-butanal and nitrostyrene using catalysts with different functional groups in the side chain.*[a]

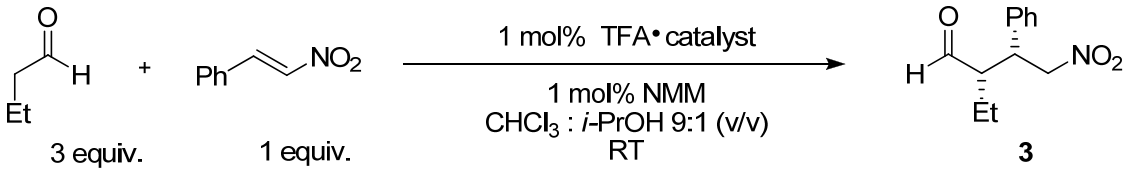

Entry	Catalyst	Time [h]	Conv. [%][b]	*syn:anti* [b]	*ee* [%][c]
1	TFA•**H-D-Pro-Pro-Asp-NH$_2$ (21)**	12	95	25 : 1	95
2	TFA•**H-D-Pro-Pro-Asn-NH$_2$ (48)**	72	44	6 : 1	72
3	TFA•**H-D-Pro-Pro-Asp(O*t*Bu)-NH$_2$ (49)**	36	30	8 : 1	64

[a] Reactions were performed at a 1.1 mmol scale (0.40 M with respect to nitrostyrene). [b] Determined by ^{1}H NMR spectroscopy of the reaction mixture. [c] Determined by chiral-phase HPLC analysis.

7.2 Modifications at the C-Terminus

As discussed above in chapter 6.2, the peptide H-D-Pro-Pro-Asp-NH$_2$ **21** adopts a β-turn conformation in the solid state, where the *C*-terminal carboxamide forms an H-bond with the oxygen of the D-Pro-Pro amide bond (Figure 7.1). Such an interaction might be important for stabilising the peptide in the transition state of the addition reaction and thus, for the observed high activity and selectivity.

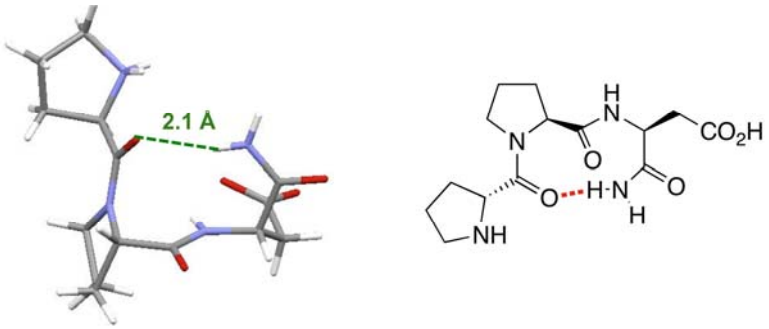

Figure 7.1. *Crystal structure and schematic of H-D-Pro-Pro-Asp-NH$_2$ **21**.*

To evaluate the importance of the *C*-terminal amide for the catalytic efficiency of peptide **21**, we prepared closely related peptides that differ in the *C*-terminal functional groups, and tested them as catalysts for the standard reaction (Figure 7.2).

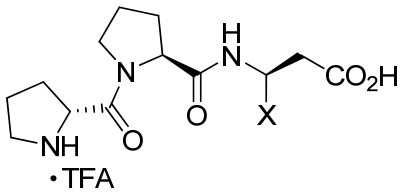

X = $CONH_2$	TFA•H-D-Pro-Pro-**Asp-NH_2 (21)**
X = H	TFA•H-D-Pro-Pro-**β-Ala-OH (50)**
X = CO_2CH_3	TFA•H-D-Pro-Pro-**Asp-OMe (51)**
X = CH_2CONH_2	TFA•H-D-Pro-Pro-**β-homo-Asp-NH_2 (52)**
X = CO_2H	TFA•H-D-Pro-Pro-**Asp-OH (53)**
X = CONHPr	TFA•H-D-Pro-Pro-**Asp-NHPr (54)**
X = CONH-●	TFA•H-D-Pro-Pro-**Asp-NH-TentaGel (55)**

Figure 7.2. *Peptides bearing different C-terminal functional groups.*

Within the structures of peptides TFA•H-D-Pro-Pro-β-Ala-OH **50** and TFA•H-D-Pro-Pro-Asp-OMe **51** the *C*-terminal carboxamide is replaced by functional groups (hydrogen and methyl ester, respectively) that are not able to function as H-bond donors. Within peptide TFA•H-D-Pro-Pro-β-homo-Asp-NH_2 **52** an additional methylene group is introduced as a spacer to the carboxamide. Peptides TFA•H-D-Pro-Pro-Asp-OH **53** and TFA•H-D-Pro-Pro-Asp-NHPr **54** bear carboxylic acid and secondary amide moieties, respectively, in place of the primary carboxamide. Finally, in analogy to peptide **54**, the solid supported TFA•H-D-Pro-Pro-Asp-NH-TentaGel **55**, which also bears a secondary amide on the *C*-terminus, was synthesised. To analyse the catalytic properties of peptides **50-55** the conjugate addition reaction between *n*-butanal and nitrostyrene served again as a test reaction using the previously established standard conditions (Table 7.2).

With all of the peptidic catalysts **50-55**, good to very good stereoselectivities and conversions after 12 h were observed (*syn:anti* ≥15:1, ≥85 % *ee*, Table 7.2, Entries 2-7). However, none of the peptides performed equally as well as the parent catalyst TFA•H-D-Pro-Pro-Asp-NH_2

21 (Table 7.2, Entry 1). This demonstrates that also peptides that cannot be stabilised by an intramolecular H-bond to form a β-turn (or another conformation which is stabilised by an interaction of the *C*-terminal carboxamide), are reasonable asymmetric catalysts, even if the peptide lacks the stereogenic center of the *C*-terminal amino acid (catalyst **50,** Table 7.2, Entry 2). At the same time, the results revealed that both the presence and the position of the *C*-terminal primary carboxamide are crucial for highly efficient asymmetric catalysis. Thus, the main contribution for the excellent asymmetric induction and catalytic activity of peptide **21** stems from the D-Pro-Pro portion whereas the *C*-terminal amide is important for the fine tuning of the stereoselectivity.

Table 7.2. *Asymmetric 1,4-addition reaction between n-butanal and nitrostyrene using catalysts with different C-terminal functionalities.* [a]

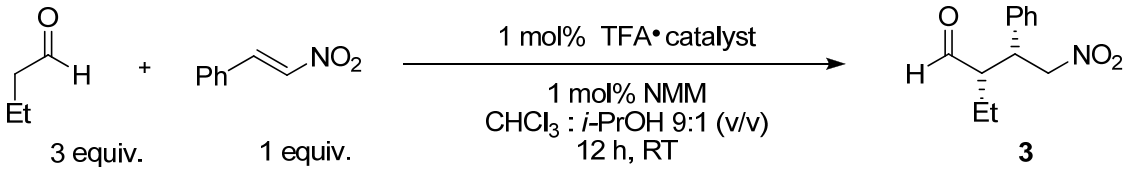

Entry	Catalyst	Conv. [%][b]	*syn:anti* [b]	*ee* [%][c]
1	TFA•**H-D-Pro-Pro-Asp-NH$_2$ (21)**	95	25 : 1	95
2	TFA•**H-D-Pro-Pro-β-Ala-OH (50)**	80	26 : 1	88
3	TFA•**H-D-Pro-Pro-Asp-OMe (51)**	96	30 : 1	89
4	TFA•**H-D-Pro-Pro-β-homo-Asp-NH$_2$ (52)**	95	19 : 1	85
5	TFA•**H-D-Pro-Pro-Asp-OH (53)**	82	21 : 1	85
6	TFA•**H-D-Pro-Pro-Asp-NHPr (54)**	85	23 : 1	92
7	TFA•**H-D-Pro-Pro-Asp-NH-TentaGel (55)**[d]	quant. (5 h)	15 : 1	91

[a] Reactions were performed at a 1.1 mmol scale (0.40 M with respect to nitrostyrene). [b] Determined by ^{1}H NMR spectroscopy of the reaction mixture. [c] Determined by chiral-phase HPLC analysis. [d] 3 mol% of catalyst was used.

In the past few years the immobilisation of catalysts became an important research topic, since this should allow for facile catalyst recycling.[129] Peptides can be readily synthesised on a solid support and directly used as catalysts, therefore they are especially appropriate for this immobilisation strategy.[130] The TentaGel immobilised catalyst **55** showed a very high activity (quantitative conversion within 5 h using 3 mol% of the catalyst, Table 7.2, Entry 7), good diastereoselectivity (*syn:anti* = 15:1) and an enantiomeric excess of 91 %. This

enantioselectivity is comparable to the result obtained with catalyst **54** (Table 7.2, Entry 6), which also bears a secondary amide at the *C*-terminus. This finding further underlines the importance of the primary *C*-terminal carboxamide for high enantioselectivity and suggests that an alternative position (e.g. a functional group at Cγ) is more suitable for immobilisation of the peptidic catalyst on a solid support.

7.3 Importance of the Spacer Length in the Side-Chain of the C-terminal Amino Acid

Next we tested the influence of the spacer from the peptidic backbone to the carboxylic acid in the side chain of the *C*-terminal amino acid on the catalytic efficiency (Figure 7.3).

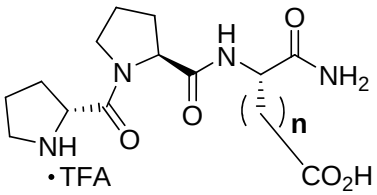

n = **1** TFA•H-D-Pro-Pro-**Asp**-NH_2 **21**

n = **2** TFA•H-D-Pro-Pro-**Glu**-NH_2 **56**

n = **3** TFA•H-D-Pro-Pro-**Aad**-NH_2 **57**

n = **4** TFA•H-D-Pro-Pro-**Api**-NH_2 **58**

n = **5** TFA•H-D-Pro-Pro-**Asu**-NH_2 **59**

Figure 7.3. *Peptides bearing different spacer length in the side-chain of the C-terminal amino acid.*

Towards this goal we compared TFA•H-D-Pro-Pro-Asp-NH_2 **21** with the peptides TFA•H-D-Pro-Pro-Glu-NH_2 **56,** TFA•H-D-Pro-Pro-Aad-NH_2 **57**, TFA•H-D-Pro-Pro-Api-NH_2 **58** and TFA•H-D-Pro-Pro-Asu-NH_2 **59** bearing up to four additional methylene groups as spacers between the backbone and the carboxylic acid. Remarkably, the glutamic acid analogue **56**, with one additional methylene group in the side chain, proved to be an even better catalyst than **21** for the conjugate addition reaction of *n*-butanal to nitrostyrene. γ-Nitroaldehyde **3** was obtained in almost perfect diastereoselectivity (*syn:anti* = 50:1, Table 7.3, Entry 2) and an excellent enantioselectivity of 97 % *ee*. Peptide **57** with yet an additional methylene group in the spacer is still a very good catalyst with an efficiency that is comparable to that of the parent peptide **21** (Table 7.3, Entry 3). Even peptides **58** and **59** with more flexible spacers

exhibited reasonable catalytic efficiencies (Table 7.3, Entries 4 and 5). However, a clear tendency towards lower activity and selectivity with increasing spacer length was observed. If the spacer from the peptidic backbone to the carboxylic acid is shorter than in peptide **21**, both activity and selectivity are significantly lower. This was established by testing the peptides TFA•H-D-Pro-Pro-D-Asn-OH **60** and TFA•H-D-Pro-Pro-D-Gln-OH **61** as catalysts for the standard reaction (Table 7.3, Entries 7 and 8). However, a direct comparison with peptide **21** is not possible, since the carboxamide is further removed by one methylene group in peptide **60** and two methylene groups in peptide **61**, respectively.

Table 7.3. *Asymmetric 1,4-addition reaction between n-butanal and nitrostyrene using catalyst **21** analogues with different spacer length in the side chain of the C-terminal amino acid.* [a]

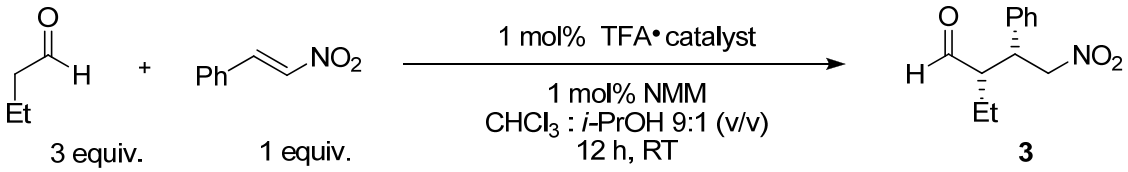

Entry	Catalyst	Conv. [%][a]	*syn:anti* [b]	*ee* [%][c]
1	TFA•**H-D-Pro-Pro-Asp-NH$_2$ (21)**	95	25 : 1	95
2	TFA•**H-D-Pro-Pro-Glu-NH$_2$ (56)**	quant.	50 : 1	97
3	TFA•**H-D-Pro-Pro-Aad-NH$_2$ (57)**	quant.	30 : 1	94
4	TFA•**H-D-Pro-Pro-Api-NH$_2$ (58)**	90	27 : 1	92
5	TFA•**H-D-Pro-Pro-Asu-NH$_2$ (59)**	80	24 : 1	86
7	TFA•**H-D-Pro-Pro-D-Asn-OH (60)**	76	20 : 1	81
8	TFA•**H-D-Pro-Pro-D-Gln-OH (61)**	45	20 : 1	87

[a] Reactions were performed at a 1.1 mmol scale (0.40 M with respect to nitrostyrene). [b] Determined by ^{1}H NMR spectroscopy of the reaction mixture. [c] Determined by chiral-phase HPLC analysis.

In summary, these findings demonstrated that a considerable degree of conformational flexibility is tolerated in the side chain of the *C*-terminal amino acid. In addition they further underline that the D-Pro-Pro motif is the major contributor to the high asymmetric induction of peptidic catalysts of the type H-D-Pro-Pro-Xaa-NH_2 where Xaa is an amino acid with a carboxylic acid in the side chain.

These results, combined with the observation that TFA•H-D-Pro-Pro-β-Ala-OH **50** is a reasonably good catalyst for the 1,4-addtion reaction of *n*-butanal and nitrostyrene (see Table 7.2) led us to investigate peptide analogues with variable distances of the *C*-terminal carboxylic acid from the D-Pro-Pro motif. Thus, catalysts of the type TFA•H-D-Pro-Pro-NH-$(CH_2)_n$-CO_2H with n = 1-4, were synthesised and tested for the standard reaction (Table 7.4).

Table 7.4. *Asymmetric 1,4-addition reaction between n-butanal and nitrostyrene using catalyst of the type TFA•H-D-Pro-Pro-NH-$(CH_2)_n$-CO_2H.* [a]

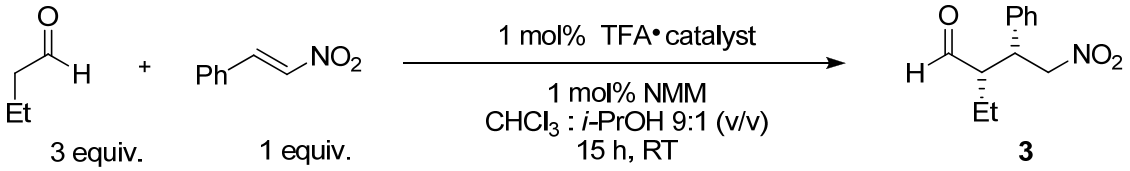

Entry	Catalyst	Conv. [%][b]	*syn:anti* [b]	*ee* [%][c]
1	TFA•**H-D-Pro-Pro-Gly-OH (62)**	86	13 : 1	77
2	TFA•**H-D-Pro-Pro-β-Ala-OH (50)**	85	26 : 1	88
3	TFA•**H-D-Pro-Pro-γ-Abu-OH (63)**	93	30 : 1	89
4	TFA•**H-D-Pro-Pro-5-Ava-OH (64)**	95	30 : 1	89

[a] Reactions were performed at a 1.1 mmol scale (0.40 M with respect to nitrostyrene). [b] Determined by ^1H NMR spectroscopy of the reaction mixture. [c] Determined by chiral-phase HPLC analysis.

Whereas TFA•H-D-Pro-Pro-Gly-OH **62** (Table 7.4, Entry 1) proved to be a much poorer catalysts in terms of selectivity for the standard reaction in comparison to peptide **50**, activity, diastereoselectivity and enantioselectivity were slightly improved using TFA•H-D-Pro-Pro-γ-Abu-OH **63** (Table 7.4, Entry 3). Similar results in comparison to peptide **50** were obtained with TFA•H-D-Pro-Pro-5-Ava-OH **64** (Table 7.4, Entry 4). These findings demonstrate that in the case of peptides of the type TFA•H-D-Pro-Pro-NH-$(CH_2)_n$-CO_2H the position of the carboxylic acid only plays a minor role in terms of activity and selectivity.

7.4 *H-D-Pro-Pro-Glu-NH$_2$ (56) and its Diastereoisomers*

Studies of catalysts of the type H-D-Pro-Pro-Xaa-OH afforded the tripeptide TFA•H-D-Pro-Pro-Glu-NH_2 **56** as improved catalyst for the addition reaction of *n*-butanal and nitrostyrene (see Chapter 7.3). Next we synthesised the diastereoisomers of this peptide and tested those for the standard reaction, to confirm that the peptide bearing the D-Pro-Pro motif is the most efficient catalyst, as found in analogous experiments with the diastereoisomers of TFA•H-Pro-Pro-Asp-NH_2 **21** (see Chapter 4.3). Interestingly, we found that both activity and diastereoselectivity for TFA•H-Pro-Pro-Glu-NH_2 **65** and TFA•H-D-Pro-Pro-Glu-NH_2 **56** are similar in this reaction. However, the enantioselctivity for peptide **65** proved to be significantly lower (87 % *ee*, Table 7.5, Entry 1).

Table 7.5. *Asymmetric 1,4-addition reaction between n-butanal and nitrostyrene. Screening of diasteroisomeric peptides of H-Pro-Pro-Glu-NH_2.*[a]

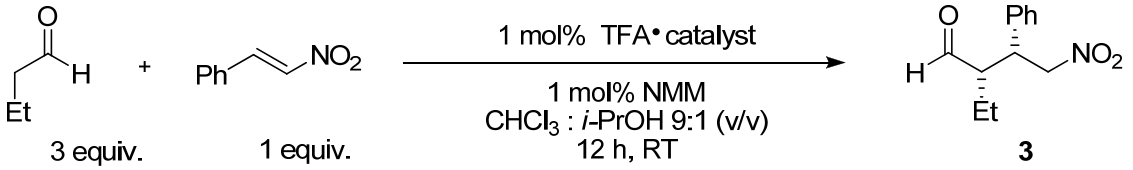

Entry	Catalyst	Conv. [%][b]	*syn : anti*[b]	*ee (syn)* [%][c]	Abs. Conf.
1	TFA•H-Pro-Pro-Glu-NH_2 **65**	quant.	50 : 1	87	*(R,S)*
2	TFA•H-**D**-Pro-Pro-Glu-NH_2 **56**	quant.	50 : 1	97	***(S,R)***
3	TFA•H-Pro-**D**-Pro-Glu-NH_2 **66**	77	38 : 1	84	*(R,S)*
4	TFA•H-Pro-Pro-**D**-Glu-NH_2 **67**	52	23 : 1	74	*(R,S)*

[a] Reactions were performed at a 1.1 mmol scale (0.40 M with respect to nitrostyrene). [b] Determined by ^{1}H NMR analysis . [c] Determined by chiral phase HPLC analysis.

On the other hand, the peptides TFA•H-Pro-D-Pro-Glu-NH_2 **66** and TFA•H-Pro-Pro-D-Glu-NH_2 **67** proved to be poorer catalysts in terms of activity and selectivity for this reaction (Table 7.5, Entries 3 and 4). These results are in good agreement with the obtained results for the diastereoisomers of H-Pro-Pro-Asp-NH_2 **1** (see Chapter 4.3).

8. TFA•H-D-Pro-Pro-Glu-NH_2 (56) as a Catalyst for Asymmetric 1,4-Addition Reactions of Aldehydes to Nitroolefins

8.1 Substrate Scope

A careful comparison of the catalytic efficiencies of TFA•H-D-Pro-Pro-Glu-NH_2 **56** and TFA•H-D-Pro-Pro-Asp-NH_2 **21** demonstrated that both the catalytic activity and stereoselectivity of peptide **56** are higher compared to those of **21** (see Chapter 7.3). Under the same conditions (3 equivalents of *n*-butanal, 1 equivalent of nitrostyrene), the conjugate addition reaction of *n*-butanal and nitrostyrene is complete within 8 h with **56** whereas 12 h are required with **21**. This higher reactivity of **56** allowed to further reduce the excess of aldehyde with respect to the nitroolefin required for good yields. Using as little as 1.5 equivalents of the aldehyde, under otherwise identical conditions, the conjugate addition product **3** was obtained within a slightly longer reaction time in the same high enantioselectivity (97% *ee*) and with slightly lower diastereoselectivity (*syn*:*anti* = 42:1) (Table 8.1, Entry 1). These improved conditions were used to evaluate the substrate scope of TFA•H-D-Pro-Pro-Glu-NH_2 **56**.

8.1.1 Addition of Aldehydes to Nitroolefins

In the presence of 1 mol% of **56** a range of aldehyde and nitroolefin combinations reacted readily with each other. The resulting γ-nitroaldehydes were obtained in excellent yields and stereoselectivities within 12-24 h at RT (Table 8.1). Aromatic nitroolefins bearing both electron-poor and electron-rich aromatic substituents (Table 8.1, Entries 6-8) as well as aliphatic nitroolefins (Table 8.1, Entries 9 and 10) reacted readily with aromatic as well as linear or β-branched aliphatic aldehydes (Table 8.1, Entries 1-10).

Table 8.1. *Asymmetric conjugate addition of aldehydes to nitroalkenes catalysed by TFA•H-D-Pro-Pro-Glu-NH$_2$* ***56***. [a]

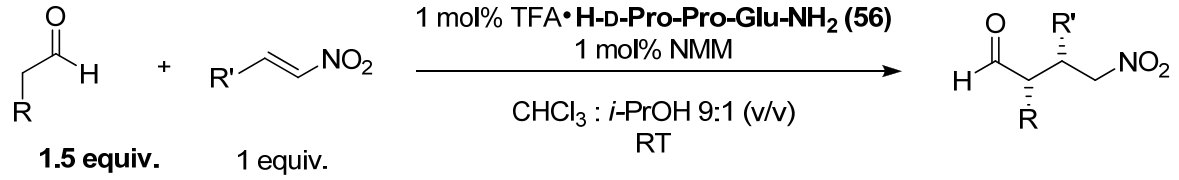

Entry	Product		Time [h]	Yield [%][b]	*syn:anti*[c]	*ee* [%][d]
1	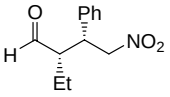	**3**	16	96	42:1	**97**
2	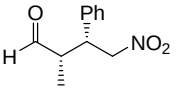	**33**	18	98	7:1	**95**
3	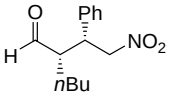	**35**	12	98	27:1	**96**
4[e]	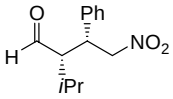	**36**	18	93	61:1	**96**
5	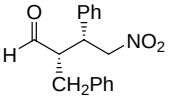	**37**	16	94	25:1	**97**
6	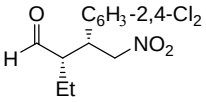	**41**	12	97	36:1	**96**
7	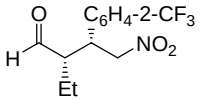	**42**	24	95	>99:1	**98**
8[e]	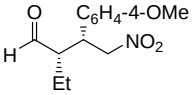	**44**	24	quant.	21:1	**95**
9[e]	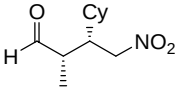	**46**	14	84	6:1	**98**
10	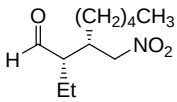	**68**	14	90	24:1 [c]	**97**

[a] Reactions were performed with 1 eq of the β-nitroolefin and 3 eq of the aldehyde with a concentration of 0.4 M with respect to the nitroolefin. [b] Isolated yield. [c] Determined by ^{1}H NMR on the crude material. [d] Determined by chiral phase HPLC analysis. [e] Use of 2 mol% of catalyst and NMM.

The best results were obtained with nitroolefins bearing electron poor aromatic substituents (e.g. Table 8.1, Entry 7), however, even with the poorest substrate combination (aliphatic nitroolefin and propanal, Table 8.1, Entry 9) a diastereoselectivity of *syn:anti* = 6:1 and an enantioselectivity of 98 % *ee* was achieved. In comparision to TFA•H-D-Pro-Pro-Asp-NH_2 **21** (see Chapter 5) the improved catalyst **56** has generally an enantioselectivity that is greater by 2-4 % *ee* at RT.

8.1.2 Addition of Aldehydes to β-Nitroacrolein Dimethylacetal (69)

β-Nitroacroleine dimethylacetal **69** is an interesting functionalised nitroolefin that has been employed in several metal- and organocatalysed conjugate addition reactions.[27,48,131-136] The addition of **69** with aldehydes leads to the corresponding γ-nitroaldehydes containing a second chemically differentiated formyl group. We tested the catalytic efficiency of TFA•H-D-Pro-Pro-Glu-NH_2 **56** in conjugate addition reactions of different aldehydes with β-nitroacroleine dimethylacetal **69**, which is easily accessible via the Henry reaction of 2,2-dimethylacetal and nitromethane, followed by the condensation with trifluoroacetic anhydride (Scheme 8.1).[135] The desired Michael acceptor **69** was obtained in an overall yield of 72 %.

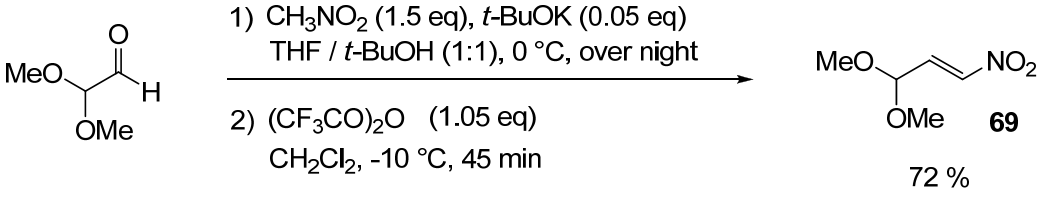

Scheme 8.1. *Synthesis of β-nitroacroleine dimethylacetal* ***69****.*

Reactions with in particular aldehydes bearing functional groups in their side chains result in highly functionalised γ-nitroaldehydes bearing four different functional groups (Table 8.2, Entry 3). Gratifyingly the highly functionalised products formed not only in yields of ≥95 % but also with high diastereoselectivities (*syn:anti* = 16:1 to >99:1) and enantioselectivities (90-95 % *ee*), using 1 mol% of catalyst **56**. These results demonstrate that TFA•H-D-Pro-Pro-Glu-NH_2 **56** is an excellent catalyst not only for aromatic and aliphatic but also functionalised aldehydes and nitroolefins.

Table 8.2. *Asymmetric conjugate addition of aldehydes to β-nitroacroleine dimethylacetal* ***69*** *catalysed by TFA•H-D-Pro-Pro-Glu-NH₂* ***56****.*[a]

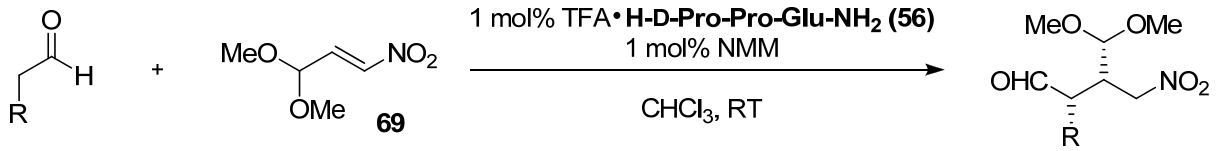

Entry	R	Product	Time [h]	yield [%][b]	*syn:anti* [c]	*ee* [%][d]
1	Et	**70**	14	quant.	68:1	**92%**
2[e]	*i*-Pr	**71**	15	95	>99:1	**95%**
3	CH_2CO_2Me	**72**	15	95	16:1	**90%**

[a] Reactions were performed at a 1.1 mmol scale (0.40 M with respect to nitrostyrene). [b] Isolated yield [c] Determined by ^1H NMR on the crude material. [d] Determined by chiral phase HPLC analysis. [e] Use of 2 mol% of catalyst and NMM.

8.2 Effect of Additives on the Catalytic Efficiency

Since the peptidic catalysts are usually prepared by solid phase peptide synthesis and removed from the acid labile resin using TFA, the corresponding TFA-salts are obtained. As a result, the addition of a base such as NMM is necessary to liberate the secondary amine and allow for catalysis (see Chapter 4.1). We were curious to test whether the presence of TFA and NMM affects the catalytic performance of the peptidic catalyst and investigated whether the high catalytic efficiency of peptide H-D-Pro-Pro-Glu-NH_2 **56** is also achieved in the absence of TFA and NMM. Thus, the TFA of the TFA•peptide **56** was removed by ion exchange chromatography and the resultig "desalted" peptide **56** tested for its catalytic efficiency in the standard reaction of *n*-butanal and nitrostyrene. In addition we tested the effect of other additives such as HCl/NMM, AcOH/NMM, NMM and TFA on the catalytic performance of the "desalted" peptidic catalyst **56** (Table 8.3). Remarkably, the "desalted" peptide **56** performed equally as well as the TFA-salt of **56** in the presence of NMM (Table 8.3, Entry 2). Furthermore, also the addition of HCl•NMM, AcOH•NMM or NMM alone did not affect the excellent catalytic efficiency of peptide **56** (Table 8.3, Entries 3-5).

Table 8.3. *H-D-Pro-Pro-Glu-NH_2* **56** *catalysed 1,4-addition reaction of n-butanal to nitrostyrene with different additives.*[a]

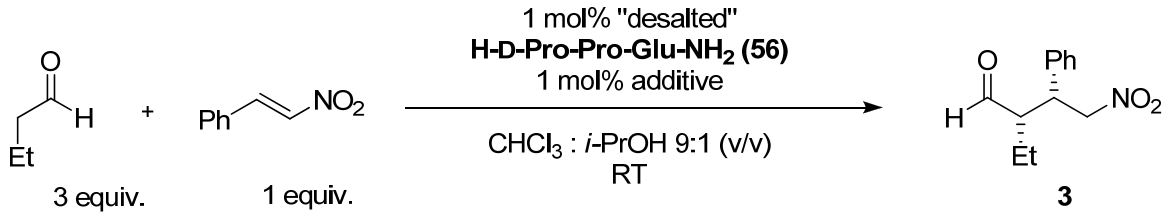

Entry	Additive	Conv. [%][b]	*syn:anti* [b]	*ee* [%][c]
1	TFA•NMM	quant.	50 : 1	97
2	none	quant.	50 : 1	97
3	AcOH•NMM	quant.	50 : 1	96
4	HCl•NMM	quant.	52 : 1	96
5	NMM	98	50 : 1	97
6[d]	TFA	16	n.d. [e]	n.d. [e]

[a] Reactions were performed at a 1.1 mmol scale (0.40 M with respect to nitrostyrene). [b] Determined by ^{1}H NMR spectroscopy of the reaction mixture. [c] Determined by chiral-phase HPLC analysis. [d] Reaction time of 72 h. [e] Not determined.

Only the addition of TFA to the "desalted" peptide **56** reduced the catalytic activity dramatically, further underlining that the secondary amine is crucial for catalysis. These results demonstrate that no additives are necessary for high catalytic efficiency of peptide **56**.

8.3 Gram Scale Synthesis of γ-Nitroalcohol (73)

To demonstrate that a scale up of the peptide **56** catalysed conjugate addition reaction of aldehydes to nitroolefins is straightforward, we performed the reaction of *n*-butanal and nitrostyrene in a quantity greater than 5 mmol. Since the corresponding γ-nitroaldehyde **3** showed a tendency to epimerise during chromatographic purification, we reduced the aldehyde *in situ* to obtain the configurationally stable γ-nitroalcohol **73**. The reaction was performed with only 1.1 equivalents of *n*-butanal, using 2 mol% of the peptidic catalyst **56** and 2 mol% NMM at 0°C. The reduction was carried out after a reaction time of 48 h using

borane•THF (Scheme 8.2). The desired product **73** was obtained after column chromatography in 95 % yield (1.2 g) and with a nearly perfect stereoselectivity (*syn:anti* >99:1, 99 % *ee*, Figure 8.1).

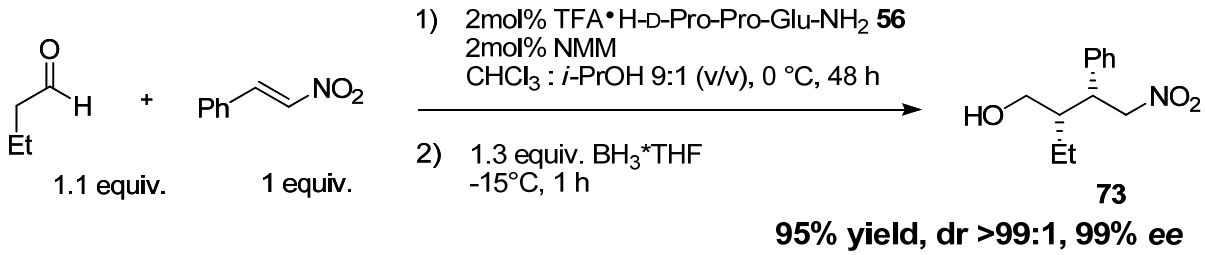

Scheme 8.2. *Gram scale synthesis of γ-nitroalcohol **73**.*

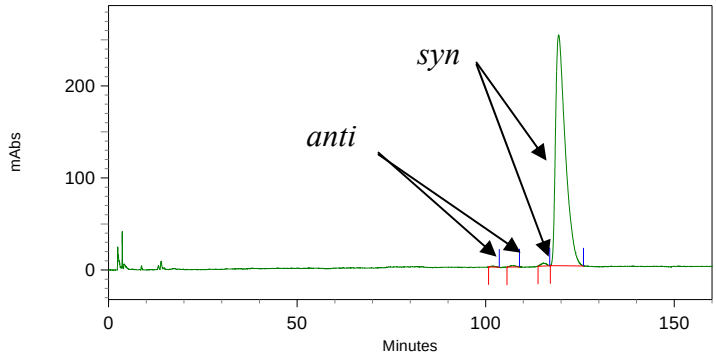

Figure 8.1. *Chiral HPLC of γ-nitroalcohol **73** (Chriacel AD-H, 210 nm).*

This experiment further underlines the efficiency of catalyst **56** for the conjugate addition reactions of aldehydes to nitroolefins. In particular the fact that the reaction between *n*-butanal and nitrostyrene occurs in a nearly atom economical manner renders this system even more attractive.

9. Conformational Studies II

9.1 X-Ray Crystal Structure Analysis of H-D-Pro-Pro-Glu-NH_2 (56)

Crystals of the catalyst H-D-Pro-Pro-Glu-NH_2 **56** which were suitable for x-ray single crystal structure analysis were obtained in an analogous manner to those of peptides **1** and **21**. Thus, crystallisation occurred with the "desalted" peptide **56** from a mixture of H_2O/MeOH/THF (see Chapter 6.2 and Experimental Section). Again, in the solid state this peptide **56** adopts a β-turn conformation with an H-bond between the *C*-terminal carboxamide and the carbonyl-oxygen of the D-Pro-Pro peptide bond as observed with **1** and **21** (Figure 9.1).

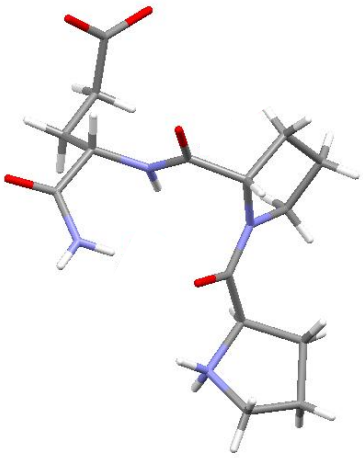

Figure 9.1. *Crystal structure of peptide* ***56***

The carboxylic acid function of the flexible glutamate side chain points away from the secondary amine of the *N*-terminal proline residue, which could be due to packing effects. However, a single rotation around the Cα-Cβ bond of the glutamate residue would bring the carboxylic acid in close proximity to the secondary amine. Thus, the obtained structure would be consistent with the conformational requirements of the previously discussed transition state model (see Chapter 6.1).

9.2 NMR Studies

9.2.1 H-D-Pro-Pro-Glu-NH_2 (56)

NMR studies of the "desalted" peptide H-D-Pro-Pro-Glu-NH_2 **56** were performed in a mixture of $CDCl_3/CD_3OD/CD_3OH$ 23:1:1 (v/v/v) in a concentration of approximately 50 mM. This solvent mixture provided for solubility of **56** and is closely related to the solvent mixture previously used for the 1,4-addition reactions ($CHCl_3$/*i*-PrOH 9:1 v/v). Under these conditions only one conformer was detected by NMR. Furthermore, strong NOEs were observed between both Hδ' of the L-proline residue and Hα of the D-proline residue with H^N of the glutamate residue (Figure 9.2). In particular the latter long range NOE is indicative for a relatively well defined turn-conformation of peptide **56** in solution, which is remarkable for a tripeptide. In contrast, two different conformers in a ratio of 78:22 and a lack of the mentioned NOEs were observed in d6-DMSO under otherwise identical conditions. These results demonstrate that peptide **56** adopts different conformations in different solvents. This is moreover in agreement with the observation of a rather high influence of the solvent on the catalytic performance of peptides in conjugate addition reactions of aldehydes to nitroolefins (see Chapter 4.1.3).

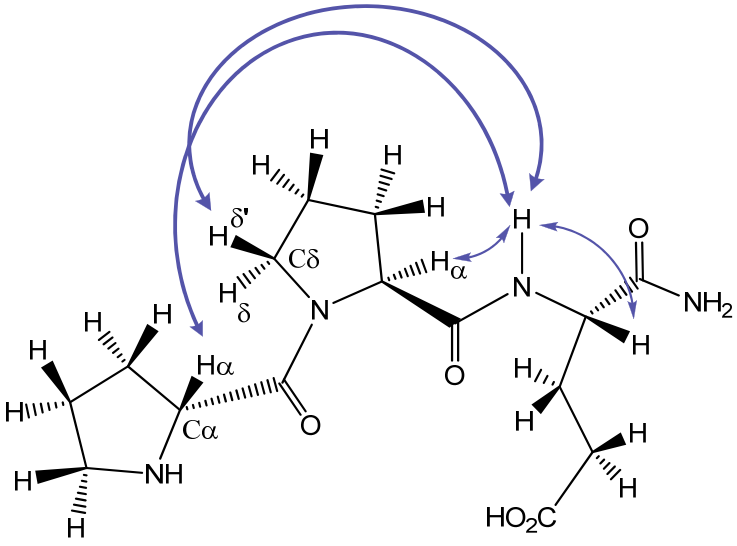

Figure 9.2. *Selected NOEs of* **56** *in* $CDCl_3/CD_3OD/CD_3OH$ *23:1:1 (v/v/v).*

9.2.2 Enamine Formation between H-D-Pro-Pro-Glu-NH_2 (56) and Phenylacetaldeyde

The formation of an enamine species upon reaction of the secondary amine of the peptidic catalyst and the corresponding aldehyde substrate is supposed to be the first crucial intermediate within the catalytic cycle proposed for the asymmetric conjugate addition reactions of aldehydes and nitroolefins (see below for details, Chapter 10). To detect such an intermediate by NMR several unsuccessful experiments with different reactive aldehydes (*n*-butanal, 3-phenylpropionaldehyde) and peptide **56** in different ratios (excess aldehyde, excess peptide, stochiometric ratio) and in different solvents ($CDCl_3$, d6-DMSO, d8-*i*-PrOH) were carried out. However, mixing phenylacetaldehyde, which is an aldehyde that reacts only slowly with nitrostyrene in the presence of peptide **56**, with an excess of the "desalted" H-D-Pro-Pro-Glu-NH_2 **56** in a mixture of $CDCl_3/CD_3OH$ 9:1 (v/v) under dry conditions led to the formation of the desired resonance stabilised enamine as well as to a second minor species which could not be assigned (Scheme 9.1, see Experimental Section).

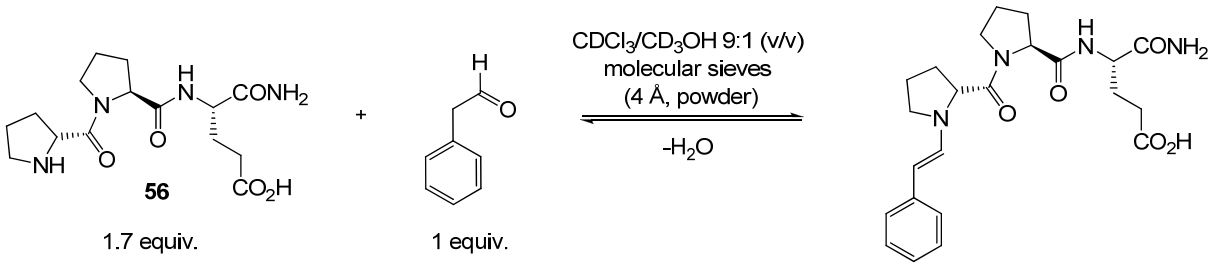

Scheme 9.1. *Formation of the enamine between peptide* ***56*** *and phenylacetaldehyde.*

Within 1 h approximately 20 % of the enamine species related to **56** was formed. The intensity of this species was regressive over time and almost vanished after 3 d. Furthermore, the addition of a trace of water to an enamine containing sample caused the immediate disappearance of this species and the increase of the original aldehyde and peptide signals. The signals of enamine was partially assigned via NOESY, ROESY and TOCSY experiments (see Experimental Section). NOEs between the vinylic protons and the δ protons of the D-Pro/Pro residues allowed for the determination of the enamine conformation as *s-trans*. This is in agreement with the proposed transition state model where the formation of an *s-trans* enamine is essential in order to obtain the correct stereoselectivtiy of the product (see Chapter 6.1).

10. Kinetic Studies of H-D-Pro-Pro-Glu-NH_2 (56) Catalysed Conjugate Addition Reaction of Aldehydes to Nitroolefins using *in situ* FT-IR Spectroscopy

In order to improve the reaction conditions and to gain further insight into the reaction mechanism of the H-D-Pro-Pro-Glu-NH_2 **56** catalysed conjugate addition reactions of aldehydes to nitroolefins, kinetic studies using *in situ* FT-IR spectroscopy were carried out. *In situ* FT-IR spectroscopy is a very convenient and accurate method allowing for real time monitoring of e.g. product formation without the need for withdrawing samples during the reaction progress.[137]

The reaction between *n*-butanal and nitrostyrene, catalysed by H-D-Pro-Pro-Glu-NH_2 **56**, was used again as standard reaction (Scheme 10.1). As shown above, this reaction proved to proceed cleanly, providing the γ-nitroaldehyde **3** in very high yield and selectivity (dr = 50:1, 97% *ee*), using 1 mol% of the catalyst (see Chapter 8.1). Since catalyst **56** was typically used as its TFA-salt, an equimolar amount of NMM as a base was always added in the kinetic experiments if not otherwise mentioned.

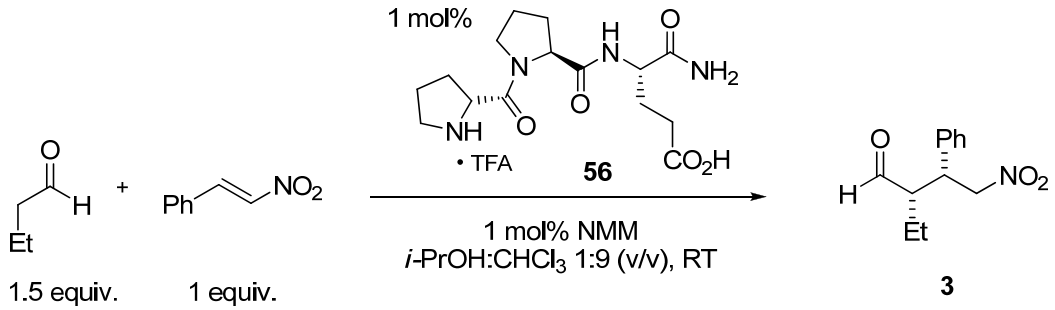

Scheme 10.1. *Asymmetric 1,4-addition reaction of butanal to nitrostyrene, catalysed by TFA• H-D-Pro-Pro-Glu-NH_2* **56**.

The proposed catalytic cycle of this reaction involves the formation of the *s-trans* enamine **I**, followed by addition to the nitrostyrene to form the intermediate iminium ion **II** that is

hydrolysed to provide the product **3** (Scheme 10.2). All measurements in this study were performed by means of *in situ* FT-IR (SiComp probe) at RT, monitoring the NO stretching absorbance of the γ-nitroaldehydes at 1554 cm^{-1} or 1555 cm^{-1}, respectively. As shown in the stack plot of the corresponding IR-spectra of the standard reaction (Figure 10.1) this absorbance is completely isolated and undisturbed by other IR-absorbances within the reaction mixture. Spectra for all following experiments were either collected every 2 min performing 256 scans or every minute with 154 scans. A typical experiment was carried out on a 2.2 mmol scale and an overall volume of 5 mL (see Experimental Section).

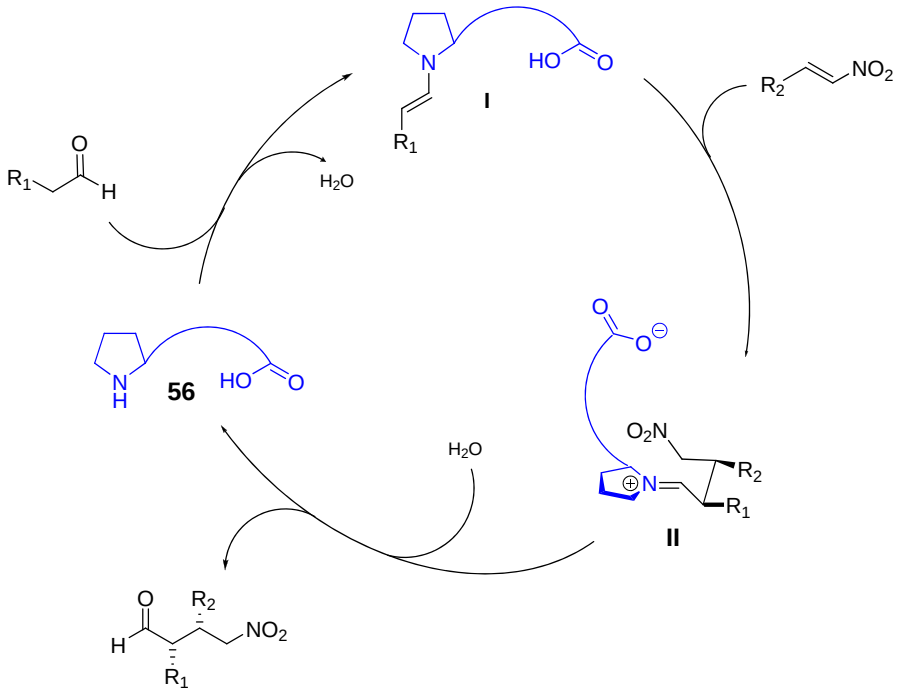

Scheme 10.2. *Proposed catalytic reaction cycle for the 1,4-addition reaction catalysed by peptide* ***56***.

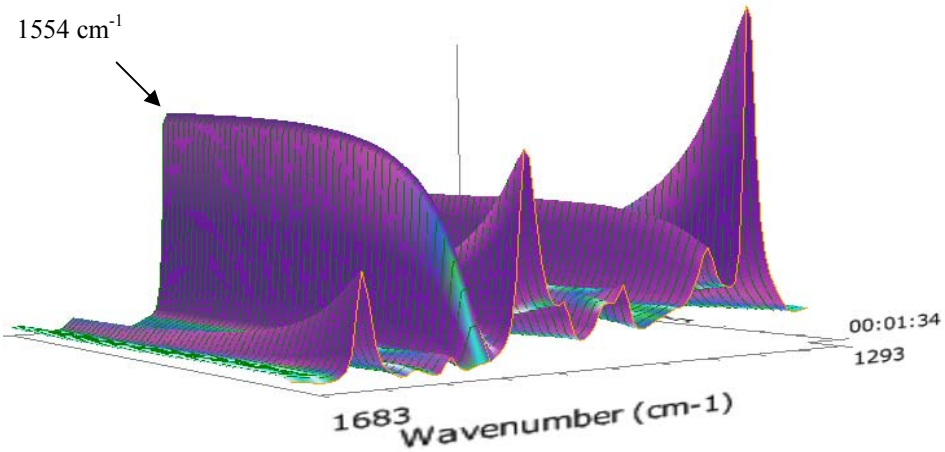

Figure 10.1. *Three-dimensional stack plot of IR spectra.*

10.1 *Initial Investigations*

In order to test whether *in situ* FT-IR spectroscpy is a suitable tool for the intended kinetic studies several initial investigations, concerning the reliability of the measurements as well as the stability of the reaction system, were carried out. Additional experiments to those described within this chapter but with minor relevance for this work are described in the appendix.

10.1.1 Fraction Conversion versus *In Situ* Measurement

To verify that the observed intensity of the absorbance corresponds to the product conversion we measured the absorbance vs. time profile for the title reaction and collected periodically samples from the reaction mixture. To determine the product conversion of the discrete samples we employed ^{1}H NMR analysis, using *i*-PrOH as an internal standard. The reaction was performed in $CHCl_3$/*i*-PrOH 9:1 (v/v) with a catalyst concentration of 4.4 mM**,** a nitrostyrene concentration of 0.44 M and an *n*-butanal concentration of 1.23 M. Figure 10.2 shows that absorbance and data points of the product conversion laid on top of each other.

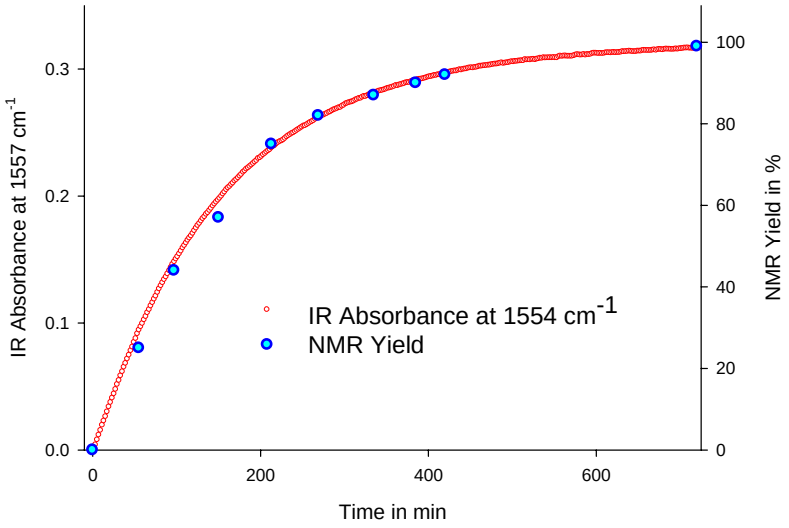

Figure 10.2. *Conversion vs. time monitored by in situ FT-IR and confirmed by ^{1}H NMR analysis.*

Under the chosen conditions the reaction was clean and went to completion within 12 h. The measured absorbance corresponded to the product conversion. Therefore no further calibration was necessary.

The addition order of *n*-butanal and nitrostyrene to the catalyst **56** does not influence the reaction progress. Figure 10.3 shows, that the conversion vs. time plots are identical when *n*-butanal was allowed to equilibrate with catalyst **56** in solution for 10 min before addition of nitrostyrene or when the addition of *n*-butanal and nitrostyrene to the catalyst **56** occured simultaneously. Furthermore, this graph demonstrates the reproducibility of the measurements.

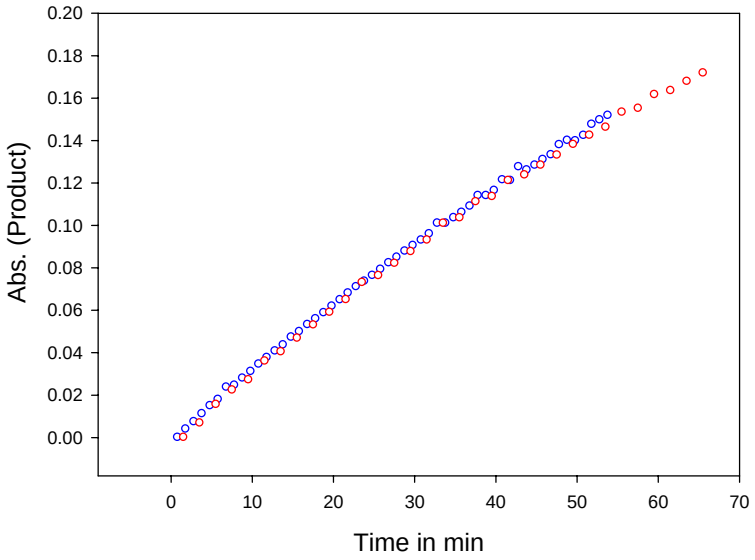

Figure 10.3. *Aldehyde – catalyst equilibration before nitrostyrene addition (blue curve) and simoultanous addition of n-butanal and nitrostyrene to the catalyst (red curve). [cat* ***56****] = 4.4 mM, [n-butanal] = 0.44 M, [nitrostyrene] = 0.44 M.*

10.1.2 Investigation of Catalyst Instabilities

To investigate whether product inhibition or catalyst deactivation is of concern, an experiment described by Blackmond[138] was carried out as follows. Two reactions with different starting concentrations of nitrostyrene but with the same excess of *n*-butanal (related to the corresponding nitrostyrene concentration of each reaction) were performed and the reaction rate vs. the concentration of nitrostyrene of both reactions was plotted. Since the

concentration of nitrostyrene was derived from the product formation, recording of the reaction progress until completion of both reactions was necessary. To reach complete conversion within less than 4 h, both reactions of this experiment were performed with the same catalyst **56** concentration of 13 mM (= 2.95 mol%). The principle of this experiment relies on the fact, that both reaction mixtures contain the same ratio between nitrostyrene and *n*-butanal at each time. However, in the reaction mixture with higher starting concentration of nitrostyrene the catalyst performed more turnovers at the same nitrostyrene concentration and the concentration of already formed product is higher. If neither the catalyst activity is decreasing nor the product in the mixture is disturbing the reaction, the plots of reaction rate vs. nitrostyrene concentration of both reactions overlay. The two reactions were realised with nitrostyrene concentrations of 0.4 M and 0.35 M, respectively, and with 0.5 M excess of *n*-butanal (Figure 10.4).

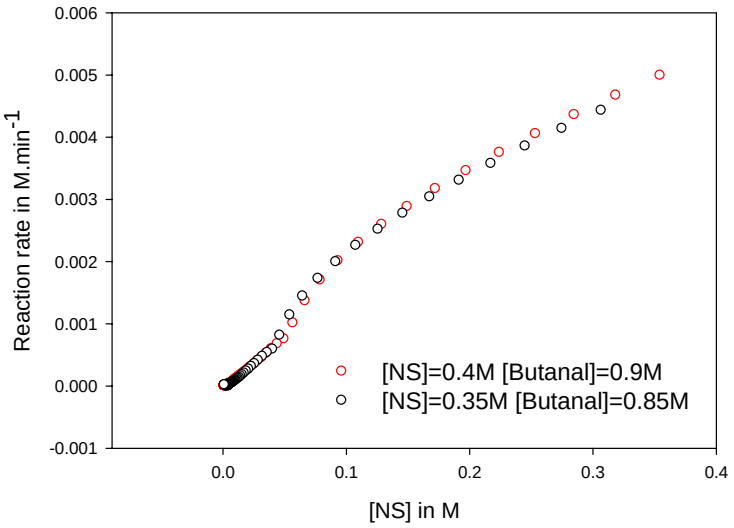

Figure 10.4. *Experiments with the same excess of 0.5M.*

Indeed, the two curves overlaped, demonstrating the absence of product inhibition and/or catalyst deactivation. To confirm this result the experiment was repeated with a different *n*-butanal excess of 0.25 M and nitrostyrene concentrations of 0.2 M and 0.17 M, respectively, under otherwise identical conditions. This also provided overlapping of both curves and underlined the absence of catalyst instabilities in this addition reaction (see Appendix for detailed information).

10.1.3 TFA•Catalyst / NMM vs. Desalted Catalyst

Next we desalted peptide **56** and performed the addition reaction with a catalyst concentration of 4.4 mM, a *n*-butanal concentration of 0.44 M and a nitrostyrene concentration of 0.44 M. In comparison to the analogous reaction with the TFA•peptide **56** and NMM, no difference in terms of product formation vs. time was observed (Figure 10.5). For both reactions >90 % conversion and identical stereoselectivities (*syn:anti* ≈ 25:1, 97 % *ee*) were observed after 5 h (conversions were determined by ^{1}H NMR with *i*-PrOH as an internal standard). This experiment underlined that the TFA has no influence on the catalytic properties of catalyst **56** (see Chapter 8.2).

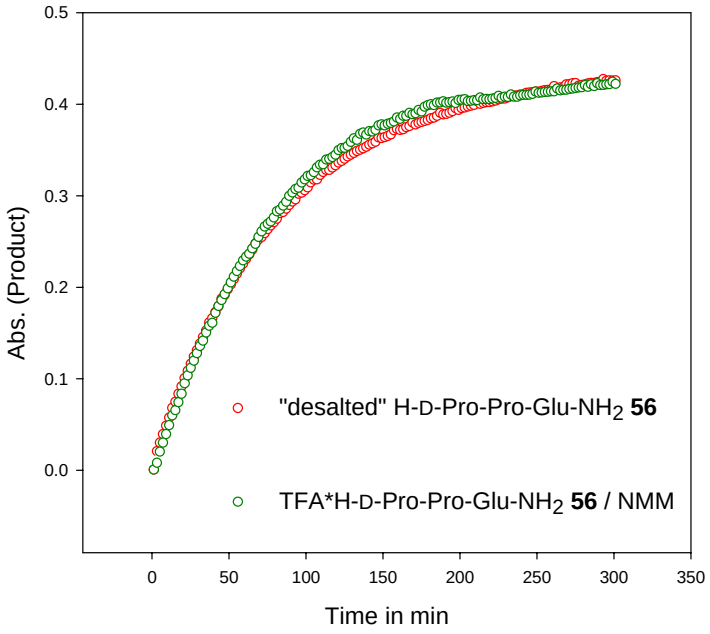

Figure 10.5. *Addition reaction of n-butanal and nitrostyrene with the desalted catalyst* ***56*** *(red curve) and the TFA•catalyst* ***56*** */ NMM.*

10.1.4 Non-linear Effects?

Before starting with the reaction progress kinetic studies of the conjugate addition of aldehydes to nitroolefins, we tested the peptide **56** catalysed reaction of *n*-butanal and nitrostyrene for non-linear effects.[139,140] The enantiomeric excess of the Michael adduct **3** was correlated with different enantiomeric excesses of catalyst **56**. Reactions were performed

with H-D-Pro-Pro-Glu-NH_2 **56** (= DLL) and its enantiomer H-Pro-D-Pro-D-Glu-NH_2 (= LDD) in various degrees of optical purities ranging from 100 % *ee* of DLL to 100 % *ee* of LDD. The plot of the determined product *ee*'s vs. the *ee* of the catalyst mixtures clearly showed a linear correlation (Figure 10.6). Thus, no non-linear effect was found which strongly indicates that only one molecule of catalyst **56** is responsible for inducing the enantioselectivity of one product molecule.

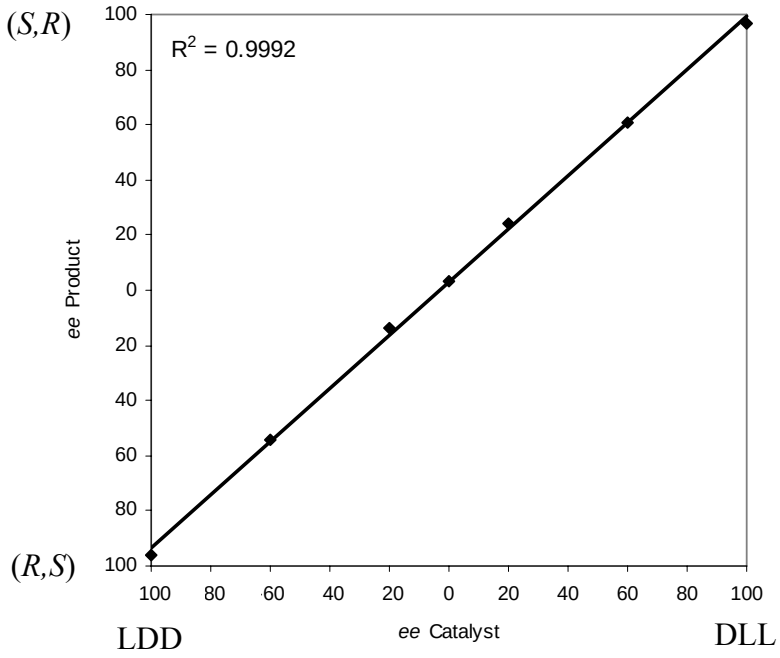

Figure 10.6. *Enantiomeric excess of product **3** vs. ee of the mixture of catalyst enantiomers. Reactions were performed using 1 mol% of catalyst mixture, 1 eq of nitrostyrene and 3 eq of n-butanal in $CHCl_3$/i-PrOH 9:1 (v/v). The ee was determined after 15 h by chiral HPLC analysis.*

10.2 Reaction Progress Kinetic Analysis

Reaction progress kinetic analysis is a tool to construct graphical rate equations with a minimal number of experiments and represents a convenient methodology to obtain a picture of complex catalytic reaction behaviour.[138] According to this we performed a number of experiments and constructed the corresponding graphical rate equations. Theroretical considerations as well as the experimental set up and the results are described in the appendix.

The experiments showed that no integer reaction orders exist in the peptide **56** catalysed conjugate addition reaction of *n*-butanal and nitrostyrene under the chosen conditions. This indicates that the reaction does not have only one rate limiting step, thus, the catalyst has no definitive "resting state".

The methodology of reaction progress kinetic analysis is only appropriate for determining integer orders within the investigated reaction. Thus, a more detailed kinetic analysis was necessary in order to identify the rate determining reaction step.

10.3 Determination of Reaction Orders: Log-Log Plots

To determine the fractional reaction orders of the peptide **56** catalysed reaction of *n*-butanal and nitrostyrene the log-log plot method was applied.[141,142] This method is based on the construction of plots of the logarithms of initial rates vs. the logarithms of the concentrations of the species being varied. Importantly, only one species is varied at the time whereas the concentrations of all other reaction participants have to remain constant. To obtain initial rates, the derivatives of [product **3**]/time was calculated at t = 15 min for all following experiments.

10.3.1 Reaction Order with Respect to the Catalyst

The reaction order with respect to catalyst **56** was studied using 6 different catalyst concentrations between 1.1 mM (0.25 mol%) and 6.6 mM (1.5 mol%) whereas concentrations of nitrostyrene and *n*-butanal were kept constant at 0.44 M (for detailed experimental set up see Appendix). The corresponding reaction profiles showed that the catalyst loading affects the reaction rate (Figure 10.7). To determine the reaction order with respect to catalyst **56** we constructed a log-log plot (Figure 10.8) of the initial reaction rates vs. the catalyst concentrations. Linear fitting of the data led to a slope of 0.98 (R^2 = 0.98). This suggests that

the reaction shows first order kinetics with respect to the catalyst **56** under the chosen conditions.

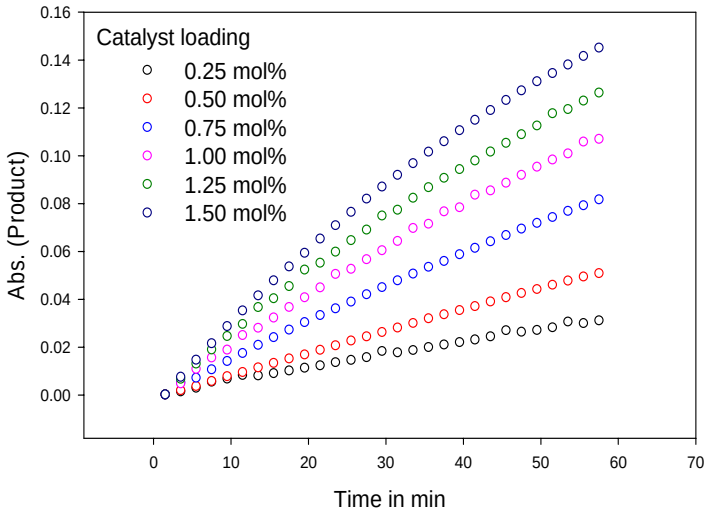

Figure 10.7. *Product formation vs. time at different catalyst loading.*

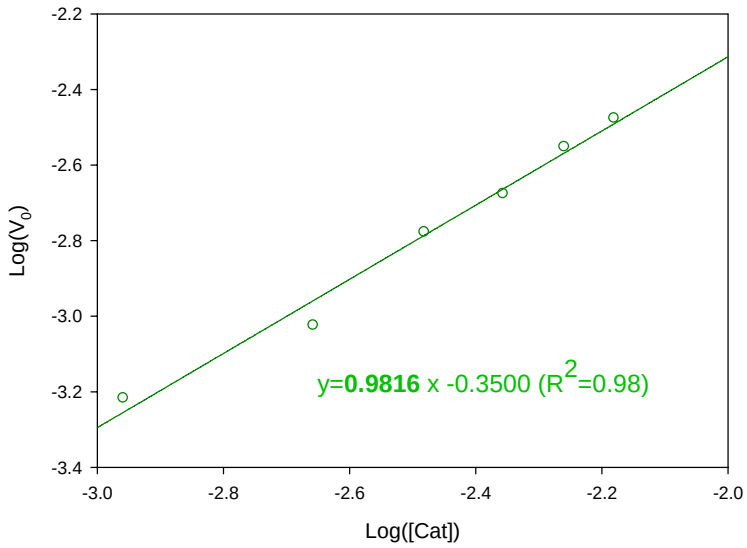

Figure 10.8. *Plot of log (initial rate) vs. log [cat **56**] providing a slope of 0.98.*

10.3.2 Reaction Order with Respect to the Aldehyde

Similar experiments were carried out to determine the reaction order with respect to *n*-butanal. For this purpose we performed 11 different reactions varying the aldehyde concentration from 0.22 M to 1.43 M at constant catalyst concentration (0.44 mM) and nitrostyrene concentration (0.44 M) (Figure 10.9, for detailed experimental set up see

Appendix). The log-log plot of the initial reaction rates versus the aldehyde concentrations showed, that the reaction is slightly influenced by the increased amount of *n*-butanal (slope of 0.35) until a certain concentration is reached ([*n*-butanal] ≈ 0.9 M). Afterwards the aldehyde concentration does not change the rate anymore and the reaction becomes zero order in aldehyde (Figure 10.10). This result suggests that at a certain concentration of *n*-butanal saturation kinetics are reached.

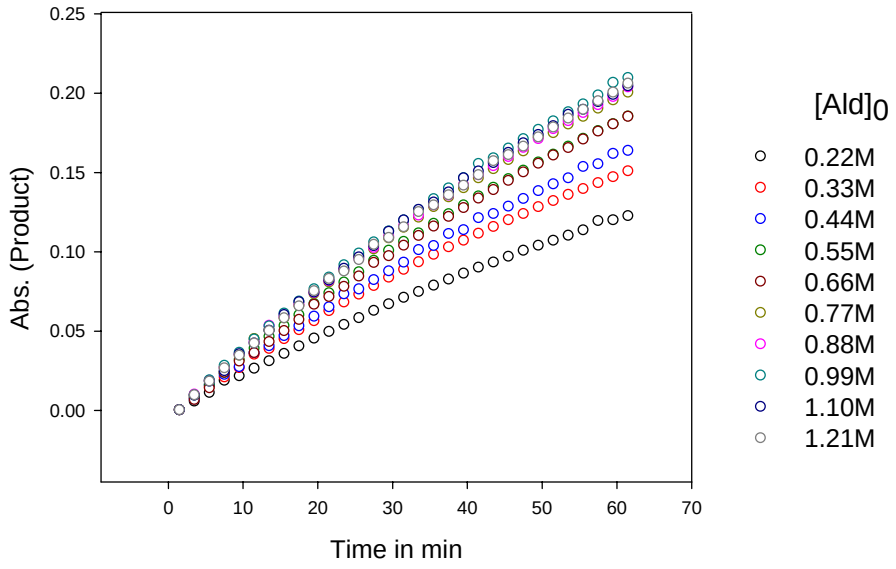

Figure 10.9. *Formation of the product* ***3*** *vs. time at different initial [n-butanal].*

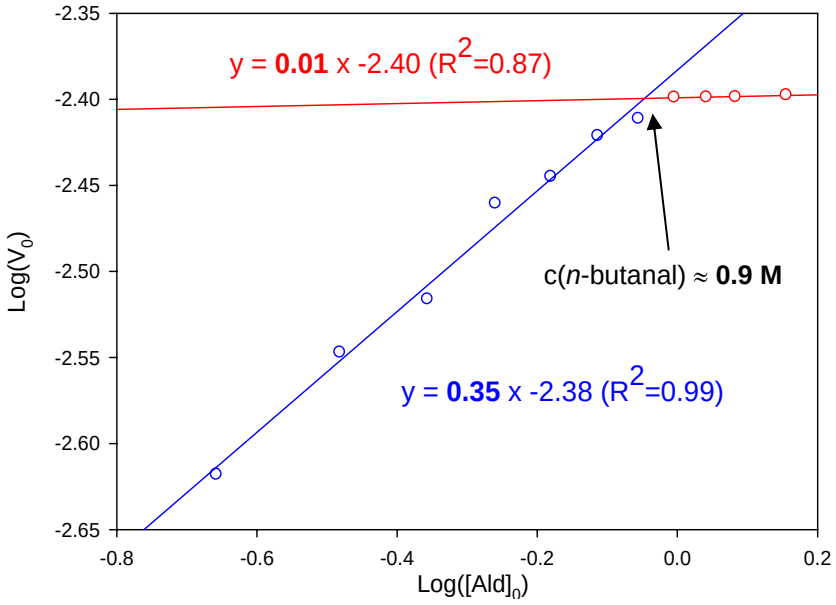

Figure 10.10. *Plot of log (initial rate) vs. log [n-butanal] providing a slope of 0.35 for [n-butanal] = 0.22 to 0.88 M and 0 for [n-butanal] = 0.99 to 1.21 M.*

To test the influence of the catalyst loading on the reaction order with respect to *n*-butanal and to confirm the observed plateau in the previous experiment, we repeated the reactions described above, using 2 mol% of the catalyst **56** instead of 1 mol% (for detailed experimental set up see Appendix). The results showed that the shape of the corresponding log-log plot (Figure 10.11) is comparable with the former plot at half catalyst concentration (1 mol%, see Figure 10.10). Up to the *n*-butanal concentration of ~0.7 M the slope is 0.32, then the plateau is reached and the slope becomes 0.

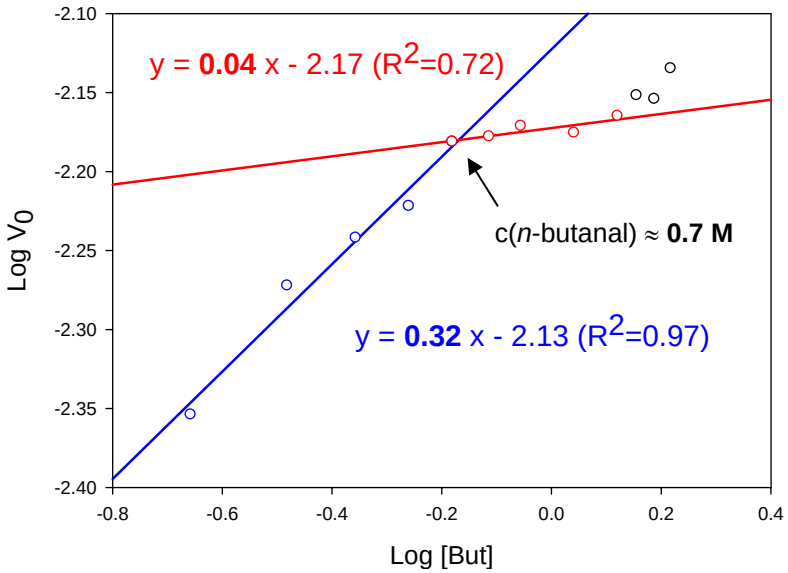

Figure 10.11. *Plot of log (initial rate) vs. log [n-butanal] shows a comparable shape to the graph in figure 10.10.*

Under these conditions the plateau is reached at a lower concentration in comparison to the experiment at lower catalyst loading (~0.9 M, see Figure 10.10). At very high *n*-butanal concentrations (1.43 M to 1.65 M) the data points do not fit with the linear regression of the plateau anymore. However these concentrations are very high compared to the concentration of *n*-butanal which is typically used in this reaction.

10.3.3 Reaction Order with Respect to the Nitrostyrene

The nitrostyrene concentration was varied in 7 different experiments from 0.22 M to 2.12 M at constant catalyst concentration (4.4 mM) and aldehyde concentration (0.44 M) (for detailed experimental set up see Appendix). The obtained reaction profiles showed that the

nitrostyrene concentration clearly affects the reaction rate, even at very high concentrations (Figure 10.12). In the log-log plot a linear correlation, providing a slope of 0.54 (R^2 = 0.98), was observed (Figure 10.13).

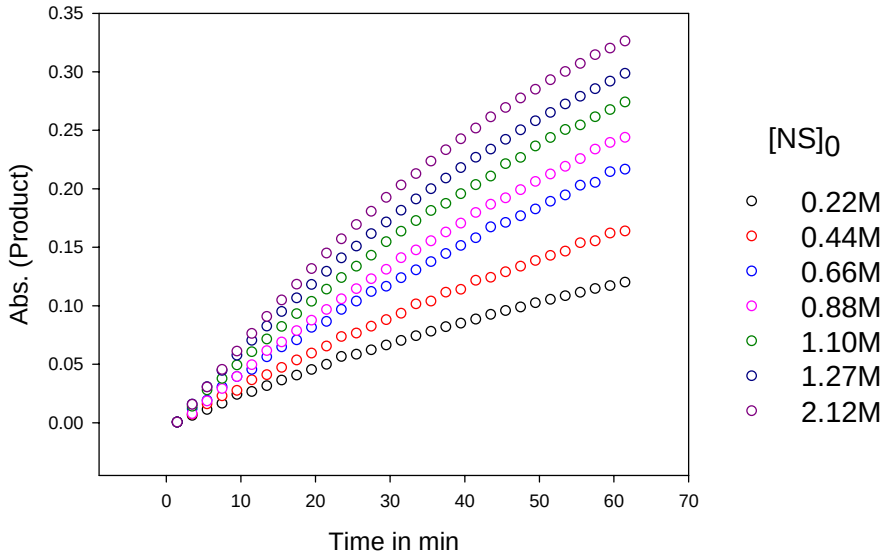

Figure 10.12. *Formation of the product* ***3*** *vs. time at different initial [nitrostyrene].*

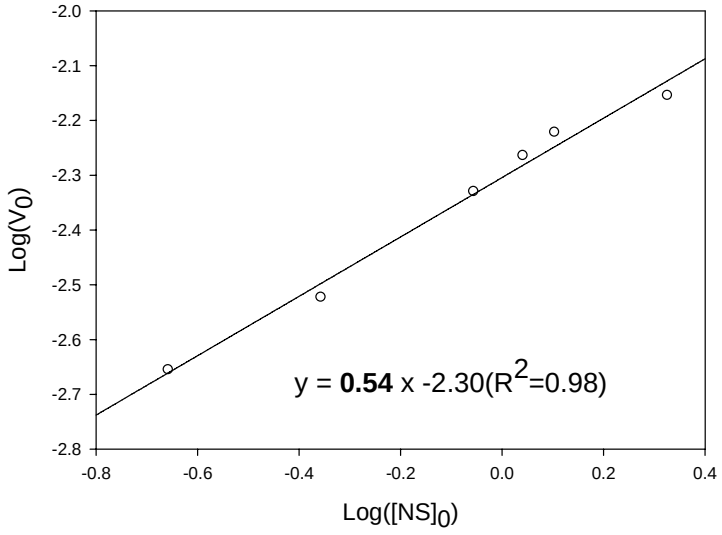

Figure 10.13. *Plot of log (initial rate) vs. log [nitrostyrene] providing a slope of 0.54. Experiments were carried out with a constant [n-butanal] of 0.44 M.*

The reaction order of ~0.5 with respect to nitrostyrene is not influenced by the aldehyde concentration as shown in a similar experiment performed at higher *n*-butanal concentration (Figure 10.14). The reactions were carried out at a constant aldehyde concentration of 0.88 M

because at this concentration the zero order plateau was observed in the experiment for aldehyde order determination described above (see Chapter 10.3.2). The obtained slope of the corresponding log-log plot was 0.53 (R^2 = 0.99) (for detailed experimental set up see Appendix).

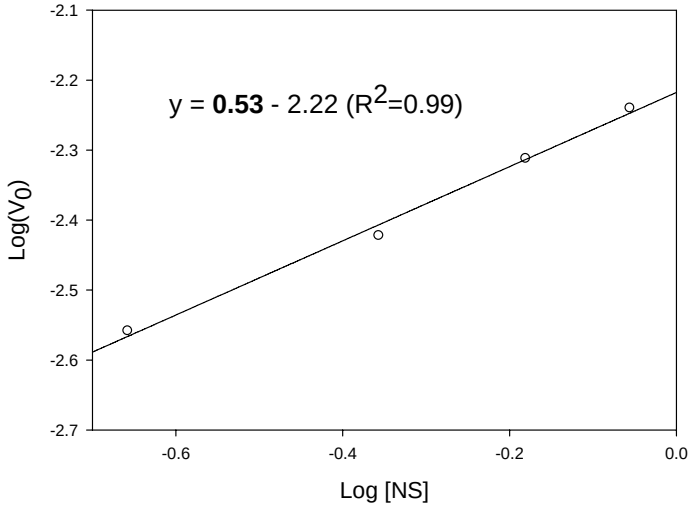

Figure 10.14. *Plot of log (initial rate) vs. log [nitrostyrene] providing a slope of 0.53. Experiments were carried out with a constant [n-butanal] of 0.88 M.*

10.3.4 Determination of Reaction Orders - Conclusions and Design of Further Experiments

The observed reaction orders with respect to the aldehyde of 0.3 to 0 at low and high aldehyde concentrations, respectively, indicate that at high aldehyde concentrations the equilibrium is shifted to the enamine **I** which becomes the resting state of the reaction.

The reaction order of ~0.5 with respect to nitrostyrene is either an indication for dimerisation of the catalyst, what can be excluded since no non-linear effects were observed (see Chapter 10.1.4), or may imply that the hydrolysis step in the reaction is closely related to the nitrostyrene addition step in terms of their reaction rates.

In order to gain further information about the kinetics of the **56** catalysed 1,4-additon reaction of aldehydes to nitroolefins and in particular to explain the obtained reaction orders with respect to *n*-butanal and nitrostyrene, additional experiments were necessary. Thus, on the one

hand, reactions with a less reactive aldehyde were performed to address the question of how the aldehyde order and the plateau of zero order, respectively, change (see Chapter 10.3.5). On the other hand, experiments with less reactive nitrostyrenes were performed to address the question wheter the reaction order of ~0.5 with respect to nitrostyrene can be influenced (see Chapter 10.3.6). Furthermore, the effect of water on the reaction order was described (see Chapter 10.3.7).

10.3.5 Less Reactive Aldehyde: Addition of Isovaleraldehyde to Nitrostyrene

Isovaleraldehyde reacts significantly slower with nitrostyrene than *n*-butanal. As shown above (see Chapter 8.1), the reaction required 2 mol% of TFA•H-D-Pro-Pro-Glu-NH_2 **56** and NMM in $CHCl_3$/*i*-PrOH 9:1 (v/v) and 1.5 equivalents aldehyde to obtain the desired product **36** after 18 h in 93 % yield (Scheme 10.3). In comparison, the reaction of *n*-butanal and nitrostyrene required only 1 mol% of catalyst **56** under the same conditions and was completed after 16 h (see Chapter 8.2).

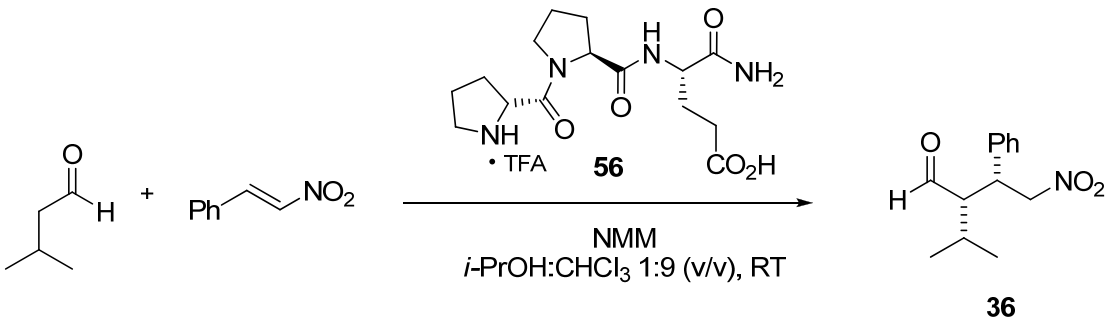

Scheme 10.3. *Asymmetric 1,4-addition of isovaleraldehyde to nitrostyrene, catalysed by H-D-Pro-Pro-Glu-NH_2* ***56****.*

We determined the influence of the aldehyde on the reaction rate by performing 9 reactions at different isovaleraldehyde concentrations of 0.22 M to 1.76 M at constant catalyst concentration (8.8 mM = 2 mol%) and nitrostyrene concentration (0.44 M) (Figure 10.15, for detailed experimental set up see Appendix).

Again, the corresponding log-log plot showed a linear correlation with a slope of 0.31 (R^2 = 98) between an isovaleraldehyde concentration of 0.22 M and 1.32 M. Afterwards the additional aldehyde is not influencing the initial rate of the reaction and a plateau is reached.

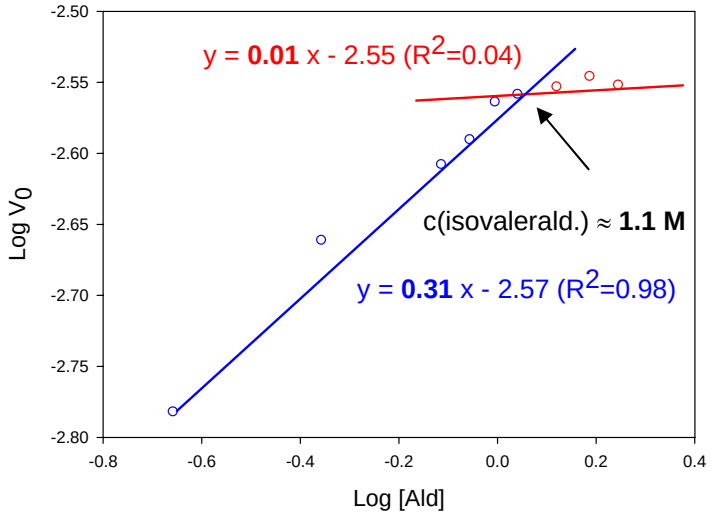

Figure 10.15. *Plot of log (initial rate) vs. log [isovaleraldehyde] providing a slope of 0.31 for [isovaleraldehyde] 0.22 to 1.1 M and 0 for [isovaleraldehyde] 1.1 to 1.76 M.*

The comparison of the two log-log plots of the reactions with *n*-butanal or isovaleraldehyde and nitrostyrene at 2 mol% of catalyst **56** showed that the initial slope of ~0.3 is identical, whereas the plateau is reached at different concentrations (Figure 10.16).

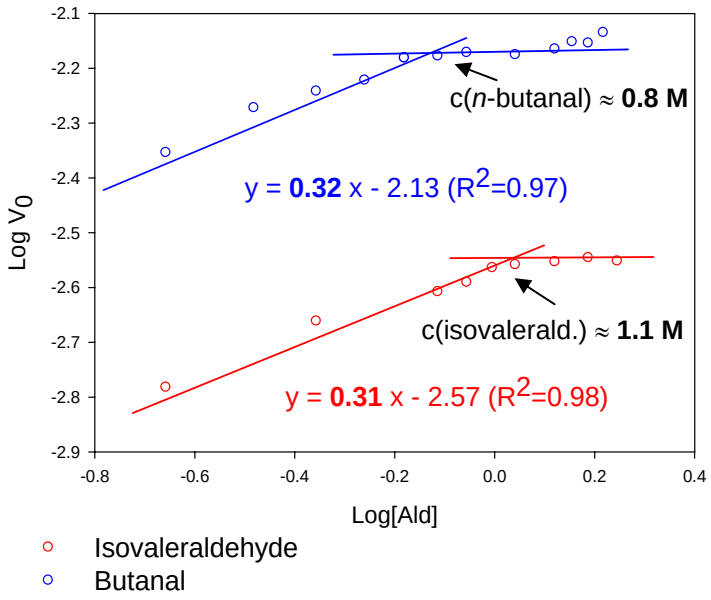

Figure 10.16. *Plot of log (initial rate) vs. log [aldehyde] of the reactions with different concentrations of n-butanal (blue curve) and isovaleraldehyde (red curve).*

In the case of *n*-butanal (blue curve) the plateau is reached at a concentration of approximately 0.8 M and for isovaleraldehyde (red curve) this concentration is approximately at 1.1 M. This indicates that for isovaleraldehyde, the less reactive Michael donor, a higher concentration is necessary to reach saturation kinetics.

10.3.6 Less Reactive Nitrostyrenes: Addition of *n*-Butanal to 4-Methoxynitrostyrene and 2,4-Dimethoxynitrostyrene

Next we addressed the question how a less reactive nitrostyrene influences the kinetics of the 1,4-addition reaction. 4-Methoxynitrostyrene reacts significantly slower with *n*-butanal than nitrostyrene (see Chapter 8.1). The reaction required 2 mol% of TFA•H-D-Pro-Pro-Glu-NH_2 **56** in $CHCl_3$/*i*-PrOH 9:1 (v/v) and 1.5 equivalents of *n*-butanal to obtain the desired product **44** after 24 h in quantitative yield (Scheme 10.4).

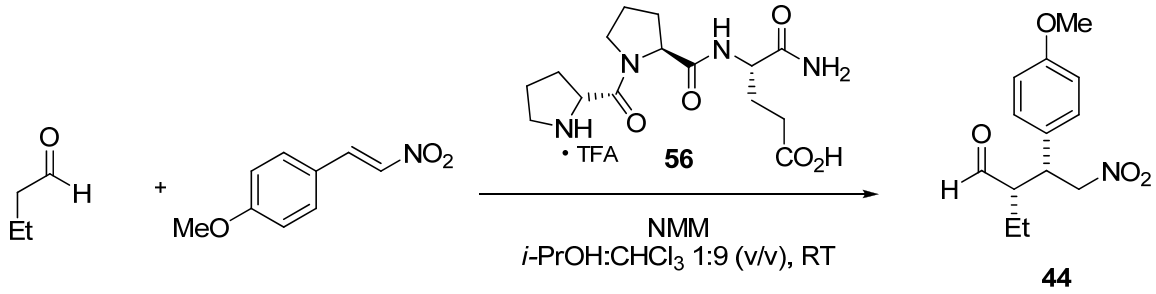

Scheme 10.4. *Asymmetric 1,4-addition reaction of n-butanal to 4-methoxynitrostyrene, catalysed by H-D-Pro-Pro-Glu-NH_2* ***56***.

The reaction order with respect to 4-methoxynitrostyrene was determined with 5 experiments at constant catalyst concentration (8.8 mM) and *n*-butanal concentration (0.44 M). The 4-methoxynitrostyrene concentration was varied between 0.1 M and 0.8 M (for detailed experimental set up see Appendix). The corresponding log-log plot showed a linear correlation (R^2 = 0.99) with a slope of 0.84 (Figure 10.17). Since the methoxy group of 4-methoxnitrostyrene is electron donating, the electrophilicity is lower compared to nitrostyrene and the process of bond formation is slower. This is a further evidence for our hypothesis that not only the C-C bond forming step but also the hydrolysis of the iminium ion **II** is rate determining. In the case of a less reactive nitroolefin the addition becomes slower and thus, "more rate determining" what causes an increase of the observed reaction order.

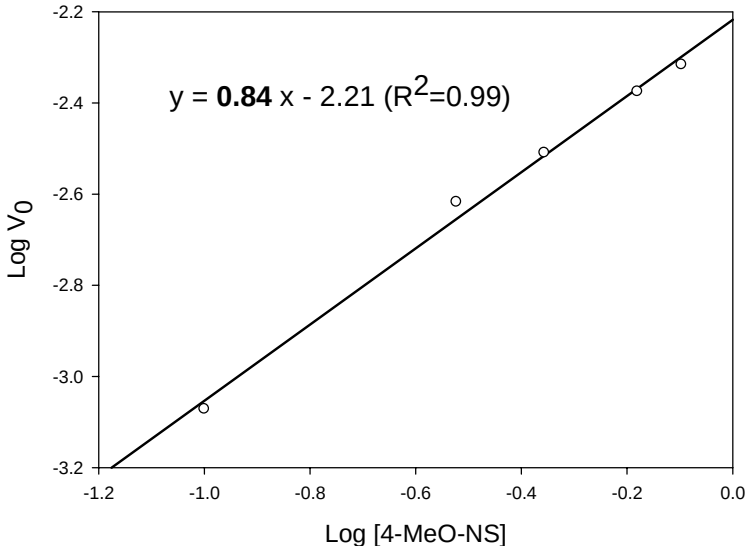

Figure 10.17. *Plot of log (initial rate) vs. log [4-MeO-NS] providing a slope of 0.84. Experiments were carried out with constant [cat **56**] = 8.8 mM and [n-butanal] = 0.44 M.*

To confirm the trend to higher reaction orders with less reactive nitroolefins, we performed the addition reaction of *n*-butanal to 2,4-dimethoxynitrostyrene which reacts significantly slower with *n*-butanal than 4-methoxynitrostyrene (Scheme 10.5).

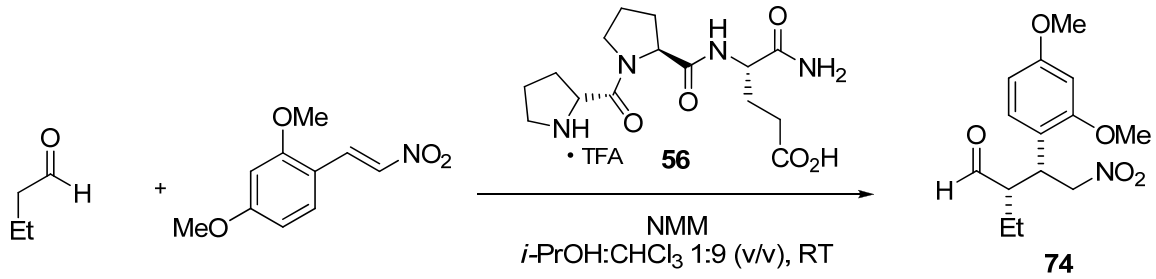

Scheme 10.5. *Asymmetric 1,4-addition reaction of n-butanal to 2,4-dimethoxynitrostyrene, catalysed by H-D-Pro-Pro-Glu-NH2 **56**.*

Reactions were carried out with different 2,4-dimethoxynitrostyrene concentrations of 0.17 M to 0.63 M at constant catalyst concentration (13.2 mM = 3 mol%) and *n*-butanal concentration (0.44M) (for detailed experimental set up see Appendix). A slope of 1.0 (R^2 = 0.99) was obtained in the log-log plot (Figure 10.18). This result strongly indicates that the C-C bond formation step in the addition reaction is much slower compared to the hydrolysis and becomes completely rate determining.

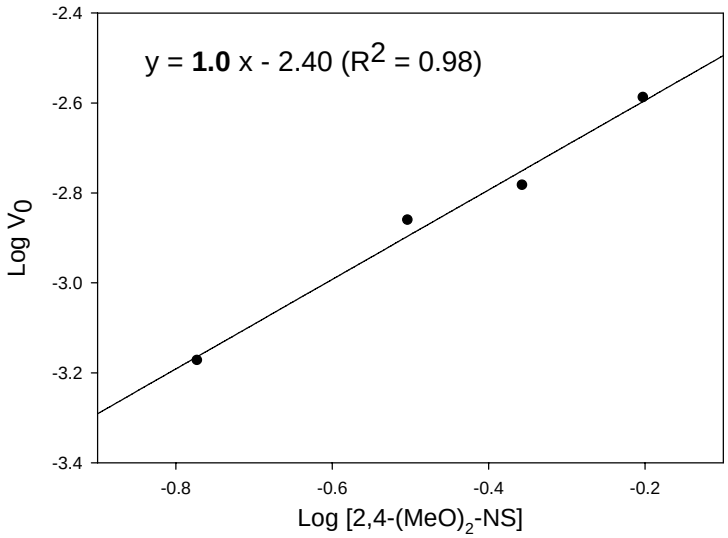

Figure 10.18. *Plot of log (initial rate) vs. log [2,4-(MeO)$_2$-NS] providing a slope of 1.0. Experiments were carried out with a constant [cat* **56***] = 13.2 mM (3 mol%) and [n-butanal] = 0.44 M.*

10.3.7 Standard Reaction, Dry Conditions and Additional Water – Influence on Reaction Rates and Reaction Orders

Next we tested the influence of the water content in the reaction mixture on reaction rate and reaction orders. The reaction does not proceed in the prescence of molecular sieves what indicates that water has to be present to a small extent in the reaction mixture (for details see Appendix). That the rate of the reaction is significantly influenced by the water content is shown in figure 10.19.

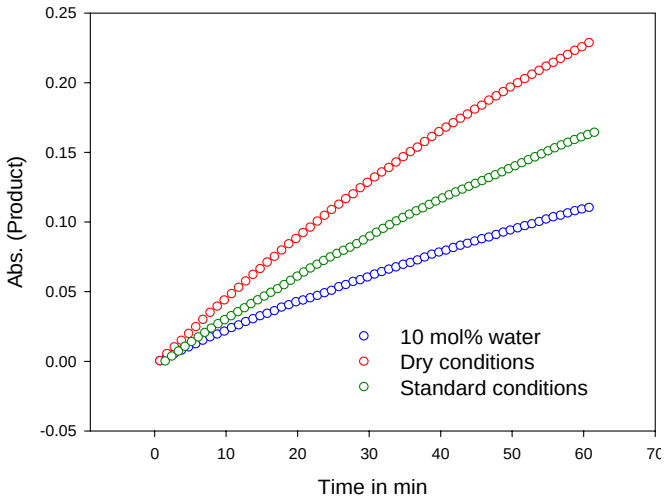

Figure 10.19. *Product formation vs. time: Reaction of nitrostyrene [0.44 M] and n-butanal [0.44 M] at standard conditions (green curve), under "dry conditions" (red curve) and with 10 mol% additional water (blue curve).*

Three addition reactions of *n*-butanal and nitrostyrene were performed under standard conditions (catalyst concentration = 4.4 mM, nitrostyrene concentration = 0.44 M and *n*-butanal concentration = 0.44 M), with additional water (same concentrations plus 10 mol% water) and under "dry conditions" (same concentrations but solvent and *n*-butanal dried with molecular sieves 3Å and dried glassware). The reaction performed under "dry conditions" occured significantly faster than the reaction at standard conditions. A conversion of >90 % was obtained in less than 5 h.

10.3.7.1 Additional Water: Reaction Order with Respect to *n*-Butanal and Nitrostyrene

Six different reactions with *n*-butanal concentrations between 0.55 M and 1.56 M at constant catalyst concentration (4.4 mM) and nitrostyrene concentration (0.44 M) with 10 mol% additional water (44 mM) (for detailed experimental set up see Appendix) were performed and a log-log plot was constructed (Figure 10.20). The data points of the log-log plot showed a linear correlation ($R^2 = 0.98$) with a similar slope of 0.37 (compared to 0.35 for the reaction without water, see Chapter 10.3.2). However no plateau was observed at high aldehyde concentrations.

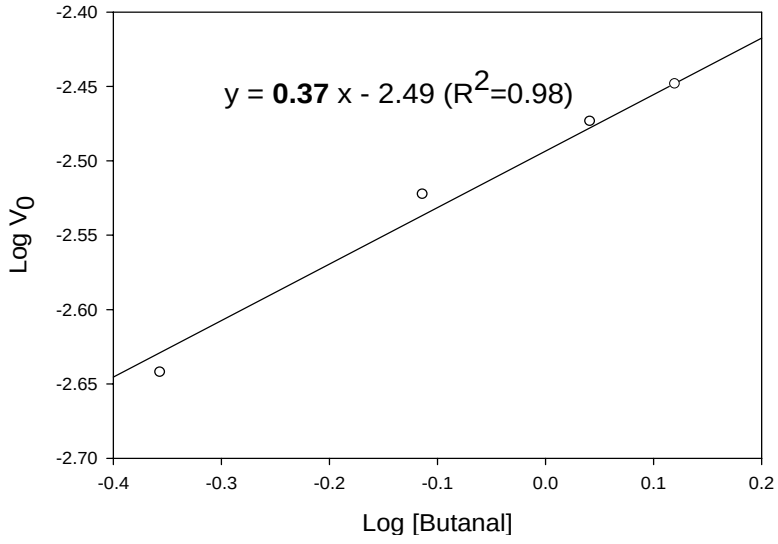

Figure 10.20. *Influence on reaction order of butanal if 10 mol% water is added to the reaction mixture: The plot of log (initial rate) vs. log [n-butanal] provides a slope of 0.37. The reactions were performed at [cat* **56***] = 4.4 mM with additional water [H_2O] = 44 mM.*

The influence of 10 mol% additional water on the reaction order with respect to nitrostyrene was tested with 5 different experiments at constant *n*-butanal concentration (0.44 M), catalyst concentration (4.4 mM) and water concentration (44 mM = 10 mol%). The nitrostyrene concentration was varied between 0.22 M and 1.10 M (for detailed experimental set up see Appendix). A slope of 0.73 (R^2 = 0.99) was obtained with the corresponding log-log plot (Figure 10.21), which is significantly higher than at standard conditions (slope = 0.54, see Chapter 10.3.3).

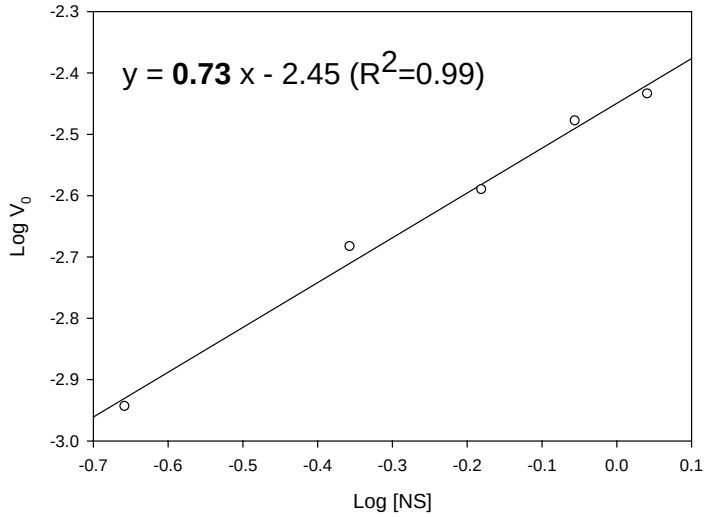

Figure 10.21. *Different nitrostyrene concentrations and 10 mol% water: The plot of log (initial rate) vs. log [nitrostyrene] provides a slope of 0.73. [cat* ***56****] = 4.4 mM, [n-butanal] = 0.44 M and [H_2O] = 44 mM.*

10.3.7.2 Dry Conditions: Reaction Order with Respect to *n*-Butanal and Nitrostyrene

Additional experiments concerning the water content were carried out under "dry conditions", allowing only the presence of water generated by enamine formation. Therefore the solvent-mixture ($CHCl_3$/*i*-PrOH 9:1 v/v) and *n*-butanal were dried over molecular sieves (3Å) and all glassware was dried for each experiment. Six reactions with different *n*-butanal concentrations between 0.22 M and 0.88 M were performed at constant catalyst concentration (4.4 mM) and nitrostyrene concentration (0.44 M) (for detailed experimental set up see Appendix). A slope of 0.29 (R^2 = 0.97) was determined in the corresponding log-log plot for low *n*-butanal concentrations whereas a plateau was reached at higher concentration (~0.7 M) (Figure 10.22).

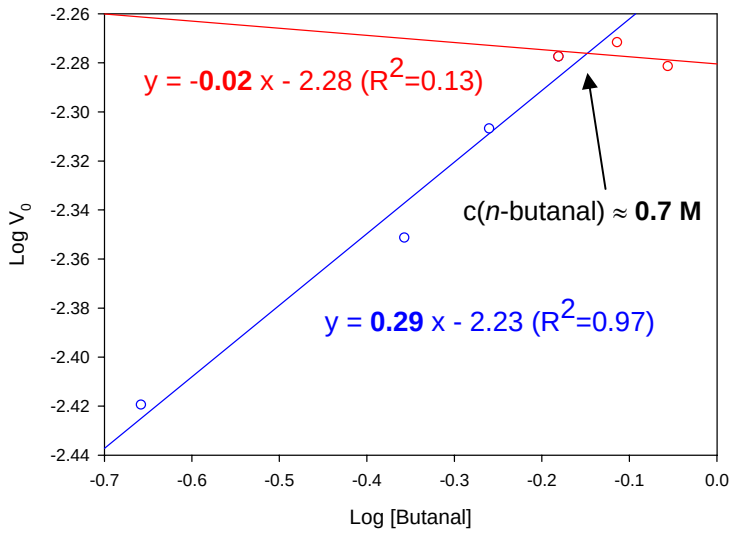

Figure 10.22. *Influence on reaction order of n-butanal under "dry conditions": The plot of log (initial rate) vs. log [n-butanal] provides a slope of 0.29. From [n-butanal] = 0.66 M to 0.88 M the reaction order is zero. Reactions were performed at [cat **56**] = 4.4 mM and [nitro-styrene]= 0.44 M.*

For the reactions of different nitrostyrene concentrations between 0.22 M and 1.10 M, at constant *n*-butanal concentration (0.44 M) and catalyst concentration (4.4 mM) under the "dry conditions" described above (for detailed experimental set up see Appendix), the log-log plot showed a slope of 0.42 (R^2 = 0.99, Figure 10.23) which is lower compared to the corresponding graph for the standard reactions (slope = 0.54, see Chapter 10.3.3).

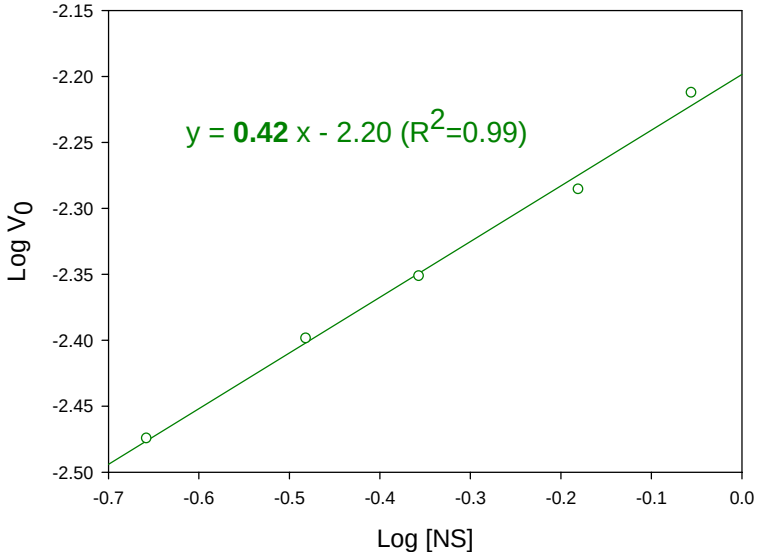

Figure 10.23. *Different nitrostyrene concentrations under "dry conditions": The plot of log (initial rate) vs. log [nitrostyrene] provides a slope of 0.42. [cat **56**] = 4.4 mM and [n-butanal] = 0.44 M.*

10.3.7.3 Dry vs. Standard vs. Additional Water - Conclusions

In comparison to the standard conditions, using standard solvents and *n*-butanal, the reaction order with respect to *n*-butanal was not significantly influenced at low aldehyde concentrations if the water content of the reaction mixture was changed. However, the level of the observed plateau was different. In the case of the reactions with 10 mol% additional water no plateau was observed whereas for the reactions under "dry conditions" a plateau was found at a lower *n*-butanal concentration (Figure 10.24). This indicates that the less water is in the reaction mixture, the less *n*-butanal is necessary to reach zero order kinetics with respect to the aldehyde. The equilibrium between free catalyst **56** and the corresponding enamine **I** is pushed to the enamine side if additional water from the solvent and the environment is absent in the reaction mixture.

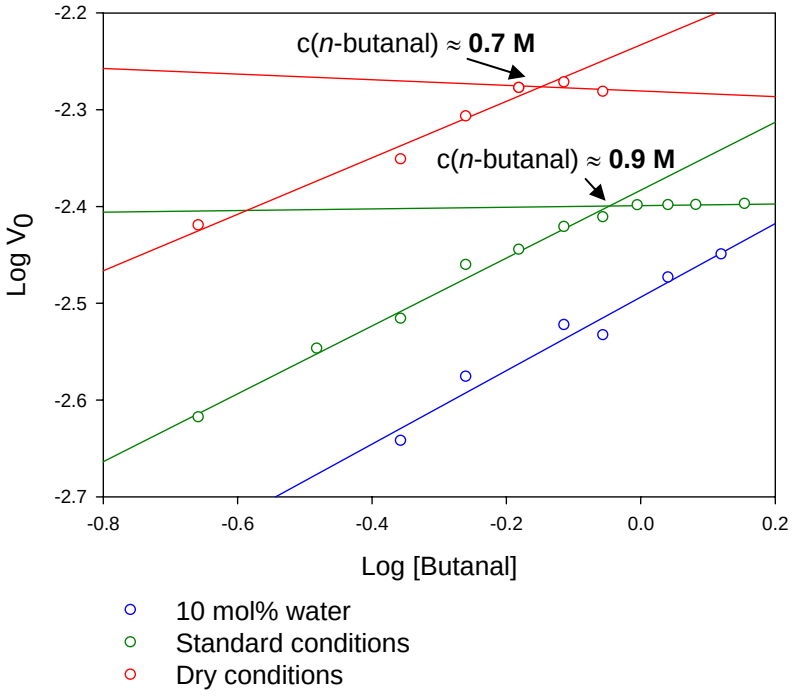

Figure 10.24. *Comparison of the log-log plots of the reactions of different n-butanal concentrations and nitrostyrene at standard conditions (green curve) with additional water (blue curve) and under "dry conditions" (red curve).*

In the case of the experiments carried out with different nitrostyrene concentrations at different water content, it was shown that the overall reaction rate is lower with higher water content. However, the reaction order with respect to nitrostyrene was found to be higher if

additional water was present in the reaction mixture and lower under “dry conditions”. This result suggests that the C-C bond formation step and the hydrolysis step are closely related to each other in terms of their rate. If additional water is absent in the reaction mixture, the hydrolysis is slower and becomes “more rate determining” in the reaction. The observed dependency on nitrostyrene is lower, thus, this process is “less rate determining”. If additional water is present in the reaction mixture, the hydrolysis occurs faster and becomes “less rate determining”, therefore the observed reaction order with respect to nitrostyrene is higher.

10.4 Summary and Conclusions

Reaction progress analysis on the 1,4-addition reaction of aldehydes to nitroolefins was performed using *in situ* FT-IR spectroscopy. The standard reaction of *n*-butanal and nitrostyrene proved to be a clean and reproducible reaction where the observed absorbance of product (NO stretching absorbance) correlated with the actual product conversion. Furthermore the reaction showed no sign of catalyst instabilities (neither catalyst deactivation nor product inhibition) and no non-linear effects were observed. The “desalted peptide” H-D-Pro-Pro-Glu-NH_2 **56** showed a comparable catalytic behaviour as the TFA salt of the peptide **56** in the presence of an equimolar amount of NMM. To determine the different orders of the reaction, we performed experiments with different concentrations of one component, whereas all other concentrations of the components were kept constant. Plots of the logarithm of the initial rate vs. the logarithm of the different concentrations were used to determine the reaction order with respect to the component whose concentration was changed. It was found that the reaction showed first order kinetics with respect to the catalyst **56**. In the case of *n*-butanal, the reaction order turned out to be approximately 0.3 at low concentrations (up to 0.8 M *n*-butanal) and zero order at higher concentrations. For nitrostyrene the reaction order was found to be approximately 0.5. A similar result was found for the reaction order with respect to *n*-butanal when the reaction was performed using a less reactive aldehyde (isovaleraldehyde). Again, the order was approximately 0.3 at low concentration and became zero order at higher concentrations. However, the concentration at which the plateau of zero order was reached, was higher for isovaleraldehyde (1.1 M and 0.8 M for *n*-butanal). The reaction order with respect to nitrostyrene was significantly increased by using a less reactive

Michael acceptor. In the case of 4-methoxynitrostyrene the reaction order was found to be approximately 0.8 and with 2,4-dimethoxynitrostyrene the reaction order was 1. The content of water strongly influenced the reaction rate. Additional water slowed down the reaction between *n*-butanal and nitrostyrene, whereas "dry conditions" increased the reaction rate. Considering the influence of the water content on the different reaction orders, we found that in the case of *n*-butanal a reaction order of approximately 0.3 remained and no plateau was reached, whereas for nitrostyrene the reaction order increased to 0.7. Under "dry conditions" the plateau was reached at a lower concentration of *n*-butanal (0.66 M in comparison to 0.8 M at standard conditions). The reaction order with respect to nitrostyrene decreased under "dry conditions" to 0.4.

The results of the experiments which were performed to investigate the reaction order with respect to aldehyde indicate that at standard conditions the catalyst has no definitive "resting state" and is present as free catalyst **56** and as enamine **I** in the reaction mixture. However, this equilibrium can be influenced either by increasing the aldehyde concentration or by performing the reaction at lower water content ("dry conditions"). In both cases the equilibrium is pushed to the enamine side. The experiments concerning the reaction order with respect to nitrostyrene suggest that the rate of the C-C bond formation step and the rate of the hydrolysis of intermediate **II** to the product **3** are very similar. It was shown that in the case of using less reactive nitroolefins, the reaction orders increase. This indicates that the C-C bond formation is slower and therefore more rate determining and the hydrolysis occurs faster in comparison. Additional water in the reaction increased the reaction order with respect to nitroolefine as well. This suggests that hydrolysis becomes faster and therefore the C-C bond formation step is again more rate determining.

11. H-D-Pro-Pro-Glu-NH_2 (56) Catalysed Asymmetric 1,4-Additions Reactions: Optimised Conditions Based on Kinetic Studies

11.1 Evaluation of Improved Reaction Conditions

In the previous chapter the kinetic studies of the TFA•H-D-Pro-Pro-Glu-NH_2 **56** catalysed conjugate addition reactions of aldehydes and nitroolefins revealed that in principle the reaction rate can be significantly increased when reactions are carried out under dry conditions (Schlenk conditions). Furthermore it was found that the reaction rate of the 1,4-addition is more dependent on the nitrostyrene than on the aldehyde concentration, thus, the reaction should occur faster when nitrostyrene instead of *n*-butanal is used in an excess. The peptide **56** catalysed conjugate addition reaction of *n*-butanal and nitrostyrene occurred without formation of side products (e.g. homoaldol products). Therefore, we assumed that no loss of yield should be obtained when the aldehyde is used as the limiting substrate. Several reactions of *n*-butanal and nitrostyrene were carried out using 1 mol% of peptide **56** and varying the reaction conditions (standard vs. dry conditions) as well as the excess of nitrostyrene (Table 11.1). In comparison to previous conditions, where 1.5 equivalents of *n*-butanal and "non dry" aldehyde and solvents were used (Table 11.1, Entry 1), the reaction with 1.5 equivalents of nitrostyrene under otherwise identical conditions occurred more than twice as fast. A conversion of greater than 95 % was observed after only 7 h (Table 11.1, Entry 2). Importantly, the selectivity was not affected (*syn:anti* = 46:1, 97 % *ee*). When the reaction was carried out under dry condition with the original ratio between *n*-butanal and nitrostyrene (1.5 eq to 1 eq), the reaction was even faster and a conversion of >95 % was observed after only 4 h (Table 11.1, Entry 3). Whereas the diastereoselectivity was slightly lower (*syn:anti* = 32:1), the enantioselectivity remained constant (97 % *ee*). The fastest conversion was observed when the reaction was carried out under dry conditions and with 1.5 equivalents of nitrostyrene (Table 11.1, Entry 4). In this case the reaction was complete after 3 h and the product was obtained with a *syn:anti* ratio of 29:1 and an enantioselectivity of 97

% *ee*. As expected, a smaller excess of nitrostyrene increased the reaction time again. However, the reaction using only 1.2 equivalents of nitrostyrene and under dry conditions still led to complete conversion to the desired product **3** in only 5 h (Table 11.1, Entry 5).

Table 11.1: *H-D-Pro-Pro-Glu-NH$_2$* ***56*** *catalysed asymmetric 1,4-addition reaction between n-butanal and nitrostyrene: Standard conditions vs. dry conditions.*[a]

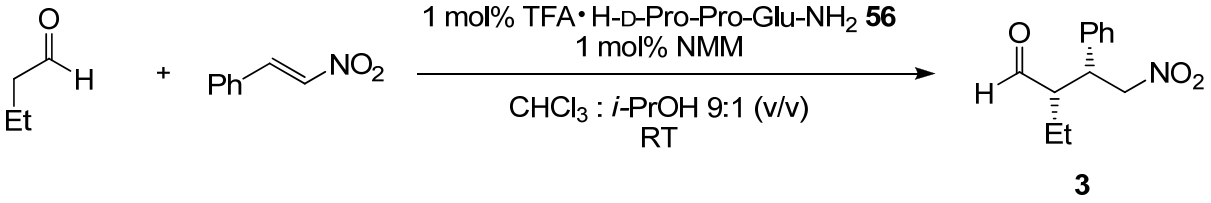

3

Entry	Conditions	***n*-Butanal** [eq]	**Nitrostyrene** [eq]	Time [h]	Conv. [%][b]	*syn : anti*[b]	*ee* [%][c]
1	**standard**	1.5	1	16	quant.	42:1	97
2	**standard**	1	1.5	7	>95	46:1	97
3	**dry**	1.5	1	4	>95	32:1	97
4	**dry**	1	1.5	3	>95	29:1	97
5	**dry**	1	1.2	5	>95	21:1	97
6	**dry, 0 °C**	1	1.5	20	>95	>99:1	98
7	**dry, 0.1mol% (56)**	1	1.5	48	>90	16:1	97

[a] Reactions were performed at a 0.44 mmol scale (0.5 M with respect to nitrostyrene). [b] Determined by ^{1}H NMR of the reaction mixture. [c] Determined by chiral HPLC analysis.

Next we tested the reaction with 1.5 equivalents of nitrostyrene and under dry conditions, carried out at 0 °C (Table 11.1, Entry 6). In this case the product **3** was obtained after 20 h in nearly perfect diastereoselectivity (*syn:anti* = >99:1) and with an enantiomeric excess of 98 %. The significantly faster reaction rate observed by using an excess of nitrostyrene under dry conditions suggests that under these conditions the catalyst loading can be further reduced. Thus, we performed the reaction of *n*-butanal and nitrostyrene with as less catalyst **56** as possible and with the aim to obtain a high yield within a reasonable reaction time. We were pleased to find that the addition reaction works with only 0.1 mol% of catalyst **56**. After 48 h the desired product **3** was obtained in a yield of 87 %, with a diastereoselectivity of *syn:anti* = 16:1 and a enantioselectivity of 97 % *ee* (Table 11.1, Entry 7).

11.2 Substrate Scope

Reactions with different substrate combinations were performed using 1 mol% of catalyst **56**. In these cases we were basically interested in the reaction time. On the other hand, we performed each reaction within 48 h using the lowest possible catalyst loading. All reactions were carried out with 1.5 equivalents of nitrostyrene and under dry conditions (Table 11.2) and led, either performed with 1 mol% or with 0.1-0.4 mol% of **56**, to the corresponding products in high to very high yields (87-98 %) and excellent enanatioselectivities (95-99 % *ee*). However, the observed diastereoselectivities were generally lower (*syn:anti* = 10:1 to 35:1, Table 11.2, Entries 1-20) than the previously obtained results for these reactions under standard conditions using 1.5 equivalents of aldehyde (see Chapter 8.1). The fastest reactions were observed between *n*-butanal and nitrostyrene (Table 11.2, Entries 1 and 2) or activated nitrostyrenes, such as 2,4-dichloronitrostyrene (Table 11.2, Entries 11 and 12) or 2-trifluoromethylnitrostyrene (Table 11.2, Entries 13 and 14). With the use of 1 mol% of **56** these reactions showed complete conversions within 3 h and 0.1 mol% of **56** sufficed to obtain full conversions within 48 h. As expected, the slowest reactions were observed with isovaleralehyde as challenging Michael donor (20 h with 1 mol% **56**, Table 11.2, Entries 7 and 8) and with 4-methoxynitrostyrene as a poor Michael acceptor (12 h with 1 mol% **56**, Table 11.2, Entries 17 and 18). For both reactions 0.4 mol% of peptide **56** were necessary to obtain high yields after 48 h. An intermediate activity was observed with the aliphatic nitroolefin *(E)*-4-methyl-1-nitropent-1-ene and *n*-butanal (Table 11.2, Entries 19-20). The reaction with 1 mol% **56** took 7 h and 0.2 mol% of **56** was necessary to obtain a high yield after 48 h. Finally, the best results in terms of activity and selectivity were obtained with the reaction between 3-phenylpropionaldehyde and 2-trifluoromethylnitrostyrene (Table 11.2, Entries 15 and 16). In this case the reaction required only 4 h with 1 mol% **56**, leading to the product **43** in 98% yield and with a *syn:anti* ratio of 32:1 and 99 % *ee*.

Table 11.2. *Asymmetric conjugate addition of aldehydes to nitroalkenes catalysed by TFA•H-D-Pro-Pro-Glu-NH_2* **56**. [a]

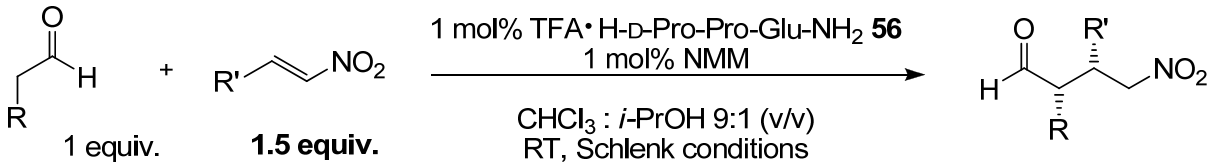

Entry	Product		Catalyst loading	Time [h]	Yield [%][b]	*syn:anti*[c]	*ee* [%][d]
1	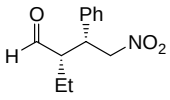	**3**	1 mol%	**3**	92	29 : 1	**97**
2			**0.1 mol%**	48	87	16 : 1	**97**
3	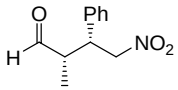	**33**	1 mol%	**7**	94	20 : 1	**95**
4			**0.2 mol%**	48	92	20 : 1	**96**
5	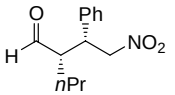	**34**	1 mol%	**6**	93	22 :1	**97**
6			**0.1 mol%**	48	98	18 :1	**96**
7	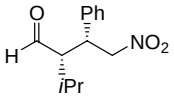	**36**	1 mol%	**20**	89	20 :1	**96**
8			**0.4 mol%**	48	93	21 : 1	**94**
9	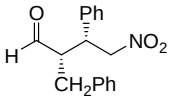	**37**	1 mol%	**5**	97	15 : 1	**98**
10			**0.1 mol%**	48	87	16 :1	**98**
11	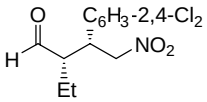	**41**	1 mol%	**3**	98	24 : 1	**97**
12			**0.1 mol%**	48	95	21 : 1	**96**
13	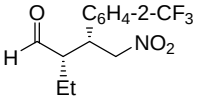	**42**	1 mol%	**3**	94	32 : 1	**98**
14			**0.1 mol%**	48	96	35 : 1	**97**
15	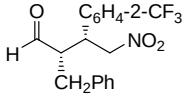	**43**	1 mol%	**4**	98	32 : 1	**99**
16			**0.1 mol%**	48	92	35 : 1	**99**
17	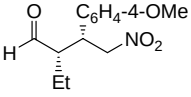	**44**	1 mol%	**12**	93	11 : 1	**95**
18			**0.4 mol%**	48	96	13 : 1	**95**
19	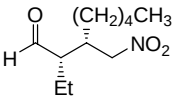	**68**	1 mol%	**7**	89	15 : 1	**97**
20			**0.2 mol%**	48	92	10 :1	**98**

[a] Reactions using 1mol% of **56** *were performed at a 0.44 mmol scale, reactions using 0.1 to 0.4 mol% of* **56** *were performed at a 2.2 mmol scale. [b]Isolated yield. [c]Determined by ^1H NMR on the crude material. [d] Determined by chiral phase HPLC analysis.*

12. Asymmetric 1,4-Addition Reaction of Aldehydes to Nitroethylene

12.1 Introduction and Initial Studies

It was shown that aliphatic, aromatic as well as funtionalised nitroolefins react readily with aldehydes in the presence of peptide **56** (see Chapter 8.1 and 11.2). Next we became interested in employing nitroethylene, the simplest of all nitroolefins, as a Michael acceptor since this would afford access to monosubstituted γ-nitroaldehydes. These would allow for conversion into monosubstituted γ^2-amino acids as important building blocks in the development of therapeutics or within foldamer research. (Scheme 12.1).[143-150] Common procedures for the synthesis of γ^2-amino acids rely on the use of chiral auxiliaries.[151-153] A direct and more efficient route would thus facilitate their accessibility.

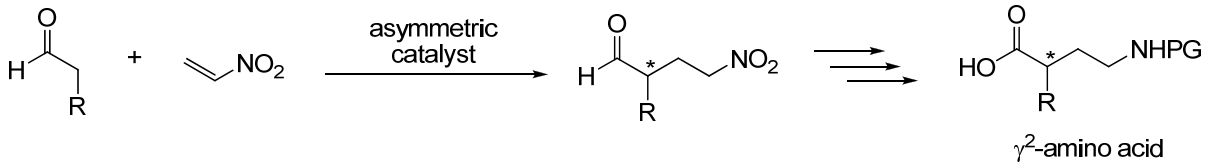

Scheme 12.1. *Potential catalytic route for the synthesis of γ^2-amino acids*

Nitroethylene was prepared following the literature via the condensation of commercially available 2-nitroethanol using phthalic anhydride.[29,154-156] It has long been known that nitroethylene has the tendency to polymerise readily.[157] Therefore, the handling of this compound is challenging. We found that if the freshly synthesised nitroethylene is immediately dissolved in chloroform, this solution remains stable over a prolonged time (stored at -20 °C) and can be conveniently used as reagent. For the very first experiment we used 3 mol% of the original lead peptide TFA•H-Pro-Pro-Asp-NH_2 **1** and 3 mol% NMM for the reaction of 1 equivalent of 3-phenylpropionaldehyde with 1.1 equivalents of nitroethylene in $CHCl_3$/*i*-PrOH 9:1 (v/v). We were pleased to oberserve formation of the desired γ-

nitroaldehyde. After 20 h a conversion of 87 % was determined by ^{1}H NMR of the reaction mixture, however, we found that the product racemised during work up and purification upon which the reliable determination of the enantiomeric excess by chiral HPLC became impossible. The *in situ* reduction of the γ-nitroaldehyde would generate the configurationally stable γ-nitroalcohol, however, the additional effort is not convenient for the screening of a large number of peptides. A solution to the problem was found by using a method reported by Gellman et al. for the determination of the enantiomeric excess using ^{1}H NMR analysis.[158] After reaction of the crude γ-nitroaldehyde with a chiral amine in the NMR tube, the *in situ* generated diastereomeric imines were detected and their ratio was determined by integration. This method proved to be simple, fast and accurate and therefore adequate for the screening of a library of peptides (for details see Experimental Section).

12.2 Catalyst Screening for the Reaction of 3-Phenylpropionaldehyde and Nitroethylene

Various catalysts which were originally developed for reactions of aldehydes and nitroolefins were then tested for the 1,4-addition reaction of 3-phenylpropionaldehyde and nitroethylene under the identical conditions as mentioned for the first experiment with catalyst **1** (Table 12.1). The same tendency as for the reactions of *n*-butanal and nitrostyrene in terms of selectivity was observed with the diastereoisomers of TFA•H-Pro-Pro-Asp-NH_2 **1** (Table 12.1, Entries 1-4), where TFA•H-D-Pro-Pro-Asp-NH_2 **21** was again the most selective catalyst (87 % *ee*), providing the product with opposite absolute configuration in comparison to the products obtained with the other diastereoisomers. With the exception of TFA•H-D-Pro-Pro-Glu-NH_2 **56** and TFA•H-D-Pro-Pro-Gln-NH_2 **75**, all other peptides, including diastereomeric tetrapeptides of TFA•H-Pro-Pro-Asp-Pro-NH_2 **6** or tripeptides of the type TFA•H-Pro-Pro-Xaa-OH, TFA•H-Pro-Pro-Xaa-NH_2, TFA•H-D-Pro-Pro-Xaa-OH and TFA•H-D-Pro-Pro-Xaa-NH_2, proved to be less selective for the test reaction than peptide **21** (Table 12.1, Entries 5-21). Interesstingly, the peptide TFA•H-D-Pro-Pro-Gln-NH_2 **75**, bearing a carboxamide instead of a carboxylic acid in the side chain of the third amino acid, showed the best *ee* of 91 % and the highest conversion with respect to nitroethylene (98 % after 20 h, Table 12.1, Entry 21). However, significant quantities of side products were detected in the

^{1}H NMR spectrum of the reaction mixture. Thus, peptide **56** which showed slightly lower selectivity (88 % *ee*) and similar conversion with respect to nitroethylene (98 % after 20 h, Table 12.1, Entry 20) was used for further studies of reaction optimisation.

Table 12.1. *Asymmetric 1,4-addition reaction between 3-phenylpropionaldehyde and nitroethylene. Peptidescreening.*[a]

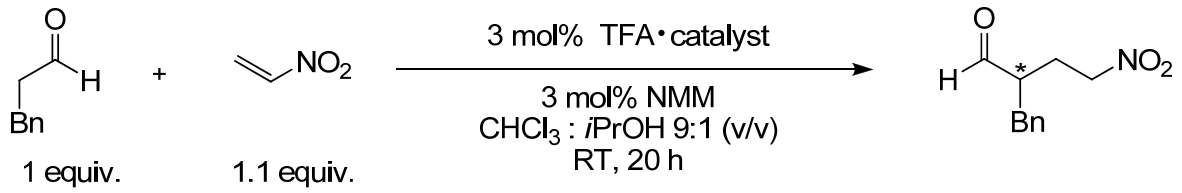

Entry	Catalyst		Conv. [%][b]	*ee* [%][c]	Abs. Conf.
1	TFA•**H-Pro-Pro-Asp-NH$_2$**	**1**	87	73	*R*
2	TFA•**H-D-Pro-Pro-Asp-NH$_2$**	**21**	77	87	*S*
3	TFA•**H-Pro-D-Pro-Asp-NH$_2$**	**19**	81	66	*R*
4	TFA•**H-Pro-Pro-D-Asp-NH$_2$**	**20**	81	65	*R*
5	TFA•**H-Pro-Pro-Asp-Pro-NH$_2$**	**6**	92	74	*R*
6	TFA•**H-D-Pro-Pro-Asp-Pro-NH$_2$**	**24**	86	73	*S*
7	TFA•**H-Pro-D-Pro-Asp-Pro-NH$_2$**	**25**	85	70	*R*
8	TFA•**H-Pro-Pro-Asp-D-Pro-NH$_2$**	**26**	76	55	*R*
9	TFA•**H-Pro-Pro-Asp-OMe**	**8**	95	62	*R*
10	TFA•**H-Pro-Pro-β-homo-Asp-OH**	**10**	83	66	*R*
11	TFA•**H-Pro-Pro-β-homo-Asp-NH$_2$**	**9**	89	61	*R*
12	TFA•**H-Pro-Pro-Glu-NH$_2$**	**14**	86	66	*R*
13	TFA•**H-Pro-Pro-Asn-OH**	**11**	98	76	*R*
14	TFA•**H-Pro-Pro-Cys(SO$_3$H)-NH$_2$**	**15**	10	n.d.	*n.d.*
15	TFA•**H-Pro-MePro-Asp-NH$_2$**	**16**	67	46	*R*
16	TFA•**H-Pro-Pro-Ser-OH**	**12**	63	63	*R*
17	TFA•**H-Pro-Pro-His-OH**	**13**	54	54	*R*
18	TFA•**H-D-Pro-Pro-Asn-OH**	**29**	95	80	*S*
19	TFA•**H-D-Pro-Pro-Asn-NH$_2$**	**48**	93	86	*S*
20	TFA•**H-D-Pro-Pro-Glu-NH$_2$**	**56**	98	88	*S*
21	TFA•**H-D-Pro-Pro-Gln- NH$_2$**	**75**	98	91	*S*

[a] Reactions were performed at a 220 μmol scale (0.9 M with respect to nitroethylene). [b] Determined by ^{1}H NMR analysis comparing aldehyde integrals of 3-phenylpropionaldehyde and product. [c] Determined by ^{1}H NMR analysis using a chiral amine.

12.3 Reaction Optimisation

12.3.1 Evaluation of Conditions using TFA•H-D-Pro-Pro-Glu-NH_2 (56)

Although the initial results obtained for the peptide **56** catalysed Michael addition of 3-phenylpropionaldehyde and nitroethylene were promising, the optimisation of this reaction turned out to be challenging. Many reactions were set up with the variation of different reaction parameters such as catalyst loading, substrate ratio, concentration and solvent. However, no satisfying results were achieved (Table 12.2, only examples).

Table 12.2. *Asymmetric 1,4-addition reaction between 3-phenylpropionaldehyde and nitroethylene. Optimization with H-D-Pro-Pro-Glu-NH_2* **56**.[a]

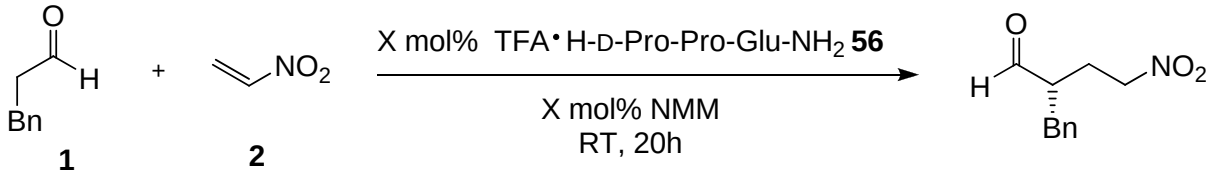

Entry	**56** [mol%]	**1** [eq]	**2** [eq]	Conc. [M] [b]	Solvent	Conv. [%] [c]	*ee* [%] [d]
1	2	1	1	1.5	$CHCl_3$: *i*-PrOH 10 : 1	69	92
2	2	1	1	1.5	$CHCl_3$: *i*-PrOH 25 : 1	55	93
4	2	2	1	1.5	$CHCl_3$: *i*-PrOH 25 : 1	85	96
5	2	1	1.5	1.5	$CHCl_3$: *i*-PrOH 25 : 1	35	90
6	2	3	1	1.36	neat $CHCl_3$	85	91
7	2	2	1	2.3	neat $CHCl_3$	72	89
8	1	2	1	2.3	neat $CHCl_3$	28	n.d.
9	1	3	1	2.3	neat $CHCl_3$	60	89
10	2	1	1.5	1	neat $CHCl_3$	22	n.d.
11	2	2	1	1	neat $CHCl_3$	79	93
12	1	2	1	1	neat $CHCl_3$	42	95
13	1	3	1	1	neat $CHCl_3$	77	94

[a] Reactions were performed at a 340 μmol scale. [b] Concentration with respect to nitroethylene. [c] Determined by ^1H NMR analysis comparing aldehyde integrals of 3-phenylpropionaldehyde and product. [d] Determined by ^1H NMR analysis using a chiral amine.

While the conversions with respect to nitroethylene were usually good, the conversions with respect to the aldehyde proved to be rather disappointing. In this respect, a white precipitate was often observed after stirring the reaction mixtures for approximately one hour, which was taken as an indication for polymerisation of nitroethylene. Nevertheless, an excess of 3-phenylpropionaldehyde (Table 12.2, Entries 2, 6-9, 11-13), a decreased concentration of the reaction mixtures (Table 12.2, Entries 10-13) and the use of neat $CHCl_3$ as solvent (Table 12.2, Entries 6-13) were beneficial in terms of conversions and selectivities. Finally, we observed that the reaction occurred faster and cleaner when the mixture was about 10 times more dilute.

12.3.2 Reaction Optimisation at Low Concentrations

Further reactions between 3-phenylpropionaldehyde and nitroethylene were then performed with 1 mol% of TFA•H-D-Pro-Pro-Asp-NH_2 **21** or TFA•H-D-Pro-Pro-Glu-NH_2 **56** in $CHCl_3$, at lower concentrations and using the aldehyde in an excess (Table 12.3). Both peptides were tested with 3 equivalents of the aldehyde at a concentration of 0.5 M with respect to nitroethylene (Table 12.3, Entries 1 and 2). The reaction with **56** was in this case not only significantly faster but also more selective (10 h, 90 % conversion, 90 % *ee*). A slightly higher activity and a notably higher selectivity was observed when the reaction with **56** was carried out with 3 equivalents aldehyde but at a concentration of 0.25 M with respect to nitroetylene (10 h, 95 % conversion, 95 % *ee*, Table 12.3, Entry 3). The reaction became slower when the aldehyde was reduced from 3 to 1.5 equivalents, however, the observed selectivity was greater than 95 % *ee* (Table 12.3, Entry 4). Best conditions were then found using 1 mol% of TFA•H-D-Pro-Pro-Glu-NH_2 **56**, 1.5 equivalents of 3-phenylpropionaldehyde and nitroethylene at a concentration of 0.1 M (Table 12.3, Entry 5). Under these conditions both conversion and the enantioselectivity were greater than 95 % after 15 h. A further decrease of the concentration to 0.05 M had a negative influence on activity and selectivity (Table 12.3, Entry 6). An increase of the catalyst loading to 3 mol% reduced the reaction time to only 5 h, however, the selectivity droped to 90 % *ee* (Table 12.3, Entry 7). Under the improved conditions the peptide TFA•H-D-Pro-Pro-Gln-NH_2 **75** showed a selectivity of greater than 95 % *ee* but only 45 % conversion was observed after 70 h. Finally we used the "desalted peptide" H-D-Pro-Pro-Asp-NH_2 **56** with and without NMM and found that both

activity and selectivity were much lower in comparison to the reactions with the TFA salt of **56**. This is in contrast to the reaction between *n*-butanal and nitrostyrene with "desalted" **56**, where additives had no influence on the catalytic performance (see Chapter 8.2).

Table 12.3. *Asymmetric 1,4-addition reaction between 3-phenylpropionaldehyde and nitroethylene. Optimization at low concentrations.*[a]

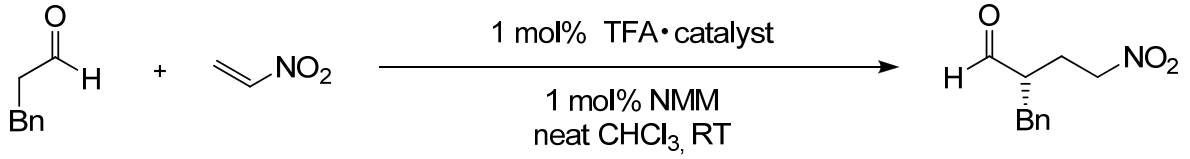

Entry	Catalyst	Aldehyde [eq]	Conc. [M] [b]	Time [h]	Conv. [%][c]	*ee* [%][d]
1	TFA•H-D-Pro-Pro-Asp-NH_2 **21**	3	0.5	30	70	85
2	TFA•H-D-Pro-Pro-Glu-NH_2 **56**	3	0.5	10	90	90
3	TFA•H-D-Pro-Pro-Glu-NH_2 **56**	3	0.25	10	95	95
4	TFA•H-D-Pro-Pro-Glu-NH_2 **56**	1.5	0.25	15	90	>95
5	TFA•H-D-Pro-Pro-Glu-NH_2 **56**	1.5	0.1	15	>95	>95
6	TFA•H-D-Pro-Pro-Glu-NH_2 **56**	1.5	0.05	15	80	90
7	TFA•H-D-Pro-Pro-Glu-NH_2 **56** (3 mol%)	1.5	0.1	5	>95	90
8	TFA•H-D-Pro-Pro-Asp-NH_2 **21**	1.5	0.1	50	85	90
9	TFA•H-D-Pro-Pro-Gln-NH_2 **75**	1.5	0.1	70	45	>95
10	TFA•H-D-Pro-Pro-Asp-NH_2 **21** desalted, no NMM	1.5	0.1	70	75	90
11	TFA•H-D-Pro-Pro-Asp-NH_2 **21** desalted, 1mol% NMM	1.5	0.1	70	40	n.d.

[a] Reactions were performed at a 220 μmol scale. [b] Concentration with respect to nitroethylene. [c] Determined by ^{1}H NMR analysis comparing aldehyde integrals of 3-phenylpropionaldehyde and product. [d] Determined by ^{1}H NMR analysis using a chiral amine.

12.4 Substrate Scope

With the best reaction parameters determined (1.5 eq aldehyde, 0.1 M nitroethylene in chloroform), we reacted a range of different aldehydes with nitroethylene in the presence of 1 mol% of **56**. As mentioned before, the resulting α-substituted γ-nitroaldehydes are prone to

racemisation upon purification by column chromatography. Thus, the aldehydes were typically reduced with borane to the corresponding alcohols before isolation. The conjugate addition reaction products were obtained in high yields and excellent enantioselectivities for a range of different aliphatic and functionalised aldehydes (Table 12.4).

Table 12.4. *Asymmetric 1,4-addition between aldehydes and nitroethylene catalysed by peptide* ***56****.*[a]

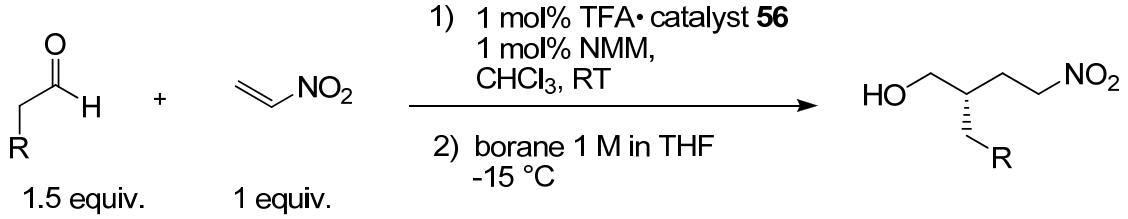

Entry	Product		Time [h]	Yield [%][b]	*ee* [%][c]
1	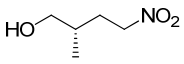	**76**	20	84	95
2	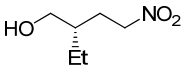	**77**	15	82	98
3	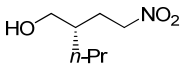	**78**	15	90	99
4	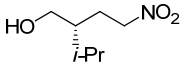	**79**	45	85	97[d]
5[e]	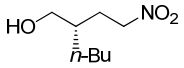	**80**	20	84	99
6	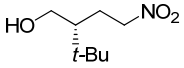	**81**	5d	67	98
7	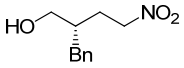	**82**	15	82	98
8	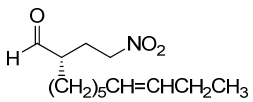	**83**	25	86	97[d]
9	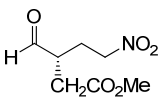	**84**	70	78	95[d]
10	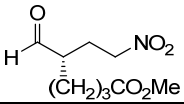	**85**	30	80	96[d]

[a]Reactions were performed at a 0.44 mmol scale. Nitroethylene was used at a conc. of 0.1 M in chloroform. [b] Isolated yield. [c] Determined by chiral-phase HPLC analysis (Chiracel AD-H). [c] Determined by ^{1}H NMR of the crude material after the addition of a chiral primary amine. [d] 3 mol% of the catalyst were used.

In all cases the desired products **76-85** were obtained in good yields and selectivities of 95-99 % *ee*. Particularly notable is that, with slightly higher amounts of catalyst (3 mol%) and longer reaction times, not only isovaleraldehyde but even neopentylaldehyde with a *tert*-butyl group at the α-carbon is tolerated as a substrate (Table 12.4, Entries 4 and 6). In addition, aldehydes bearing functional groups such as alkenes and esters also reacted readily with nitroethylene in the presence of only 1 mol% of peptide **56** (Table 12.4, Entries 8-10). A limitation with respect to the substrate scope was found in the application of β-functionalised aldehydes. 3-(methylthio)propionaldehyde and even the Cbz-protected 3-amino-propionaldehyde were both reactive substrates and the corresponding addition products were isolated in high yields after the *in situ* reduction, however, the enantionselectivities remained poor due to racemisation. Another inapplicable substrate was benzyloxyacetaldehyde. Again, a high conversion but a low enantioselectivity was obtained. However, in this case we assume that the α-proton is very acidic what caused racemisation and thus low selectivity of the corresponding addition product.

12.5 Derivatisation of γ-Nitroalcohol (82)

12.5.1 Synthesis of γ-Butyrolactone (86)

The γ-nitroalcohol **82** was readily converted into the chiral γ-lactone **86**, using $NaNO_2$ and acetic acid in DMSO (Scheme 12.2).[28] **86** was obtained in a yield of 89 % with retention of the optical purity as shown by chiral HPLC (Figure 12.1). Monosubstituted γ-lactones are useful precursors to a multitude of biologically active compounds.[159] Besides, **86** was used to assign the absolute configuration by comparison of the optical rotation with the literature.[160]

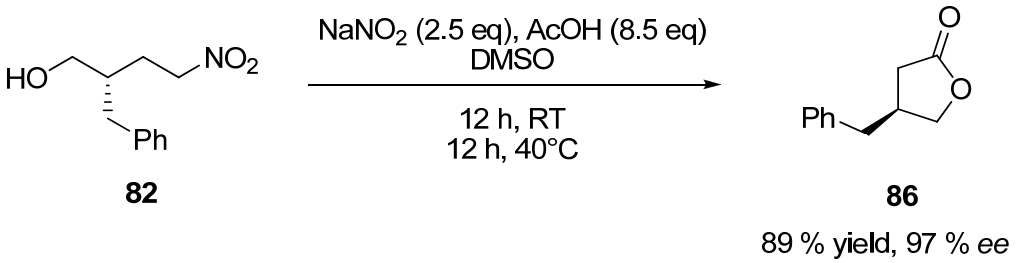

Scheme 12.2. *Synthesis of γ-lactone **86** from γ-nitroalcohol **82**.*

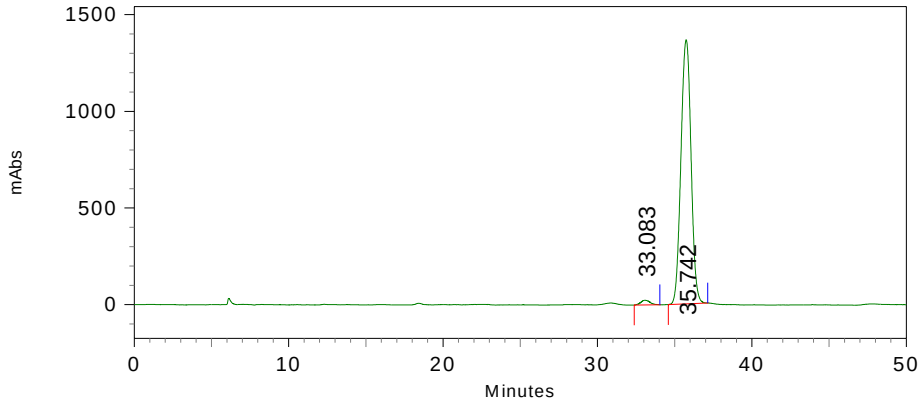

Figure 12.1. *Chiral HPLC of γ-lactone* ***86*** *(97 % ee).*

12.5.2 Synthesis of Monosubstituted γ^2-Amino Acid (87)

The conversion of the conjugate addition products to γ^2-amino acids proved to be straightforward. As an illustration, nitroalcohol **82** was oxidised to the carboxylic acid using Jones reagent followed by reduction of the nitro group with Raney-Ni and Fmoc protection of the resulting amino acid (Scheme 12.3). The Fmoc-protected γ^2-amino acid **87** was obtained in an overall yield of 81 % with retention of optical purity as determined by ^{1}H NMR analysis after the reaction of **86** with a chiral amine (for details see Experimental Section).

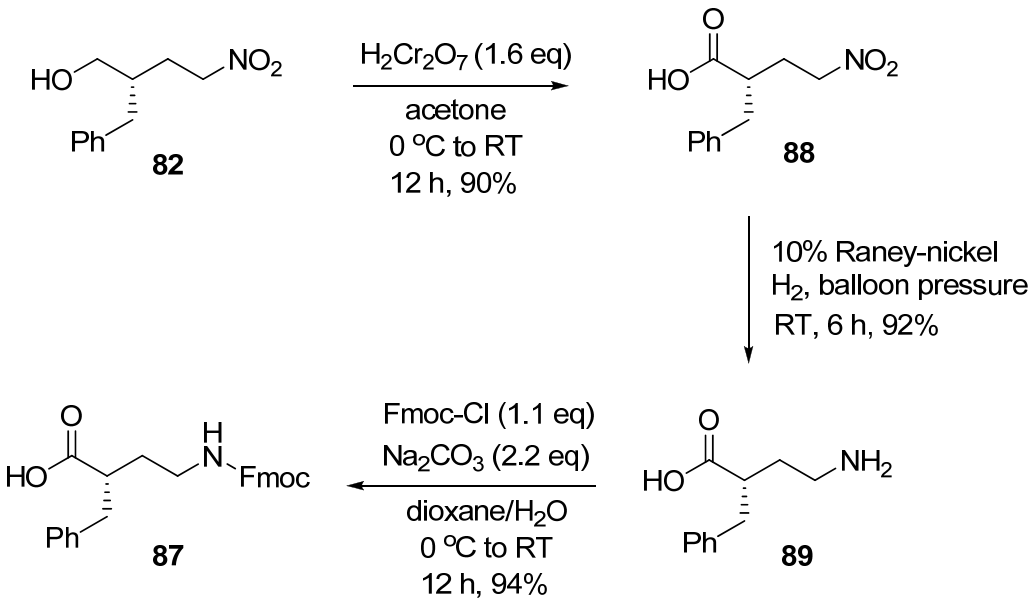

Scheme 12.3. *Synthesis of γ-lactone* ***87*** *from γ-nitroalcohol* ***82***.

12.6 Conclusions

In conclusion TFA•H-D-Pro-Pro-Glu-NH_2 **56** is an excellent asymmetric catalyst for conjugate addition reactions of aldehydes to nitroethylene, affording monosubstituted γ-nitroaldehydes in high yields and enantioselectivities requiring only a small excess of the aldehyde (1.5 eq) and as little as 1 mol% of the catalyst. The products can be readily converted into γ-butyrolactones and monosubstituted γ^2-amino acids.

13. Summary and Outlook

Within this thesis, the development of peptides as highly efficient catalysts for asymmetric conjugate addition reactions of aldehydes to nitroolefins is described.

The tripeptide TFA•H-Pro-Pro-Asp-NH_2 **1** was originally developed and established as an efficient catalyst for asymmetric aldol reactions. Based on insight gained from conformational analysis it was predicted that **1** and closely related peptides may also serve as catalysts for asymmetric 1,4-addition reactions. Indeed, TFA•H-D-Pro-Pro-Asp-NH_2 **21** proved to be a highly effective catalyst for asymmetric conjugate addition reactions of aldehydes to nitroolefins. A broad scope of different substrate combinations including aliphatic and aromatic nitroolefins as well as linear, β-branched and aromatic aldehydes reacted readily in the presence of as little as 1 mol% of **21** to the desired γ-nitroaldehydes in high yields (82-99 %), high diastereoselectivities (*syn:anti* = 4:1->99:1) and very high enantioselectivities (88-98 % *ee*). Thus, **21** proved to be significantly more active and applicable to a broader substrate scope compared to other amine based catalysts that had previously been developed for 1,4-addition reactions of aldehydes to nitroolefins. In addition, the peptidic catalyst **21** also offered solutions to other challenges encountered with the other amine based catalysts and allowed for using only a small excess of the aldehyde providing the products within a reasonable reaction time.

Analysis of the structural and functional prerequisites for high catalytic efficiency within catalysts **21** led then to the establishment of the closely related peptide TFA•H-D-Pro-Pro-Glu-NH_2 **56** as an even more effective catalyst for conjugate addition reactions of aldehydes and nitroolefins including the functionalised β-nitroacrolein dimethylacetal (up to quant. yields, *syn:anti* ratio up to >99:1, up to 99 % ee). Even nitroethylene, the simplest of all nitroolefins, reacts readily with functionalised and non-functionalised aldehydes. The derivatisation of the corresponding products offered a new entry into the synthesis of monosubstituted γ^2-amino acids, previously only accessible by using chiral auxiliaries.

Extensive kinetic studies allowed for further insight into the reaction mechanism and led to the establishment of improved reaction conditions. Only as little as 0.1 mol% of **56** was required for the corresponding reactions, which is the lowest catalyst loading that has been

achieved for enamine catalysis to date. A further benefit of the peptidic catalyst is that, in contrast to many other organocatalysts, no additives are necessary to obtain the desired products in very high yields and selectivities. Further conformational studies indicated that peptide **56** is more rigid than usual tripeptides but still bear a significant degree of conformational freedom. Therefore, the right degree of flexibility might be the key to the effectiveness of peptides as asymmetric catalysts.

These studies demonstrate the high potential of short peptides as efficient catalysts and establish a basis for further investigations. These may include the application of peptides as catalysts for other 1,4-addition reactions using different Michael donors (e.g. ketones, malonates, nitroalkanes) and Michael acceptors (e.g. α,β-unsaturated aldehydes and ketones, β-disubstitued nitroolefins). Also new challenging transformations such as e.g. α-alkylation of aldehydes or complex cascade reactions might become accessible by using peptides as catalysts.

IV.
Experimental Section

14. General Aspects

Materials and reagents were of the highest commercially available grade purchased from Fluka, Aldrich, Lancaster, Acros, Riedel, TCI or Alfa Aesar and used without further purification. Resins for solid phase synthesis were obtained from Novabiochem (Merck Biosciences), Rapp Polymere or Bachem AG and amino acid derivatives from Bachem AG or from the Poly Peptide Group. Reactions requiring anhydrous conditions were carried out using oven-dried glassware (overnight at 110 °C), which was assembled hot and cooled under nitrogen. Reactions were monitored by thin layer chromatography using aluminium-backed Merck silica gel 60 F_{254} plates. Compounds were visualized by UV, ceric ammonium molybdate (CAM), $KMnO_4$ and/or ninhydrin solutions. Flash chromatography was performed using Merck or Fluka silica gel 60, particle size 40-63 μm. Solvents for extractions and for column chromatography were previously distilled. Yields given are based upon chromatographically and spectroscopically (^{1}H and ^{13}C NMR) pure materials. ^{1}H and ^{13}C NMR spectra were recorded on a Bruker DMX600, DPX500, DPX400 or av250 spectrometer. Chemical shifts are reported in ppm using TMS, TSP (sodium salt) or the residual solvent peak as a reference. The assignement of the signals of complex compounds was carried out by COSY, HMQC and HMBC analysis. Ion exchange was performed using Dowex® resin (1x2-400) from Sigma-Aldrich or VariPure™ IPE tubes from Varian. Electrospray (ESI) mass spectra were recorded on a Finnigan MAT LCQ and on a Bruker esquire 3000plus spectrometer. Analytical grade methanol was used as the carrier solvent, with samples prepared to a final concentration of approximately 1 mg/mL. High resolution mass spectroscopy (HRMS) was carried out on an Applied Biosystems Sciex QStar Pular spectrometer (MS Service UNI-Bern). Elemental analysis was performed on a Perkin-Elmer 240 Analyser (Dr. W. Kirsch, UNI-Basel). Normal Phase HPLC analysis was carried out on an analytical HPLC with a diode array detector SPD-M10A from Shimadzu using Chiracel columns (AD, AD-H, AS-H, OD-H) (250 mm x 4.6 mm) from Daicel or on a ReproSil Chrial-AM (250 mm x 4.6 mm) column from 'Dr.Maisch'. GC analyses were performed on a Focus GC with a flame ionization detector (FID) from Brechbühler AG using a Chiraldex G-TA column. Optical rotations were measured on a Perkin Elmer Polarimeter 341. CD-spectra were measured on an Applied Biophysics Chirascan spectrometer. For automated peptide synthesis, a Syro I Peptide Synthesizer (MultiSynTech) was employed. *In situ* FT-

IR spectroscopy was carried out on a ReactIR R4000 (SiComp probe connected to an MCT detector with K6 conduit) from Mettler Toledo. Karl-Fischer titrations were performed with a Titrando KF titrator from Metrohm (Bachem AG, Bubendorf). X-ray analysis was performed on a Nonius KappaCCD diffractometer at 173K (M. Neuburger, UNI-Basel).

15. General Protocols

15.1 General Protocols for Solid-Phase Peptide Synthesis

Peptides were prepared on solid-phase polymeric supports following the general protocols for manual or automated Fmoc/*t*Bu peptide synthesis.[161] Prior to manual peptide synthesis, reaction vessels were silylated to reduce the tendency of the resin beads to stick to the glass surfaces. This was achieved through overnight agitation of reaction vessels containing a solution of 10 % (v/v) TMSCl in anhydrous toluene. Before use, reaction vessels were washed with CH_2Cl_2 (5x) and 'baked out' at 110 ^oC overnight.

Protocol A1: *Functionalisation of Rink Amide AM/MBHA and Sieber Amide resin*
Rink and Sieber resins are usually Fmoc-protected as supplied and must be deprotected prior to the first amino acid functionalisation as follows: 20 % (v/v) piperidine in DMF was added to the resin (pre-swollen in DMF and drained) and the reaction mixture was agitated for 10 min, drained, rinsed with neat DMF, and treated with 20 % (v/v) piperidine in DMF once more for a further 10 min. The resin was then washed alternatively with DMF and CH_2Cl_2 (5x each). The coupling of the first amino acid occurred under the same conditions as described for general solid phase synthesis using HCTU/*i*-Pr_2NEt or DIC/HOBt (Protocol B & C).

Protocol A2: *Functionalisation of Wang resin*
To a suspension of Wang OH resin (pre-swollen in CH_2Cl_2), was added a solution of the Fmoc amino acid (3 eq), *N*-methylimidazole (2.5 eq) and MSNT (3 eq) in anhydrous CH_2Cl_2 (THF may be required to aid dissolution of MSNT). The reaction mixture was agitated at RT for 1 h, then washed alternatively with DMF (5x) and CH_2Cl_2 (5x). Functionalisation of the resin was determined by quantitative Fmoc test.[162]

Protocol A3: *Functionalisation of 2-Chlorotrityl chloride resin*

A preformed solution of the Fmoc amino acid (4 eq) and *i*-Pr_2NEt (5 eq) dissolved in anhydrous CH_2Cl_2 was added to a suspension of the resin (pre-swollen in anhydrous CH_2Cl_2). The reaction mixture was agitated for 1 h and washed with a mixture of CH_2Cl_2/MeOH/*i*-Pr_2NEt (17:2:1 v/v/v, 5x), CH_2Cl_2 (5x), DMF (5x) and CH_2Cl_2 (5x). Functionalisation of the resin was determined by quantitative Fmoc test.[162]

Protocol B1: *Manual peptide synthesis using HCTU/i-Pr_2NEt*

i-Pr_2NEt (6 eq) was added to a solution of the Fmoc-amino acid (2 eq) and HCTU (2 eq) in the minimum amount of DMF necessary. The coupling cocktail was aged for 2 min and then added directly to the amino-functionalised resin (pre-swollen in DMF and drained). The reaction mixture was agitated for 45 - 60 min before washing alternatively with DMF (5x) and CH_2Cl_2 (5x). The completeness of each coupling was monitored using standard tests according to the functionalisation of the *N*-terminus (Chloranil,[163] TNBS[162, 164] or Kaiser[165] test). In the case of incomplete functionalisation of the resin, the entire coupling procedure was repeated. In the case of complete coupling, the Fmoc deprotection was performed as follows: A solution of 20 % (v/v) piperidine in DMF was added to the resin (pre-swollen in DMF) and the reaction mixture was agitated for 5 min, drained, and the piperidine treatment repeated a second time for 10 min. Finally the resin was thoroughly washed with DMF (5x) and CH_2Cl_2 (5x). The completeness of deprotection was monitored using standard tests according to the functionalisation of the free *N*-teminus (Chloranil,[163] TNBS[162, 164] or Kaiser[165] test). The entire protocol was then repeated for the next cycle. The final Fmoc deprotection was omited when the corresponding Boc-amino acid was employed for the last coupling.

Protocol B2: *Manual peptide synthesis using DIC/HOBt*

A solution of the Fmoc-amino acid (2 eq) and HOBt (2 eq) dissolved in the minimum amount of DMF necessary was added to the suspension of the amino-functionalised resin (pre-swollen in CH_2Cl_2 and drained). The mixture was agitated for 2 min before addition of DIC (2 eq) and then agitated for a further 45-60 min. The suspension was washed alternatively with DMF (5x) and CH_2Cl_2 (5x). The completeness of each coupling was monitored using standard tests according to the functionalisation of the *N*-terminus (Chloranil,[163] TNBS[162, 164] or Kaiser[165] test). In the case of incomplete functionalisation of the resin, the entire coupling procedure

was repeated. In the case of complete coupling, the Fmoc deprotection was performed as follows: A solution of 20 % (v/v) piperidine in DMF was added to the resin (pre-swollen in DMF) and the reaction mixture was agitated for 5 min, drained, and the piperidine treatment repeated a second time for 10 min. Finally the resin was thoroughly washed with DMF (5x) and CH_2Cl_2 (5x). The completeness of deprotection was monitored using standard tests according to the functionalisation of the free *N*-teminus (Chloranil,[163] TNBS[162, 164] or Kaiser[165] test). The entire protocol was then repeated for the next cycle. The final Fmoc deprotection was omited when the corresponding Boc-amino acid was employed for the last coupling.

Protocol C: *Automated peptide synthesis*

i-Pr_2NEt (12 eq as a 3 M solution in *N*-methylpyrrolidone) was added to a solution of Fmoc-amino acid (4 eq) and HCTU (4 eq) in DMF. The activated amino acid was added to the amino-functionalized resin, swollen in DMF (≈100 mM concentration) and the mixture was agitated for 1.5 h before washing with DMF (5x). The Fmoc deprotection was performed by the addition of 40 % (v/v) piperidine in DMF to the resin (preswollen in DMF). The reaction mixture was agitated for 3 min, drained and the piperidine treatment repeated for 10 min. Finally the resin was washed with DMF (7x). The entire protocol was then repeated for the next cycle. The final Fmoc deprotection was omited when the corresponding Boc-amino acid was employed for the last coupling.

Protocol D: *Cleavage from the solid support and isolation of peptides*

The solid supported peptides were cleaved from the resin by agitation in a mixture of acid in CH_2Cl_2 (Wang resin = TFA/CH_2Cl_2 1:1 v/v, Rink Amide resin = TFA/CH_2Cl_2 1:1 v/v and 2-chlorotrityl chloride resin = neat TFA) for 1 h and then repeated for a further 30 min. The acidic filtrates were combined and removal of all volatiles under reduced pressure followed by precipitation with Et_2O afforded the crude peptides as their trifluoroacetate salts. Peptide salts were then triturated with Et_2O (at least 3 times) and filtered over a fine glass frit (grade 3) or a syringe filter, dried under high vacuum and used without further purification unless specifically stated.

15.2 General Protocols for 1,4-Addition Reactions

Protocol E: *1,4-Addition reaction of aldehydes to nitroolefins*

Standard conditions:

Calculated for 1 mol% TFA•H- D-Pro-Pro-Glu-NH_2 ***56*** *(454.4 g/mol)*

NMM (5.0 µL, 44 µmol, 0.1 eq) was dissolved in the specified solvent (10 mL). 1 mL of this solution was added to the catalyst (2.0 mg, 4.40 µmol. 0.01 eq) and the mixture was stirred for 5 min. The nitroolefin (0.44 mmol, 1 eq) and the aldehyde (0.66-1.32 mmol, 1.5-3 eq) were added and the reaction mixture (homogenous solution) was stirred or shaken (thermo shaker) at the specified temperature. The progress of the reaction was followed by TLC or by ^{1}H NMR spectroscopy of the crude reaction mixture (~100 µL + 400 µL $CDCl_3$). After completion, the reaction mixture was directly separated by flash column chromatography on silica gel eluting with a mixture of pentanes and EtOAc. Collected fractions were concentrated *in vacuo* and the product was dried under high vaccum.

Schlenk conditions:

Glassware was heated out under N_2 flow. All solvents (crown cap quality), aldehydes and stock-solutions were dried with molecular sieves (3 Å, activated in microwave for 2 min at 750 W) and stored under a N_2 atmosphere. Reactions were set up under a N_2 atmosphere.

Calculated for 1 mol% TFA•H- D-Pro-Pro-Glu-NH_2 ***56*** *(454.4 g/mol)*

NMM stock-solution (44 mM; 100 µL, 0.01 eq) was added to the catalyst (2.0 mg, 4.40 µmol. 0.01 eq). The aldehyde (0.44 mmol, 1 eq), the nitroolefin stock-solution (1.34 M; 1230 µL, 0.66 mmol, 1.5 eq) and solvent (0.5 mL) were added and the reaction mixture (homogenous solution) was stirred at RT. The progress of the reaction was followed by ^{1}H NMR spectroscopy of the crude reaction mixture (~100 µL + 400 µL $CDCl_3$). After completion, the reaction mixture was directly separated by flash column chromatography on silica gel eluting with a mixture of pentanes and EtOAc. Collected fractions were concentrated *in vacuo* and the product was dried under high vaccum.

Calculated for 0.1 mol% TFA•H- D-Pro-Pro-Glu-NH_2 ***56*** *(454.4 g/mol)*

NMM stock-solution (0.44 mM; 50 µL, 0.001 eq), the aldehyde (2.20 mmol, 1 eq) and solvent (3.5 mL) were added to the catalyst (1 mg, 2.20 µmol, 0.001 eq). The nitroolefin (3.30 mmol,

1.5 eq) was added as a solid and the reaction mixture (homogenous solution) was stirred at RT. The progress of the reaction was followed by ^{1}H NMR spectroscopy of the crude reaction mixture (~100 µL + 400 µL $CDCl_3$). After completion, the reaction mixture was directly separated by flash column chromatography on silica gel eluting with a mixture of pentanes and EtOAc. Collected fractions were concentrated *in vacuo* and the product was dried under high vaccum.

Protocol F: *1,4-Addition reaction of aldehydes to nitroethylene*
Calculated for 1 mol% TFA•H-D-Pro-Pro-Glu-NH_2 ***56*** *(454.4 g/mol)*
The aldehyde (0.66 mmol, 1.5 eq) and NMM (4.40 µmol, 0.01 eq = 2.2 mL from a 2 mM NMM stock-solution in chloroform) were added to the catalyst (2mg, 4.40 µmol, 0.01 eq). Nitroethylene (0.44 mmol, 1.0 eq = 2.2 mL from a 0.2 M nitroethylene stock-solution in chloroform) was added and the reaction mixture (homogenous solution) was stirred or shaken (thermo shaker) at RT. The progress of the reaction was followed by ^{1}H NMR spectroscopy of the crude reaction mixture (~100 µL + 400 µL $CDCl_3$). After completion of the reaction, the mixture was cooled to -15 °C (ice/salt bath) and borane 1M in THF (0.75 mmol, 1.7 eq) was added. The mixture was stirred for 1 h at -15 °C. After completion of the reduction, the mixture was quenched with AcOH (2.2 mmol, 5 eq) and the solvent was evaporated. The crude product was directly separated by flash column chromatography on silica gel eluting with a mixture of pentanes and EtOAc. Collected fractions were concentrated *in vacuo* and the product was dried under high vaccum.

15.3 General Protocol for Ion Exchange of Peptides

Protocol G: *Ion pair extraction with VariPure tube*
The desalting occurred by ion pair extraction using a VariPure™ IPE tube (Varian, Inc.). The crude TFA•peptide (50-100 mg) was dissolved in water (1.5 mL) and loaded on the VariPure™ IPE tube which was previously rinsed with MeOH (2 mL). After eluting without pressure, the tube was washed with water until no more peptide was traced (TLC spots visualised with ninhydrin). Peptide containing fractions were pooled and lyophilised. The desalted peptide was obtained as a white solid (~80%). The absence of TFA was confirmed by ^{19}F NMR analysis.

16. Peptides, Building Blocks and Substrates

16.1 Characterisation Index

Peptides prepared by solid-phase synthesis

TFA•H-Pro-Pro-Asp-NH_2 **1**
TFA•H-Pro-Pro-OH **4**
TFA•H-Pro-Asp-NH_2 **5**
TFA•H-Pro-Pro-Asp-Pro-NH_2 **6**
TFA•H-Pro-Pro-Asp-Pro-Pro-NH_2 **7**
TFA•H-Pro-Pro-β-homo-Asp-NH_2 **9**
TFA•H-Pro-Pro-β-homo-Asp-OH **10**
TFA•H-Pro-Pro-Asn-OH **11**
TFA•H-Pro-Pro-Ser-OH **12**
TFA•H-Pro-Pro-His-OH **13**
TFA•H-Pro-Pro-Gly-OH **14**
TFA•H-Pro-Pro-Cys(SO_3H)-NH_2 **15**
TFA•H-Pro-MePro-Asp-NH_2 **16**
TFA•Me-Pro-Pro-Asp-NH_2 **17**
Ac-Pro-Pro-Asp-NH_2 **18**
TFA•H-D-Pro-Pro-Asp-NH_2 **21**
TFA•H-Pro-D-Pro-Asp-NH_2 **19**
TFA•H-Pro-Pro-D-Asp-NH_2 **20**
TFA•H-D-Pro-Pro-Asp-Pro-NH_2 **24**
TFA•H-Pro-D-Pro-Asp-Pro-NH_2 **25**
TFA•H-Pro-Pro-D-Asp-Pro-NH_2 **22**
TFA•H-Pro-Pro-Asp-D-Pro-NH_2 **26**
TFA•H-Pro-Pro-D-Asp-D-Pro-NH_2 **27**
TFA•H-Pro-D-Pro-Asp-D-Pro-NH_2 **23**
TFA•H-Pro-D-Pro-D-Asp-Pro-NH_2 **28**
TFA•H-D-Pro-Pro-Asn-OH **29**
TFA•H-D-Pro-Pro-D-Asn-OH **30**
TFA•H-D-Pro-Pro-Ser-OH **31**
TFA•H-D-Pro-Pro-His-OH **32**
TFA•H-Pro-D-Ala-D-Asp-NH_2 **2**
TFA•H-D-Pro-Pro-Asn-NH_2 **48**
H-D-Pro-Pro-Asp(O*t*Bu)-NH_2 **49** (desalted)
TFA•H-D-Pro-Pro-β-homo-Asp-NH_2 **52**
TFA•H-D-Pro-Pro-Asp-OH **53**
TFA•H-D-Pro-Pro-Asp-NH-TentaGel **55**
TFA•H-D-Pro-Pro-Gly-OH **62**
TFA•H-D-Pro-Pro-β-Ala-OH **50**
TFA•H-D-Pro-Pro-γ-Abu-OH **63**
TFA•H-D-Pro-Pro-Glu-NH_2 **56**
H-D-Pro-Pro-Glu-NH_2 **56** (desalted)
TFA•H-D-Pro-Pro-Aad-NH_2 **57**
TFA•H-D-Pro-Pro-Api-NH_2 **58**
TFA•H-D-Pro-Pro-Asu-NH_2 **59**
TFA•H-D-Pro-Pro-D-Asn-OH **60**
TFA•H-D-Pro-Pro-D-Gln-OH **61**
TFA•H-Pro-Pro-Glu-NH_2 **65**
TFA•H-Pro-D-Pro-Glu-NH_2 **66**
TFA•H-Pro-Pro-D-Glu-NH_2 **67**
TFA•H-D-Pro-Pro-Gln-NH_2 **75**

Peptides prepared by solution-phase synthesis

Boc-Pro-Pro-OH **90**

Boc-D-Pro-Pro-OH **91**

TFA•H-Pro-Pro-Asp-OMe **8**

TFA•H-D-Pro-Pro-Asp-OMe **51**

TFA•H-D-Pro-Pro-Asp-NHPr **54**

TFA•H-D-Pro-Pro-5-Ava-OH **64**

Boc-Pro-2-MePro-OH **92**

Synthesis of non-commercial available building blocks

Fmoc- β-homo-Asp(O*t*Bu)-OH **93**

N-Me-Pro-OH **94**

HCl•H-5-Ava-OMe **95**

H-Asp(O*t*Bu)-NHPr **96**

Synthesis of non-commercial available substrates

(E)-1-Nitro-1-cyclohexylethene

(E)-4-Methyl-1-nitropent-1-ene

(E)-1-Nitro-1-heptene

(E)-3,3-Dimethoxy-1-nitro-propene **69**

Nitroethylene

16.2 Peptides Prepared by Solid-Phase Synthesis

Peptides on solid support were prepared eighter by automated or by manual synthesis (Fmoc/*t*Bu strategy)[161] according to the general procedures and obtained as white solids and in yields of 70 % to 95 % unless otherwise stated.

TFA•H-Pro-Pro-Asp-NH_2 (1)

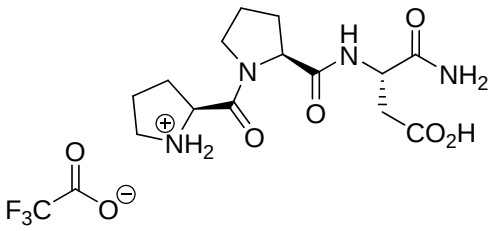

Prepared on Rink Amide AM resin (0.62 mmol/g) on a 10 mmol scale according to the general protocols for functionalisation of Rink Amide AM resin (Protocol A1) and for manual peptide synthesis using DIC/HOBt (Protocol B2). Fmoc-Asp(O*t*Bu)-OH was used for the first and Fmoc-Pro-OH for the second and third coupling. Cleavage from the solid support and isolation of the peptide was carried out according to the general protocol (Protocol D).

^{1}H-NMR (500 MHz, d6-DMSO, 23°C): The conformers were observed in the ratio 5:2. Major conformer: δ = 8.15 (d, *J* = 8.0 Hz, 1H), 7.13 (s, 1H), 7.11 (s, 1H), 4.47 (dd, *J* = 8.3 Hz, 5.9 Hz, 1H), 4.41 (dt, *J* = 6.7 Hz, 14.4 Hz, 1H), 4.36 (dd, *J* = 8.5 Hz, 5.2 Hz, 1H), 3.63 (m, 1H), 3.45 (m, 1H), 3.24 (m, 1H), 3.16 (m, 1H), 2.65, (dd, *J* = 16.4 Hz, 6.3 Hz, 1H), 2.51 (dd, *J* = 16.4 Hz, 6.9 Hz, 1H), 2.39 (m, 1H), 2.12 (m, 1H), 1.97-1.79 (m, 6H); Minor conformer: δ = 8.57 (d, *J* = 8.1 Hz, 1H), 7.41 (s, 1H), 7.13 (s, 1H), 4.53 (dt, *J* = 5.3 Hz, 7.7 Hz, 1H), 4.42 (m, 1H), 3.93 (t, *J* = 8.4 Hz, 1H), 3.52 (m, 1H), 3.42 (m, 1H), 3.35 (m, 1H), 3.27 (m, 1H), 2.72, (dd, *J* = 16.5 Hz, 5.4 Hz, 1H), 2.55 (dd, *J* = 16.3 Hz, 8.6 Hz, 1H), 2.39 (m, 1H), 2.24 (m, 1H), 2.04 (m, 1H), 1.97-1.79 (m, 5H).

^{13}C-NMR (125.6 MHz, d6-DMSO, 23°C): Major conformer: δ = 172.2, 171.9, 170.7, 167.1, 60.0, 58.3, 49.3, 46.8, 45.9, 36.0, 28.9, 27.9, 24.5, 23.5; Minor conformer: δ = 172.0, 172.0, 170.6, 166.8, 58.9, 58.4, 49.5, 47.4, 45.5, 36.3, 31.6, 27.3, 23.6, 22.0.

MS (ESI): *m/z* (%): 327.4 (100) $[M+H]^+$, 349.5 (24) $[M+Na]^+$. M = 326.3 calcd for $C_{14}H_{22}N_4O_5$.

TFA•H-Pro-Pro-OH (4)

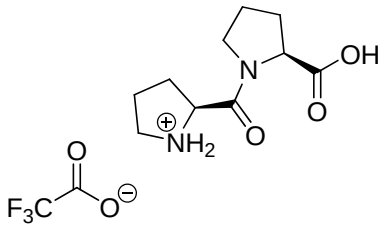

Prepared on 2-Chlorotrityl resin (1.60 mmol/g) on a 4 mmol scale according to the general protocols for functionalisation of 2-Chlorotrityl resin (Protocol A3) and for manual peptide synthesis using DIC/HOBt (Protocol B2). Fmoc-Pro-OH was used for the first and Boc-Pro-OH for the second coupling. Cleavage from the solid support and isolation of the peptide was carried out according to the general protocol (Protocol D). The peptide was precipitated as a golden gum by addition of Et_2O and dried *in vacuo* to a golden foam (99 %).

^{1}H NMR (400 MHz, D_2O, 22°C): δ = 4.29 (t, *J* = 7.8 Hz, 2H), 3.41 (m, 2H), 3.30 (m, 2H), 2.16 (m, 2H), 1.93 (m, 2H), 1.84 (m, 4H).

^{13}C NMR (100 MHz, D_2O, 22°C): δ = 168.3, 60.6, 45.2, 27.2, 22.6.

MS (ESI)**:** *m/z* (%): 211.1 (100) $[M-H]^-$. M = 212.2 calcd for $C_{10}H_{16}N_2O_3$.

TFA•H-Pro-Asp-NH_2 (5)

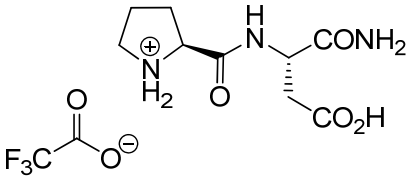

Prepared on Rink Amide AM Resin (0.62 mmol/g) on a 150 µmol scale according to the general protocols for functionalisation of Rink Amide AM resin (Protocol A1) and for automated peptide synthesis (Protocol C). Fmoc-Asp(O*t*Bu)-OH was used for the first and Fmoc-Pro-OH for the second coupling. Cleavage from the solid support and isolation of the peptide was carried out according to the general protocol (Protocol D).

^{1}H NMR (400 MHz, D_2O, 22°C): δ = 4.68 (m, 1H), 4.41 (dd, J = 6.6 Hz, 8.6 Hz, 1H), 3.42 (m, 2H), 2.99 – 2.80 (m, 2H), 2.46 (m, 1H), 2.18 – 2.02 (m, 3H).

^{13}C NMR (100 MHz, D_2O, 22°C): δ = 177.5, 172.7, 172.4, 62.8, 53.6, 49.6, 39.0, 32.7, 26.9.

MS (ESI)**:** *m/z* (%): 230.1 (100) $[M+H]^+$. M = 229.2 calcd for $C_9H_{15}N_3O_4$.

TFA•H-Pro-Pro-Asp-Pro-NH_2 (6)

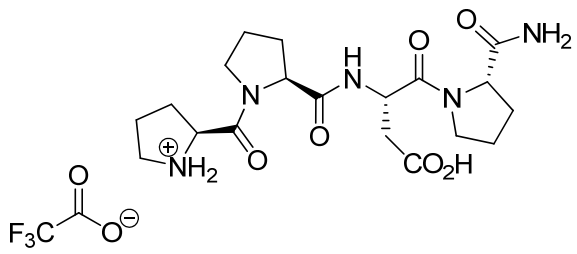

Prepared on Rink Amide AM Resin (0.71 mmol/g) on a 200 µmol scale according to the general protocols for functionalisation of Rink Amide AM resin (Protocol A1) and for automated peptide synthesis (Protocol C). Fmoc-Pro-OH was used for the first, the third and the fourth coupling, Fmoc-Asp(O*t*Bu)-OH was used for the second coupling. Cleavage from the solid support and isolation of the peptide was carried out according to the general protocol (Protocol D).

^{1}H-NMR (400 MHz, d6-DMSO, 23°C): The conformers were observed in the ratio 7:2:1. Major conformer: δ = 9.38 (s, 1H), 8.51 (m, 1H), 8.33 (d, *J* = 7.9 Hz, 1H), 6.99 (s, 1H), 6.98 (s, 1H), 4.77 (dd, *J* = 14.7 Hz, 6.9 Hz, 1H), 4.46 (m, 1H), 4.34 (m, 1H), 4.15 (m, 1H), 3.66-3.35 (m, 4H), 3.20 (m, 2H), 2.80 (m, 1H), 2.40 (m, 1H), 2.16-1.70 (m, 12H). Signals of minor conformers: δ = 8.79 (d, J = 7.8 Hz), 8.15 (d, *J* = 7.9 Hz), 7.08 (s), 7.06 (s), 7.04 (s), 4.89-4.82 (m), 4.21-4.18 (m).

^{13}C NMR (100 MHz, d6-DMSO, 22°C): Major conformer: δ = 173.4, 172.1, 170.6, 168.9, 166.5, 59.7, 59.5, 58.2, 47.4, 46.7, 46.5, 45.7, 35.9, 29.2, 29.0, 27.8, 24.4, 24.1, 23.5. No signals of minor conformers observed.

MS (ESI)**:** *m/z* (%): 422.2 (100) $[M-H]^-$. M = 423.5 calcd for $C_{19}H_{29}N_5O_6$.

TFA•H-Pro-Pro-Asp-Pro-Pro-NH$_2$ (7)

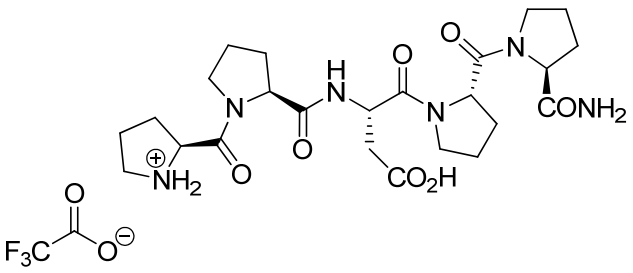

Prepared on Rink Amide AM Resin (0.62 mmol/g) on a 150 µmol scale according to the general protocols for functionalisation of Rink Amide AM resin (Protocol A1) and for automated peptide synthesis (Protocol C). Fmoc-Pro-OH was used for the first, the second, the fourth and the fifth coupling, Fmoc-Asp(O*t*Bu)-OH was used for the third coupling. Cleavage from the solid support and isolation of the peptide was carried out according to the general protocol (Protocol D).

^{1}H-NMR (400 MHz, D_2O, 23°C): δ = 4.96 (dd, *J* = 5.1 Hz, 8.8 Hz, 1H), 4.66 (m, 2H), 4.47 (dd, *J* = 6.2 Hz, 8.5 Hz, 1H), 4.38 (dd, *J* = 5.4 Hz, 8.5 Hz, 1H), 3.80 (m, 1H), 3.69 (m, 2H), 3.58 (m, 1H), 3.42 (m, 2H), 2.95 (m, 1H), 2.72 (dd, *J* = 8.8 Hz, 17.0 Hz, 1H), 2.57 (m, 1H), 2.33 (m, 3H), 2.12 – 1.85 (m, 14H).

^{13}C NMR (100 MHz, D_2O, 22°C): δ = 177.1, 176.9, 176.7, 175.5, 173.2, 171.5, 63.8, 63.7, 62.6, 62.4, 51.9, 51.3, 51.3, 51.2, 51.1, 50.1, 38.3, 33.0, 32.8, 31.8, 31.6, 28.1, 28.1, 27.3.

MS (ESI)**:** *m/z* (%): 521.2 (100) $[M+H]^+$. M = 520.6 calcd for $C_{24}H_{36}N_6O_7$.

TFA•H-Pro-Pro-β-homo-Asp-NH$_2$ (9)

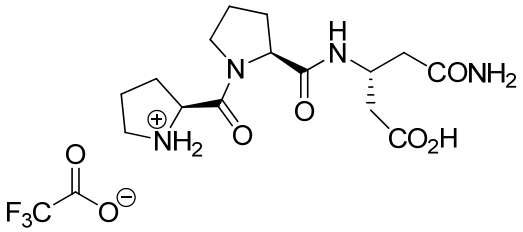

Prepared on Rink Amide AM resin (0.62 mmol/g) on a 2 mmol scale according to the general protocols for functionalisation of Rink Amide AM resin (Protocol A1) and for manual peptide synthesis using HCTU/*i*-Pr_2NEt (Protocol B1). Fmoc-β-homo-Asp(O*t*Bu)-OH **93** was used for the first and Fmoc-Pro-OH for the second and third coupling. Cleavage from the solid support and isolation of the peptide was carried out according to the general protocol (Protocol D).

^{1}H NMR (400 MHz, D_2O, 25°C) δ = 4.47 (dd, *J* = 6.6 Hz, 8.6 Hz, 1H), 4.41 (m, 1H), 4.25 (dd, *J* = 6.1 Hz, 8.4 Hz, 1H), 3.54 (m, 1H), 3.45 (m, 1H), 3.26 (m, 2H), 2.54 (dd, *J* = 2.3 Hz, 6.8 Hz, 2H), 2.45 (dd, *J* = 5.1 Hz, 14.6 Hz, 2H), 2.35 (dd, *J* = 9.2 Hz, 14.6 Hz, 1H), 2.15 (m, 1H), 2.00-1.80 (m, 5H), 1.75 (m, 1H).

^{13}C NMR (100 MHz, D_2O, 25°C) δ = 175.8, 175.0, 173.2, 168.4, 61.2, 59.5, 48.0, 47.0, 44.5, 39.8, 38.7, 30.0, 28.7, 24.9, 24.3.

MS (ESI): *m/z* (%): 341.3 (100) $[M+H]^+$. M = 340.4 calcd for $C_{15}H_{24}N_4O_5$.

TFA•H-Pro-Pro-β-homo-Asp-OH (10)

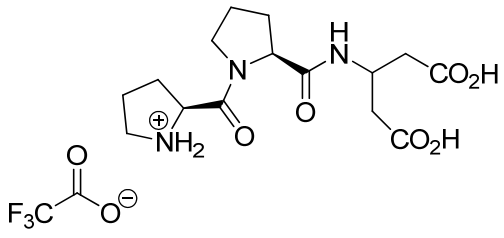

Prepared on Wang resin (1.0 mmol/g) on a 2 mmol scale according to the general protocols for functionalisation of Wang resin (Protocol A2) and for manual peptide synthesis using HCTU/*i*-Pr_2NEt (Protocol B1). Fmoc-β-homo-Asp(O*t*Bu)-OH **93** was used for the first and Fmoc-Pro-OH for the second and third coupling. Cleavage from the solid support and isolation of the peptide was carried out according to the general protocol (Protocol D).

^{1}H NMR (400 MHz, D_2O, 25°C) δ = 4.48-4.30 (m, 2H), 4.19 (dd, *J* = 6.0 Hz, 8.4 Hz, 1H), 3.47 (m, 1H), 3.39 (m, 1H), 3.22 (m, 2H), 2.61-2.46 (m, 3H), 2.41 (dd, *J* = 8.8 Hz, 16.0 Hz, 2H), 2.08 (m, 1H), 1.94-1.73 (m, 5H), 1.68 (m, 1H).

^{13}C NMR (100 MHz, D_2O, 25°C) δ = 175.0, 174.9, 173.1, 168.3, 61.2, 59.4, 48.0, 46.9, 43.9, 38.6, 38.5, 29.8, 28.7, 24.8, 24.2.

MS (ESI): *m/z* (%): 342.2 (100) $[M+H]^+$. M = 341.4 calcd for $C_{15}H_{23}N_3O_6$.

TFA•H-Pro-Pro-Asn-OH (11)

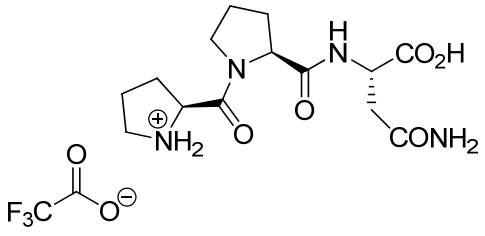

Prepared on Wang resin (1.0 mmol/g) on a 2 mmol scale according to the general protocols for functionalisation of Wang resin (Protocol A2) and for manual peptide synthesis using HCTU/*i*-Pr_2NEt (Protocol B1). Fmoc-Asn(Trt)-OH was used for the first and Fmoc-Pro-OH for the second and third coupling. Cleavage from the solid support and isolation of the peptide was carried out according to the general protocol (Protocol D).

^{1}H NMR (400 MHz, D_2O, 25°C) δ = 4.58 (dd, J = 6.1 Hz, 6.2 Hz, 1H), 4.50 (dd, J = 6.1 Hz, 8.5 Hz, 1H), 4.37 (dd, J = 5.3 Hz, 8.5 Hz, 1H), 3.56 (m, 1H), 3.48 (m, 1H), 3.28 (m, 2H), 2.73 (d, J = 6.2 Hz, 2H), 2.44 (m, 1H), 2.20 (m, 1H), 2.02-1.78 (m, 6H).

^{13}C NMR (100 MHz, D_2O, 25°C) δ = 175.0, 174.3, 173.8, 168.5, 60.9, 59.5, 49.8, 48.0, 47.0, 36.4, 29.6, 28.8, 24.9, 24.2.

MS (ESI): *m/z* (%): 327.2 (100) $[M+H]^+$. M = 326.3 calcd for $C_{14}H_{22}N_4O_5$.

TFA•H-Pro-Pro-Ser-OH (12)

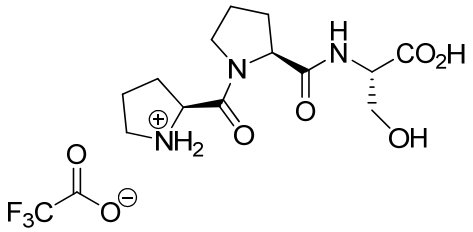

Prepared on Wang resin (1.0 mmol/g) on a 2 mmol scale according to the general protocols for functionalisation of Wang resin (Protocol A2) and for manual peptide synthesis using HCTU/*i*-Pr_2NEt (Protocol B1). Fmoc-Ser(*t*Bu)-OH was used for the first and Fmoc-Pro-OH for the second and third coupling. Cleavage from the solid support and isolation of the peptide was carried out according to the general protocol (Protocol D).

^{1}H-NMR (500 MHz, D_2O, 23°C): δ = 4.63 (m, 1H), 4.54 (m, 1H), 4.49 (m, 1H), 3.93 (dd, *J* = 11.7 Hz, 4.6Hz, 2H), 3.70 (m, 1H), 3.59 (m, 1H), 3.39 (m, 2H), 2.55 (m, 1H), 2.35 (m, 1H), 2.02 (m, 6H).

^{13}C-NMR (125.6 MHz, D_2O, 23°C): δ = 173.7, 173.2, 168.0, 60.9, 60.4, 59.0, 54.9, 47.7, 46.6, 29.3, 28.3, 24.5, 23.8.

MS (ESI): *m/z* (%): 300 (100) $[M+H]^+$. M = 299.3 calcd for $C_{13}H_{21}N_3O_5$.

TFA•H-Pro-Pro-His-OH (13)

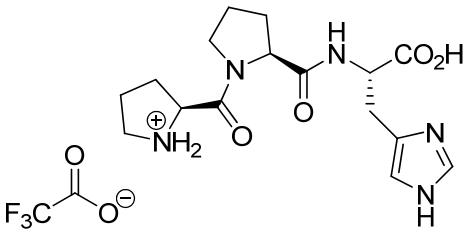

Prepared on Wang resin (1.0 mmol/g) on a 2 mmol scale according to the general protocols for functionalisation of Wang resin (Protocol A2) and for manual peptide synthesis using HCTU/*i*-Pr_2NEt (Protocol B1). Fmoc-His(Trt)-OH was used for the first and Fmoc-Pro-OH for the second and third coupling. Cleavage from the solid support and isolation of the peptide was carried out according to the general protocol (Protocol D).

^{1}H-NMR (500 MHz, D_2O, 23°C): δ = 8.60 (s, 1H), 7.33 (s, 1H), 4.72 (m, 1H), 4.61 (m, 1H), 4.43 (m, 1H), 3.67 (m, 1H), 3.57 (m, 1H), 3.39 (m, 2H), 3.31 (dd, *J* = 15.6 Hz, 5.2 Hz, 1H), 3.21 (dd, *J* = 15.4 Hz, 7.9 Hz, 1H), 2.54 (m, 1H), 2.29 (m, 1H), 2.01 (m, 5H), 1.87 (m, 1H).

^{13}C-NMR (125.6 MHz, D_2O, 23°C): δ = 173.4, 167.9, 133.3, 128.5, 117.2, 60.5, 59.0, 51.9, 47.7, 46.6, 29.3, 28.3, 26.1, 24.5, 23.8.

MS (ESI): *m*/*z* (%): 350 (100) $[M+H]^+$. M = 349.4 calcd for $C_{16}H_{23}N_5O_4$.

TFA•H-Pro-Pro-Gly-OH (14)

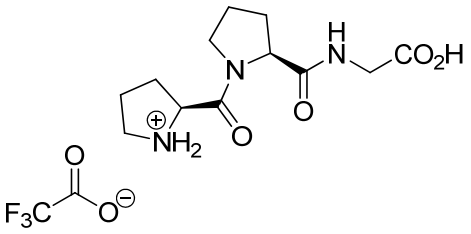

Prepared on Wang resin (1.0 mmol/g) on a 2 mmol scale according to the general protocols for functionalisation of Wang resin (Protocol A2) and for manual peptide synthesis using HCTU/*i*-Pr_2NEt (Protocol B1). Fmoc-Gly-OH was used for the first and Fmoc-Pro-OH for the second and third coupling. Cleavage from the solid support and isolation of the peptide was carried out according to the general protocol (Protocol D).

^{1}H NMR (400 MHz, D_2O, 25°C) δ = 4.51 (dd, *J* = 6.9 Hz, 7.2 Hz, 1H), 4.39 (dd, *J* = 6.5 Hz, 7.3 Hz, 1H), 3.93 (d, *J* = 18.0 Hz, 1H), 3.83 (d, *J* = 18.0 Hz, 1H), 3.59 (m, 1H), 3.47 (m, 1H), 3.29 (m, 2H), 2.44 (m, 1H), 2.24 (m, 1H), 1.91 (m, 6H).

^{13}C NMR (100 MHz, D_2O, 25°C) δ = 174.6, 173.3, 168.5, 60.9, 59.5, 48.1, 47.0, 41.4, 29.8, 28.7, 24.9, 24.2.

MS (ESI): *m*/*z* (%): 270.3 (100) $[M+H]^+$. M = 269.3 calcd for $C_{12}H_{19}N_3O_4$.

TFA•H-Pro-Pro-Cys(SO_3H)-NH_2 (15)

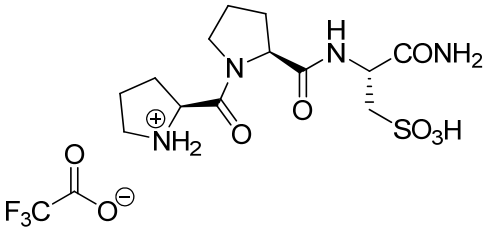

Prepared on Rink Amide MBHA resin (0.63 mmol/g) on a 2 mmol scale according to the general protocols for functionalisation of Rink Amide MBHA resin (Protocol A1) and for manual peptide synthesis using DIC/HOBt (Protocol B2). Fmoc-Cys(SO_3H)-OH was used for the first and Fmoc-Pro-OH for the second and third coupling. Cleavage from the solid support and isolation of the peptide was carried out according to the general protocol (Protocol D).

^{1}H-NMR (600 MHz, d6-DMSO, 25°C): The conformers were observed in the ratio 1:1. Conformer 1: δ = 9.29 (1H), 8.61 (1H), 8.52 (d, *J* = 8.2 Hz, 1H), 7.04 (1H), 6.89 (1H), 4.65 (m, 1H), 4.49 (m, 1H), 4.48 (m, 1H), 3.64 (m, 1H), 3.53 (m, 1H), 3.24 (m, 1H), 3.17 (m, 1H), 2.98 (dd, *J* = (13.9 Hz, 3.1 Hz, 1H), 2.83 (dd, *J* = 13.9 Hz, 11 Hz, 1H), 2.35 (m, 1H), 2.18 (m, 1H), 2.26 (m, 1H), 2.02 (m, 1H), 1.97 (m, 1H), 1.89 (m, 1H), 1.92 (m, 2H). Conformer 2: δ = 8.99 (1H), 8.68 (1H), 8.35 (d, *J* = 6.4 Hz, 1H), 7.41 (1H), 7.13 (1H), 4.35 (m, 1H), 4.29 (m, 1H), 4.18 (m, 1H), 3.51 (m, 1H), 3.39 (m, 1H), 3.17 (m, 2H), 2.85 (dd, *J* = 13.7 Hz, 6 Hz, 1H), 2.78 (dd, *J* = 13.7 Hz, 6 Hz, 1H), 2.31 (m, 1H), 2.14 (m, 1H), 1.94 (m, 2H), 1.89 (m, 1H), 1.81 (m, 1H), 1.81 (m, 2H).

^{13}C NMR (151 MHz, d6-DMSO, 25°C): Conformer 1: δ = 172.1, 171.0, 167.5, 59.6, 58.3, 51.6, 50.3, 46.7, 45.6, 31.0, 27.6, 24.2, 23.2. Conformer 2: 172.1, 170.1, 167.3, 60.6, 57.4, 50.6, 50.0, 46.9, 45.8, 22.3, 22.0.

HRMS (ESI) *m/z*: calcd for $C_{13}H_{23}N_4O_6S$ 363.1338; found, 363.1331.

TFA•H-Pro-2-MePro-Asp-NH$_2$ (16)

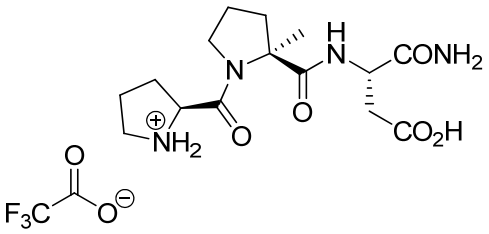

Prepared on Rink Amide AM resin (0.35 mmol/g) on a 0.4 mmol scale according to the general protocols for functionalisation of Rink Amide AM resin (Protocol A1) and for manual peptide synthesis using HCTU/*i*-Pr$_2$NEt (Protocol B1). Fmoc-Asp(O*t*Bu)-OH was used for the first coupling. The second coupling was carried out by using 4.0 eq Boc-Pro-2-methylproline-OH **94** and 4.0 eq HCTU/12.0 eq *i*-Pr$_2$NEt. Cleavage from the solid support and isolation of the peptide was carried out according to the general protocol (Protocol D) but using neat TFA.

^{1}H NMR (400 MHz, D$_2$O, 25°C): δ = 4.69 (m, 1H), 4.59 (m, 1H), 3.71 (m, 1H), 3.57 (m, 1H), 3.38 (m, 1H), 3.26 (m, 1H), 2.87, (dd, *J* = 15.4 Hz, 5.3 Hz, 1H), 2.76 (dd, *J* = 15.4 Hz, 7.5 Hz, 1H), 2.56 (m, 1H), 2.11 (m, 1H), 2.07-1.79 (m, 6H),1.52 (s, 3H).

^{13}C NMR (100 MHz, D$_2$O, 25°C) δ = 176.8, 175.7, 174.5, 169.6, 64.9, 60.8, 51.2, 49.5, 48.3, 38.2, 31.3, 30.1, 26.3, 25.5, 21.9.

MS (ESI): *m/z* (%): 341.4 (92) $[M+H]^+$. M = 340.4 calcd for $C_{15}H_{24}N_4O_5$.

TFA•Me-Pro-Pro-Asp-NH_2 (17)

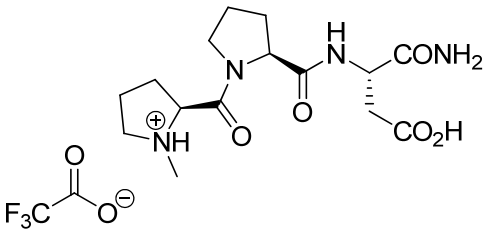

Prepared on Rink Amide AM resin (0.62 mmol/g) on a 3 mmol scale according to the general protocols for functionalisation of Rink Amide AM resin (Protocol A1) and for manual peptide synthesis using HCTU/*i*-Pr_2NEt (Protocol B1). Fmoc-Asp(O*t*Bu)-OH was used for the first coupling. The second coupling was performed with Fmoc-Pro-OH and the third coupling with *N*-Me-Pro-OH **94**. Cleavage from the solid support and isolation of the peptide was carried out according to the general protocol (Protocol D).

^{1}H-NMR (400 MHz, d6-DMSO, 25°C): The conformers were observed in the ratio 1.5:1. Major conformer: δ = 9.68 (br s, 1H) 8.22 (d, *J* = 8.0 Hz, 1H) 7.16 (s, 1H), 7.11 (s, 1H), 4.48 (m, 3H), 3.59 (m, 2H), 3.41 (m, 1H), 3.11 (m, 1H), 2.79 (s, 3H), 2.59 (m, 2H), 2.49 (m, 1H), 2.18–1.70 (m, 7H). Minor conformer: 9.74 (br s, 1H), 8.71 (d, *J* = 8.0 Hz, 1H), 7.46 (s, 1H), 7.16 (s, 1H), 4.53 (m, 1H), 4.33 (m, 1H), 4.85 (m, 1H), 3.59 (m, 2H), 3.41 (m, 1H), 3.11 (m, 1H), 2.73 (s, 3H), 2.59 (m, 2H), 2.25 (m, 1H), 2.18–1.70 (m, 7H).

^{13}C NMR (100 MHz, d6-DMSO, 25 ^{o}C): Major conformer: δ = 173.2, 173.0, 172.7, 171.5, 67.8, 60.8, 56.6, 50.3, 47.6, 36.9, 32.4, 29.8, 28.1, 25.2, 23.0. Minor conformer: 173.2, 173.1, 172.7, 171.7, 67.8, 59.9, 56.1, 50.4, 48.1, 36.9, 32.4, 29.8, 28.3, 25.2, 22.9.

HRMS (ESI) *m/z:* calcd for $C_{15}H_{25}N_4O_5$ 341.1824; found, 341.1823.

Ac-Pro-Pro-Asp-NH_2 (18)

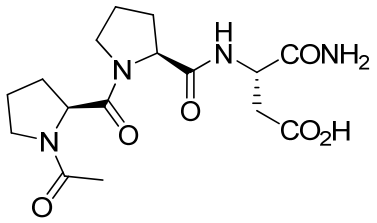

Prepared on Rink Amide AM resin (0.62 mmol/g) on a 3 mmol scale according to the general protocols for functionalisation of Rink Amide AM resin (Protocol A1) and for manual peptide synthesis using HCTU/*i*-Pr_2NEt (Protocol B1). Fmoc-Asp(O*t*Bu)-OH was used for the first coupling. The second and third coupling was performed with Fmoc-Pro-OH. *N*-terminal acetylation occured as follows: Et_3N (20 eq) and Ac_2O (20 eq) were added to the amine-functionalised resin (pre-swollen in CH_2Cl_2) to a final concentration of ~100 mM in CH_2Cl_2. The mixture was agitated for 1 h and then washed alternatively with DMF (5x) and CH_2Cl_2 (5x). The completeness of acetylation was monitored using the standard chloranil test.[163] Cleavage from the solid support and isolation of the peptide was carried out according to the general protocol (Protocol D).

^{1}H-NMR (400 MHz, d6-DMSO, 25°C): The conformers were observed in the ratio 3:1. Major conformer: δ = 10.50 (br s, 1H), 7.89 (d, *J* = 8.2 Hz, 1H), 7.15 (s, 1H), 6.99 (s, 1H), 4.51 (dd, *J* = 8.3 Hz, 3.2 Hz, 1H), 4.40 (m, 1H), 4.20 (dd, *J* = 8.3 Hz, 4.8 Hz 1H), 3.68 (m, 1H), 3.52 (m, 2H), 3.34 (m, 1H), 2.68 (dd, *J* = 16.4 Hz, 5.5 Hz, 1H), 2.57 (dd, *J* = 16.4 Hz, 7.3 Hz, 1H), 2.30–1.55 (m, 8H), 1.94 (s, 3H). Minor conformer: 10.50 (br s, 1H), 8.36 (d, *J* = 8.2 Hz, 1H), 7.37 (s, 1H), 7.22 (s, 1H), 4.72 (dd, *J* = 8.6 Hz, 2.5 Hz), 4.47 (m, 1H), 4.30 (dd, *J* = 8.1 Hz, 4.8 Hz, 1H), 3.68 (m, 1H), 3.52 (m, 2H), 3.34 (m, 1H), 2.76, (dd, *J* = 16.4 Hz, 4.9 Hz, 1H), 2.68 (dd, *J* = 16.4 Hz, 5.5 Hz, 1H), 2.30–1.55 (m, 8H), 1.76 (s, 3H).

^{13}C NMR (100 MHz, d6-DMSO, 25 ^{o}C): Major conformer: δ = 173.3, 173.1, 172.1, 171.7, 168.9, 61.0, 58.2, 50.1, 48.4, 47.7, 36.5, 29.5, 29.2, 25.5, 25.1, 22.9. Minor conformer: δ = 173.3, 173.2, 172.7, 172.7, 169.3, 59.5, 59.2, 50.2, 47.5, 46.9, 36.5, 29.4, 29.2, 25.5, 25.2, 23.1.

HRMS (ESI) *m/z:* calcd for $C_{16}H_{24}N_4O_6Na$ 391.1593; found, 391.1589.

TFA•H-D-Pro-Pro-Asp-NH_2 (21)

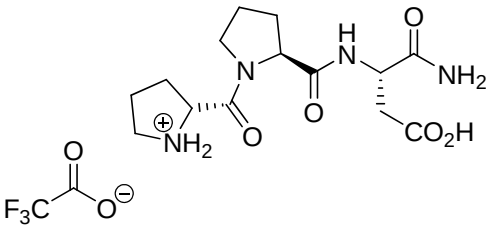

Prepared on Rink Amide AM resin (0.62 mmol/g) on a 10 mmol scale according to the general protocols for functionalisation of Rink Amide AM resin (Protocol A1) and for manual peptide synthesis using DIC/HOBt (Protocol B2). Fmoc-Asp(O*t*Bu)-OH was used for the first coupling. The second coupling was performed with Fmoc-Pro-OH and the third coupling with Fmoc-D-Pro-OH. Cleavage from the solid support and isolation of the peptide was carried out according to the general protocol (Protocol D).

^{1}H NMR (400 MHz, D_2O, 25°C) δ = 4.71 (dd, *J* = 5.3 Hz, 8.4 Hz, 1H), 4.64 (dd, *J* = 7.1 Hz, 8.7 Hz, 1H), 4.46 (dd, J = 3.7 Hz, 8.6 Hz, 1H), 3.73 (m, 1H), 3.60 (m, 1H), 3.42 (m, 1H), 2.97 (dd, *J* = 5.3 Hz, 16.9 Hz, 1H), 2.84 (dd, *J* = 8.4 Hz, 16.8 Hz, 1H), 2.55 (m, 1H), 2.31 (m, 1H), 2.11-1.97 (m, 6H).

^{13}C NMR (100 MHz, $CDCl_3$, 25°C) δ = 175.2, 174.5, 174.3, 168.9, 61.4, 58.8, 50.4, 48.1, 47.1, 35.8, 29.9, 28.5, 24.7, 24.4.

HRMS (ESI) *m/z*: calcd for $C_{14}H_{23}N_4O_5$ 327.1668; found, 327.1661.

TFA•H-Pro-D-Pro-Asp-NH_2 (19)

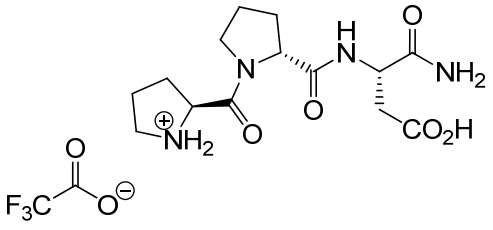

Prepared on Rink Amide AM Resin (0.62 mmol/g) on a 150 µmol scale according to the general protocols for functionalisation of Rink Amide AM resin (Protocol A1) and for automated peptide synthesis (Protocol C). Fmoc-Asp(O*t*Bu)-OH was used for the first

coupling. The second coupling was performed with Fmoc-D-Pro-OH and the third coupling with Fmoc-Pro-OH. Cleavage from the solid support and isolation of the peptide was carried out according to the general protocol (Protocol D).

^{1}H NMR (400 MHz, D_2O, 25°C) δ = 4.75 (dd, J = 4.8 Hz, 8.4 Hz, 1H), 4.63 (m, 1H), 3.73 (td, J = 6.5 Hz, 10.1 Hz, 1H), 3.62 (td, J = 7.0, 10.0, 1H), 3.42 (m, 2H), 2.97 (dd, J = 4.8 Hz, 17.0 Hz, 1H), 2.85 (dd, J = 8.4 Hz, 17.0 Hz, 1H), 2.56 (m, 1H), 2.30 (m, 1H), 2.12-1.93 (m, 6H).

^{13}C NMR (100 MHz, $CDCl_3$, 25°C) δ = 175.4, 174.6, 174.6, 168.5, 61.5, 59.7, 50.3, 48.2, 47.1, 35.9, 29.8, 28.6, 24.9, 24.4.

HRMS (ESI) *m/z*: calcd for $C_{14}H_{23}N_4O_5$ 327.1668; found, 327.1668.

TFA•H-Pro-Pro-D-Asp-NH$_2$ (20)

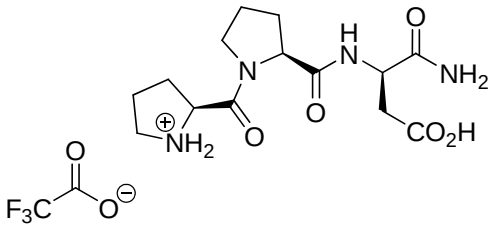

Prepared on Rink Amide AM Resin (0.62 mmol/g) on a 150 μmol scale according to the general protocols for functionalisation of Rink Amide AM resin (Protocol A1) and for automated peptide synthesis (Protocol C). Fmoc-D-Asp(O*t*Bu)-OH was used for the first coupling. The second and the third coupling were performed with Fmoc-Pro-OH. Cleavage from the solid support and isolation of the peptide was carried out according to the general protocol (Protocol D).

^{1}H NMR (400 MHz, D_2O, 25°C) δ = 4.77 (m, 1H), 4.64 (m, 1H), 4.51 (dd, J = 5.9 Hz, 8.5 Hz, 1H), 3.71 (m, 1H), 3.62 (m, 1H), 3.42 (m, 2H), 2.89 (dd, J = 5.1 Hz, 15.8 Hz, 1H), 2.80 (dd, J = 7.6 Hz, 15.7 Hz, 1H), 2.62 (m, 1H), 2.32 (m, 1H), 2.12-1.89 (m, 6H).

^{13}C NMR (100 MHz, $CDCl_3$, 25°C) δ = 175.3, 174.6, 173.9, 168.8, 61.2, 59.8, 50.1, 48.4, 47.3, 37.1, 30.2, 29.1, 25.2, 24.6.

HRMS (ESI) *m/z*: calcd for $C_{14}H_{23}N_4O_5$ 327.1668; found, 327.1668.

TFA•H-D-Pro-Pro-Asp-Pro-NH_2 (24)

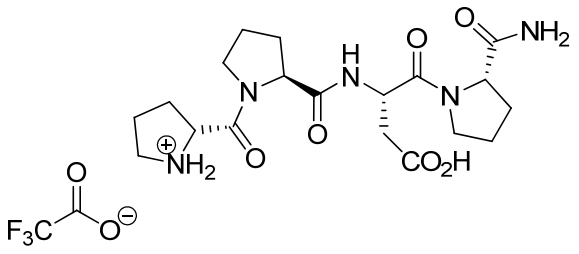

Prepared on Rink Amide AM Resin (0.71 mmol/g) on a 200 μmol scale according to the general protocols for functionalisation of Rink Amide AM resin (Protocol A1) and for automated peptide synthesis (Protocol C). Fmoc-Pro-OH was used for the first and the third coupling, Fmoc-Asp(O*t*Bu)-OH was used for the second and Fmoc-D-Pro-OH for the fourth coupling. Cleavage from the solid support and isolation of the peptide was carried out according to the general protocol (Protocol D).

^{1}H-NMR (400 MHz, d6-DMSO, 23°C): The conformers were observed in the ratio10:5:2:1. Major conformer: δ = 9.44 (m, 1H), 8.55 (m, 1H), 8.42 (d, J = 7.8 Hz, 1H), 6.99 (s, 2H), 4.77 (dm, J = 14.3 Hz, 1H), 4.48 (m, 1H), 4.31 (dd, J = 8.7 Hz, 2.9 Hz, 1H), 4.17 (m, 1H), 3.62 (m, 2H), 3.43 (m, 2H), 3.20 (m, 2H), 2.81 (m, 1H), 2.40 (m, 1H), 2.21-1.62 (m, 12H). Signals of minor conformers: δ = 9.26 (m), 8.62 (d, J = 7.8 Hz), 8.36 (d, J = 7.3), 8.22 (d, J = 7.8 Hz), 7.09 (s), 7.05 (s), 4.83 (m), 4.55 (m).

^{13}C NMR (100 MHz, d6-DMSO, 22°C): Major conformer: δ = 173.5, 172.1, 170.8, 168.9, 166.4, 59.8, 59.7, 58.3, 47.5, 46.7, 46.5, 45.7, 35.9, 29.3, 29.2, 27.9, 24.2, 24.0, 23.6. Signals of minor conformers: δ = 173.4, 171.9, 170.9, 167.0, 59.3, 58.1, 45.6, 28.3, 23.8.

HRMS (ESI) *m/z*: calcd for $C_{19}H_{30}N_5O_6$ 424.2196; found, 424.2193.

TFA•H-Pro-D-Pro-Asp-Pro-NH_2 (25)

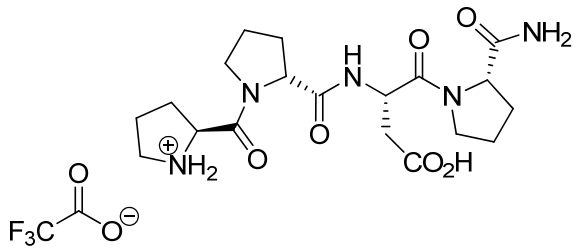

Prepared on Rink Amide AM Resin (0.71 mmol/g) on a 200 µmol scale according to the general protocols for functionalisation of Rink Amide AM resin (Protocol A1) and for automated peptide synthesis (Protocol C). Fmoc-Pro-OH was used for the first and the fourth coupling, Fmoc-Asp(O*t*Bu)-OH was used for the second and Fmoc-D-Pro-OH for the third coupling. Cleavage from the solid support and isolation of the peptide was carried out according to the general protocol (Protocol D).

^{1}H-NMR (400 MHz, d6-DMSO, 23°C): The conformers were observed in the ratio 10:5:1. Major conformer: δ = 9.44 (br s, 1H), 8.53 (m, 1H), 8.42 (d, J = 8.5 Hz, 1H), 7.02 (s, 2H), 4.89 (dm, J = 15.6, 1H), 4.46 (m, 1H), 4.32 (dd, J = 8.6 Hz, 2.7 Hz, 1H), 4.18 (m, 1H), 3.63 (m, 2H), 3.42 (m, 2H), 3.19 (m, 2H), 2.78 (m, 1H), 2.41 (m, 1H), 2.19-1.68 (m, 12H). Signals of minor conformers: δ = 9.32 (br s), 8.66 (d, J = 7.6 Hz), 8.03 (d, J = 8.2 Hz), 6.99 (s), 4.81 (m), 4.54 (m), 4.12 (m).

^{13}C NMR (100 MHz, d6-DMSO, 22°C): Major conformer: δ = 173.4, 172.2, 170.5, 168.7, 166.3, 59.8, 59.8, 58.4, 47.2, 46.7, 46.5, 45.6, 36.3, 29.6, 29.3, 27.7, 24.1, 23.9, 23.5. Signals of minor conformers: δ = 173.4, 173.3, 172.1, 59.1, 58.1, 35.7, 23.8.

MS (ESI)**:** *m/z* (%): 424.2 (100) $[M+H]^+$. M = 423.5 calcd for $C_{19}H_{29}N_5O_6$.

TFA•H-Pro-Pro-D-Asp-Pro-NH_2 (22)

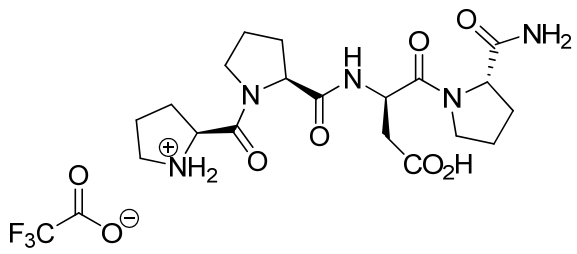

Prepared on Rink Amide AM Resin (0.71 mmol/g) on a 200 μmol scale according to the general protocols for functionalisation of Rink Amide AM resin (Protocol A1) and for automated peptide synthesis (Protocol C). Fmoc-Pro-OH was used for the first the third and the fourth coupling, Fmoc-D-Asp(O*t*Bu)-OH was used for the second coupling. Cleavage from the solid support and isolation of the peptide was carried out according to the general protocol (Protocol D).

^{1}H-NMR (400 MHz, d6-DMSO, 23°C): The conformers were observed in the ratio 5:3:2:1. Major conformer: δ = 9.42 (br s, 1H), 8.48 (m, 1H), 8.09 (d, J = 8.2 Hz, 1H), 7.16 (s, 1H), 6.94 (s, 1H), 4.44 (m, 4H), 3.64-3.31 (m, 4H), 3.30-3.05 (m, 2H), 2.75 (m, 1H), 2.39 (m, 1H), 2.29-1.69 (m, 12H). Signals of minor conformers: δ = 9.34 (br s, 1H), 8.56 (d, J = 8.1 Hz), 8.00 (d, J = 8.3 Hz), 7.56 (s), 7.50 (s), 7.35 (s), 7.23 (s), 7.18 (s), 7.02 (s), 4.33-3.95 (m).

^{13}C NMR (100 MHz, d6-DMSO, 22°C): Major conformer: δ = 173.4, 171.7, 170.7, 168.9, 166.6, 59.9, 59.5, 58.2, 47.4, 46.7, 45.9, 45.8, 36.1, 29.5, 29.2, 28.0, 24.4, 24.2, 23.5. Signals of minor conformers: δ = 175.2, 171.5, 168.8, 59.4, 35.7, 23.8.

MS (ESI)**:** *m/z* (%): 424.2 (100) $[M+H]^+$. M = 423.5 calcd for $C_{19}H_{29}N_5O_6$.

TFA•H-Pro-Pro-Asp-D-Pro-NH_2 (26)

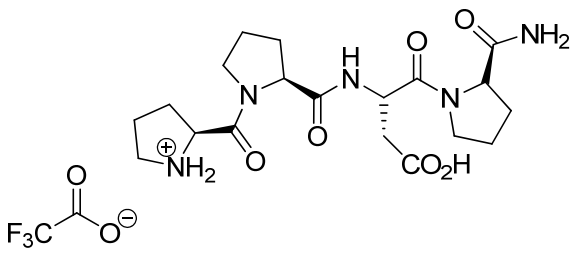

Prepared on Rink Amide AM Resin (0.71 mmol/g) on a 200 µmol scale according to the general protocols for functionalisation of Rink Amide AM resin (Protocol A1) and for automated peptide synthesis (Protocol C). Fmoc-D-Pro-OH was used for the first coupling, Fmoc-Asp(O*t*Bu)-OH was used for the second and Fmoc-Pro-OH for the third and fourth coupling. Cleavage from the solid support and isolation of the peptide was carried out according to the general protocol (Protocol D).

^{1}H-NMR (500 MHz, d6-DMSO, 23°C): The conformers were observed in the ratio 13:3:3:1. Major conformer: δ = 9.46 (br s, 1H), 8.60 (d, *J* = 7.8 Hz, 1H), 8.43 (m, 1H), 6.97 (s, 1H), 6.82 (s, 1H), 4.62 (ddm, *J* = 14.0 Hz, 8.2 Hz, 1H), 4.46-4.37 (m, 1H), 4.31 (dd, *J* = 8.5 Hz, 5.0 Hz), 4.12 (dd, *J* = 8.8 Hz, 4.4 Hz), 3.58 (m, 2H), 3.46 (m, 2H), 3.13 (m, 2H), 2.75 (dd, *J* = 16.4 Hz, 8.5 Hz, 1H), 2.35 (m, 2H), 2.11-1.94 (m, 2H), 1.93-1.70 (m, 9H). Signals of minor conformers: δ = 9.27 (br s), 8.90 (d, *J* = 8.0 Hz), 8.83 (d, *J* = 8.2 Hz), 8.33 (s, *J* = 7.4), 7.91 (s), 7.54 (s), 7.44 (s), 7.25 (s), 7.18 (s), 7.03 (s), 4.83 (m), 4.53 (m), 4.17 (dd, *J* = 8.6 Hz, 3.9 Hz), 2.61 (m), 2.49 (m), 2.21 (m).

^{13}C NMR (126 MHz, d6-DMSO, 23°C): Major conformer: δ = 173.0, 172.3, 171.5, 169.3, 167.2, 60.4, 60.0, 58.6, 48.3, 47.2, 47.2, 46.4, 36.3, 29.6, 29.6, 28.4, 24.8, 24.8, 24.1. Signals of minor conformers: δ = 174.0, 172.0, 171.2, 171.0, 169.8, 168.9, 167.2, 167.0, 60.0, 59.9, 59.9, 59.3, 58.9, 58.8, 48.0, 47.8, 46.9, 46.2, 36.1, 32.1, 32.1, 29.7, 29.5, 28.6, 28.3, 24.7, 24.0, 22.5, 22.4.

MS (ESI)**:** *m/z* (%): 424.2 (100) $[M+H]^+$. M = 423.5 calcd for $C_{19}H_{29}N_5O_6$.

TFA•H-Pro-Pro-D-Asp-D-Pro-NH_2 (27)

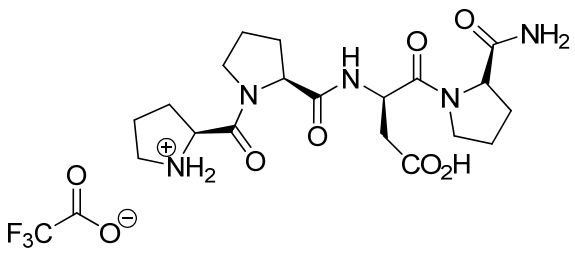

Prepared on Rink Amide AM Resin (0.71 mmol/g) on a 200 µmol scale according to the general protocols for functionalisation of Rink Amide AM resin (Protocol A1) and for automated peptide synthesis (Protocol C). Fmoc-D-Pro-OH was used for the first coupling, Fmoc-D-Asp(O*t*Bu)-OH was used for the second and Fmoc-Pro-OH for the third and fourth coupling. Cleavage from the solid support and isolation of the peptide was carried out according to the general protocol (Protocol D).

^{1}H-NMR (500 MHz, d6-DMSO, 23°C): The conformers were observed in the ratio 9:5:4:2. Major conformer: δ = 9.35 (m, 1H), 8.45 (m, 1H), 8.01 (d, J = 8.3 Hz, 1H), 7.15 (s, 1H), 6.90 (s, 1H), 4.50 (m, 1H), 4.42 (m, 2H), 4.12 (m, 1H), 3.60-3.03 (m, 6H), 2.70 (m, 1H), 2.35 (m, 1H), 2.00-1.68 (m, 12H). Signals of minor conformers: δ = 8.57 (d, J = 7.8 Hz, 8.47 (d, J = 7.3 Hz), 7.97 (s, J = 8.0), 7.61 (s), 7.54 (s), 7.23 (s), 7.20 (s), 7.18 (s), 6.95 (s), 4.57 (m), 4.26 (m), 4.22 (m).

^{13}C NMR (126 MHz, d6-DMSO, 23°C): Major conformer: δ = 174.1, 173.1, 170.8, 168.8, 167.4, 60.0, 59.8, 58.8, 48.9, 47.2, 47.1, 46.3, 36.1, 29.9, 29.4, 28.3, 24.7, 24.5, 24.0. Signals of minor conformers: δ = 60.1, 59.0, 49.0, 46.8, 46.2, 45.6, 36.0, 32.2, 32.2, 28.3, 28.0, 24.7, 24.6, 24.0, 22.8, 22.5.

MS (ESI)**:** *m/z* (%): 424.2 (100) $[M+H]^+$. M = 423.5 calcd for $C_{19}H_{29}N_5O_6$.

TFA•H-Pro-D-Pro-Asp-D-Pro-NH_2 (23)

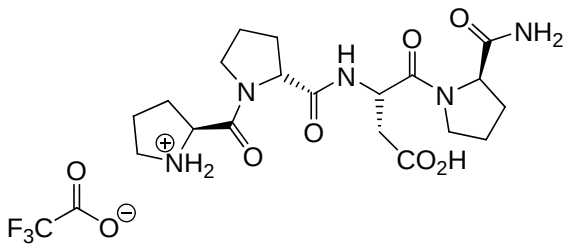

Prepared on Rink Amide AM Resin (0.71 mmol/g) on a 200 μmol scale according to the general protocols for functionalisation of Rink Amide AM resin (Protocol A1) and for automated peptide synthesis (Protocol C). Fmoc-D-Pro-OH was used for the first and third coupling, Fmoc-Asp(O*t*Bu)-OH was used for the second and Fmoc-Pro-OH for the fourth coupling. Cleavage from the solid support and isolation of the peptide was carried out according to the general protocol (Protocol D).

^{1}H-NMR (400 MHz, d6-DMSO, 23°C): The conformers were observed in the ratio 10:4:3:2. Major conformer: δ = 9.43 (s, 1H), 8.49 (m, 1H), 8.51 (d, J = 8.1 Hz, 1H), 6.96 (s, 1H), 6.87 (s, 1H), 4.82 (m, 1H), 4.50 (m, 1H), 4.32 (m, 1H), 4.19 (m, 1H), 3.74-3.33 (m, 4H), 3.30-3.08 (m, 2H), 2.75 (m, 1H), 2.37 (m, 1H), 2.21-1.52 (m, 12H). Signals of minor conformers: δ = 9.32 (s), 8.76 (d, J = 7.7 Hz), 8.71 (d, J = 7.9 Hz), 8.48 (d, J = 8.2 Hz), 7.62 (s), 7.44 (s), 7.28 (s), 7.25 (s), 7.06 (s), 6.91 (s), 4.68 (m), 4.59 (m).

^{13}C NMR (100 MHz, d6-DMSO, 22°C): Major conformer: δ = 173.4, 171.8, 170.8, 168.8, 166.5, 59.9, 59.8, 58.4, 47.4, 46.7, 46.7, 45.7, 36.0, 29.5, 29.1, 27.8, 24.2, 23.9, 23.6. Signals of minor conformers: δ = 173.2, 171.7, 171.6, 171.5, 171.4, 171.2, 170.6, 169.3, 168.7, 166.2, 59.6, 59.4, 59.1, 58.0, 46.3, 35.2, 31.7, 31.7, 31.5, 28.4, 24.0, 23.8, 21.6.

MS (ESI)**:** *m/z* (%): 424.2 (100) $[M+H]^+$. M = 423.5 calcd for $C_{19}H_{29}N_5O_6$.

TFA•H-Pro-D-Pro-D-Asp-Pro-NH_2 (28)

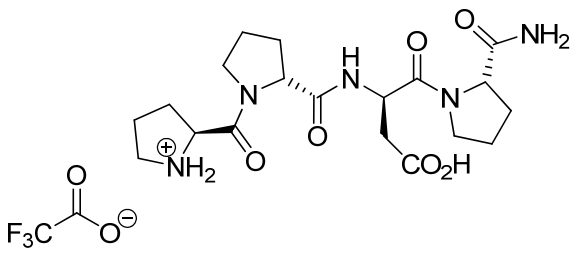

Prepared on Rink Amide AM Resin (0.71 mmol/g) on a 200 µmol scale according to the general protocols for functionalisation of Rink Amide AM resin (Protocol A1) and for automated peptide synthesis (Protocol C). Fmoc-Pro-OH was used for the first and fourth coupling, Fmoc-D-Asp(O*t*Bu)-OH was used for the second and Fmoc-D-Pro-OH for the third coupling. Cleavage from the solid support and isolation of the peptide was carried out according to the general protocol (Protocol D).

^{1}H-NMR (400 MHz, d6-DMSO, 23°C): The exact ratio of conformers could not be determined. A minimum of three conformers are existent according to the ^{1}H-NMR spectra. Major conformer: δ = 9.43 (br s, 1H), 8.63 (m, 1H), 8.29 (d, J = 8.3, 1H), 6.92 (s, 2H), 4.55 (m, 2H), 4.36 (m, 1H), 4.17 (m, 1H), 3.71-3.31 (m, 4H), 3.20 (m, 2H), 2.77 (m, 1H), 2.38 (m, 1H), 2.22-1.60 (m, 12H). Signals of minor conformers: δ = 9.28 (br s), 9.15 (br s), 8.52 (m), 8.36 (m), 8.15 (d, J = 8.1 Hz), 7.56 (s), 7.53 (s), 7.23 (s), 7.22 (s), 7.19 (s), 7.18 (s).

^{13}C NMR (100 MHz, d6-DMSO, 23°C): Major conformer: δ = 173.5, 171.7, 171.0, 168.8, 166.5, 59.8, 59.7, 58.3, 47.5, 46.8, 46.6, 45.7, 35.8, 29.3, 29.2, 27.8, 24.2, 24.0, 23.5. Signals of minor conformers: δ = 173.5, 173.2, 171.5, 171.0, 170.8, 168.7, 46.7, 29.4, 28.3, 28.2, 23.9.

MS (ESI)**:** *m/z* (%): 446.4 (100) $[M+Na]^+$. M = 423.5 calcd for $C_{19}H_{29}N_5O_6$.

TFA•H-D-Pro-Pro-Asn-OH (29)

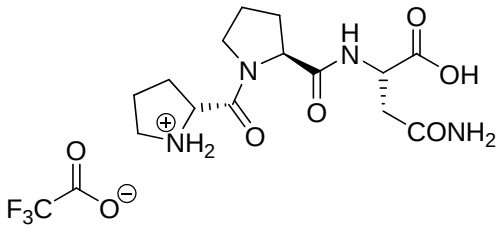

Prepared on Wang resin (1.0 mmol/g) on a 2 mmol scale according to the general protocols for functionalisation of Wang resin (Protocol A2) and for manual peptide synthesis using HCTU/*i*-Pr_2NEt (Protocol B1). Fmoc-Asn(Trt)-OH was used for the first coupling. Fmoc-Pro-OH was used for the second and Fmoc-D-Pro-OH for the third coupling. Cleavage from the solid support and isolation of the peptide was carried out according to the general protocol (Protocol D).

^{1}H-NMR (400 MHz, D_2O, 25°C): δ = 4.55 (dd, *J* = 6.4 Hz, 8.5 Hz, 1H), 4.51 (dd, *J* = 6.4 Hz, 8.6 Hz, 1H), 4.39 (dd, *J* = 5.4 Hz, 8.6 Hz, 1H), 3.46 (m, 1H), 3.40 (m, 1H), 3.33 (m, 2H), 2.70 (dd, *J* = 5.8 Hz, 15.4 Hz, 1H), 2.65 (dd, *J* = 6.4 Hz, 15.2 Hz, 1H), 2.35 (m, 1H), 2.18 (m, 1H), 2.12-1.70 (m, 6H).

^{13}C-NMR (100 MHz, D_2O, 25°C): δ = 175.0, 174.3, 173.7, 168.5, 60.9, 59.5, 49.8, 48.0, 47.0, 36.4, 29.6, 28.8, 24.9, 24.2.

MS (ESI): *m*/*z* (%): 327.2 (100) $[M+H]^+$. M = 326.3 calcd for $C_{14}H_{22}N_4O_5$.

TFA•H-D-Pro-Pro-D-Asn-OH (30)

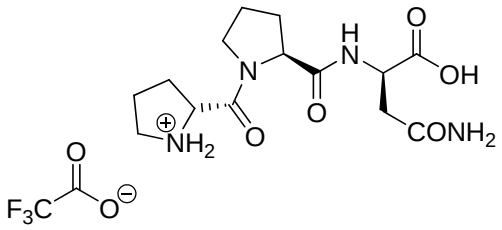

Prepared on Wang resin (1.0 mmol/g) on a 2 mmol scale according to the general protocols for functionalisation of Wang resin (Protocol A2) and for manual peptide synthesis using HCTU/*i*-Pr_2NEt (Protocol B1). Fmoc-D-Asn(Trt)-OH was used for the first coupling. Fmoc-

Pro-OH was used for the second and Fmoc-D-Pro-OH for the third coupling. Cleavage from the solid support and isolation of the peptide was carried out according to the general protocol (Protocol D).

^{1}H-NMR (400 MHz, D_2O, 25°C): δ = 4.62 (dd, J = 6.1 Hz, 8.5 Hz, 1H), 4.55 (dd, J = 6.1 Hz, 8.6 Hz, 1H), 4.38 (dd, J = 5.4 Hz, 8.6 Hz, 1H), 3.52 (m, 1H), 3.45 (m, 1H), 3.34 (m, 2H), 2.80 (dd, J = 5.8 Hz, 15.8 Hz, 1H), 2.76 (dd, J = 6.3 Hz, 15.6 Hz, 1H), 2.34 (m, 1H), 2.19 (m, 1H), 1.95-1.70 (m, 6H).

^{13}C-NMR (100 MHz, D_2O, 25°C): δ = 175.0, 174.3, 173.7, 168.5, 60.9, 59.4, 49.7, 48.0, 47.0, 36.4, 29.6, 28.7, 24.9, 24.2.

MS (ESI): *m/z* (%): 327.2 (100) $[M+H]^+$. M = 326.3 calcd for $C_{14}H_{22}N_4O_5$.

TFA•H-D-Pro-Pro-Ser-OH (31)

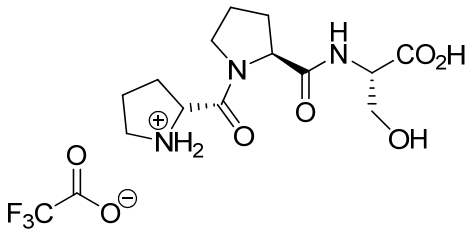

Prepared on Wang resin (1.0 mmol/g) on a 2 mmol scale according to the general protocols for functionalisation of Wang resin (Protocol A2) and for manual peptide synthesis using HCTU/*i*-Pr_2NEt (Protocol B1). Fmoc-Ser(*t*Bu)-OH was used for the first coupling. Fmoc-Pro-OH was used for the second and Fmoc-D-Pro-OH for the third coupling. Cleavage from the solid support and isolation of the peptide was carried out according to the general protocol (Protocol D).

^{1}H-NMR (400 MHz, D_2O, 23°C): δ = 4.63 (dd, *J* = 8.6 Hz, 7.0 Hz, 1H), 4.53 (m, 2H), 4.00 (dd, *J* = 11.6 Hz, 4.8 Hz, 1H), 3.90 (dd, *J* = 12.0 Hz, 4.0 Hz, 1H), 3.73 (m, 1H), 3.60 (m, 1H), 3.42 (m, 2H), 2.55 (m, 1H), 2.33 (m, 1H), 2.06 (m, 6H).

^{13}C-NMR (100 MHz, D_2O, 23°C): δ = 174.4, 173.6, 168.3, 61.3, 61.0, 59.6, 55.3, 48.1, 47.0, 30.0, 28.4, 24.6, 24.3.

MS (ESI): *m*/*z* (%): 300.1 (100) $[M+H]^+$. M = 299.3 calcd for $C_{13}H_{21}N_3O_5$.

TFA•H-D-Pro-Pro-His-OH (32)

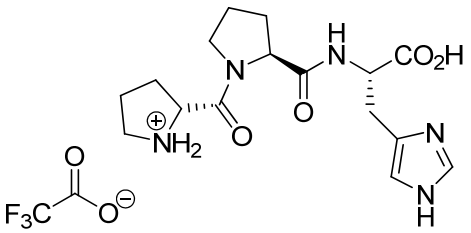

Prepared on Wang resin (1.0 mmol/g) on a 2 mmol scale according to the general protocols for functionalisation of Wang resin (Protocol A2) and for manual peptide synthesis using HCTU/*i*-Pr_2NEt (Protocol B1). Fmoc-His(Trt)-OH was used for the first coupling. Fmoc-Pro-OH was used for the second and Fmoc-D-Pro-OH for the third coupling. Cleavage from the solid support and isolation of the peptide was carried out according to the general protocol (Protocol D).

^{1}H-NMR (400 MHz, D_2O / CD_3OD 5:1, 23°C): δ = 8.63 (d, *J* = 1.3 Hz, 1H), 7.34 (s, 1H), 4.68 (dd, *J* = 5.2 Hz, 8.0 Hz, 1H), 4.61 (m, 1H), 4.44 (dd, *J* = 3.3 Hz, 8.8 Hz, 1H), 3.72 (m, 1H), 3.58 (m, 1H), 3.50 – 3.34 (m, 3H), 3.18 (dd, *J* = 8.1 Hz, 15.5 Hz, 1H), 2.56 (m, 1H), 2.29 (m, 1H), 2.12 – 1.92 (m, 6H).

^{13}C-NMR (100 MHz, D_2O / CD_3OD 5:1, 23°C): δ = 176.8, 176.4, 170.8, 136.3, 131.9, 120.2, 63.7, 62.2, 55.5, 49.6, 32.5, 31.0, 29.5, 27.2, 26.9, 17.1, one signal probably below CD_3OD.

MS (ESI): *m*/*z* (%): 350.2 (100) $[M+H]^+$. M = 349.4 calcd for $C_{16}H_{23}N_5O_4$.

TFA•H-Pro-D-Ala-D-Asp-NH_2 (2)

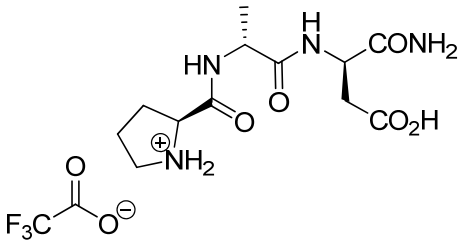

Prepared on Rink Amide AM Resin (0.71 mmol/g) on a 200 µmol scale according to the general protocols for functionalisation of Rink Amide AM resin (Protocol A1) and for automated peptide synthesis (Protocol C). Fmoc-D-Asp(O*t*Bu)-OH was used for the first coupling, Fmoc-D-Ala-OH was used for the second and Fmoc-Pro-OH for the third coupling. Cleavage from the solid support and isolation of the peptide was carried out according to the general protocol (Protocol D).

^{1}H-NMR (400 MHz, D_2O, 22°C): δ = 4.40 (dd, *J* = 7.9 Hz, 5.3 Hz, 1H), 4.27 (dd, *J* = 8.6 Hz, 6.7 Hz, 1H), 4.22 (q, *J* = 7.2 Hz, 1H), 3.27 (m, 2H), 2.54 (dd, *J* = 15.9 Hz, 5.3 Hz, 1H), 2.48 (dd, *J* = 15.9 Hz, 7.9 Hz, 1H), 2.31 (m, 1H), 1.92 (m, 3H), 1.26 (d, *J* = 7.2 Hz, 3H).

^{13}C NMR (100 MHz, $CDCl_3$, 22°C): δ = 177.6, 176.0, 174.3, 169.7, 59.7, 51.3, 50.0, 46.4, 38.4, 29.5, 23.7, 16.2. MS (ESI): m/z (%): 301.4 (100) $[M+H]^+$, 323.4 (24) $[M+Na]^+$.

MS (ESI): *m/z* (%): 301.4 (100) $[M+H]^+$, 323.4 (25) $[M+Na]^+$. M = 300.3 calcd for $C_{12}H_{20}N_4O_5$.

TFA•H-D-Pro-Pro-Asn-NH_2 (48)

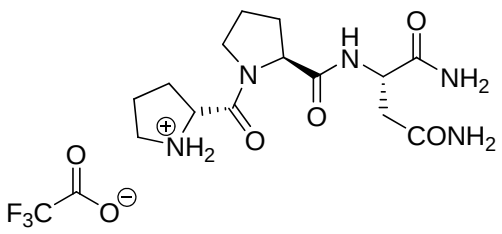

Prepared on Rink Amide AM Resin (0.71 mmol/g) on a 200 µmol scale according to the general protocols for functionalisation of Rink Amide AM resin (Protocol A1) and for automated peptide synthesis (Protocol C). Fmoc-Asn(Trt)-OH was used for the first coupling.

Fmoc-Pro-OH was used for the second and Fmoc-D-Pro-OH for the third coupling. Cleavage from the solid support and isolation of the peptide was carried out according to the general protocol (Protocol D).

^{1}H NMR (400 MHz, D_2O, 25°C) δ = 4.70 (dd, J = 5.4 Hz, 8.6 Hz, 1H), 4.66 (dd, J = 6.8 Hz, 8.6 Hz, 1H), 4.48 (dd, J = 3.9 Hz, 8.5 Hz, 1H), 3.76 (m, 1H), 3.62 (m, 1H), 3.44 (m, 2H), 2.87 (dd, J = 5.5 Hz, 15.5 Hz, 1H), 2.76 (dd, J = 8.8 Hz, 15.5 Hz, 1H), 2.57 (m, 1H), 2.34 (m, 1H), 2.14 – 1.98 (m, 6H).

^{13}C NMR (100 MHz, D_2O, 25°C) δ = 177.6, 177.2, 176.6, 171.2, 63.7, 62.0, 53.1, 50.4, 49.4, 38.9, 32.2, 30.8, 27.0, 26.7.

HRMS (ESI) *m/z*: calcd for $C_{14}H_{23}N_5O_4$ 326.1828; found, 326.1826.

H-D-Pro-Pro-Asp(O*t*Bu)-NH_2 (49) (desalted)

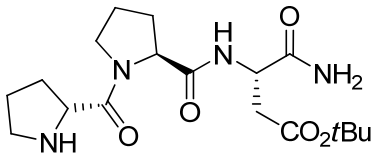

Prepared on Sieber Amide resin (0.41 mmol/g) at a 0.45 mmol scale according to the general protocols for functionalisation of Sieber Amide resin (Protocol A1) and for manual peptide synthesis (Protocol B1) but using 3 eq of each of amino acid derivative, 3 eq of HCTU and 9 eq of *i*-Pr_2NEt. Fmoc-Asp(O*t*Bu)-OH was used for the first coupling. Fmoc-Pro-OH was used for the second and Fmoc-D-Pro-OH for the third coupling. The *N*-terminal proline fmoc group was removed by piperidine treatment (3 x 5 min), and the crude peptide was cleaved by treatment of the resin with 1% TFA/CH_2Cl_2 (10 x 2 min using 10 x 10 mL). After each acidolysis treatment, the cleavage solution containing the protected peptide was immediately run into a cooled (0 ^oC) solution of 5 % pyridine in MeOH (30 mL), and following collection of CH_2Cl_2 washings (10 x 5 mL), the cleavage solution was concentrated *in vacuo* almost to dryness. The crude peptide was dissolved in chloroform (500 µL), and the resulting golden coloured solution loaded onto acetate charged ion-exchange resin (Dowex 1x2-400) eluting with water. Product containing fractions (visualised on silica TLC by ninhydrin) were pooled and concentrated by centrifugal evaporation, affording the title peptide as a stiff colourless glass (65 %).

^{1}H NMR (400 MHz, D_2O, 25°C) δ = 4.71 (dd, J = 5.8 Hz, 8.4 Hz, 1H), 4.66 (dd, J = 7.1 Hz, 8.8 Hz, 1H), 4.47 (dd, J = 3.5 Hz, 9.0 Hz, 1H), 3.75 (m, 1H), 3.62 (m, 1H), 3.44 (m, 2H), 2.91 (dd, J = 5.8 Hz, 16.4 Hz, 1H), 2.75 (dd, J = 8.5 Hz, 16.3 Hz, 1H), 2.57 (m, 1H), 2.34 (m, 1H), 2.14 – 1.96 (m, 6H), 1.46 (s, 9H).

^{13}C NMR (100 MHz, D_2O, 25°C) δ = 177.5, 176.6, 174.1, 171.2, 86.2, 63.8, 62.1, 52.9, 50.4, 49.4, 39.6, 32.3, 30.8, 29.9, 27.0, 26.7.

HRMS (ESI) *m/z*: calcd for $C_{18}H_{31}N_4O_5$ 383.2294; found, 383.2304.

TFA•H-D-Pro-Pro-β-homo-Asp-NH$_2$ (52)

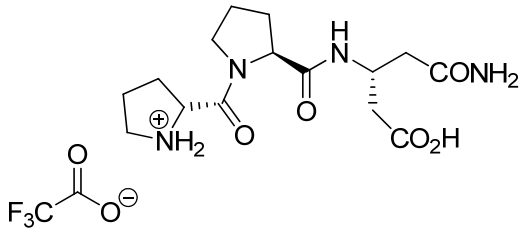

Prepared on Rink Amide AM resin (0.62 mmol/g) on a 2 mmol scale according to the general protocols for functionalisation of Rink Amide AM resin (Protocol A1) and for manual peptide synthesis using HCTU/*i*-Pr_2NEt (Protocol B1). Fmoc-β-homo-Asp(O*t*Bu)-OH **93** was used for the first coupling. Fmoc-Pro-OH was used for the second and Fmoc-D-Pro-OH for the third coupling. Cleavage from the solid support and isolation of the peptide was carried out according to the general protocol (Protocol D).

^{1}H NMR (400 MHz, D_2O, 25°C) δ = 4.63 (dd, J = 6.8 Hz, 8.8 Hz, 1H), 4.55 (m, 1H), 4.38 (dd, J = 3.6 Hz, 8.8 Hz, 1H), 3.72 (m, 1H), 3.58 (m, 1H), 3.42 (m, 2H), 2.66 – 2.45 (m, 5H), 2.27 (m, 1H), 2.11 – 1.93(m, 6H).

^{13}C NMR (100 MHz, D_2O, 25°C) δ = 178.6, 178.0, 176.2, 171.1, 64.2, 62.4, 50.7, 49.8, 47.4, 42.7, 41.8, 32.9, 31.2, 27.2, 27.1.

HRMS (ESI) *m/z*: calcd for $C_{15}H_{25}N_4O_5$ 341.1824; found, 341.1829.

TFA•H-D-Pro-Pro-Asp-OH (53)

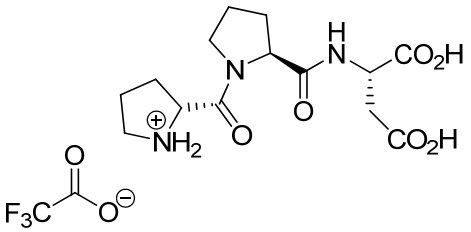

Prepared on Wang resin (1.0 mmol/g) on a 2 mmol scale according to the general protocols for functionalisation of Wang resin (Protocol A2) and for manual peptide synthesis using HCTU/*i*-Pr_2NEt (Protocol B1). Fmoc-Asp(O*t*Bu)-OH was used for the first coupling. Fmoc-Pro-OH was used for the second and Fmoc-D-Pro-OH for the third coupling. Cleavage from the solid support and isolation of the peptide was carried out according to the general protocol (Protocol D).

^{1}H NMR (400 MHz, D_2O, 25°C) δ = 4.77 (dd, *J* = 5.7 Hz, 6.6 Hz, 1H), 4.63 (dd, J = 7.3 Hz, 8.5 Hz, 1H), 4.49 (dd, J = 3.3 Hz, 8.6 Hz, 1H), 3.73 (m, 1H), 3.60 (m, 1H), 3.42 (m, 2H), 2.97 (m, 2H), 2.56 (m, 1H), 2.32 (m, 1H), 2.12 – 1.97 (m, 6H).

^{13}C NMR (100 MHz, D_2O, 25°C) δ = 177.4, 177.0, 176.8, 171.1, 63.8, 62.4, 52.3, 50.7, 49.7 38.5, 32.6, 31.2, 27.3, 27.0.

HRMS (ESI) *m/z*: calcd for $C_{14}H_{22}N_3O_6$ 328.1508; found, 328.1500.

TFA•H-D-Pro-Pro-Asp-NH-TentaGel (55) (solid supported)

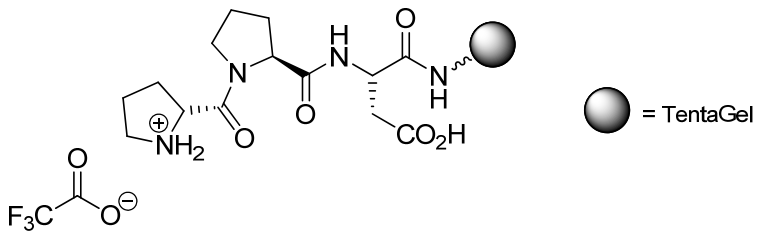

Prepared on TentaGel S NH_2 resin (0.27 mmol/g) on a 70 μmol scale according to the general protocol for automated peptide synthesis (Protocol C). No special treatment was required for the functionalisation of the resin (first coupling). Fmoc-Asp(O*t*Bu)-OH was used for the first

coupling. Fmoc-Pro-OH was used for the second and Boc-D-Pro-OH for the third coupling. The *t*-butyl protecting groups were removed by treatment of the resin with a mixture of TFA/CH_2Cl_2 1:2 within 2 h followed by washing with CH_2Cl_2 (5x), CH_2Cl_2 / Et_3N (9:1 v/v) (5x), CH_2Cl_2 (5x) and Et_2O (5x). The resin was then dried under high vacuum.

TFA•H-D-Pro-Pro-Gly-OH (62)

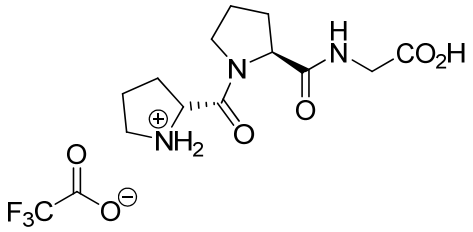

Prepared on Wang resin (1.0 mmol/g) on a 2 mmol scale according to the general protocols for functionalisation of Wang resin (Protocol A2) and for manual peptide synthesis using HCTU/*i*-Pr_2NEt (Protocol B1). Fmoc-Gly-OH was used for the first coupling. Fmoc-Pro-OH was used for the second and Fmoc-D-Pro-OH for the third coupling. Cleavage from the solid support and isolation of the peptide was carried out according to the general protocol (Protocol D).

^{1}H NMR (400 MHz, D_2O / CD_3OD 2:1, 25°C) δ= 4.61 (dd, *J* = 7.4 Hz, 8.3 Hz, 1H), 4.49 (dd, *J* = 3.2 Hz, 8.6 Hz, 1H), 3.98 (d, *J* = 17.8 Hz, 1H), 3.92 (d, *J* = 17.8 Hz, 1H), 3.75 (m, 1H), 3.59 (m, 1H), 3.41 (m, 2H), 2.56 (m, 1H), 2.31 (m, 1H), 2.05 (m, 6H).

^{13}C NMR (100 MHz, D_2O / CD_3OD 2:1, 25°C) δ= 176.9, 176.0, 170.8, 63.8, 62.3, 50.5, 49.6, 44.1, 32.6, 31.1, 27.1, 27.0.

MS (ESI): *m*/*z* (%): 270.2 (100) $[M+H]^+$. M = 269.3 calcd for $C_{12}H_{19}N_3O_4$.

TFA•H-D-Pro-Pro-β-Ala-OH (50)

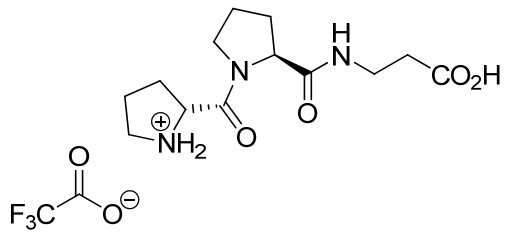

Prepared on Wang resin (1.0 mmol/g) on a 2 mmol scale according to the general protocols for functionalisation of Wang resin (Protocol A2) and for manual peptide synthesis using HCTU/*i*-Pr_2NEt (Protocol B1). Fmoc-β-Ala-OH was used for the first coupling. Fmoc-Pro-OH for the second and Fmoc-D-Pro-OH for the third coupling. Cleavage from the solid support and isolation of the peptide was carried out according to the general protocol (Protocol D).

^{1}H NMR (400 MHz, D_2O / CD_3OD 12:1, 25°C) δ = 4.63 (dd, J = 7.1 Hz, 8.7 Hz, 1H), 4.39 (dd, J = 4.0 Hz, 8.9 Hz, 1H), 3.73 (m, 1H), 3.60 (m, 1H), 3.57 – 3.36 (m, 4H), 2.61 (t, J = 6.5 Hz, 2H), 2.58 (m, 1H), 2.28 (m, 1H), 2.14 – 1.92 (m, 6H).

^{13}C NMR (100 MHz, D_2O / CD_3OD 12:1, 25°C) δ = 179.0, 176.8, 171.1, 64.1, 62.3, 51.5, 49.7, 38.3, 36.4, 32.8, 31.1, 27.8, 27.0.

HRMS (ESI) *m/z*: calcd for $C_{13}H_{22}N_3O_4$ 384.1610; found, 384.1604.

TFA•H-D-Pro-Pro-γ-Abu-OH (63)

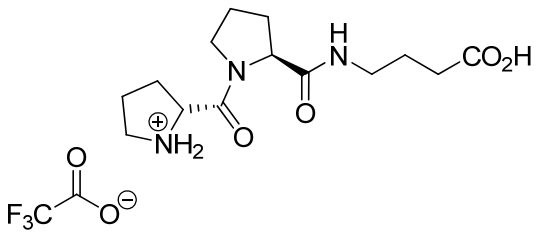

Prepared on Wang resin (1.0 mmol/g) on a 2 mmol scale according to the general protocols for functionalisation of Wang resin (Protocol A2) and for manual peptide synthesis using HCTU/*i*-Pr_2NEt (Protocol B1). Fmoc-γ-Abu-OH was used for the first coupling. Fmoc-Pro-

OH for the second and Fmoc-D-Pro-OH for the third coupling. Cleavage from the solid support and isolation of the peptide was carried out according to the general protocol (Protocol D).

^{1}H NMR (400 MHz, D_2O, 25°C) δ = 4.63 (dd, J = 6.9 Hz, 8.9 Hz, 1H), 4.38 (dd, J = 4.1 Hz, 8.9 Hz, 1H), 3.73 (m, 1H), 3.60 (m, 1H), 3.42 (m, 2H), 3.24 (dt, J = 3.3 Hz, 6.7 Hz, 2H), 2.56 (m, 1H), 2.37 (t, J = 7.4 Hz, 2H), 2.28 (m, 1H), 2.13 – 1.94 (m, 6H), 1.80 (p, J = 7.1 Hz, 2H).

^{13}C NMR (100 MHz, D_2O, 25°C) δ = 180.9, 176.7, 170.9, 64.1, 62.2, 51.6, 49.6, 41.5, 33.9, 32.7, 31.1, 27.2, 26.9, 26.8.

MS (ESI): m/z (%): 298.2 (100) $[M+H]^+$. M = 297.4 calcd for $C_{14}H_{23}N_3O_4$.

TFA•H-D-Pro-Pro-Glu-NH$_2$ (56)

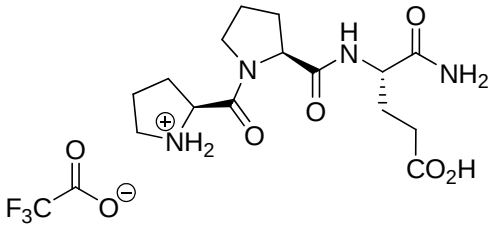

Prepared on Rink Amide AM resin (0.62 mmol/g) on a 15 mmol scale according to the general protocols for functionalisation of Rink Amide AM resin (Protocol A1) and for manual peptide synthesis using DIC/HOBt (Protocol B2). Fmoc-Glu(O*t*Bu)-OH was used for the first and Fmoc-Pro-OH for the second coupling. Boc-D-Pro-OH was applied for the third coupling. Cleavage from the solid support and isolation of the peptide was carried out according to the general protocol (Protocol D).

^{1}H NMR (400 MHz, D_2O, 25°C) δ = 4.51 (dd, J = 7.1 Hz, 8.8 Hz, 1H), 4.34 (dd, J = 3.6 Hz, 9.0 Hz, 1H), 4.23 (dd, J = 5.2 Hz, 9.5 Hz, 1H), 3.60 (m, 1H), 3.49 (m, 1H), 3.29 (m, 2H), 2.40 (m, 3H), 2.19 (m, 1H), 2.08-1.80 (m, 8H).

^{13}C NMR (100 MHz, D_2O, 25°C) δ = 177.4, 176.2, 174.5, 168.6, 61.2, 59.6, 53.2, 48.0, 47.0, 30.3, 29.8, 28.5, 26.4, 24.7, 24.3.

For detailed assignement of ^{1}H and ^{13}C NMR signals in d6-DMSO and $CDCl_3/CD_3OD/CD_3OH$ 23:1:1 (v/v/v) see Chapter 18.4.1.

HRMS (ESI) *m/z*: calcd for $C_{15}H_{25}N_4O_5$ 341.1824; found, 341.1821.

Desalting of H-D-Pro-Pro-Glu-NH_2 (56)

The peptide desalting occurred by ion pair extraction using a VariPure^{TM} IPE tube according to the general procecure (Protocol G) with TFA•H-D-Pro-Pro-Glu-NH_2 **56** (80 mg, 176 µmol). The desalted H-D-Pro-Pro-Glu-NH_2 was obtained as a white solid (49 mg, 81 %).

TFA•H-D-Pro-Pro-Aad-NH_2 (57)

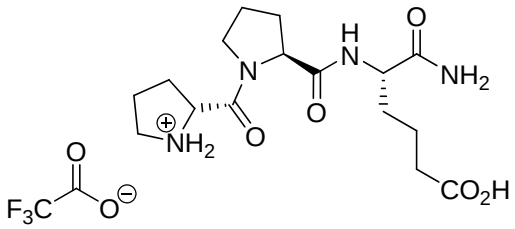

Prepared on Rink Amide AM Resin (0.71 mmol/g) on a 200 µmol scale according to the general protocols for functionalisation of Rink Amide AM resin (Protocol A1) and for automated peptide synthesis (Protocol C). Fmoc-Aad(O*t*Bu)-OH was used for the first coupling. Fmoc-Pro-OH was used for the second and Fmoc-D-Pro-OH for the third coupling. Cleavage from the solid support and isolation of the peptide was carried out according to the general protocol (Protocol D).

^{1}H NMR (400 MHz, D_2O, 25°C) δ = 4.64 (dd, *J* = 7.0 Hz, 8.7 Hz, 1H), 4.48 (dd, *J* = 3.5 Hz, 8.9 Hz, 1H), 4.28 (dd, *J* = 5.4 Hz, 8.8 Hz, 1H), 3.76 (m, 1H), 3.61 (m, 1H), 3.43 (m, 2H), 2.56 (m, 1H), 2.41 (t, *J* = 7.2 Hz, 2H), 2.33 (m, 1H), 2.12 – 1.93 (m, 6H), 1.91 – 1.62 (m, 4H).

^{13}C NMR (100 MHz, D_2O, 25°C) δ= 181.7, 179.6, 177.2, 171.4, 63.9, 62.4, 56.6, 50.8, 49.8, 36.5, 33.3, 32.7, 31.2, 27.4, 27.1, 23.9.

MS (ESI): *m/z* (%):355.2 (100) $[M+H]^+$. M = 354.4 calcd for $C_{16}H_{26}N_4O_5$.

TFA•H-D-Pro-Pro-Api-NH_2 (58)

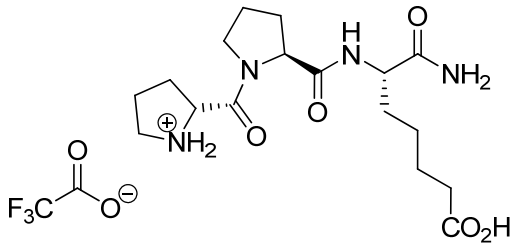

Prepared on Rink Amide AM Resin (0.62 mmol/g) on a 100 µmol scale according to the general protocols for functionalisation of Rink Amide AM resin (Protocol A1) and for automated peptide synthesis (Protocol C). Fmoc-Api(O*t*Bu)-OH [= (*S*)-Fmoc-2-amino-pimelic acid-7-tert-butyl ester] was used for the first coupling. Fmoc-Pro-OH was used for the second and Fmoc-D-Pro-OH for the third coupling. Cleavage from the solid support and isolation of the peptide was carried out according to the general protocol (Protocol D).

^{1}H NMR (400 MHz, D_2O, 25°C) δ = 4.64 (m, 1H), 4.47 (dd, *J* = 3.5 Hz, 8.9 Hz, 1H), 4.27 (dd, *J* = 5.5 Hz, 9.0 Hz, 1H), 3.72 (m, 1H), 3.60 (m, 1H), 3.43 (m, 2H), 2.66 (m, 1H), 2.32 (m, 3H), 2.05 (m, 5H), 1.79 (m, 3H), 1.62 (m, 2H), 1.42 (m, 2H).

^{13}C NMR (100 MHz, D_2O, 25°C) δ = 182.4, 179.7, 177.0 171.2, 63.7, 62.2, 56.5, 50.6, 49.6, 37.0, 33.4, 32.5, 31.0, 27.6, 27.2, 26.9, 26.9

MS (ESI): *m*/*z* (%): 369.2 (100) $[M+H]^+$. M = 368.4 calcd for $C_{17}H_{28}N_4O_5$.

TFA•H-D-Pro-Pro-Asu-NH_2 (59)

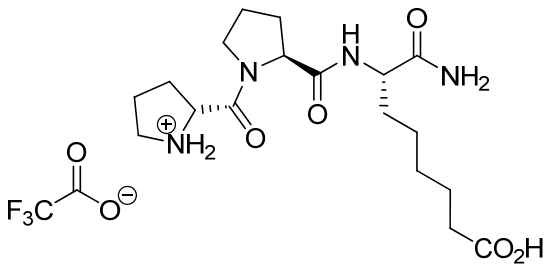

Prepared on Rink Amide AM Resin (0.62 mmol/g) on a 100 µmol scale according to the general protocols for functionalisation of Rink Amide AM resin (Protocol A1) and for automated peptide synthesis (Protocol C). Fmoc-Asu(O*t*Bu)-OH [= (*S*)-Fmoc-2-amino-

suberic acid-8-tert-butyl ester] was used for the first coupling. Fmoc-Pro-OH was used for the second and Fmoc-D-Pro-OH for the third coupling. Cleavage from the solid support and isolation of the peptide was carried out according to the general protocol (Protocol D).

^{1}H NMR (400 MHz, D_2O, 25°C) δ = 4.64 (dd, *J* = 7.3 Hz, 8.5 Hz, 1H), 4.48 (dd, *J* = 3.5 Hz, 9.0 Hz, 1H), 4.26 (dd, *J* = 5.6 Hz, 9.0 Hz, 1H), 3.73 (m, 1H), 3.61 (m, 1H), 3.43 (m, 2H), 2.55 (m, 1H), 2.37 – 2.26 (m, 3H), 2.04 (m, 5H), 1.78 (m, 3H), 1.59 (td, *J* = 7.3 Hz, 14.2 Hz, 2H), 1.30 (m, 4H).

^{13}C NMR (100 MHz, D_2O, 25°C) δ = 183.0, 179.7, 176.8, 171.0, 63.5, 62.0, 56.4, 50.4, 49.4, 37.3, 33.4, 32.3, 30.8, 30.4, 27.5, 27.2, 27.0 26.7.

MS (ESI): *m/z* (%): 383.3 (100) $[M+H]^+$. M = 382.5 calcd for $C_{18}H_{30}N_4O_5$.

TFA•H-D-Pro-Pro-D-Asn-OH (60)

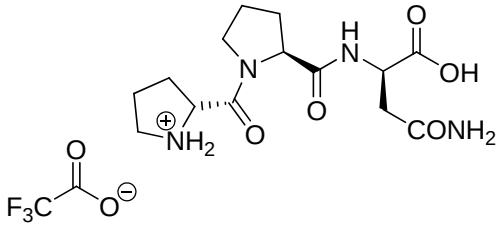

Prepared on Wang resin (1.0 mmol/g) on a 2 mmol scale according to the general protocols for functionalisation of Wang resin (Protocol A2) and for manual peptide synthesis using HCTU/*i*-Pr_2NEt (Protocol B1). Fmoc-D-Asn(Trt)-OH was used for the first coupling. Fmoc-Pro-OH for the second and Fmoc-D-Pro-OH for the third coupling. Cleavage from the solid support and isolation of the peptide was carried out according to the general protocol (Protocol D).

^{1}H NMR (400 MHz, D_2O, 25°C) δ = 4.62 (dd, *J* = 6.1 Hz, 8.5 Hz, 1H), 4.55 (dd, *J* = 6.1 Hz, 8.6 Hz, 1H), 4.38 (dd, *J* = 5.4 Hz, 8.6 Hz, 1H), 3.52 (m, 1H), 3.45 (m, 1H), 3.34 (m, 2H), 2.80 (dd, *J* = 5.8 Hz, 15.8 Hz, 1H), 2.76 (dd, *J* = 6.3 Hz, 15.6 Hz, 1H), 2.34 (m, 1H), 2.19 (m, 1H), 1.95-1.70 (m, 6H).

^{13}C NMR (100 MHz, D_2O, 25°C) δ = 175.0, 174.3, 173.7, 168.5, 60.9, 59.4, 49.7, 48.0, 47.0, 36.4, 29.6, 28.7, 24.9, 24.2.

MS (ESI): *m*/*z* (%): 327.2 (100) $[M+H]^+$. M = 326.3 calcd for $C_{14}H_{22}N_4O_5$.

TFA•H-D-Pro-Pro-D-Gln-OH (61)

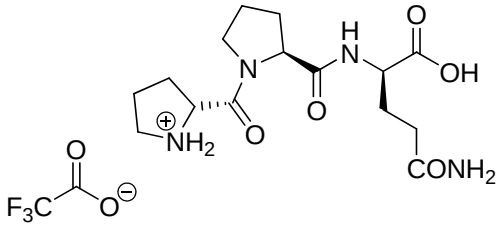

Prepared on Wang resin (1.0 mmol/g) on a 2 mmol scale according to the general protocols for functionalisation of Wang resin (Protocol A2) and for manual peptide synthesis using HCTU/*i*-Pr_2NEt (Protocol B1). Fmoc-D-Gln(Trt)-OH was used for the first coupling. Fmoc-Pro-OH for the second and Fmoc-D-Pro-OH for the third coupling. Cleavage from the solid support and isolation of the peptide was carried out according to the general protocol (Protocol D).

^{1}H NMR (400 MHz, D_2O, 25°C) δ = 4.51 (dd, *J* = 7.1 Hz, 8.8 Hz, 1H), 4.36 (dd, *J* = 3.5 Hz, 8.6 Hz, 1H), 4.28 (dd, *J* = 5.0 Hz, 9.2 Hz, 1H), 3.61 (m, 1H), 3.48 (m, 1H), 3.28 (m, 2H), 2.41 (m, 1H), 2.24 (m, 3H), 2.08 (m, 1H), 1.92 (m, 7H).

^{13}C NMR (100 MHz, D_2O, 25°C) δ = 178.3, 175.0, 174.2, 168.5, 61.2, 59.7, 52.6, 48.0, 47.0, 31.5, 30.1, 28.4, 26.7, 24.5, 24.3.

MS (ESI): *m*/*z* (%): 341.3 (100) $[M+H]^+$. M = 340.4 calcd for $C_{15}H_{24}N_4O_5$.

TFA•H-Pro-Pro-Glu-NH_2 (65)

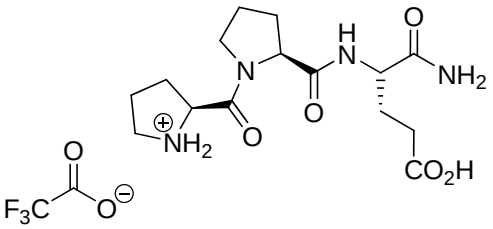

Prepared on Rink Amide AM Resin (0.71 mmol/g) on a 200 µmol scale according to the general protocols for functionalisation of Rink Amide AM resin (Protocol A1) and for automated peptide synthesis (Protocol C). Fmoc-Glu(O*t*Bu)-OH was used for the first coupling. Fmoc-Pro-OH was used for the second and the third coupling. Cleavage from the solid support and isolation of the peptide was carried out according to the general protocol (Protocol D).

^{1}H NMR (400 MHz, D_2O, 25°C) δ = 4.51 (dd, *J* = 6.3 Hz, 8.5 Hz, 1H), 4.36 (dd, *J* = 6.3 Hz, 8.2 Hz, 1H), 4.20 (dd, *J* = 5.5 Hz, 9.1 Hz, 1H), 3.57 (m, 1H), 3.45 (m, 1H), 3.29 (m, 2H), 2.42 (m, 3H), 2.21 (m, 1H), 2.07-1.72 (m, 8H).

^{13}C NMR (100 MHz, D_2O, 25°C) δ = 177.4, 176.2, 174.2, 168.4, 60.9, 59.5, 53.2, 48.1, 47.0, 30.2, 29.7, 28.7, 26.5, 25.0, 24.2.

MS (ESI): *m*/*z* (%): 341.3 (100) $[M+H]^+$. M = 340.4 calcd for $C_{15}H_{24}N_4O_5$.

TFA•H-Pro-D-Pro-Glu-NH_2 (66)

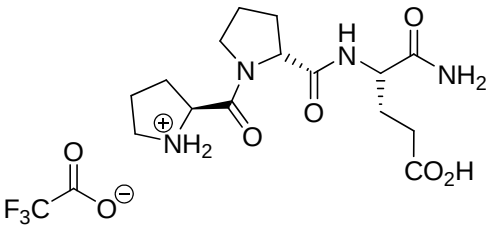

Prepared on Rink Amide AM Resin (0.71 mmol/g) on a 200 µmol scale according to the general protocols for functionalisation of Rink Amide AM resin (Protocol A1) and for automated peptide synthesis (Protocol C). Fmoc-Glu(O*t*Bu)-OH was used for the first coupling. Fmoc-D-Pro-OH was used for the second and Fmoc-Pro-OH for the third coupling.

Cleavage from the solid support and isolation of the peptide was carried out according to the general protocol (Protocol D).

^{1}H NMR (400 MHz, D_2O, 25°C) δ = 4.49 (dd, *J* = 7.1 Hz, 8.8 Hz, 1H), 4.34 (dd, *J* = 4.4 Hz, 8.8 Hz, 1H), 4.23 (dd, *J* = 4.8 Hz, 9.8 Hz, 1H), 3.60 (m, 1H), 3.47 (m, 1H), 3.29 (m, 2H), 2.47-2.37 (m, 3H), 2.19 (m, 1H), 2.07 (m, 1H), 2.01-1.78 (m, 7H).

^{13}C NMR (100 MHz, D_2O, 25°C) δ = 177.4, 176.3, 174.6, 168.4, 61.3, 59.6, 53.2, 48.0, 47.0, 30.5, 29.9, 28.5, 26.3, 24.7, 24.3.

MS (ESI): *m*/*z* (%): 341.2 (100) $[M+H]^+$. M = 340.4 calcd for $C_{15}H_{24}N_4O_5$.

TFA•H-Pro-Pro-D-Glu-NH_2 (67)

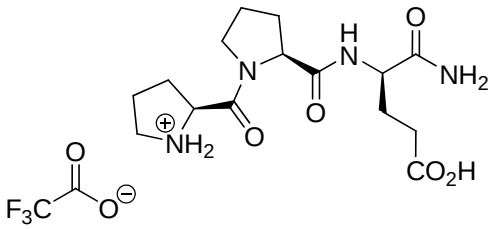

Prepared on Rink Amide AM Resin (0.71 mmol/g) on a 200 μmol scale according to the general protocols for functionalisation of Rink Amide AM resin (Protocol A1) and for automated peptide synthesis (Protocol C). Fmoc-D-Glu(O*t*Bu)-OH was used for the first coupling. Fmoc-Pro-OH was used for the second and for the third coupling. Cleavage from the solid support and isolation of the peptide was carried out according to the general protocol (Protocol D).

^{1}H NMR (400 MHz, D_2O, 25°C) δ = 4.50 (dd, *J* = 6.4 Hz, 8.5 Hz, 1H), 4.35 (dd, *J* = 7.1 Hz, 7.7 Hz, 1H), 4.24 (dd, *J* = 4.7 Hz, 9.9 Hz, 1H), 3.59 (m, 1H), 3.45 (m, 1H), 3.27 (m, 2H), 2.50-2.30 (m, 3H), 2.21 (m, 1H), 2.09 (m, 1H), 2.02-1.75 (m, 7H).

^{13}C NMR (100 MHz, D_2O, 25°C) δ = 177.3, 176.3, 174.4, 168.4, 61.2, 59.5, 53.0, 48.1, 47.0, 30.4, 29.7, 28.7, 26.4, 25.1, 24.2.

MS (ESI): *m*/*z* (%): 341.2 (100) $[M+H]^+$. M = 340.4 calcd for $C_{15}H_{24}N_4O_5$.

TFA•H-D-Pro-Pro-Gln-NH_2 (75)

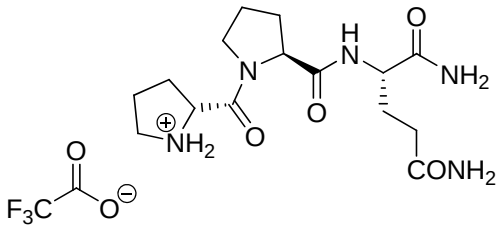

Prepared on Rink Amide AM Resin (0.71 mmol/g) on a 200 µmol scale according to the general protocols for functionalisation of Rink Amide AM resin (Protocol A1) and for automated peptide synthesis (Protocol C). Fmoc-Gln(Trt)-OH was used for the first coupling. Fmoc-Pro-OH was used for the second and Fmoc-D-Pro-OH for the third coupling. Cleavage from the solid support and isolation of the peptide was carried out according to the general protocol (Protocol D).

^{1}H-NMR (400 MHz, D_2O / CD_3OD 5 : 1, 23°C): δ = 4.63 (m, 1H), 4.46 (dd, *J* = 3.0 Hz, 8.9 Hz, 1H), 4.29 (dd, *J* = 4.9 Hz, 9.5 Hz, 1H), 3.74 (m, 1H), 3.61 (m, 1H), 3.42 (m, 2H), 2.55 (m, 1H), 2.40 (t, *J* = 7.4 Hz, 2H), 2.33 (m, 1H), 2.17 – 1.93 (m, 8H).

^{13}C-NMR (100 MHz, D_2O / CD_3OD 5 : 1, 23°C): δ =180.8, 178.7, 176.9, 171.2, 64.0, 62.4, 56.0, 50.7, 49.7, 34.3, 32.5, 31.2, 29.9, 27.4, 27.0.

MS (ESI): *m*/*z*(%): 340.2 (100) $[M+H]^+$. M = 339.4 calcd for $C_{15}H_{25}N_5O_4$.

16.3 Peptides Prepared by Solution-Phase Synthesis

Boc-Pro-Pro-OH (90)

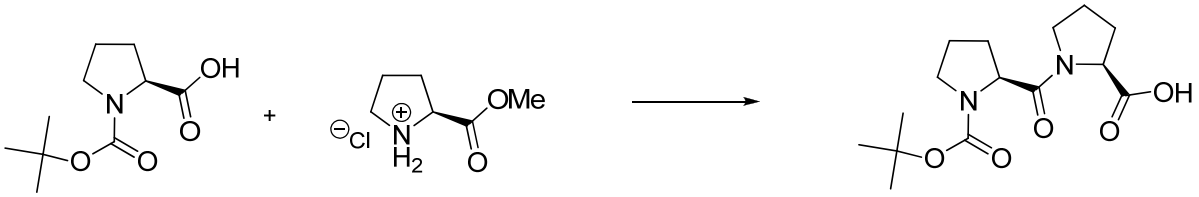

Boc-Pro-OH (16.4 g, 76.1 mmol, 1.05 eq), EDC•HCl (16.68 g, 87.0 mmol, 1.2 eq) and HOBt•H_2O (13.3 g, 87.0 mmol, 1.2 eq) were charged into a 1L flask and 200 mL of dry CH_2Cl_2 was added with stirring while the contents were cooled to 0^{o}C in an ice-bath. *i*-Pr_2NEt (15.0 mL, 90.6 mmol, 1.25 eq) was added dropwise over 10 min, and the resulting yellow solution was stirred for an additional 10 min before HCl•H-Pro-OMe (12.0 g, 72.5 mmol, 1.0 eq) was added as a solid. The resulting homogeneous yellow reaction mixture was stirred at RT for 4 h and diluted with 200 mL of 0.1 M HCl. The layers were separated and the aqueous phase extracted with CH_2Cl_2 (3 x 30 mL). The combined organic phases were washed with 1 M $NaHCO_3$ solution (100 mL), water (100 mL) and brine (100 mL). The dried ($MgSO_4$) organic phases were filtered through a short plug of silicagel (10 mm, 4 cm dia) and the crude protected dipeptide solution was concentrated *in vacuo* at 30 ^{o}C. The resulting light yellow oil was chromatographed over silicagel eluting with 2 % (v/v) MeOH/CH_2Cl_2 (TLC visualised with ninhydrin), product containing fractions combined and concentrated *in vacuo* to afford Boc-Pro-Pro-OMe as a clear colourless oil (21.7 g, 92 %).

The obtained Boc-Pro-Pro-OMe (13.7 g, 42.0 mmol, 1.0 eq) was dissolved in a mixture of 1:1:1 (v/v/v) THF/MeOH/4M NaOH (250 mL) and the resulting cloudy mixture was stirred at RT for 2 h until the lower layer of oil was consumed and the starting material showed complete conversion by TLC (CH_2Cl_2/MeOH 9:1 v/v, ninhydrin). The basic aqueous layer was washed with CH_2Cl_2 (3 x 100 mL) and was then acidified (to pH 2) with concentrated HCl (30% aq). The resulting colourless suspension was extracted with EtOAc (5 x 75 mL). The combined EtOAc layers were washed with brine (1 x 100 mL) and dried over anhydrous Na_2SO_4. The solvents were evaporated *in vacuo* yielding a sticky foam which was dissolved in a minimum amount of CH_2Cl_2 (40 mL). Pentane (200 mL) was added slowly and the mixture was unltrasonicated until a colourless suspension was obtained. Evaporation of the

solvents and drying under high vaccum yielded Boc-Pro-Pro-OH **90** as a white solid (10.2 g, 78 %).

^{1}H NMR (400 MHz, $CDCl_3$, 23°C): Rotamers were observed around the *t*Bu singlet in a approximate ratio 2:1: δ = 4.69 - 4.38 (m, 2H), 3.83 - 3.39 (m, 4H), 2.40 - 1.87 (m, 8H), 1.46 and 1.40 (2 × s, $(CH_3)_3$ rotamers, 9H).

^{13}C NMR (100 MHz, $CDCl_3$, 23°C): Mixture of rotamers: δ = 174.7, 174.4, 172.5, 172.2, 154.6, 153.5, 80.0, 79.8, 60.0, 59.9, 57.7, 57.6, 47.3, 46.9, 46.7, 30.2, 29.4, 28.45, 28.4, 27.2, 27.0, 25.0, 24.3, 23.7.

MS (ESI): *m/z* (%): 313.4 (100) $[M+H]^+$. M = 312.4 calcd for $C_{15}H_{24}N_2O_5$.

Boc-D-Pro-Pro-OH (91)

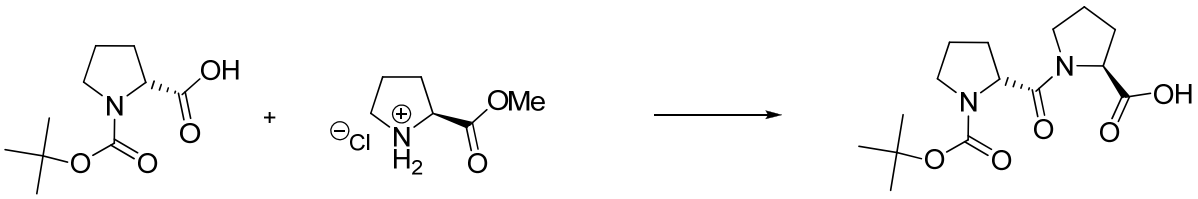

Boc-D-Pro-Pro-OH **91** was prepared in analogy to Boc-Pro-Pro-OH **90** (peptide coupling and soaponification), using Boc-D-Pro-OH (10.0 g, 46.5 mmol, 1.05 eq), EDC•HCl (10.2 g, 53.1 mmol, 1.2 eq), HOBt•H_2O (8.1 g, 53.1 mmol, 1.2 eq), *i*-Pr_2NEt (9.2 mL, 55.3 mmol, 1.25 eq) and HCl•H-Pro-OMe (7.3 g, 44.3 mmol, 1.0 eq). The product was obtained as a white solid (10.4 g, 72 % overall).

^{1}H NMR (400 MHz, $CDCl_3$, 23°C): Rotamers were observed around the *t*Bu singlet in a approximate ratio 2:1: δ = 10.21 (s br, 1H), 4.54 (m, 1H), 4.39 (m, 1H), 3.95 - 3.28 (m, 4H), 2.45 - 1.68 (m, 8H), 1.37 and 1.33 (2 × s, $(CH_3)_3$ rotamers, 9H).

^{13}C NMR (100 MHz, $CDCl_3$, 23°C): Mixture of rotamers: δ = 175.6, 174.3, 172.0, 171.5, 154.9, 153.4, 143.7, 80.6, 80.4, 60.5, 57.9, 57.7, 47.5, 46.9, 46.6, 30.2, 29.1, 28.5, 28.4, 28.3, 28.1, 28.0, 27.0, 24.8, 24.7, 24.7, 23.7.

MS (ESI): *m/z* (%): 335.1 (100) $[M+Na]^+$. M = 312.4 calcd for $C_{15}H_{24}N_2O_5$.

TFA•H-Pro-Pro-Asp-OMe (8)

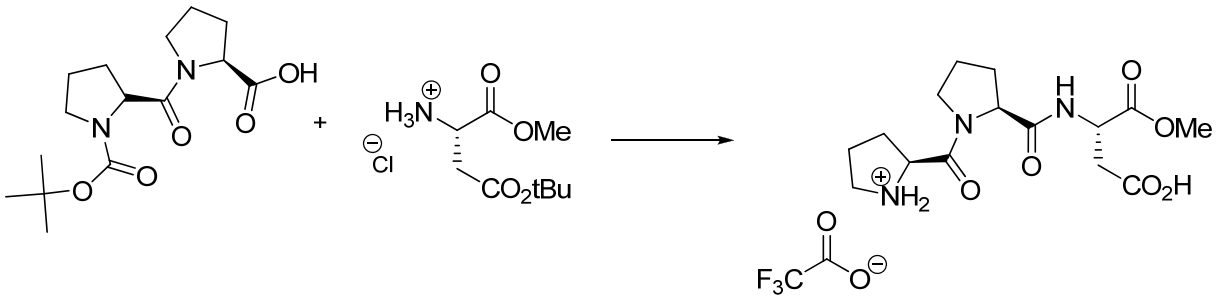

Boc-Pro-Pro-OH **90** (500 mg, 1.6 mmol, 1.0 eq), H-Asp(O*t*Bu)-OMe•HCl (384 mg, 1.6 mmol, 1.0 eq) and EDC•HCl (368 mg, 1.9 mmol, 1.2 eq) were charged into a 50 mL flask. 10 mL EtOAc and 1mL DMF were added with stirring. *i*-Pr_2NEt (320 µL, 1.9 mmol, 1.2 eq) was added and the cloudy mixture was stirred at RT over night. The TLC (EtOAc/MeOH 10:1 v/v) showed complete conversion of the starting material. The resulting clear solution was diluted with EtOAc (20 mL) and extracted with 0.1M HCl (5 mL), H_2O (5 mL), $NaHCO_3$ 10 % aq (5 mL) and brine (2x 5 mL). The organic layer was dried ($MgSO_4$) and concentrated *in vacuo* at 30 °C to a colourless oil which was then chromatographed over silicagel eluting with a gradient of neat EtOAc to 10% (v/v) MeOH in EtOAc. Product containing fractions were combined and concentrated *in vacuo*. A mixture of TFA/CH_2Cl_2 2:1 (v/v) (2 mL) was added to the obtained Boc-D-Pro-Pro-Asp(O*t*Bu)-OMe and the solution was stirred for 1 h. All volatailes were removed *in vacuo* followed by precipitation of the remaining oil with Et_2O (10 mL). The precipitate was filtered over a syringe filter and triturated with Et_2O (3x 3 mL). Drying under high vaccum yielded TFA•H-Pro-Pro-Asp-OMe **8** as a white solid (355 mg, 65 %).

^{1}H-NMR (400 MHz, d6-DMSO, 23°C): The conformers were observed in the ratio 4:1. Major conformer: δ = 9.89 (s, 1H), 8.45 (br s, 1H), 8.42 (d, *J* = 8.2 Hz, 1H), 4.55 (dd, *J* = 13.9, 6.4 Hz, 1H), 4.46 (m, 1H), 4.11 (dd, *J* = 8.3, 4.8 Hz, 1H), 3.60 (m, 1H), 3.58 (s, 3H), 3.42 (m, 1H), 3.23 (m, 1H), 3.16 (m, 1H), 2.75 (m, 1H), 2.65 (m, 1H), 2.40 (m, 1H), 2.12 (m, 1H), 2.94–1.72 (m, 6H). Minor conformer: δ = 9.80 (s, 1H), 8.55 (br s, 1H), 8.88 (d, *J* = 7.6 Hz, 1H), 4.61 (m, 1H), 4.46 (m, 1H), 4.11 (dd, *J* = 8.3, 4.7 Hz, 1H), 3.87 (m, 1H), 3.61 (s, 3H), 3.60 (m, 1H), 3.45 (m, 1H), 3.23 (m, 1H), 2.78, (m, 1H), 2.60 (m, 1H), 2.40 (m, 1H), 2.26 (m, 1H), 2.94–1.72 (m, 6H).

^{13}C NMR (100 MHz, d6-DMSO, 25 °C): Major conformer: δ = 172.4, 172.3, 172.2, 171.8, 60.2, 59.1, 52.9, 49.4, 47.6, 46.6, 36.7, 29.9, 28.7, 25.2, 24.4. Minor Conformer: δ = 172.36, 171.91, 171.67, 171.56, 60.37, 59.16, 53.12, 49.51, 47.15, 46.37, 36.38, 29.81, 28.85, 25.13, 24.41.

HRMS (ESI) *m/z*: calcd for $C_{15}H_{24}N_3O_6$ 342.1665; found, 342.1654.

TFA•H-D-Pro-Pro-Asp-OMe (51)

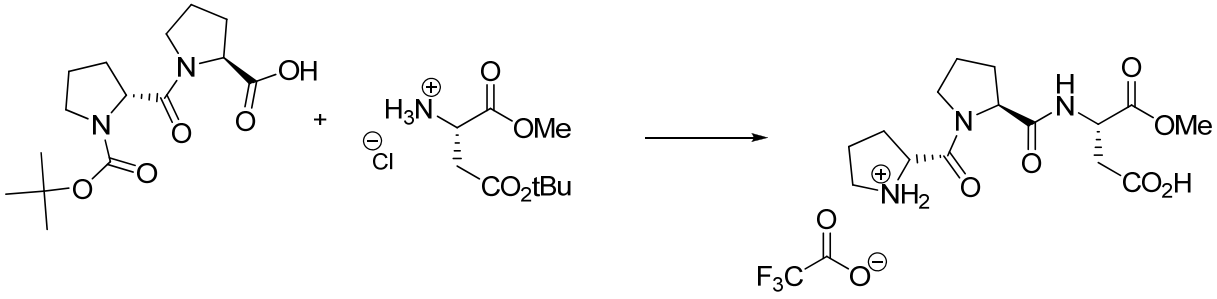

TFA•H-D-Pro-Pro-Asp-OMe **51** was prepared in analogy to TFA•H-Pro-Pro-Asp-OMe **8** using Boc-D-Pro-Pro-OH **91** (600 mg, 1.92 mmol, 1.0 eq), H-Asp(O*t*Bu)-OMe•HCl (461 mg, 1.92 mmol, 1.0 eq), EDC•HCl (442 mg, 2.3 mmol, 1.2 eq) and *i*-Pr_2NEt (384 µL, 2.3 mmol, 1.2 eq). The product was obtained as a white solid (427 mg, 69 % overall).

^{1}H NMR (400 MHz, D_2O, 25°C) δ= 4.81 (m, 1H); 4.63 (dd, *J* = 7.0 Hz, 8.8 Hz, 1H), 4.48 (dd, *J* = 3.3 Hz, 1H), 3.76 (s, 3H), 3.73 (m, 1H), 3.60 (m, 1H), 3.42 (m, 2H), 2.99 (d, *J* = 6.1 Hz, 2H), 2.56 (m, 1H), 2.33 (m, 1H), 2.14 – 1.97 (m, 6H).

^{13}C NMR (100 MHz, D_2O, 25°C) δ= 177.3, 177.0, 175.6, 171.1, 63.8, 62.4, 56.3, 52.3, 50.7, 49.8, 38.4, 32.7, 31.2, 27.3, 27.1.

HRMS (ESI) *m/z*: calcd for $C_{15}H_{24}N_3O_6$ 342.1665; found, 342.1669.

TFA•H-D-Pro-Pro-Asp-NHPr (54)

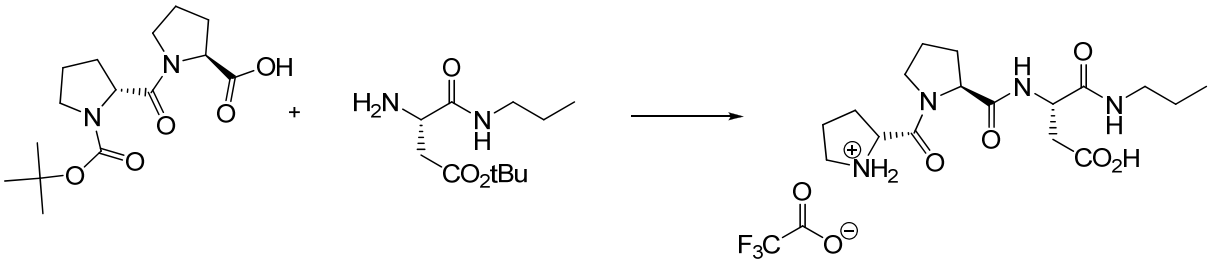

Boc-D-Pro-Pro-OH **91** (406 mg, 1.3 mmol, 1.0 eq), H-Asp(O*t*Bu)-NHPr **96** (300 mg, 1.3 mmol, 1.0 eq) and EDC•HCl (299 mg, 1.56 mmol, 1.2 eq) were charged into a 50 mL flask. 10 mL EtOAc and 1mL DMF were added with stirring. *i*-Pr_2NEt (271 µL, 1.56 mmol, 1.2 eq) was added and the mixture was stirred for 90 min. According to the TLC (EtOAc/MeOH 10:1 v/v) approximately 50 % of the starting material was converted. Therefore HOBt (88 mg, 0.65 mmol, 0.5 eq) was added and stirring was continued for 90 min. The reaction mixture was then diluted with EtOAc (20 mL) and extracted with 0.1M HCl (5 mL), H_2O (5 mL), $NaHCO_3$ 10 % aq (5 mL) and brine (2x 5 mL). The organic layer was dried ($MgSO_4$) and concentrated *in vacuo* at 30 °C. The obtained colourless oil was then chromatographed over silicagel eluting with 10% v/v MeOH in EtOAc. Product containing fractions were combined and concentrated *in vacuo*. A mixture of TFA/CH_2Cl_2 2:1 (v/v) (2 mL) was added to the obtained Boc-D-Pro-Pro-Asp(O*t*Bu)-NHPr and the solution was stirred for 1 h. All volatailes were removed *in vacuo* followed by precipitation of the remaining oil with Et_2O (10 mL). The precipitate was filtered over a syringe filter and triturated with Et_2O (3x 3 mL). Drying under high vaccum yielded TFA•H-Pro-Pro-Asp-NHPr **54** as a white solid (408 mg, 68 %).

^{1}H NMR (400 MHz, D_2O, 25°C) δ = 4.64 (m, 2H), 4.46 (dd, *J* = 3.0 Hz, 8.9 Hz, 1H), 3.73 (m, 1H), 3.60 (m, 1H), 3.43 (m, 2H), 3.17 (m, 2H), 2.91 (ddd, *J* = 1.36 Hz, 6.08 Hz, 16.61 Hz, 1H), 2.81 (ddd, *J* = 1.29 Hz, 7.97 Hz, 16.7 Hz, 1H), 2.56 (m, 1H), 2.31 (m, 1H), 2.14 – 1.96 (m, 6H), 1.49 (m, 2H), 0.85 (t, *J* = 7.4 Hz, 3H).

^{13}C NMR (100 MHz, D_2O, 25°C) δ = 177.1, 176.8, 175.0, 171.3, 63.9, 62.4, 53.7 50.8, 49.8, 44.4, 38.6, 32.7, 31.1, 27.3, 27.0, 24.9, 13.6.

HRMS (ESI) *m/z*: calcd for $C_{17}H_{29}N_4O_5$ 369.2137; found, 369.2148.

TFA•H-D-Pro-Pro-5-Ava-OH (95)

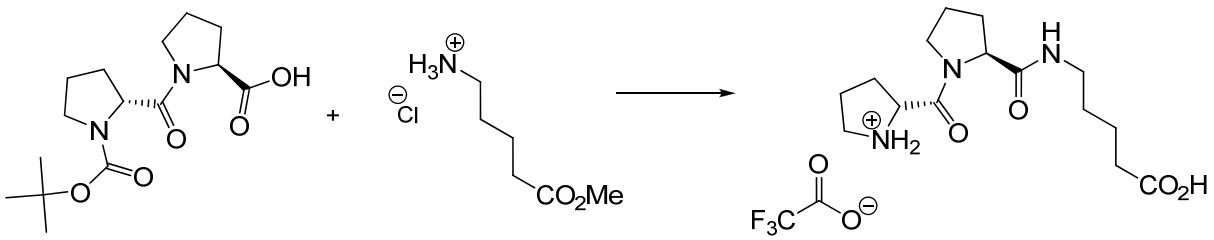

Boc-D-Pro-Pro-OH **91** (820 mg, 2.62 mmol, 1.0 eq), HCl•H-5-Ava-OMe **95** (440 mg, 2.62 mmol, 1.0 eq), *i*-Pr_2NEt (1.0 mL, 5.77 mmol, 2.2 eq) and EDC•HCl (605 mg, 3.14 mmol, 1.2 eq) were suspended in EtOAc (25 mL) and stirred over night at RT. To the resulting turbid solution was added DMF (4 mL) and after ultrasonication a colourless solution was obtained which was stirred for a further 2 h at RT. TLC (EtOAc/MeOH 10:1 v/v, visualised with ninhydrin and $KMnO_4$) showed complete conversion. The reaction mixture was diluted with EtOAc (100 mL) and successively extracted with 0.1 M HCl (20 mL), H_2O (20 mL), aqueous $NaHCO_3$ 10% (20 mL), H_2O (20 mL) and brine (20 mL). The organic layer was dried ($MgSO_4$), and concentrated under reduced pressure. The resulting oil was chromatographed over silicagel eluting with EtOAc (250 mL) and EtOAc/MeOH 20:1 (v/v) (250 mL). The desired Boc-D-Pro-Pro-5-Ava-OMe was obtained as a colourless oil (0.95 g, 85 %).

100 mg Boc-D-Pro-Pro-5-Ava-OMe (0.235 mmol, 1.0 eq) was dissolved in 1 mL MeOH and 260 µL (0.260 mmol, 1.1 eq) of an aqueous solution of 0.1 M NaOH was added. The reaction mixture was then stirred for 1 h at RT (TLC showed approximately 50 % conversion). Additional 0.1 M aq NaOH (260 µL, 0.260 mmol, 1.1 eq) was added and the mixture was stirred for another 2 h (TLC showed complete conversion). The reaction mixture was concentrated *in vacuo* and the residue was diluted in water (5 mL) before extraction with EtOAc (2x 5 mL). The collected organic layers were dried ($MgSO_4$) and concentrated under reduced pressure. The corresponding Boc-D-Pro-Pro-5-Ava-OH was obtained as a white powder (80 mg) which was dissolved in CH_2Cl_2 (3 mL). TFA (300 µL) was added and the reaction mixture was stirred for 1 h at RT before all volatiles were removed *in vacuo*. The obtained oil was dried under high vacuum and afterwards lyophilised, however, the desired title compound **95** remained a colourless oil (81 mg, 81 % overall).

^{1}H NMR (400 MHz, D_2O, 25°C): δ = 4.50 (dd, *J* = 7.0 Hz, 8.8 Hz, 1H), 4.26 (dd, *J* = 4.2 Hz, 8.9 Hz, 1H), 3.60 (td, *J* = 6.3 Hz, 6.3 Hz, 10.2 Hz, 1H), 3.48 (ddd, *J* = 3.4 Hz, 7.3 Hz, 14.2 Hz, 1H), 3.30 (m, 2H), 3.90 (m, 2H), 2.43 (ddd, *J* = 6.8 Hz, 8.9 Hz, 13.0 Hz, 1H), 2.27 (t, *J* = 7.1 Hz, 2H), 2.16 (ddd, *J* = 5.8 Hz, 8.8 Hz, 12.4 Hz, 1H), 1.70-2.00 (m, 6H), 1.36-1.52 (m., 4H).

^{13}C NMR (100 MHz, CDCl3, 25°C) *δ* = 178.3, 171.4, 168.8, 62.0, 59.9, 47.5, 47.1, 39.3, 33.0, 29.8, 28.9, 28.1, 25.4, 24.6, 21.0.

MS (ESI): *m/z*: 312.2 $[M+H]^+$. M = 311.2 calcd for $C_{15}H_{25}N_3O_4$.

Boc-Pro-2-MePro-OH (92)

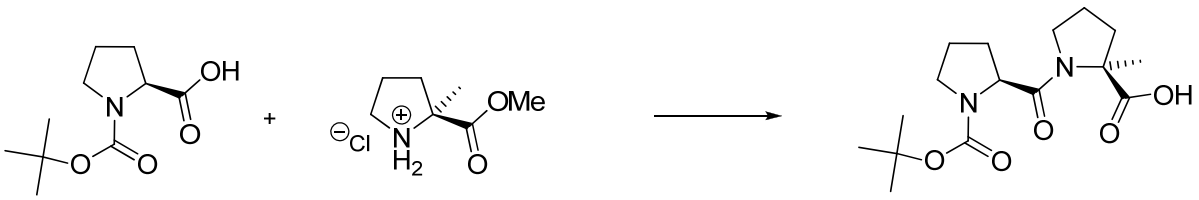

Boc-Pro-OH (7.55 g, 35.1 mmol, 1.05 eq), EDC•HCl (7.70 g, 40.2 mmol, 1.2 eq), HOBt•H_2O (6.16 g, 40.2 mmol, 1.2 eq), were charged into a 500 mL flask and 100 mL of dry CH_2Cl_2 was added with stirring and cooling to 0 ^{o}C under N_2. *i*-Pr_2NEt (2.25 eq, 75.15 mmol, 12.9 mL) was added over 10 min, and the resulting slightly yellow solution was stirred for an additional 10 min prior to addition of solid HCl•H-2-MePro-OMe (1.0 eq, 33.4 mmol, 6.0 g). The resulting homogeneous yellow reaction mixture was stirred at RT for 4 h and diluted with 100 mL of 0.1 M HCl. The layers were separated and the aqueous phase extracted with CH_2Cl_2 (3 x 30 mL). The combined organic phases were washed with 1 M $NaHCO_3$ solution (50 mL), water (50 mL) and brine (50 mL). The dried ($MgSO_4$) organic phases were filtered through a short plug of silicagel (10 mm, 4 cm dia) and the crude protected dipeptide solution was concentrated *in vacuo* at 30 ^{o}C. The resulting light yellow oil was chromatographed over silicagel eluting with 2 % (v/v) MeOH/CH_2Cl_2 (TLC visualised with ninhydrin), product containing fractions combined and concentrated *in vacuo* to afford the pure Boc-Pro-2-MePro-OMe as a clear colourless oil (10.3 g, 90 %).

The obtained Boc-Pro-2-MePro-OMe (9.70 g, 28.5 mmol, 1.0 eq) was then dissolved in a mixture of 1:1:1 (v/v/v) THF/MeOH/4M NaOH (100 mL) and the resulting cloudy mixture was stirred at RT for 2 h until the lower layer of oil was consumed and the starting material showed complete conversion by TLC (CH_2Cl_2/MeOH 98:2 v/v, ninhydrin-dip). The basic aqueous layer was washed with CH_2Cl_2 (3 x 50 mL) and was then acidified (to pH 2) with concentrated HCl (30 % aq). The resulting colourless suspension was extracted with EtOAc (5 x 40 mL). The combined EtOAc layers were washed with brine (1 x 50 mL) and dried over anhydrous Na_2SO_4. The solvents were evaporated *in vacuo* yielding a sticky foam which was dissolved in a minimum amount of CH_2Cl_2 (30 mL). Pentane (150 mL) was added slowly and the mixture was ultrasonicated until a colourless suspension was obtained. Evaporation of the solvents and drying on high vacuum yielded Boc-Pro-2-MePro-OH **92** as a white solid (7.44 g, 80 %).

^{1}H NMR (400 MHz, $CDCl_3$, 23°C) Rotamers were observed around the *t*Bu singlet in a approximate ratio 3:1: δ = 10.9 (br s, 1H), 4.29 (m, 1H), 3.69 - 3.30 (m, 4H), 2.30 - 1.83 (m, 8H), 1.67 (s, 3H), 1.44 and 1.36 (2 × s, $(CH_3)_3$ rotamers, 9H).

^{13}C NMR (100 MHz, $CDCl_3$): Mixtures of rotamers: δ = 178.4, 177.8, 172.4, 171.8, 154.4, 153.7, 80.1, 79.7, 72.3, 72.9, 67.8, 67.4, 49.8, 49.2, 46.5, 46.1, 42.3, 41.6, 29.5, 29.1, 28.5, 28.0, 25.6, 25.1, 24.5, 24.0, 20.3, 19.7.

MS (ESI): *m/z* (%): 327.4 (100) $[M+H]^+$. M = 326.4 calcd for $C_{16}H_{26}N_2O_5$.

16.4 Synthesis of Non-Commercial Available Building Blocks

Fmoc-β-homo-Asp(O*t*Bu)-OH **93** and *N*-Me-Pro-OH **94** were originally prepared by Dr. J. D. Revell during his post doctoral studies in the Wennemers group at the University of Basel (2004 – 2008).

Fmoc-β-homo-Asp(O*t*Bu)-OH (93)

The synthesis of Fmoc-β-homo-Asp(O*t*Bu)-OH **93** occurred via seven steps starting from dimethyl 3-oxoglutarate and ammonium acetate according to Crossley et al.[166]

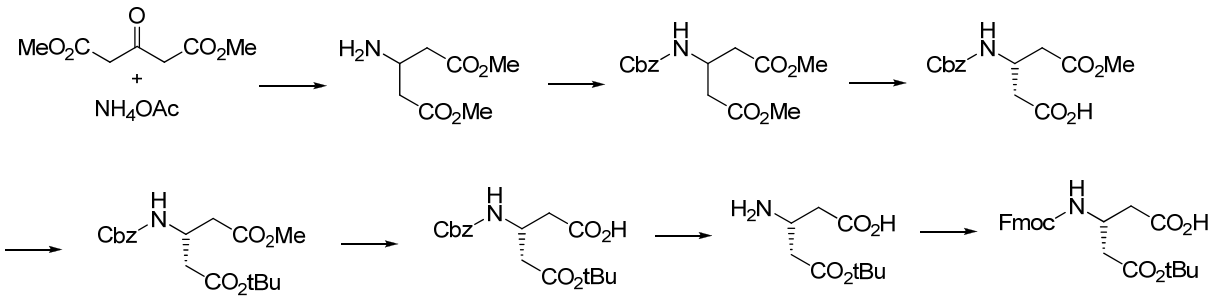

Dimethyl 3-aminoglutarate

A solution of dimethyl-3-oxoglutarate (50.0 g, 287 mmol) and ammonium acetate (250 g, 3.24 mol, 11.3 eq) in dry MeOH (800 mL) was stirred over molecular sieves (3Å; 100 g) for 2 d at RT. The mixture was acidified to pH 3 by addition of methanolic HCl (5M). Sodium cyanoborohydride (22.6 g, 360 mmol, 1.25 eq) was added, and the mixture reacidified to pH 3 and then stirred for 1 h at RT. The mixture was filtered through Celite and the methanol removed. The residual oil was basified to pH 9, with cooling, by addition of sodium hydroxide (10 M); water was then added until the solution was homogenous. The aqueous layer was extracted with CH_2Cl_2 (5 x 200 mL). The combined organic extracts were washed with saturated NaCl (2 x 100 mL) and dried (Na_2SO_4) and the solvent removed, affording the crude product as an oil which was distilled under reduced pressure yielding dimethyl-3-aminoglutarate as a colourless oil (29.4 g, 58 %).

^{1}H NMR (400 MHz, $CDCl_3$, 25°C) δ = 3.61 (s, 6 H; OC*H*$_3$), 3.38 (m, 1H; C*H*), 2.48 (d, *J* = 6 Hz, 4H; C*H*$_2$), 1.79 (br s, 2H; N*H*$_2$).

b.p. 67-70 ^{o}C at 0.07 mbar.

Dimethyl 3-benzyloxycarbonylaminoglutarate

To dimethyl 3-aminoglutarate (20.0 g, 114 mmol) dissolved in aq $NaHCO_3$ (1M; 2 eq, 228 mmol = 228 mL) was added a solution of benzyl chloroformate (19.4 g, 16.0 mL, 114 mmol) at 0 ^{o}C. The mixture was stirred for 3 h at RT then extracted with diethyl ether (5 x 100 mL). The combined ether extracts were washed with HCl (3M; 3 x 50 mL), saturated $NaHCO_3$ (2 x 25 mL), brine (2 x 25 mL), and dried (Na_2SO_4), and the solvent removed to give an oil. Chromatography of the oil on silica gel eluting with 30% EtOAc/*n*-pentanes gave dimethyl 3-benzyloxycarbonylaminoglutarate as a colourless oil (32.15 g, 91 %).

^{1}H NMR (400 MHz, $CDCl_3$, 25°C) δ = 7.24 (m, 5H; Ar*H*), 5.55 (br d, 1H; N*H*), 5.05 (s, C*H*$_2$Ar; 2H), 4.35 (m, 1H; C*H*), 3.65 (s, 6H; OC*H*$_3$), 2.69 (d, *J* = 6 Hz, 4H; C*H*$_2$).

Methyl hydrogen (3S)-3-benzyloxycarbonylaminoglutarate

To a mixture of dimethyl 3-benzyloxycarbonylaminoglutarate (15.4 g, 49.8 mmol) in phosphate buffer (0.5M; pH 8.0) (1.5 L) and acetone (45 mL) was added pig liver esterase (PLE; 20,000 units). The mixture was stirred at 25 ^{o}C for 7 h. The pH of the mixture was checked periodically and NaOH (0.1M) was added dropwise to maintain the pH at 8.0.

The resultant solution was acidified to pH 2 by addition of concentrated HCl, and extracted with CH_2Cl_2 (4 x 500 mL). The combined extracts were washed with saturated NaCl (500 mL), dried over Na_2SO_4, and concentrated *in vacuo* to afford the crude half-ester as a white solid. Recrystallisation from $CHCl_3$/*n*-pentanes gave the title compound as fine, colourless white needles (11.8 g, 80 %).

^{1}H NMR (400 MHz, $CDCl_3$, 25°C) δ = 8.58 (br s, 1H; CO_2*H*), 7.30 (m, 5H; Ar*H*), 5.75 (br d, 1H; N*H*), 5.05 (s, 2H; C*H*$_2$Ar), 4.30 (m, 1H; C*H*), 3.60 (s, 3H; C*H*$_3$), 2.68 (d, *J* = 6 Hz, 4H; C*H*$_2$).

$[\alpha]_D^{25}$ = +0.70^o (c = 6.0, $CHCl_3$).

Methyl tert-butyl (3R)-3-benzyloxycarbonylaminoglutarate

To a solution of the half-ester (6.29 g, 21.3 mmol) in dry CH_2Cl_2 (25 mL) was added DMAP (250 mg, 2.0 mmol) and *tert*-butanol (10 mL). DCC (4.56 g, 22 mmol) was added to the stirred solution at 0 ^oC, and after stirring at this temperature for 5 min, the mixture was allowed to warm to RT and stirred for a further 3 h. The mixture was filtered and the solvent removed. The residue was taken up in EtOAc (250 mL), refiltered, washed with HCl (1M, 125 mL), saturated $NaHCO_3$ (125 mL), and saturated NaCl (125 mL), and dried (Na_2SO_4). The solvent was removed to give an oil which was chromatographed over SiO_2, eluting with CH_2Cl_2 to afford the pure title compound as a colourless oil (6.25 g, 84 %).

^{1}H NMR (400 MHz, $CDCl_3$, 25°C) δ = 7.24 (m, 5H; Ar*H*), 5.30-5.65 (br d, 1H; N*H*), 5.05 (s, 2H; CH_2Ar), 4.15-4.50 (br m, 1H; C*H*), 3.65 (s, 3H; OCH_3), 2.65 (d, *J* = 6 Hz, 2H; CH_2), 2.40 (d, *J* = 6 Hz, 2H; CH_2), 1.45 (s, 9H; OC(CH_3)$_3$).

$[\alpha]_D^{25}$ = –1.12^o (c = 3.5, $CHCl_3$).

tert-Butyl hydrogen (3R)-3-benzyloxycarbonylaminoglutarate

To a stirred solution of the diester (10.5 g, 29.9 mmol) in MeOH (100 mL) was added lithium hydroxide solution (1M; 35 mmol, 35 mL). The solution was stirred for 2.5 h at RT, then diluted with water (500 mL) and extracted with CH_2Cl_2 (4 x 250 mL). The aqueous layer was acidified to pH 2 by addition of concentrated HCl and then extraced with CH_2Cl_2 (6 x 200 mL). The combined extracts were washed with saturated NaCl (250 mL), dried (Na_2SO_4), and the solvent removed to afford the half-ester as a colourless gum (8.39 g, 83 %).

^{1}H NMR (400 MHz, $CDCl_3$, 25°C) δ = 7.24 (m, 5H, Ar*H*); 5.75 (br d, 1H, N*H*); 5.05 (s, 2H; CH_2), 4.30 (m, 1H; C*H*), 2.70 (d, *J* = 6 Hz, 2H; CH_2), 2.60 (d, *J* = 6 Hz, 2H; CH_2), 1.45 (s, 9H; OC(CH_3)$_3$).

$[\alpha]_D^{25}$ = –1.1^o (c = 2.4, $CHCl_3$).

tert-Butyl hydrogen (3R)-3-aminoglutarate

To a solution of *tert*-Butyl hydrogen (3*R*)-3-benzyloxycarbonylaminoglutarate (6.07 g, 18.0 mmol) in EtOAc (250 mL) was added under argon palladium on charcoal (10 % w/w, 520

mg) and the reaction mixture was hydrogenated at RT under atmospheric pressure for 12 h. Following filtration of the reaction mixture through Celite, concentration of the filtrate and washings afforded the title compound as a colourless glass (3.55 g, 97 %).

^{1}H NMR (400 MHz, $CDCl_3$, 25°C) δ = 5.85 (br s, 2H; N*H*$_2$), 4.38 (m, 1H; C*H*), 2.62 (d, *J* = 6 Hz, 2H; C*H*$_2$), 2.47 (d, *J* = 6 Hz, 2H; C*H*$_2$), 1.40 (s, 9H; OC(C*H*$_3$)$_3$).

Fmoc-β-homo-L-Asp(OtBu)-OH **93**

To an ice-cold stirred solution of *tert*-butyl hydrogen (3*R*)-3-aminoglutarate (3.25 g, 16.0 mmol) and Na_2CO_3 (35.0 mmol) dissolved in a mixture of water (100 mL) and dioxane (50 mL) was added dropwise a solution of 9-fluorenylmethoxycarbonyl chloride (4.66 g, 18.0 mmol) in dioxane (50 mL) over 1 h. The rapidly stirred solution was allowed to warm to RT and stirred overnight, extracted with diethyl ether (2 x 100 mL) and the aqueous portion acidified with HCl (4 M) to a final pH of 2 at which point the title compound precipitated as a white curd which was filtered and washed well with ice-cold water. The filter cake was dried under high vacuum, affording the title compound **93** as a fine white powder (6.39 g, 94 %).

^{1}H NMR (400 MHz, $CDCl_3$, 25°C) δ = 11.0 (bs, 1H), 7.75 (d, *J* = 7.5 Hz, 2H), 7.58 (d, *J* = 7.3 Hz, 2H), 7.39 (dd, *J* = 7.3 Hz, 7.4 Hz, 2H), 7.30 (dd, *J* = 7.3 Hz, 7.4 Hz, 2H), 5.80 (d, *J* = 9.0 Hz, 1H), 4.37 (d, *J* = 7.1 Hz, 2H), 4.22 (m,1H), 2.85-2.35 (m, 4H), 1.45 (s, 9H).

^{13}C NMR (100 MHz, $CDCl_3$, 25°C) δ = 176.3, 171.1, 156.2, 144.3, 141.8, 128.2, 127.5, 125.6, 120.5, 82.1, 67.5, 47.6, 45.5, 39.8, 38.5, 28.5.

MS (ESI): *m*/*z* (%): 448.3 (100) $[M+Na]^+$. M = 425.5 calcd for $C_{24}H_{27}NO_6$.

$[\alpha]_D^{25}$ = +2.4 (c = 1.00, $CHCl_3$).

***N*-Me-Pro-OH (94)**[167]

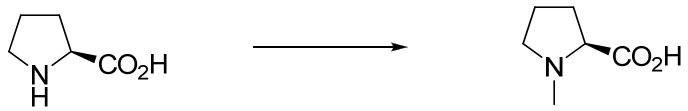

To a solution of L-proline (2.0 g, 17.4 mmol, 1 eq) in MeOH (20 mL) was added formaldehyde (2.0 mL of 37 % w/w in H_2O). 10 % Pd/C catalyst (500 mg) was added cautiously (under N_2) and the resulting mixture was hydrogenated at atmosphere pressure (balloon) over 24 h. The catalyst was removed by filtration over Celite, (washing with MeOH) and the combined filtrates were concentrated under reduced pressure. The grey residue was dissolved in MeOH/toluene (1:1 v/v, 100 mL) and concentrated to provide a solid, which was recrystallized from methanol-diethyl ether to afford *N*-methyl L-proline **94** as fine colourless needles (2.18 g, 98 %).

^{1}H NMR (400 MHz, D_2O, 23°C) δ = 3.72-3.64 and 3.57-3.50 (m, 1H), 2.98-2.90 (m, 1H), 2.75 (s, 3H), 2.35-2.25 (m, 1H), 2.00-1.76 (m, 3H).

^{13}C NMR (100 MHz, $CDCl_3$ 23°C) δ = 173.1, 70.2, 55.8, 40.3, 28.3, 22.4.

MS (ESI): *m*/*z* (%): 130.1 (100) $[M+H]^+$. M = 129.2 calcd for $C_6H_{11}NO_2$.

HCl•H-5-Ava-OMe (95)

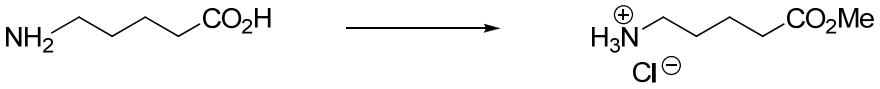

A white suspension of 5-aminovaleric acid (2.5 g, 21.3 mmol, 1.0 eq) and 15 mL MeOH was cooled to 0 °C in an ice bath. Thionyl chloride (3.9 mL, 53.4 mmol, 2.5 eq) was added dropwise within 15 min and the resulting solution was refluxed over night. All volatiles (solvent and excess thionyl chloride) were removed under reduced pressure. The obtained pale yellow mass was suspended in EtOAc (20 mL), ultrasonicated and filtrated to afford the desired product **95** as a white powder (3.4 g, 95 %).

^{1}H NMR (400 MHz, CD_3OD, 25°C) δ = 4.87 (s, 3H; NH_3^+), 3.67 (s, 3H; CH_3), 2.94 (t, J = 6.80 Hz, 2H; $CH_2CO_2CH_3$), 2.41 (t, J = 6.90 Hz, 2H; $CH_2NH_3^+$), 1.69 (m, 4H; $CH_2CH_2CH_2NH_3^+$).

^{13}C NMR (100 MHz, CD_3OD-d4, 25°C) δ= 174.2, 51.1, 39.4, 33.0, 27.0, 21.7.

MS (ESI): *m/z*: 132.1 $[M+H]^+$. M = 131.18 calcd for $C_6H_{13}NO_2$.

H-Asp(O*t*Bu)-NHPr (96)

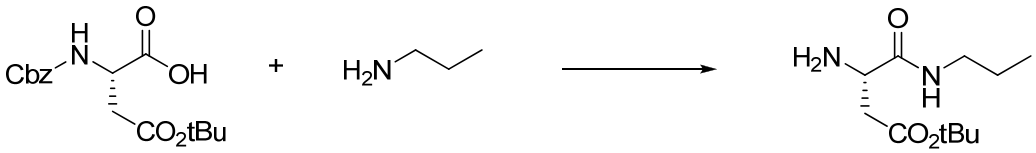

To a solution of Cbz-Asp(O*t*Bu)-OH (2.0 g, 6.2 mmol, 1 eq) in EtOAc (30 mL) was added propylamine (516 µL, 6.2 mmol, 1 eq) and EDC•HCl (1.4 g, 7.4 mmol, 1.2 eq). The resulting suspension was stirred at RT. After 2.5 h the mixture became a cloudy solution. Additional EDC•HCl (230 mg, 1.23 mmol, 0.2 eq) was added and the mixture was stirred for 1 h. The TLC (EtOAc/pentanes 2:1 v/v) showed complete conversion of the starting material. The reaction mixture was dissolved in EtOAc (150 mL) and extracted with 0.1 M HCl (2x 20 mL), Na_2CO_3 (5 % aq; 2x 20 mL) and brine (3x 20 mL). The dried ($MgSO_4$) organic phase was concentrated *in vacuo* to afford Cbz-Asp(O*t*Bu)-NHPr as a colourless oil (1.82 g, 81 %).

The obtained Cbz-Asp(O*t*Bu)-NHPr (1.52g, 4.2 mmol, 1 eq) was dissolved in MeOH (15 mL) and palladium on charcoal (10 % w/w, 150 mg) was added. The reaction mixture was hydrogenated (H_2 ballon) at RT for 5 h. The TLC (MeOH/EtOAc 1:10 v/v) showed complete conversion of the starting material. Following filtration (syringe filter), concentration of the filtrate *in vacuo* and drying under high vacuum afforded the title compound **96** as a colourless oil (916 mg, 96 %).

^{1}H NMR (400 MHz, D_2O, 23°C) δ = 7.38 (m, 1H; CON*H*), 3.64 (m, 1H; H_2NCH), 3.22 (dd, J = 6.4 Hz, 13.7 Hz, 2H; $NHCH_2$), 2.86 (dd, J = 3.8 Hz, 16.6 Hz, 1H; CH_2CO_2tBu), 2.50 (dd, J = 8.5 Hz, 16.6 Hz, 1H; CH_2CO_2tBu), 1.64 (m, 2H; H_2N), 1.53 (m, 2H; CH_2CH_3), 1.45 (s, 9H; $C(CH_3)$), 0.93 (t, J = 7.4 Hz, 3H; CH_2CH_3).

^{13}C NMR (100 MHz, $CDCl_3$ 23°C) δ = 173.3, 171.4, 81.1, 52.1, 40.9, 40.7, 28.1, 22.8, 11.4.

MS (ESI): *m/z* (%): 175 (100) $[M\text{-Boc}]^+$, 231.0 (30) $[M+H]^+$. M = 230.3 calcd for $C_{11}H_{22}N_2O_3$.

16.5 Synthesis of Non-Commercial Available Substrates

***(E)*-4-Methyl-1-nitropent-1-ene**[168,169]

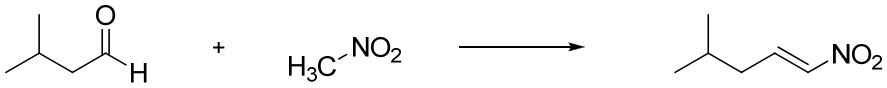

A 100 mL round-bottom flask was charged with isovaleraldehyde (5.2 mL, 48.1 mmol, 1.0 eq) and nitromethane (2.2 mL, 49.1 mmol, 1.02 eq) in 10 mL ethanol. The solution was cooled to 0 °C with an ice-bath. An aqueous solution of 10 M NaOH (4.8 mL, 48.1 mmol, 1.0 eq) was added dropwise within 20 min under vigorous stirring. A thick, white suspension was formed which was diluted with 10 mL of ethanol. After 10 min AcOH (2.75 mL, 48.1 mmol, 1.0 eq) was added and the reaction mixture became a yellow solution. 10 mL of water were added and after 10 min the yellow solution was extracted with Et_2O (2x 200 mL). The combined organic phases were washed with water (3x 50 mL, pH 6) dried ($MgSO_4$) and concentrated *in vacuo*. The corresponding nitro alcohol was obtained as a yellow oil (6.5 g).

The oil (6.5 g, 44.2 mmol, 1.0 eq) was dissolved in CH_2Cl_2 (50 mL). The obtained solution was cooled to -5 °C and trifluoroacetic anhydride (6.5 mL, 46.4 mmol, 1.05 eq) was added. Triethylamine (13 mL, 92.8 mmol, 2.1 eq) was carefully added within 20 min by syringe in a way the temperature remained around -5 °C. The reaction mixture was stirred for 1 h at -5 °C and afterwards allowed to warm to RT. The reaction mixture was diluted with CH_2Cl_2 (150 mL) and extracted with saturated aq NH_4Cl (2x 50 mL). The organic phase was dried ($MgSO_4$) and concentrated *in vacuo*. The residue was filtered over a plug of silica, eluting with EtOAc/pentanes 1:10 (v/v). Kugelrohr-distillation (120 °C, 20 mbar) afforded the pure (E)-4-methyl-1-nitropent-1-ene as a yellow oil (3.2 g, 52 % overall).

^{1}H NMR (400 MHz, CD_3OD, 25°C) δ = 7.25 (td, *J* = 13.4 Hz, 9.0 Hz, 1H; CH_2CH=CH), 6.97 (td, *J* = 13.2 Hz, 1.3 Hz, 1H; CH=C*H*NO_2), 2.15 (m, 2H; $CHCH_2$), 1.77-1.89 (m, 1H; $(CH_3)_2CH$), 0.96 (d, *J* = 6.7 Hz, 1H; CH_3).

^{13}C NMR (100 MHz, $CDCl_3$, 25°C) δ = 141.5, 140.1, 37.2, 27.7, 22.2 (2).

***(E)*-1-Nitro-1-cyclohexylethene**[168,169]

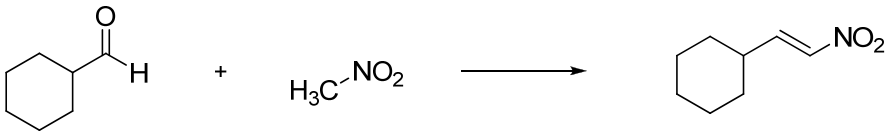

Preparation was according to *(E)*-4-methyl-1-nitropent-1-ene using cyclohexane-carboxaldehyde (5.2 mL, 45.4 mmol, 1.0 eq), nitromethane (2.5 mL, 46.2 mmol, 1.02 eq), ethanol (10 mL), aq 10 M NaOH (4.5 mL, 45.4 mmol, 1.0 eq) and conc. acetic acid (2.6 mL, 45.4 mmol, 1.0 eq). The product was obtained after filtration over a plug of silica, eluting with EtOAc/pentanes 1:10 (v/v), as a yellow oil (6.25g, 89 % overall).

^{1}H NMR (400 MHz, $CDCl_3$, 25°C): δ = 7.15 (dd, *J*= 7.2 Hz, 13.5 Hz, 1H), 6.93 (dd, *J*= 1.4 Hz, 13.5 Hz, 1H), 2.20-2.32 (m, 1H, C*H*CH=CH), 1.12-1.86 (m, 10H, *H*-cyclohexyl)

^{13}C NMR (100 MHz, $CDCl_3$, 25°C) δ = 147.3, 138.2, 37.5, 31.4 (2), 25.6, 25.4 (2).

***(E)*-1-Nitro-1-heptene**[168,169]

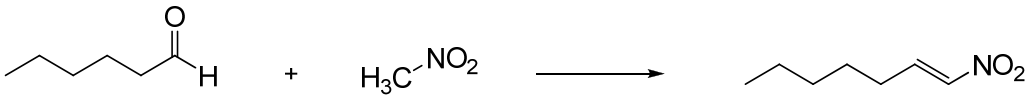

Preparation was according to *(E)*-4-methyl-1-nitropent-1-ene using *n*-hexanal (5.5 mL, 45.6 mmol, 1.0 eq), nitromethane (2.5 mL, 46.4 mmol, 1.02 eq), ethanol (10 mL), aq 10 M NaOH (4.5 mL, 45.4 mmol, 1.0 eq) and conc. acetic acid (2.6 mL, 45.4 mmol, 1.0 eq). The product was obtained after filtration over a plug of silica, eluting with EtOAc/pentanes 1:10 (v/v), as a yellow oil (6.0 g, 92 % overall).

^{1}H NMR (400 MHz, $CDCl_3$, 25°C) δ = 7.28 (td, *J* = 7.5 Hz, 13.4 Hz, 1H; CH_2CH=CH), 6.98 (td, *J* = 1.5 Hz, 13.4 Hz, 1H; CH=C*H*NO_2), 2.26 (m, 2H; $CHCH_2$), 1.52 (m, 2H; CH_2), 1.33 (m, 4H; CH_2), 0.90 (t, *J* = 7.1 Hz, 3H; CH_3).

^{13}C NMR (100 MHz, $CDCl_3$, 25°C) δ = 142.8, 139.5, 31.2, 28.4, 27.4, 22.3, 13.9.

***(E)*-3,3-Dimethoxy-1-nitro-propene = β-Nitroacrolein dimethylacetal (69)**[135]

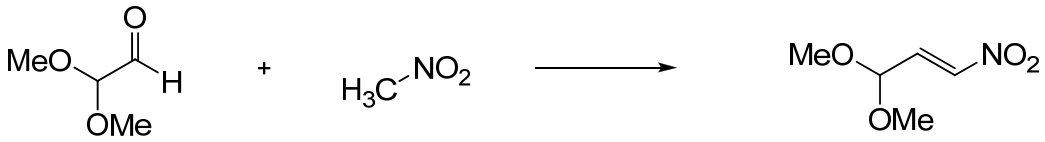

69

2,2-Dimethoxyacetaldehyde (60% w/w in H_2O, 20 mL, 133 mmol, 1 eq) and nitromethane (8.8 mL, 199.5 mmol, 1.5 eq) were dissolved in THF (30 mL) and *t*-BuOH (30 mL). The solution was stirred and cooled to 0 °C in an ice-bath and potassium *tert*-butoxide (746 mg, 6.65 mmol, 0.05 eq) was added as a solid. The reaction mixture was stirred for 1 h at 0 °C and over night at RT. The TLC (*n*-hexanes/EtOAc 1:1 v/v) showed complete conversion of the starting material. The mixture was then diluted with water (100 mL) and the resulting aqueous phase was extracted with diethyl ether (2x 250 mL, 2x 100 mL). The combined organic phases were dried ($MgSO_4$) and concentrated *in vacuo*. Drying under high vaccum yielded 1,1-dimethoxy-3-nitropropan-2-ol as a slightly yellow oil (21g, 96 %).

The obtained 1,1-dimethoxy-3-nitropropan-2-ol (10g, 60.6 mmol, 1 eq) was dissolved in CH_2Cl_2 (50 mL) and cooled to -10 °C in an ice/salt-bath. Trifluoroacetic anhydride (8.84 mL, 63.6 mmol, 1.05 eq) was added dropwise under stirring within 15 min (exothermic, temperature was kept below 12 °C) and the reaction mixture was stirred for a further 30 min. The TLC (*n*-hexanes/EtOAc 1:1 v/v) showed complete conversion of the starting material. The mixture was then diluted with CH_2Cl_2 (100 mL) and extracted with saturated aq NH_4Cl (2x 50 mL). The combined aqueous layer was back-extracted with CH_2Cl_2 (2x 50 mL) and the combined organic phases were concentrated *in vacuo* whereas TFA – salt was precipitating. After filtration, washing and concentration, chromatography of the crude product on silica gel eluting with EtOAc/pentanes 1:10 (v/v) gave *(E)*-3,3-dimethoxy-1-nitro-propene **69** as a yellow oil (7.0 g, 75 %).

^{1}H NMR (400 MHz, $CDCl_3$, 25°C) δ = 7.19 (dd, *J* = 1.4 Hz, 13.4 Hz, 1H; CH=C*H*-NO_2), 7.02 (dd, *J* = 3.3 Hz, 13.4 Hz, 1H; C*H*=CH-NO_2), 5.12 (dd, *J* = 1.5 Hz, 3.3 Hz, 1H; $(CH_3O)_2CH$), 3.35 (s, 6H; $(CH_3O)_2$).

^{13}C NMR (100 MHz, $CDCl_3$, 25°C) δ = 142.6, 136.5, 97.9, 53.0 (2).

CHN: Anal. Calcd for $C_5H_9NO_4$: C 40.82; H 6.17; N 9.52. Found: C 40.92; H 6.02; N 9.45.

Nitroethylene[29,154-156]

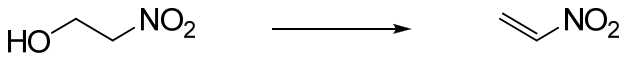

2-Nitroethanol (5g, 54.9 mmol, 1 eq) and phtalic anhydride (9g, 60.7 mmol, 1.1 eq) were charged into a 50 mL flask, equipped with a magnetic stirrer and a vacuum distillation setup (short fractional distillation column and spider). The apparatus was evacuated to about 95 mbar and the oil bath was heated. The solid reaction mixture became a clear solution (oil bath: ~120 °C) and at 123 °C (oil bath: ~180 °C) distillation of the product occurred. The distillate was collected until the distillation ceased to give a cloudy pale yellow solution, containing a mixture of nitroethylene and water which was immediately filtered through a plug of Na_2SO_4 (2 cm in a 20 mL syringe with filter). After isolation by Kugelrohr distillation, the yellow oil (1.8 g, 45 %) was immediately dissolved in chloroform (J. T. Baker, 7386, stabilized with about 0.75 % ethanol) and stored as this stock-solution (c ≤ 1M) at -20°C. The concentration of the stock-solution was confirmed from the ^{1}H NMR analysis using an internal standard (*i*-PrOH). The nitroethylene solution was stable over prolonged periods (≥2 month) at -20°C.

^{1}H NMR of stock-solution in $CHCl_3$ (400 MHz, $CDCl_3$, 25°C): 7.14 (dd, *J* = 7.4 Hz, 14.9 Hz, 1H; CH_2=C*H*), 6.65 (dd, *J* = 2.2 Hz, 14.9 Hz, 1H; CH_2=CH), 5.91 (br d, *J* = 6.0 Hz, 1H; CH_2=CH).

17. 1,4-Addition Products and Derivatives

17.1 Characterisation Index

1,4-Addition products of aldehydes and nitroolefins

(2*S*,3*R*)-2-Methyl-4-nitro-3-phenylbutanal **33**

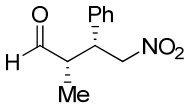

(2*S*,3*R*)-2-Ethyl-4-nitro-3-phenylbutanal **3**

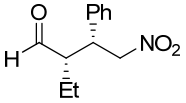

(2*S*,3*R*)-2-Propyl-4-nitro-3-phenylbutanal **34**

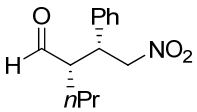

(2*S*,3*R*)-2-Butyl-4-nitro-3-phenylbutanal **35**

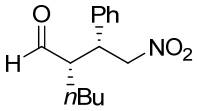

(2*S*,3*R*)-2-Isopropyl-4-nitro-3-phenylbutanal **36**

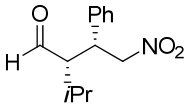

(2*S*,3*R*)-2-Benzyl-4-nitro-3-phenylbutanal **37**

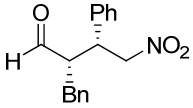

(2*S*,3*R*)-3-(4-Bromophenyl)-2-ethyl-4-nitrobutanal **38**

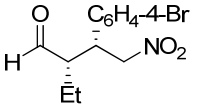

(2*S*,3*R*)-3-(4-Fluorophenyl)-2-ethyl-4-nitrobutanal **39**

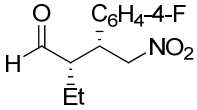

(2*S*,3*R*)-3-(4-Chlorophenyl)-2-ethyl-4-nitrobutanal **40**

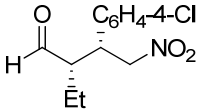

(2*S*, 3*R*)-3-(2,4-Dichlorophenyl)-2-ethyl-4-nitrobutyraldehyde **41**

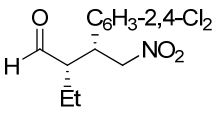

(2*S*, 3*R*)-2Ethyl-4-nitro-3-(2-trifluoromethylphenyl)butanal **42**

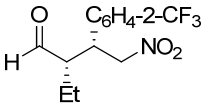

(2*S*, 3*R*)-2-Benzyl-4-nitro-3-(2-trifluoromethylphenyl)butanal **43**

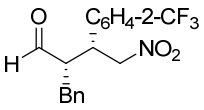

(2*S*, 3*R*)-2Ethyl-4-nitro-3-(4-methoxyphenyl)butanal **44**

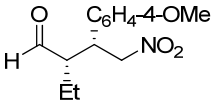

(2*S*, 3*R*)-2-Methyl-4-nitro-3-(thien-2-yl)butanal **45**

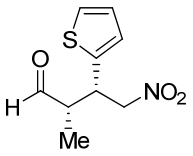

(2*S*, 3*S*)-3-Cylohexyl-2-methyl-4-nitrobutanal **46**

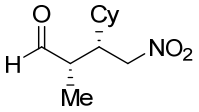

(2*S*, 3*S*)-2-Ethyl-3-nitromethyloctanal **47**

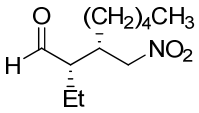

(2*S*,3*S*)-2-Ethyl-5-methyl-3-(nitromethyl)hexanal **68**

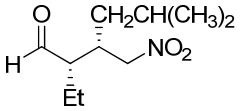

(2*S*,3*S*)-2-Ethyl-4,4-dimethoxy-3-(nitromethyl)butanal **70**

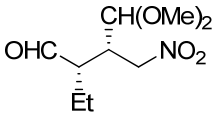

(2*S*,3*S*)-2-Isopropyl-4,4-dimethoxy-3-(nitromethyl)butanal **71**

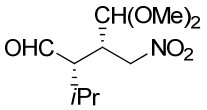

(3*S*,4*S*)-Methyl-3-formyl-5,5-dimethoxy-
4-(nitromethyl)pentanoate **72**

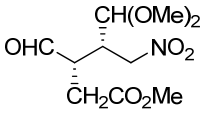

(2*S*,3*R*)-3-(2,4-Dimethoxyphenyl)-2-ethyl-4-nitrobutanal **74**

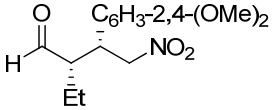

(2*S*,3*R*)-2-Ethyl-4-nitro-3-phenylbutan-1-ol **73**
(Gramm scale synthesis)

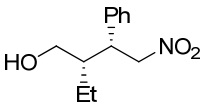

1,4-Addition products of aldehydes and nitroethylene

(2*S*)-Methyl-4-nitrobutan-1-ol **76**

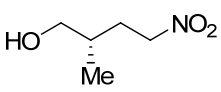

(2*S*)-Ethyl-4-nitrobutan-1-ol **77**

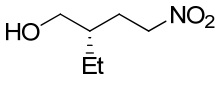

(2*S*)-(2-Nitroethyl)pentan-1-ol **78**

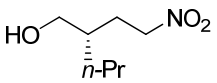

(2*S*)-(2-Nitroethyl)hexan-1-ol **79**

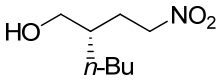

(2*R*)-3-Methyl-(2-nitroethyl)butan-1-ol **80**

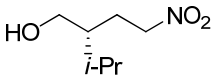

(2*R*)-3,3-Dimethyl-(2-nitroethyl)butan-1-ol **81**

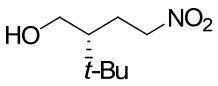

(2*S*)-Benzyl-4-nitrobutan-1-ol **82**

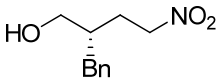

(2*S*)-(2-Nitroethyl)-*cis*-8-undecanal **83**

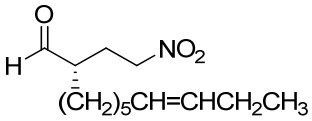

(3*R*)-Methyl-formyl-5-nitropentanoate **84**

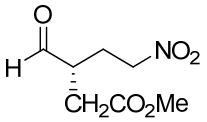

(3*S*)-Methyl-formyl-5-nitroheptanoate **85**

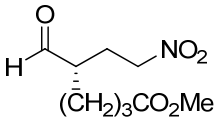

Derivatives of 1,4-addition products

(2*S*)-Benzyl-γ-butyrolactone **86**

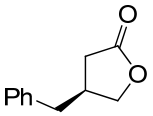

(2*S*)-2-(Methylphenyl)-4-nitrobutanoic acid **88**

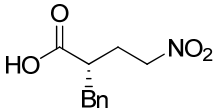

(2*S*)-2-(Methylphenyl)-4-aminobutanoic acid **89**

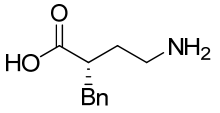

(2*S*)-4-(9-Fluorenylmethoxycarbonyl)
-2-(methylphenyl)-butanoic acid **87**

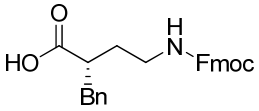

Enantiomeric excess determination of Fmoc-γ-amino acid via formation of chiral amide **97**

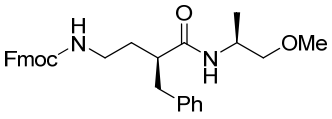

17.2 1,4-Addition Products of Aldehydes and Nitroolefins

Diastereoselectivities were determined by ^{1}H NMR analysis of the crude reaction mixture (~100 µL + 400 µL $CDCl_3$): The *syn* to *anti* integral ratio of the aldehyde signals and other separated signals was measured. Assignment of the stereoisomers was carried out by comparison with literature and chromatographic data obtained using enantiomeric peptides H-D-Pro-Pro-Glu-NH_2 **56** and H-Pro-D-Pro-D-Glu-NH_2 or diastereomeric peptides H-Pro-Pro-Asp-NH_2 **1** and H-D-Pro-Pro-Asp-NH_2 **21** as catalysts for reactions performed under otherwise identical conditions. Peptides **56**/H-Pro-D-Pro-D-Glu-NH_2 and **1/21** have opposite enantioselectivity.

Products usually epimerised during chromatography to a certain extend without affecting the enantiomeric excess. Only the *syn* isomers of the following reported products were characterized by NMR spectroscopy.

(2*S*,3*R*)-2-Methyl-4-nitro-3-phenylbutanal (33)[24]

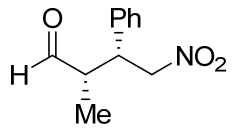

Prepared from *n*-propanal and *trans*-β-nitrostyrene according to the general procedure (Protocol E). Purified by preparative chromatography on silica gel (pentanes/EtOAc 10:1 v/v). A pale yellow oil was obtained.

^{1}H NMR (400 MHz, $CDCl_3$, 25°C) δ = 9.72 (d, J = 1.7 Hz, 1H; C*H*O), 7.32 (m, 3H; Ph), 7.17 (m, 2H; Ph), 4.80 (dd, J = 5.5 Hz, 12.7 Hz, 1H; CH_2NO$_2$), 4.68 (dd, J = 9.31 Hz, 12.7 Hz, 1H; CH_2NO$_2$), 3.81 (dt, J = 5.6 Hz, 9.2 Hz, 1H; C*H*Ph), 2.79 (m, 1H; C*H*CHO), 1.00 (d, J = 7.3 Hz, 3H, CH_3).

^{13}C NMR (100 MHz, $CDCl_3$, 25°C) δ = 202.2, 136.5, 129.1 (2), 128.1, 128.0 (2), 78.1, 48.4, 44.0, 12.1.

CHN: Anal. Calcd for $C_{11}H_{13}NO_3$: C 63.76; H 6.32; N 6.76. Found: C 63.75; H 6.35; N 6.64.

The enantiomeric excess was determined by HPLC using a Chiracel OD-H column (*n*-hexane/*i*-PrOH 90:10, 25°C) at 1 mL/min, UV detection at 254 nm: t_R : (*syn,* major) = 23.5 min, (*syn*, minor) = 34.4 min.

(2*S*,3*R*)-2-Ethyl-4-nitro-3-phenylbutanal (3)[24]

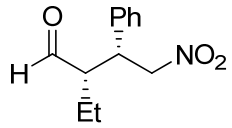

Prepared from *n*-butanal and *trans*-β-nitrostyrene according to the general procedure (Protocol E). Purified by preparative chromatography on silica gel (pentanes/EtOAc 10:1 v/v). A colourless oil was obtained.

^{1}H NMR (400 MHz, $CDCl_3$, 25°C) δ = 9.72 (d, J = 2.6 Hz, 1H; C*H*O), 7.32 (m, 3H; Ph), 7.18 (m, 2H; Ph), 4.72 (dd, J = 5.0 Hz, 12.7 Hz, 1H; CH_2NO$_2$), 4.63 (dd, J = 9.7 Hz, 12.7 Hz, 1H; CH_2NO$_2$), 3.79 (dt, J = 5.0 Hz, 9.8 Hz, 1H; C*H*Ph), 2.68 (dddd, J = 2.6 Hz, 5.0 Hz, 7.6 Hz, 10.1 Hz, 1H, C*H*CHO), 1.51 (m, 2H; CH_2CH$_3$), 0.84 (t, J = 7.5 Hz; CH_3).

^{13}C NMR (100 MHz, $CDCl_3$, 25°C) δ = 203.1, 136.8, 129.1 (2), 128.1, 128.0 (2), 78.5, 55.0, 42.7, 20.4, 10.7.

CHN: Anal. Calcd for $C_{12}H_{15}NO_3$: C 65.14; H 6.83; N 6.33. Found: C 65.18; H 6.97; N 6.36.

The enantiomeric excess was determined by HPLC using a Chiracel AD-H column (*n*-hexane/*i*-PrOH 99.5:0.5, 25°C) at 0.9 mL/min, UV detection at 254 nm: t_R : (*syn,* minor) = 36.8 min, (*syn*, major) = 47.9 min.

(2*S*,3*R*)-2-Propyl-4-nitro-3-phenylbutanal (34)[72]

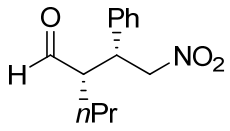

Prepared from *n*-pentanal and *trans*-β-nitrostyrene according to the general procedure (Protocol E). Purified by preparative chromatography on silica gel (pentanes/ EtOAc 15:1 v/v). A colourless oil was obtained.

^{1}H NMR (400 MHz, $CDCl_3$, 25°C) δ = 9.71 (d, J = 2.8 Hz, 1H; C*H*O), 7.33 (m, 3H; Ph), 7.18 (m, 2H; Ph), 4.71 (dd, J = 12.8 Hz, 5.3 Hz, 1H; CH_2NO$_2$), 4.65 (dd, J = 12.8 Hz, 9.4 Hz, 1H; CH_2NO$_2$), 3.78 (dt, J = 9.6 Hz, 5.3 Hz, 1H; C*H*Ph), 2.71 (m, 1H; C*H*CHO), 1.54 – 1.11 (m, 4H; CH_2CH_2CH$_3$), 0.80 (t, J = 7.1 Hz, 3H; CH_3).

^{13}C NMR (100 MHz, $CDCl_3$, 25°C) δ = 203.2, 136.8, 129.1 (2), 128.1, 127.9 (2), 78.4, 53.8, 43.2, 29.5, 19.8, 13.9

CHN: Anal. Calcd for $C_{13}H_{17}NO_3$: C 66.36; H 7.28; N 5.95. Found: C 66.33; H 7.33; N 5.93.

The enantiomeric excess was determined by HPLC using a Chiracel OD-H column (*n*-hexane/*i*-PrOH 80:20, 25°C) at 1 mL/min, UV detection at 254 nm: t_R : (*syn,* major) = 11.7 min, (*syn*, minor) = 15.9 min.

(2*S*,3*R*)-2-Butyl-4-nitro-3-phenylbutanal (35)[24]

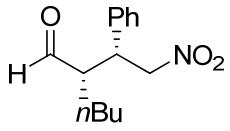

Prepared from *n*-hexanal and *trans*-β-nitrostyrene according to the general procedure (Protocol E). Purified by preparative chromatography on silica gel (pentanes/EtOAc 10:1 v/v). A pale yellow oil was obtained.

^{1}H NMR (400 MHz, $CDCl_3$, 25°C) δ = 9.70 (d, *J* = 2.8 Hz, 1H; C*H*O), 7.32 (m, 3H; Ph), 7.17 (m, 2H; Ph), 4.71 (dd, *J* = 9.5 Hz, 12.8 Hz, 1H; CH_2NO$_2$), 4.64 (dd, *J* = 9.5 Hz, 12.8 Hz, 1H; CH_2NO$_2$), 3.78 (dt, *J* = 5.3 Hz, 9.6 Hz, 1H; C*H*Ph), 2.60 (m, 1H; C*H*CHO), 1.54 – 1.09 (m, 6H; CH_2CH_2CH_2CH$_3$), 0.78 (t, *J* = 7.0 Hz, 3H; CH_3).

^{13}C NMR (100 MHz, $CDCl_3$, 25°C) δ = 203.2, 136.8, 129.1 (2), 128.1, 128.0 (2), 78.4, 53.9, 43.1, 28.5, 27.0, 22.5, 13.6.

CHN: Anal. Calcd for $C_{14}H_{19}NO_3$: C 67.45; H 7.68; N 5.62. Found: C 67.53; H 7.70; N 5.70.

The enantiomeric excess was determined by HPLC using a Chiracel OD-H column (*n*-hexane/*i*-PrOH 80:20, 25°C) at 1 mL/min, UV detection at 254 nm: t_R : (*syn,* major) = 10.9 min, (*syn*, minor) = 13.7 min.

(2*S*,3*R*)-2-Isopropyl-4-nitro-3-phenylbutanal (36)[24]

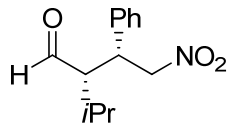

Prepared from isovaleric aldehyde and *trans*-β-nitrostyrene according to the general procedure (Protocol E). Purified by preparative chromatography on silica gel (pentanes/EtOAc 10:1 v/v). A pale yellow oil was obtained.

^{1}H NMR (400 MHz, $CDCl_3$, 25°C) δ = 9.93 (d, *J* = 2.4 Hz, 1H; C*H*O), 7.32 (m, 3H; Ph), 7.19 (m, 2H; Ph), 4.67 (dd, *J* = 4.4 Hz, 12.5 Hz, 1H; CH_2NO$_2$), 4.57 (dd, *J* = 10.0 Hz, 12.5 Hz, 1H; CH_2NO$_2$), 3.90 (dt, *J* = 4.4 Hz, 10.3 Hz, 1H; C*H*Ph), 2.77 (ddd, *J* = 2.4 Hz, 4.1 Hz, 10.8 Hz, 1H; C*H*CHO), 1.72 (d sept., *J* = 4.2 Hz, 7.1 Hz, 1H; C*H*(CH$_3$)$_2$), 1.10 (d, *J* = 7.2 Hz, 3H; CH_3), 0.88 (d, *J* = 7.0 Hz, 3H; CH_3).

^{13}C NMR (100 MHz, $CDCl_3$, 25°C) δ = 204.3, 137.0, 129.1 (2), 128.1, 127.9 (2), 79.0, 58.7, 41.9, 27.9, 21.6, 16.9.

CHN: Anal. Calcd for $C_{13}H_{17}NO_3$: C 66.36; H 7.28; N 5.95. Found: C 66.44; H 7.16; N 6.07.

The enantiomeric excess was determined by HPLC using a Chiracel AD-H column (*n*-hexane/*i*-PrOH 97:3, 25°C) at 0.5 mL/min, UV detection at 254 nm: t_R : (*syn,* minor) = 22.8 min, (*syn*, major) = 26.6 min.

(2*S*,3*R*)-2-Benzyl-4-nitro-3-phenylbutanal (37)[170]

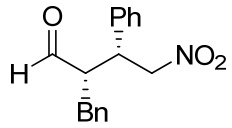

Prepared from 3-phenylpropionaldehyde and *trans*-β-nitrostyrene according to the general procedure (Protocol E). Purified by preparative chromatography on silica gel (pentanes/EtOAc 10:1 v/v). A pale yellow oil was obtained.

^{1}H NMR (400 MHz, $CDCl_3$, 25°C) δ = 9.64 (d, *J* = 2.3 Hz, 1H; C*H*O), 7.33 – 7.11 (m, 8H; Ph), 6.95 (m, 2H; Ph), 4.65 (m, 2H; CH_2NO$_2$), 3.76 (dt, *J* = 6.1 Hz, 8.7 Hz, 1H; C*H*Ph), 3.04 (ddt, *J* = 2.3 Hz, 6.0 Hz, 8.6 Hz, 1H; C*H*CHO), 2.69 (m, 2H; CH_2Ph).

^{13}C NMR (100 MHz, $CDCl_3$, 25°C) δ = 203.0, 137.1, 136.6, 129.3 (2), 128.8 (2), 128.7 (2), 128.3, 128.0 (2), 126.9, 78.0, 55.3, 43.5, 34.3.

CHN: Anal. Calcd for $C_{17}H_{17}NO_3$: C 72.07; H 6.05; N 4.94. Found: C 72.09; H 6.02; N 4.70.

The enantiomeric excess was determined by HPLC using a Chiracel AD-H column (*n*-hexane/*i*-PrOH 97.5:2.5, 25°C) at 1 mL/min, UV detection at 254 nm: t_R : (*syn,* minor) = 21.9 min, (*syn*, major) = 25.1 min.

(2*S*,3*R*)-3-(4-Bromophenyl)-2-ethyl-4-nitrobutanal (38)

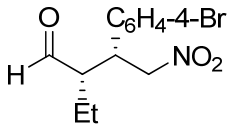

Prepared from *n*-butanal and *trans*-4-bromo-β-nitrostyrene according to the general procedure (Protocol E). Purified by preparative chromatography on silica gel (pentanes/EtOAc 10:1 v/v). A colourless oil was obtained.

^{1}H NMR (400 MHz,$CDCl_3$, 25°C) δ= 9.71 (d, *J* = 2.3 Hz, 1H; C*H*O), 7.48 (d, *J* = 8.4 Hz, 2H; Ph), 7.07 (d, *J* = 8.4 Hz, 2H; Ph), 4.72 (dd, *J* = 4.8 Hz, 12.8 Hz, 1H; CH_2NO_2), 4.60 (dd, *J* = 9.9 Hz, 12.8 Hz, 1H; CH_2NO_2), 3.77 (dt, *J* = 4.8 Hz, 9.9 Hz, 1H; C*H*Ph), 2.67 (m, 1H; C*H*CHO), 1.58–1.43 (m, 2H; CH_2CH_3), 0.84 (t, *J* = 7.5 Hz, 3H; CH_3)

^{13}C NMR (100 MHz, $CDCl_3$, 25°C) δ= 202.6, 135.9, 132.3 (2), 129.7 (2), 122.1, 78.2, 54.7, 42.1, 20.3, 10.5.

CHN: Anal. Calcd for $C_{12}H_{14}BrNO_3$: C 48.02; H 4.70; N 4.67. Found: C 48.12; H 4.72; N 4.73.

The enantiomeric excess was determined by HPLC using a Chiracel AD-H column (*n*-hexane/*i*-PrOH 98.5:1.5, 25°C) at 1 mL/min, UV detection at 254 nm: t_R : (*syn,* minor) = 30.4 min, (*syn*, major) = 42.9 min.

(2*S*,3*R*)-3-(4-Fluorophenyl)-2-ethyl-4-nitrobutanal (39)

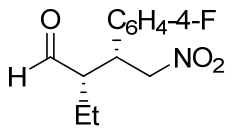

Prepared from *n*-butanal and *trans*-4-fluoro-β-nitrostyrene according to the general procedure (Protocol E). Purified by preparative chromatography on silica gel (pentanes/EtOAc 10:1 v/v). A colourless oil was obtained.

^{1}H NMR (400 MHz,$CDCl_3$, 25°C) δ= 9.72 (d, *J* = 2.4 Hz, 1H; C*H*O), 7.17 (m, 2H; Ph), 7.04 (m, 2H; Ph), 4.72 (dd, *J* = 4.8 Hz, 12.7 Hz, 1H; CH_2NO_2), 4.59 (dd, *J* = 9.9 Hz, 12.7 Hz, 1H; CH_2NO_2), 3.80 (dt, *J* = 4.8 Hz, 10.0 Hz, 1H; C*H*Ph), 2.67 (m, 1H; C*H*CHO), 1.58–1.43 (m, 2H; CH_2CH_3), 0.84 (t, *J* = 7.5 Hz, 3H; CH_3).

^{13}C NMR (100 MHz, $CDCl_3$, 25°C) δ= 202.8, 162.3 (d, J_{CF} = 247.4 Hz), 132.5 (d, J_{CF} = 3.4 Hz), 129.6 (2) (d, J_{CF} = 8.1 Hz), 116.1 (2) (d, J_{CF} = 21.6 Hz), 78.5, 54.9, 41.9, 20.3, 10.5.

CHN: Anal. Calcd for $C_{12}H_{14}FNO_3$: C 60.24; H 5.90; N 5.85. Found: C 60.39; H 5.96; N 5.72.

The enantiomeric excess was determined by HPLC using a Chiracel AD-H column (*n*-hexane/*i*-PrOH 98.5:1.5, 25°C) at 1 mL/min, UV detection at 254 nm: t_R : (*syn,* minor) = 26.6 min, (*syn*, major) = 34.4 min.

(2*S*,3*R*)-3-(4-Chlorophenyl)-2-ethyl-4-nitrobutanal (40)

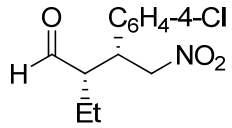

Prepared from *n*-butanal and *trans*-4-chloro-β-nitrostyrene according to the general procedure (Protocol E). Purified by preparative chromatography on silica gel (pentanes/EtOAc 10:1 v/v). A colourless oil was obtained.

^{1}H NMR (400 MHz,$CDCl_3$, 25°C) δ= 9.72 (d, *J* = 2.3 Hz, 1H; C*H*O), 7.33 (m, 1H; Ph), 7.13 (m, 1H; Ph), 4.72 (dd, *J* = 4.8 Hz, 12.8 Hz, 1H; CH_2NO_2), 4.60 (dd, *J* = 9.9 Hz, 12.8 Hz, 1H; CH_2NO_2), 3.79 (dt, *J* = 4.8 Hz, 10.0 Hz, 1H; C*H*Ph), 2.67 (m, 1H; C*H*CHO), 1.50 (m, 2H; CH_2CH_3), 0.84 (t, *J* = 7.5 Hz, 3H; CH_3).

^{13}C NMR (100 MHz, $CDCl_3$, 25°C) δ= 202.7, 135.3, 134.0, 129.3 (4), 78.3, 54.68, 42.0, 20.3, 10.5.

CHN: Anal. Calcd for $C_{12}H_{14}ClNO_3$: C 56.37; H 5.52; N 5.48. Found: C 56.29; H 5.55; N 5.54.

The enantiomeric excess was determined by HPLC using a Chiracel AD-H column (*n*-hexane/*i*-PrOH 98.5:1.5, 25°C) at 1 mL/min, UV detection at 254 nm: t_R : (*syn,* minor) = 27.3 min, (*syn*, major) = 38.1 min.

(2*S*, 3*R*)-3-(2,4-Dichlorophenyl)-2-ethyl-4-nitrobutyraldehyde (41)

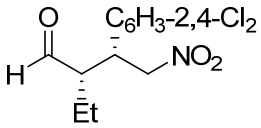

Prepared from *n*-butanal and *trans*-2,4-dichloro-β-nitrostyrene according to the general procedure (Protocol E). Purified by preparative chromatography on silica gel (pentanes/EtOAc 10:1 v/v). A colourless oil was obtained.

^{1}H NMR (400 MHz, $CDCl_3$, 25°C) δ= 9.73 (d, *J* = 2.1 Hz, 1H; C*H*O), 7.44 (d, *J* = 2.1 Hz, 1H; Ph), 7.27 (m, 1H; Ph), 7.17 (d, *J* = 8.5 Hz, 1H; Ph), 4.85 (dd, *J* = 9.2 Hz, 13.0 Hz, 1H; CH_2NO$_2$), 4.68 (dd, *J* = 4.5 Hz, 13.0 Hz, 1H; CH_2NO$_2$), 4.30 (dt, *J* = 4.4 Hz, 9.5 Hz, 1H; C*H*Ph), 2.94 (m, 1H; C*H*CHO), 1.57 (m, 2H; CH_2CH$_3$), 0.88 (t, *J* = 7.5 Hz, 3H; CH_3).

^{13}C NMR (100 MHz, $CDCl_3$, 25°C) δ= 202.4, 135.0, 134.5, 133.1, 130.3, 127.8 (2), 76.5, 53.7, 38.7, 20.4, 10.6.

CHN: Anal. Calcd for $C_{12}H_{13}Cl_2NO_3$: C 49.68; H 4.52; N 4.83. Found: C 49.65; H 4.55; N 4.81.

The enantiomeric excess was determined by HPLC using a Chiracel AD-H column (*n*-hexane/*i*-PrOH 98.5:1.5, 25°C) at 1 mL/min, UV detection at 254 nm: t_R : (*syn,* minor) = 18.0 min, (*syn*, major) = 20.0 min.

(2*S*, 3*R*)-2Ethyl-4-nitro-3-(2-trifluoromethylphenyl)butanal (42)[43]

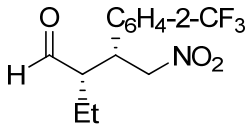

Prepared from *n*-butanal and *trans*-β-nitro-2-(trifluoromethyl)styrene according to the general procedure (Protocol E). Purified by preparative chromatography on silica gel (pentanes/EtOAc 15:1 v/v). A colourless oil was obtained.

^{1}H NMR (400 MHz, $CDCl_3$, 25°C) δ = 9.77 (dd, *J* = 1.7 Hz, 2.8 Hz, 1H; C*H*O), 7.73 (d, *J* = 7.9 Hz, 1H; Ph), 7.58 (t, *J* = 7.7 Hz, 1H; Ph), 7.43 (t, *J* = 7.6 Hz, 1H; Ph), 7.35 (d, *J* = 7.8 Hz, 1H; Ph) 4.81 (ddd, *J* = 1.4 Hz, 7.2 Hz, 12.6 Hz, 1H; CH_2NO$_2$) 4.63 (ddd, *J* = 1.5 Hz, 4.9 Hz, 12.6 Hz, 1H; CH_2NO$_2$), 4.17 (m, 1H; C*H*Ph), 2.91 (m, 1H; C*H*CHO), 1.60 (m, 1H; CH_2CH$_3$), 1.38 (m, 1H; CH_2CH$_3$), 0.87 (dt, *J* = 1.5 Hz, 7.7 Hz, 3H; CH_3).

^{13}C NMR (100 MHz, $CDCl_3$, 25°C) δ = 203.0, 136.2, 132.6, 128.2 (2), 128.1, 126.9, 126.9, 77.9, 55.5, 38.2, 21.3, 11.3.

CHN: Anal. Calcd for $C_{13}H_{14}F_3NO_3$: C 53.98; H 4.88; N 4.84. Found: C 53.99; H 4.90; N 4.72.

The enantiomeric excess was determined by HPLC using a Chiracel AD-H column (*n*-hexane/*i*-PrOH 99:1, 25°C) at 0.8 mL/min, UV detection at 254 nm: t_R : (*syn,* minor) = 19.5 min, (*syn*, major) = 21.6 min.

(2*S*, 3*R*)-2-Benzyl-4-nitro-3-(2-trifluoromethylphenyl)butanal (43)

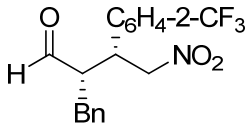

Prepared from 3-phenylpropionaldehyde and *trans*-β-nitro-2-(trifluoromethyl)styrene according to the general procedure (Protocol E). Purified by preparative chromatography on silica gel (pentanes/EtOAc 10:1 to 5:1 v/v). A colourless oil was obtained.

^{1}H NMR (400 MHz,$CDCl_3$, 25°C) δ= 9.72 (d, *J* = 2.2 Hz, 1H; C*H*O), 7.75 (d, *J* = 7.9 Hz, 1H; Ph), 7.60 (t, *J* = 7.64, 1H; Ph), 7.45 (t, *J* = 8.4, 2H; Ph), 7.24 (m, 3H; Ph), 7.03 (d, *J* = 7.1 Hz, 2H; Ph), 4.86 (dd, *J* = 7.4 Hz, 12.7 Hz, 1H; C$H_2$$NO_2$), 4.69 (dd, *J* = 4.7 Hz, 12.7 Hz, 1H; C$H_2$$NO_2$), 4.22 (m, 1H; C*H*$CH_2NO_2$), 3.36 (m, 1H; C*H*CHO), 2.83 (dd, *J* = 10.9 Hz, 14.0 Hz, 1H; CH_2Ph), 2.63 (dd, *J* = 4.4 Hz, 14.1 Hz, 1H; CH_2Ph).

^{13}C NMR (100 MHz, $CDCl_3$, 25°C) δ= 203.1, 137.0, 136.2, 132.7, 128.9, 128.8 (2), 128.6 (2), 128.3, 127.9, 127.0, 125.4, 122.7, 77.4, 55.5, 39.0, 35.4.

CHN: Anal. Calcd for $C_{18}H_{16}F_3NO_3$: C 61.54; H 4.59; N 3.99. Found: C 61.74; H 4.63; N 3.81.

The enantiomeric excess was determined by HPLC using a Chiracel AD-H column (*n*-hexane/*i*-PrOH 98.5:1.5, 25°C) at 1 mL/min, UV detection at 254 nm: t_R : (*syn,* minor) = 20.7 min, (*syn*, major) = 27.5 min.

(2*S*, 3*R*)-2Ethyl-4-nitro-3-(4-methoxyphenyl)butanal (44)[43]

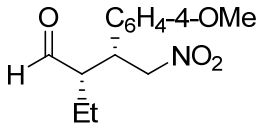

Prepared from *n*-butanal and *trans*-4-methoxy-β-nitrostyrene according to the general procedure (Protocol E). Purified by preparative chromatography on silica gel (pentanes/EtOAc 10:1 v/v). A pale yellow oil was obtained.

^{1}H NMR (400 MHz,$CDCl_3$, 25°C) δ= 9.71 (d, *J* = 2.7 Hz, 1H; C*H*O), 7.09 (m, 2H; Ph), 6.87 (m, 2H; Ph), 4.69 (dd, *J* = 5.0 Hz, 12.5 Hz, 1H; C$H_2$$NO_2$), 4.58 (dd, *J* = 9.8 Hz, 12.5 Hz, 1H; C$H_2$$NO_2$), 3.79 (s, 3H; OC$H_3$), 3.47 (dt, *J* = 5.0 Hz, 9.9 Hz, 1H; C*H*Ph), 2.63 (m, 1H; C*H*CHO), 1.51 (m, 2H; CH_2CH_3), 0.83 (t, *J* = 7.5 Hz, 3H; CH_3).

^{13}C NMR (100 MHz, $CDCl_3$, 25°C) δ= 203.3, 159.2, 129.0 (2), 128.5, 114.5 (2), 78.8, 55.2, 55.2, 42.0, 20.3, 10.7.

CHN: Anal. Calcd for $C_{13}H_{17}NO_4$: C 62.17; H 6.82; N 5.57. Found: C 61.85; H 6.68; N 5.47.

The enantiomeric excess was determined by HPLC using a Chiral AM column (*n*-hexane/*i*-PrOH 99.6:0.4, 25°C) at 1.2 mL/min, UV detection at 254 nm: t_R : (*syn,* minor) = 52.2 min, (*syn*, major) = 77.2 min.

(2*S*, 3*R*)-2-Methyl-4-nitro-3-(thien-2-yl)butanal (45)[136]

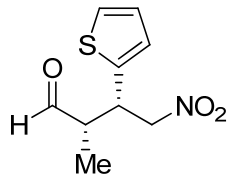

Prepared from *n*-propanal and *trans*-2-(2-nitrovinyl)thiophene according to the general procedure (Protocol E). Purified by preparative chromatography on silica gel (pentanes/EtOAc 10:1 v/v). A colourless oil was obtained.

^{1}H NMR (400 MHz, $CDCl_3$, 25°C) δ = 9.68 (d, *J* = 2.7 Hz, 1H; C*H*O), 7.33 (d, *J* = 2.7 Hz, 1H; Ph), 7.33 (t, *J* = 2.7 Hz, 1H; Ph), 7.33 (d, *J* = 2.7 Hz, 1H; Ph), 4.94 (dd, *J* = 12.7 Hz, 5.5 Hz, 1H; C*H*$_2$NO$_2$), 4.84 (dd, *J* = 12.7 Hz, 10.1 Hz, 1H; C*H*$_2$NO$_2$), 3.92 (dt, *J* = 4.9 Hz, 9.7 Hz, 1H; C*H*Ph), 2.85-2.93 (m, 1H; C*H*CHO), 0.79 (d, *J* = 7.5 Hz, 1H; C*H*$_3$).

^{13}C NMR (100 MHz, $CDCl_3$, 25°C) δ = 201.7, 138.8, 127.1, 126.7, 125.3, 78.4, 48.8, 39.4, 11.5.

CHN: Calcd for $C_9H_{11}NO_3S$: C 50.69; H 5.20; N 6.57. Found: C 50.64; H 5.17; N 6.58

The enantiomeric excess was determined by HPLC using a Chiracel AD column (*n*-hexane/*i*-PrOH 98.5:1.5, 25°C) at 1 mL/min, UV detection at 254 nm: t_R : (*syn,* minor) = 31.2 min, (*syn*, major) = 43.9 min.

(2*S*, 3*S*)-3-Cylohexyl-2-methyl-4-nitrobutanal (46)[136]

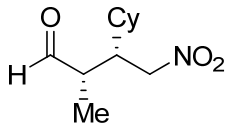

Prepared from *n*-propanal and *trans*-1-nitro-1-cyclohexyl-ethene according to the general procedure (Protocol E). Purified by preparative chromatography on silica gel (pentanes/EtOAc 15:1 v/v). A colourless oil was obtained.

^{1}H NMR (400 MHz,$CDCl_3$, 25°C) δ = 9.69 (d, *J* = 0.8 Hz, 1H; C*H*O), 4.59 (dd, *J* = 5.4 Hz, 13.3 Hz, 1H; CH_2NO_2), 4.39 (dd, *J* = 6.8 Hz, 13.3 Hz, 1H; CH_2NO_2), 2.77 – 2.54 (m, 2H; C*H*CHO, C*H*Cy), 1.81 – 1.50 (m, 5H; Cy), 1.41 (m, 1H; Cy), 1.27 – 0.93 (m, 5H; Cy), 1.20 (d, *J* = 7.0 Hz, 3H; CH_3).

^{13}C NMR (100 MHz, $CDCl_3$, 25°C) δ = 203.1, 75.8, 46.6, 43.5, 38.0, 31.6, 30.0, 26.4, 26.2, 26.0, 10.7.

CHN: Anal. Calcd for $C_{11}H_{19}NO_3$: C 61.95; H 8.98; N 6.57. Found: C 61.92; H 8.81; N 6.53.

The enantiomeric excess was determined by HPLC using a Chiracel AS-H column (*n*-hexane/*i*-PrOH 90:10, 25°C) at 0.5 mL/min, UV detection at 210 nm: t_R : (*syn,* major) = 18.4 min, (*syn*, minor) = 19.6 min.

(2*S*, 3*S*)-2-Ethyl-3-nitromethyloctanal (47)

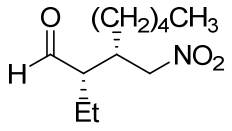

Prepared from *n*-butanal and 1-nitro-1-heptene according to the general procedure (Protocol E). Purified by preparative chromatography on silica gel (pentanes/EtOAc 15:1 v/v). A colourless oil was obtained.

^{1}H NMR (400 MHz,$CDCl_3$, 25°C) δ= 9.71 (d, *J* = 1.5 Hz, 1H; C*H*O), 4.42 (m, 2H; CH_2NO_2), 2.65 (m, 1H; C*H*CH_2NO_2), 2.41 (dtd, *J* = 1.5 Hz, 4.82 Hz, 6.33 Hz, 1H; C*H*CHO), 1.59–1.23 (m, 10H; CH_2), 1.00 (t, *J* = 7.4 Hz, 3H; CH_3); 0.88 (t, *J* = 6.9 Hz, 3H; CH_3)

^{13}C NMR (100 MHz, $CDCl_3$, 25°C) δ= 203.1, 53.9, 37.3, 36.8, 31.6, 29.0, 26.4, 22.3, 18.6, 13.9, 12.1.

CHN: Anal. Calcd for $C_{11}H_{21}NO_3$: C 61.37; H 9.83; N 6.51. Found: C 61.5; H 9.85; N 6.38.

The enantiomeric excess was determined by HPLC using a Chiracel AS-H column (*n*-hexane/*i*-PrOH 98.5:1.5, 25°C) at 0.5 mL/min, UV detection at 210 nm: t_R : (*syn,* major) = 21.1 min, (*syn*, minor) = 22.7 min.

(2*S*,3*S*)-2-Ethyl-5-methyl-3-(nitromethyl)hexanal (68)

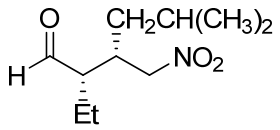

Prepared from *n*-butanal and *(E)*-4-methyl-1-nitropent-1-ene according to the general procedure (Protocol E). Purified by preparative chromatography on silica gel (pentanes/EtOAc 20:1 v/v). A colourless oil was obtained.

^{1}H NMR (400 MHz,$CDCl_3$, 25°C) δ= 9.72 (d, *J* = 1.3 Hz, 1H), 4.47 (dd, *J* = 6.4 Hz, 12.5 Hz, 1H), 4.42 (dd, *J* = 6.6 Hz, 12.5 Hz, 1H), 2.73 (m, 1H), 2.43 (dtd, *J* = 1.3 Hz, 4.7 Hz, 6.0 Hz, 1H), 1.80 (m, 1H), 1.61 (m, 1H), 1.50 (dqd, *J* = 4.9 Hz, 7.4 Hz, 14.8 Hz, 1H), 1.24 (m, 2H), 1.01 (t, *J* = 7.4 Hz, 3H), 0.92 (d, *J* = 4.9, 3H), 0.90 (d, *J* = 4.9 Hz, 3H).

^{13}C NMR (100 MHz, $CDCl_3$, 25°C) δ= 203.0, 77.1, 54.0, 38.3, 34.7, 25.2, 22.7, 22.0, 18.5, 12.2.

CHN: Anal. Calcd for $C_{10}H_{19}NO_3$: C 59.68; H 9.51; N 6.96. Found: C 59.83; H 9.26; N 6.80.

The enantiomeric excess was determined by HPLC using a Chiracel AD-H column (*n*-hexane/*i*-PrOH 99.25:0.75, 25°C) at 0.3 mL/min, UV detection at 210 nm: t_R : (*syn*, minor) = 29.5 min, (*syn,* major) = 33.0 min.

(2*S*,3*S*)-2-Ethyl-4,4-dimethoxy-3-(nitromethyl)butanal (70)[48]

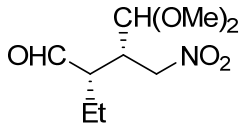

Prepared from *n*-butanal and *(E)*-3,3-dimethoxy-1-nitropropene according to the general procedure in neat $CHCl_3$. Purified by preparative chromatography on silica gel (pentanes/EtOAc 5:1 v/v). A colourless oil was obtained.

^{1}H NMR (400 MHz,$CDCl_3$, 25°C) δ = 9.64 (d, *J* = 1.4 Hz, 1H; C*H*O), 4.61 (dd, *J* = 7.2 Hz, 13.7 Hz, 1H; C$H_2$$NO_2$), 4.37 (m, 2H; C$H_2$$NO_2$, C*H*$(OMe)_2$), 3.38 (s, 3H, OC$H_3$), 3.36 (s, 3H, OC$H_3$), 3.04 (m, 1H; C*H*$CH_2NO_2$), 2.55 (s, 1H; C*H*CHO), 1.82 (m, 1H; C$H_2$$CH_3$), 1.49 (m, 1H; C$H_2$$CH_3$), 1.03 (t, *J* = 7.4 Hz, 3H; CH_3).

^{13}C NMR (100 MHz, $CDCl_3$, 25°C) δ = 202.6, 104.4, 73.3, 55.3, 55.3, 51.3, 41.1, 19.5, 12.4.

CHN: Anal. Calcd for $C_9H_{17}NO_5$: C 49.31; H 7.82; N 6.39. Found: C 49.29; H 7.56; N 6.26.

The enantiomeric excess was determined by HPLC using a Chiracel AS-H column (*n*-hexane/*i*-PrOH 95:5, 25°C) at 0.5 mL/min, UV detection at 210 nm: t_R : (*syn,* major) = 24.1 min, (*syn*, minor) = 26.4 min.

(2*S*,3*S*)-2-Isopropyl-4,4-dimethoxy-3-(nitromethyl)butanal (71)[48]

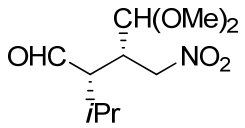

Prepared from isovaleric aldehyde and *(E)*-3,3-dimethoxy-1-nitropropene according to the general procedure in neat $CHCl_3$ (Protocol E). Purified by preparative chromatography on silica gel (pentanes/EtOAc 15:1 v/v). A colourless oil was obtained.

^{1}H NMR (400 MHz,$CDCl_3$, 25°C) δ = 9.75 (dd, *J* = 0.5 Hz, 2.5 Hz, 1H; C*H*O), 4.61 (dd, *J* = 8.9 Hz, 14.0 Hz, 1H; CH_2NO$_2$), 4.42 (dd, *J* = 3.0 Hz, 14.0 Hz, 1H; CH_2NO$_2$), 4.32 (d, *J* = 4.6 Hz, 1H; C*H*(OMe)$_2$), 3.38 (s, 3H; OCH_3), 3.38 (s, 3H; OCH_3), 3.04 (m, 1H; C*H*CH$_2$NO$_2$), 2.61 (ddd, *J* = 2.6 Hz, 3.9 Hz, 9.0 Hz, 1H; C*H*CHO), 2.03 (sept.d, *J* = 6.7 Hz, 8.7 Hz, 1H; C*H*(CH$_3$)$_2$), 1.08 (d, *J* = 6.8 Hz, 3H; CH_3), 1.03 (d, *J* = 6.6 Hz, 3H; CH_3).

^{13}C NMR (100 MHz, $CDCl_3$, 25°C) δ = 204.3, 105.3, 73.0, 56.0, 55.4 (2), 40.2, 27.2, 20.9, 20.8.

CHN: Anal. Calcd for $C_{10}H_{19}NO_5$: C 51.49; H 8.21; N 6.00. Found: C 51.52; H 8.10; N 6.00.

The enantiomeric excess was determined by HPLC using a Chiracel AS-H column (*n*-hexane/*i*-PrOH 99:1, 25°C) at 0.8 mL/min, UV detection at 210 nm: t_R : (*syn,* major) = 19.1 min, (*syn*, minor) = 22.8 min.

(3*S*,4*S*)-Methyl-3-formyl-5,5-dimethoxy-4-(nitromethyl)pentanoate (72)

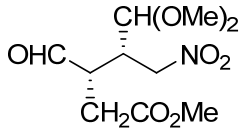

Prepared from methyl-4-oxybutanoate and *(E)*-3,3-dimethoxy-1-nitropropene according to the general procedure in neat $CHCl_3$ (Protocol E). Purified by preparative chromatography on silica gel (pentanes/EtOAc 5:1 v/v). A colourless oil was obtained.

^{1}H NMR (400 MHz,$CDCl_3$, 25°C) δ = 9.66 (s, 1H; C*H*O), 4.57 (dd, *J* = 6.7 Hz, 13.9 Hz, 1H; CH_2NO_2), 4.41 (dd, *J* = 6.5 Hz, 13.9 Hz, 1H; CH_2NO_2), 4.33 (d, *J* = 5.1 Hz, 1H, C*H*$(OMe)_2$), 3.71 (s, 3H; CO_2CH_3), 3.39 (s, 3H; OCH_3), 3.38 (s, 3H; OCH_3), 3.23 (ddt, J = 3.3 Hz, 5.2 Hz, 6.6 Hz, 1H; C*H*CH_2NO_2), 3.09 (m, 1H; C*H*CHO), 2.87 (dd, *J* = 8.20 Hz, 17.22 Hz, 1H; CH_2CO_2Me), 2.48 (dd, *J* = 5.21 Hz, 17.22 Hz, 1H; CH_2CO_2Me).

^{13}C NMR (100 MHz, $CDCl_3$, 25°C) δ = 200.1, 172.0, 104.3, 73.4, 56.3, 55.4, 52.2, 45.7, 40.7, 30.5.

CHN: Anal. Calcd for $C_{10}H_{17}NO_7$: C 45.63; H 6.51; N 5.32. Found: C 45.90; H 6.40; N 5.40.

The enantiomeric excess was determined by HPLC using a Chiracel AD-H column (*n*-hexane/*i*-PrOH 97.5:2.5, 25°C) at 0.5 mL/min, UV detection at 210 nm: t_R : (*syn*, minor) = 57.2 min, (*syn,* major) = 75.4 min.

(2*S*,3*R*)-3-(2,4-Dimethoxyphenyl)-2-ethyl-4-nitrobutanal (74)

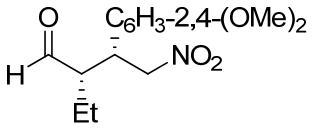

Prepared from *n*-butanal and 2,4-dimethoxy-β-nitrostyrene according to the general procedure (Protocol E). Purified by preparative chromatography on silica gel (pentanes/CH_2Cl_2 3:1 v/v). A colourless oil was obtained.

^{1}H NMR (400 MHz, $CDCl_3$, 25°C) δ = 9.68 (d, *J* = 2.7 Hz, 1H; C*H*O), 6.98 (d, *J* = 8.3 Hz, 1H; Ph), 6.44 (d, *J* = 2.4 Hz, 1H; Ph), 6.42 (dd, *J* = 2.4 Hz, 8.3 Hz, 1H; Ph), 4.79 (dd, *J* = 9.6 Hz, 12.4 Hz, 1H; CH_2NO_2), 4.60 (dd, *J* = 4.9 Hz, 12.4 Hz, 1H; CH_2NO_2), 3.92 (dt, *J* = 4.9 Hz, 9.7 Hz, 1H; C*H*Ph), 3.80 (s, 3H; OCH_3), 3.78 (s, 3H; OCH_3), 2.85-2.93 (m, 1H; C*H*CHO), 1.37-1.55 (m, 2H; CH_2CH_3), 0.79 (t, *J* = 7.5 Hz, 1H; CH_3).

^{13}C NMR (100 MHz, $CDCl_3$, 25°C) δ = 204.3, 161.1, 158.9, 131.5, 117.1, 104.9, 99.6, 77.7, 55.8, 55.7, 54.0, 39.5, 20.9, 11.1.

CHN: Anal. Calcd for $C_{14}H_{19}NO_5$: C 59.78; H 6.81; N 4.98. Found: C 59.80; H 6.78; N 4.97.

The enantiomeric excess was not determined.

(2*S*,3*R*)-2-Ethyl-4-nitro-3-phenylbutan-1-ol (73) (gram scale synthesis)

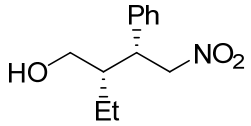

TFA•H-D-Pro-Pro-Glu-NH_2 **56** (62.0 mg, 0.136 mmol, 0.02 eq) was suspended in 1 mL of *i*-PrOH and NMM (15 µL, 0.136 mmol, 0.02 eq), butyraldehyde (675 µL, 7.5 mmol, 1.1 eq) and $CHCl_3$ (9 mL) were added. The colourless solution was then cooled to 0 °C and β-nitrostyrene (1.01 g, 6.80 mmol, 1.0 eq) was added. The yellow solution was stirred for 24 h at 0 °C. TLC (pentanes/EtOAc 10:1 v/v) showed complete conversion of the reaction and ^{1}H NMR of the crude reaction mixture showed a dr of >99:1 of the formed Michael adduct. The reaction mixture was cooled to -15°C and a solution of borane in THF (1M, 8.0 mL, 8.2 mmol, 1.2 eq) was added dropwise. After stirring for 1 h at -15 °C the TLC (pentanes/EtOAc 5:1) showed complete conversion. The mixture was quenched with an excess of conc. AcOH (2.0 mL, 31.7 mmol, 4.7 eq) and concentrated under reduced pressure. The crude product was dissolved in CH_2Cl_2/pentanes 1:2 (v/v) and purified by flash chromatography over silica gel using pentanes/EtOAc 5:1 (v/v) to obtain 1.34 g (93%) of the desired product **73** as a colourless oil.

^{1}H NMR (400 MHz, $CDCl_3$, 25°C) δ = 7.36 (m, 2H; Ph), 7.30 (m, 1H; Ph), 7.25 (m, 2H; Ph), 4.94 (dd, *J* = 12.7 Hz, 5.5 Hz, 1H; C*H*$_2$NO$_2$), 4.84 (dd, *J* = 12.7 Hz, 10.1 Hz, 1H; C*H*$_2$NO$_2$), 3.79 (dd, *J* = 11.1 Hz, 3.4 Hz, 1H; C*H*$_2$OH), 3.73 (ddd, *J* = 10.1 Hz, 7.7 Hz, 5.6 Hz, 1H; C*H*Ph), 3.63 (dd, *J* = 11.1 Hz, 6.0 Hz, 1H; C*H*$_2$OH), 1.79 (m, 2H; C*H*CH$_2$OH and CH$_2$O*H*), 1.40 (dqd, *J* = 15.0 Hz, 7.5 Hz, 4.0 Hz, 1H; C*H*$_2$CH$_3$), 1.23 (qdd, *J* = 14.3 Hz, 9.0 Hz, 7.3 Hz, 1H; C*H*$_2$CH$_3$), 0.92 (t, *J* = 7.4 Hz, 3H, C*H*$_3$).

^{13}C NMR (100 MHz, $CDCl_3$, 25°C) δ = 139.1, 129.2, 128.6, 127.9, 79.2, 62.5, 46.3, 45.8, 21.9, 12.1.

CHN: Anal. Calcd for $C_{12}H_{17}NO_3$: C 64.55; H 7.67; N 6.27. Found: C 64.30; H 7.66; N 6.21.

The diastereomeric ratio (*syn* to *anti*) and the enantiomeric excess were determined by HPLC using a Chiracel AD-H column (*n*-hexane/*i*-PrOH 99.4:0.6, 25°C) at 1.2 mL/min, UV detection at 210 nm: t_R : (*anti*, minor) = 101.7, (*anti*, major) = 107.4, (*syn*, minor) = 115.5 min, (*syn,* major) = 119.4 min.

17.3 1,4-Addition Products of Aldehydes and Nitroethylene

ee determination by chiral HPLC or chiral GC: For the determination of the signals corresponding to the two enantiomers, reactions were performed with H-D-Pro-Pro-Glu-NH_2 **56** and the enantiomeric H-Pro-D-Pro-D-Glu-NH_2 under otherwise identical conditions. Peptides **56** and H-Pro-D-Pro-D-Glu-NH_2 have opposite enantioselectivity.

ee determination by ^1H NMR spectroscopy: To determine the ee of the γ-nitroaldehydes a procedure developed by Gellman *et al.* was used.[158] This involves formation of diastereomeric imines by addition of (*S*)-(+)-1-methoxy-2-propylamine to the reaction mixture. In a typical experiment, approximately 1 mL of the reaction mixture was evaporated and re-dissolved in 0.5 mL $CDCl_3$. 60 µl of (*S*)-(+)-1-methoxy-2-propylamine were added, the mixture was shaken and the ^1H NMR spectrum (400 MHz, $CDCl_3$, 25°C) measured immediately. The *ee* was determined by integration of the signals corresponding to the imine proton.

Assignment of the absolute configuration: For the assignment of the absolute configuration, (2*S*)-benzyl-4-nitrobutan-1-ol **82** was converted into the known (2*S*)-benzyl-γ-butyrolactone **86** (see below). The optical rotation of **86** was in agreement with the published data.[160,171]

(2*S*)-Methyl-4-nitrobutan-1-ol (76)

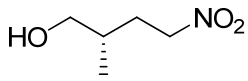

Prepared from propanal and nitroethylene according to the general procedure (Protocol F). Purified by preparative chromatography on silica gel (pentanes/EtOAc 3:1 v/v). A colourless oil was obtained.

^{1}H NMR (400 MHz, $CDCl_3$, 25°C) δ = 4.50 (m, 2H; C*H*$_2$NO$_2$), 3.59 (dd, *J* = 5.2 Hz, 10.6 Hz, 1H; C*H*$_2$OH), 3.50 (dd, *J* = 6.5 Hz, 10.5 Hz, 1H; C*H*$_2$OH), 2.21 (m, 1H; C*H*$_2$CH$_2$NO$_2$), 1.90 (m, 1H; C*H*$_2$CH$_2$NO$_2$), 1.78 (m, 1H; C*H*CH$_3$), 1.46 (s, 1H; O*H*), 0.98 (d, *J* = 6.6 Hz, 3H; C*H*$_3$).

^{13}C NMR (100 MHz, $CDCl_3$, 25°C) δ = 74.0, 67.4, 33.1, 31.1, 16.2.

CHN: Anal. Calcd for $C_5H_{11}NO_3$: C 45.10; H 8.33; N 10.52. Found: C 44.99; H 8.08; N 10.37

$[\alpha]_D^{20}$ = -15.3 (c = 1.0, $CHCl_3$, 95 % *ee*).

The enantiomeric excess was determined by HPLC using a Chiracel AD-H column (*n*-hexane/*i*-PrOH 95:5, 25°C) at 0.5 mL/min, UV detection at 210 nm: t_R : (minor) = 39.2 min, (major) = 41.7 min.

(2*S*)-Ethyl-4-nitrobutan-1-ol (77)

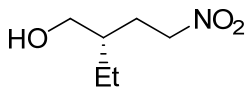

Prepared from *n*-butanal and nitroethylene according to the general procedure (Protocol F). Purified by preparative chromatography on silica gel (pentanes/EtOAc 7:1 v/v). A colourless oil was obtained.

^{1}H NMR (400 MHz, $CDCl_3$, 25°C) δ= 4.51 (t, *J* = 7.4 Hz, 2H; C*H*$_2$NO$_2$), 3.68 (dd, *J* = 4.5 Hz, 10.7 Hz, 1H; C*H*$_2$OH), 3.56 (dd, *J* = 6.3 Hz, 10.7 Hz, 1H; C*H*$_2$OH), 2.10 (m, 2H; C*H*$_2$CH$_2$NO$_2$), 1.54 (m, 1H; C*H*Et), 1.47-1.31 (m, 2H; C*H*$_2$CH$_3$), 0.94 (t, *J* = 7.2 Hz, 3H; C*H*$_3$).

^{13}C NMR (100 MHz, $CDCl_3$, 25°C) δ= 74.2, 64.7, 39.3, 29.2, 23.5, 11.1.

MS (ESI): *m/z* (%): 170.7 (100) $[M+Na]^+$. M = 147.2 calcd for $C_6H_{13}NO_3$.

$[\alpha]_D^{20}$ = -0.5 (c = 1.0, $CHCl_3$, 98 % *ee*).

The enantiomeric excess was determined by HPLC using a Chiracel AD-H column (*n*-hexane/*i*-PrOH 92.5:7.5, 25°C) at 0.5 mL/min, UV detection at 210 nm: t_R : (minor) = 20.1 min, (major) = 22.6 min.

(2*S*)-(2-Nitroethyl)pentan-1-ol (78)

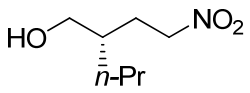

Prepared from *n*-pentanal and nitroethylene according to the general procedure (Protocol F). Purified by preparative chromatography on silica gel (pentanes/EtOAc 3:1 v/v). A colourless oil was obtained.

^{1}H NMR (400 MHz, $CDCl_3$, 25°C) δ= 4.52 (t, *J* = 7.4 Hz, 2H; C*H*$_2$NO$_2$), 3.68 (dd, *J* = 4.4 Hz, 10.7 Hz, 1H; C*H*$_2$OH), 3.54 (dd, *J* = 6.4 Hz, 10.7 Hz, 1H; C*H*$_2$OH)), 2.10 (m, 2H; C*H*$_2$CH$_2$NO$_2$), 1.62 (m, 1H; C*H*Pr), 1.46 (s, 1H; O*H*), 1.46 – 1.23 (m, 4H; C*H*$_2$C*H*$_2$CH$_3$), 0.92 (t, *J* = 7.1 Hz, 3H; C*H*$_3$).

^{13}C NMR (100 MHz, $CDCl_3$, 25°C) δ= 74.1, 65.1, 37.6, 33.1, 29.6, 19.9, 14.2.

CHN: Anal. Calcd for $C_7H_{15}NO_3$: C 52.16; H 9.38; N 8.69. Found: C 52.31; H 9.42; N 8.50.

$[\alpha]_D^{20}$ = -4.2 (c = 1.0, $CHCl_3$, 99 % *ee*).

The enantiomeric excess was determined by HPLC using a Chiracel AD-H column (*n*-hexane/*i*-PrOH 97.5:2.5, 25°C) at 0.5 mL/min, UV detection at 210 nm: t_R : (minor) = 53.4 min, (major) = 55.8 min.

(2*S*)-(2-Nitroethyl)hexan-1-ol (79)

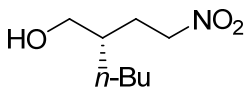

Prepared from *n*-hexanal and nitroethylene according to the general procedure (Protocol F). Purified by preparative chromatography on silica gel (pentanes/EtOAc 5:1 v/v). A colourless oil was obtained.

^{1}H NMR (400 MHz, $CDCl_3$, 25°C) δ = 4.44 (t, J = 7.4 Hz, 2H; CH_2NO$_2$), 3.61 (dd, J = 4.4 Hz, 10.7 Hz, 1H; CH_2OH), 3.47 (dd, J = 6.4 Hz, 10.7 Hz, 1H; CH_2OH), 2.02 (m, 2H; CH_2CH$_2$NO$_2$), 1.53 (m, 1H; C*H*Bu), 1.45 (s, 1H; O*H*), 1.33 – 1.19 (m, 6H; CH_2CH_2CH_2CH$_3$), 0.84 (t, J = 6.8 Hz, 3H; CH_3).

^{13}C NMR (100 MHz, $CDCl_3$, 25°C) δ = 74.2, 65.1, 37.8, 30.5, 29.6, 28.9, 22.8, 14.0.

CHN: Anal. Calcd for $C_8H_{17}NO_3$: C 54.84; H 9.78; N 7.99. Found: C 54.88; H 9.81; N 7.77;

$[\alpha]_D^{20}$ = -4.3 (c = 1.0, $CHCl_3$, 99 % *ee*).

The enantiomeric excess was determined by HPLC using a Chiracel AD-H column (*n*-hexane/*i*-PrOH 97.5:2.5, 25°C) at 0.5 mL/min, UV detection at 210 nm: t_R : (minor) = 48.6 min, (major) = 51.4 min.

(2*R*)-3-Methyl-(2-nitroethyl)butan-1-ol (80)

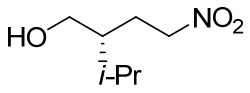

Prepared from isovaleraldehyde and nitroethylene according to the general procedure (Protocol F). Purified by preparative chromatography on silica gel (pentanes/EtOAc 5:1 v/v). A colourless oil was obtained.

^{1}H NMR (400 MHz, $CDCl_3$, 25°C) δ= 4.53 (m, 2H; C*H*$_2$NO$_2$), 3.72 (dd, *J* = 4.6 Hz, 10.7 Hz, 1H; C*H*$_2$OH), 3.59 (dd, *J* = 7.1 Hz, 10.7 Hz, 1H; C*H*$_2$OH), 2.15 (m, 1H; C*H*$_2$CH$_2$NO$_2$), 2.10 (m, 1H; C*H*$_2$CH$_2$NO$_2$), 1.76 (m, 1H; C*Hi*-Pr or C*H*(CH$_3$)$_2$), 1.42 (m, 2H; O*H*, C*Hi*-Pr or C*H*(CH$_3$)$_2$), 0.92 (d, *J* = 6.9 Hz, 6H; (C*H*$_3$)$_2$).

^{13}C NMR (100 MHz, $CDCl_3$, 25°C) δ= 74.8, 63.9, 43.7, 28.7, 27.2, 19.6, 19.3.

CHN: Anal. Calcd for $C_7H_{15}NO_3$: C 52.16; H 9.38; N 8.69. Found: C 52.21; H 9.28; N 8.69.

$[\alpha]_D^{20}$ = +5.6 (c = 1.0, $CHCl_3$, 97 % *ee*).

The enantiomeric excess was determined by ^{1}H NMR (400 MHz, $CDCl_3$, 25°C) after the addition of (*S*)-(+)-1-methoxy-2-propylamine to the crude nitroaldehyde: minor diastereoisomer δ= 7.48 (d, *J* = 5.5 Hz), major diastereoisomer δ= 7.40 (d, *J* = 5.9 Hz).

(2*R*)-3,3-Dimethyl-(2-nitroethyl)butan-1-ol (81)

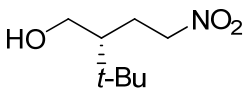

Prepared from 3,3-dimethylbutyraldehyde and nitroethylene according to the general procedure (Protocol F). Purified by preparative chromatography on silica gel (pentanes/EtOAc 5:1 v/v). A colourless oil was obtained.

^{1}H NMR (400 MHz, $CDCl_3$, 25°C) δ = 4.65 (ddd, *J* = 5.6 Hz, 8.5 Hz, 13.0 Hz, 1H; C*H*$_2$NO$_2$), 4.53 (dt, *J* = 7.9 Hz, 12.9 Hz, 1H; C*H*$_2$NO$_2$), 3.91 (ddd, *J* = 0.7 Hz, 3.7 Hz, 10.6 Hz, 1H; C*H*$_2$OH), 3.58 (dd, *J* = 7.7 Hz, 10.6 Hz, 1H; C*H*$_2$OH), 2.31 (m, 1H; C*H*$_2$CH$_2$NO$_2$), 1.96 (m, 1H; C*H*$_2$CH$_2$NO$_2$)), 1.31 (m, 2H; O*H*, C*Ht*Bu), 0.94 (s, 9H; (C*H*$_3$)$_3$).

^{13}C NMR (100 MHz, $CDCl_3$, 25°C) δ = 75.8, 63.7, 47.5, 32.6, 27.8 (3), 27.0.

CHN: Anal. Calcd for $C_8H_{17}NO_3$: C 54.84; H 9.78; N 7.99. Found: C 54.84; H 9.79; N 7.96.

$[\alpha]_D^{20}$ = +11.7 (c = 1.0, $CHCl_3$, 98% *ee*).

The enantiomeric excess was determined by chiral GC using a Chiraldex G-TA column (30m x 0.25mm x 0.12 μm film thickness) at 130°C isotherm / 60 kPa (H_2): t_R : (minor) = 55.5 min, (major) = 56.5 min.

(2*S*)-Benzyl-4-nitrobutan-1-ol (82)

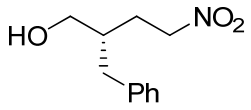

Prepared from 3-phenylpropionaldehyde and nitroethylene according to the general procedure (Protocol F). Purified by preparative chromatography on silica gel (pentanes/EtOAc 5:1 v/v). A colourless oil was obtained.

^{1}H NMR (400 MHz, $CDCl_3$, 25°C) δ = 7.31 (m, 2H; Ph), 7.22 (m, 1H; Ph), 7.17 (m, 2H; Ph), 4.47 (m, 2H; C*H*$_2$NO$_2$), 3.65 (m, 1H; C*H*$_2$OH), 3.53 (m, 1H; C*H*$_2$OH), 2.71 (dd, *J* = 7.8 Hz, 13.7 Hz, 1H; C*H*$_2$Ph), 2.63 (dd, *J* = 6.9 Hz, 13.7 Hz, 1H; C*H*$_2$Ph), 2.12 (m, 2H; C*H*$_2$CH$_2$NO$_2$), 1.94 (m, 1H; C*H*Bn).

^{13}C NMR (100 MHz, $CDCl_3$, 25°C) δ = 139.2, 129.0 (2), 128.6 (2), 126.4, 74.0, 64.3, 39.7, 37.5, 29.3.

CHN: Anal. Calcd for $C_{11}H_{15}NO_3$: C 63.14; H 7.23; N 6.69. Found: C 63.03; H 7.41; N 6.40.

$[\alpha]_D^{20}$ = +10.5 (c = 1.0, $CHCl_3$, 98 % *ee*).

The enantiomeric excess was determined by HPLC using a Chiracel AD-H column (*n*-hexane/*i*-PrOH 92.5:7.5, 25°C) at 0.5 mL/min, UV detection at 254 nm: t_R : (minor) = 28.1 min, (major) = 30.3 min.

(2*S*)-(2-Nitroethyl)-*cis*-8-undecanal (83)

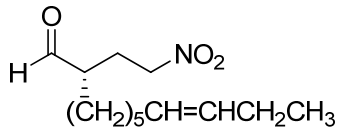

Prepared from *cis*-8-undecanal and nitroethylene according to the general procedure (Protocol F) without reduction. Purified by preparative chromatography on silica gel (pentanes/EtOAc 20:1 v/v). A colourless oil was obtained.

^{1}H NMR (400 MHz, $CDCl_3$, 25°C) δ = 9.67 (s, 1H; C*H*O), 5.36 (m, 2H; C*H*=C*H*), 4.45 (m, 2H; C$H_2$$NO_2$), 2.47 (m, 1H; C*H*CHO), 2.32 (tdd, *J* = 6.4 Hz, 9.0 Hz, 15.1 Hz, 1H; C$H_2$$CH_2NO_2$), 2.13 (m, 1H; C$H_2$$CH_2NO_2$), 2.02 (m, 4H; alkyl-H), 1.76 (m, 1H; alkyl-H), 1.52 (m, 1H; alkyl-H), 1.42 – 1.29 (m, 6H; alkyl-H), 0.97 (t, *J* = 7.5 Hz, 3H; CH_3).

^{13}C NMR (100 MHz, $CDCl_3$, 25°C) δ = 202.8, 131.9, 128.7, 73.3, 48.4, 29.4, 29.1, 28.7, 26.9, 26.5, 25.5, 20.5, 14.4.

MS (FAB): *m/z* (%): 242.1 (100) $[M+H]^+$. M = 241.3 calcd for $C_{13}H_{23}NO_3$.

The enantiomeric excess was determined by ^{1}H NMR (400 MHz, $CDCl_3$, 25°C) after the addition of (*S*)-(+)-1-methoxy-2-propylamine to the crude nitroaldehyde: minor diastereoisomer δ = 7.48 (d, *J* = 5.7 Hz), major diastereoisomer δ = 7.40 (d, *J* = 6.5 Hz).

(3*R*)-Methyl-formyl-5-nitropentanoate (84)

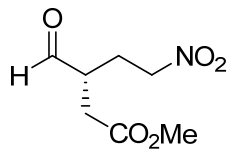

Prepared from methyl-4-oxobutanoate and nitroethylene according to the general procedure (Protocol F) without reduction. Purified by preparative chromatography on silica gel (pentanes/EtOAc 5:1 v/v). A colourless oil was obtained.

^{1}H NMR (400 MHz, $CDCl_3$, 25°C) δ = 9.67 (s, 1H; C*H*O), 4.44 (m, 2H; CH_2NO$_2$), 3.65 (s, 3H; CH_3), 2.82 (m, 1H; C*H*CHO), 2.72 (dd, J = 6.6 Hz, 16.8 Hz, 1H; CH_2CO$_2$Me), 2.54 (dd, J = 6.1 Hz, 16.8 Hz, 1H; CH_2CO$_2$Me), 2.41 (m, 1H; CH_2CH$_2$NO$_2$), 2.08 (m, 1H; CH_2CH$_2$NO$_2$).

^{13}C NMR (100 MHz, $CDCl_3$, 25°C) δ = 200.5, 171.2, 72.8, 52.3, 44.6, 33.0, 25.7.

CHN: Anal. Calcd for $C_7H_{11}NO_5$: C 44.45; H 5.86; N 7.40. Found: C 44.49; H 5.92; N 7.00.

The enantiomeric excess was determined by ^{1}H NMR (400 MHz, $CDCl_3$, 25°C) after the addition of (*S*)-(+)-1-methoxy-2-propylamine to the crude nitroaldehyde: minor diastereoisomer δ = 7.61 (d, J = 4.0 Hz), major diastereoisomer δ = 7.50 (d, J = 5.2 Hz).

(3*S*)-Methyl-formyl-5-nitroheptanoate (85)

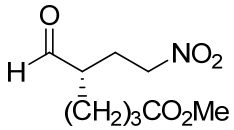

Prepared from adipic-semialdehyde-methylester and nitroethylene according to the general procedure (Protocol F) without reduction. Purified by preparative chromatography on silica gel (pentanes/EtOAc 4:1 v/v). A colourless oil was obtained.

^{1}H NMR (250 MHz, $CDCl_3$, 25°C) δ = 9.67 (s, 1H; C*H*O), 4.59 (m, 2H; C$H_2$$NO_2$), 3.69 (s, 3H; C$H_3$), 2.55 – 2.10 (m, 5H; C$H_2$$CO_2$Me, C*H*CHO, C$H_2$$CH_2NO_2$), 1.85 – 1.50 (m, 4H; (CH_2C$H_2$$CH_2CO_2$Me).

^{13}C NMR (100 MHz, $CDCl_3$, 25°C) δ = 202.2, 173.2, 73.1, 51.7, 48.2, 33.5, 27.9, 25.3, 21.8.

CHN: Anal. Calcd for $C_9H_{15}NO_5$: C 49.76; H 6.96; N 6.45. Found: C 49.93; H 6.93; N 6.30.

The enantiomeric excess was determined by ^{1}H NMR (400 MHz, $CDCl_3$, 25°C) after the addition of (*S*)-(+)-1-methoxy-2-propylamine to the crude nitroaldehyde: minor diastereoisomer δ = 7.50 (d, J = 5.5 Hz), major diastereoisomer δ = 7.42 (d, J = 6.4 Hz).

17.4 Derivatives of 1,4-Addition Products

(2*S*)-Benzyl-γ-butyrolactone (86)

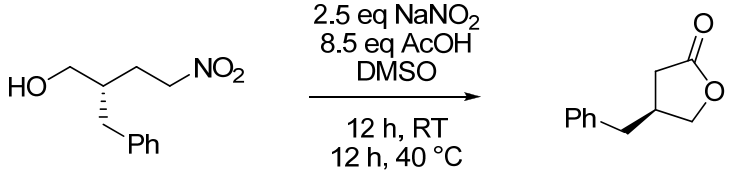

82 **86**

The title compound was prepared according to a literature procedure.[28]
(2*S*)-2-Benzyl-4-nitrobutan-1-ol **82** (210 mg, 1 mmol, 1 eq) was dissolved in DMSO (1.5 mL), $NaNO_2$ (173 mg, 2.5 mmol, 2.5 eq) and acetic acid (487 µL, 8.5 mmol, 8.5 eq) was added and the mixture was stirred for 12 h at RT. An excess of $MgSO_4$ was added and the mixture was stirred for another 12 h at 40 °C. The mixture was allowed to cool to RT and HCl 1M (20 mL) was added. The aqueous phase was extracted with CH_2Cl_2 (3 x 15 mL) and the combined organic layers were dried over $MgSO_4$. The solvent was removed under vacuum and the crude material was purified by preparative chromatography on silica gel (pentanes/EtOAc 4:1 v/v) affording a colourless oil (157 mg, 89 %).

^{1}H NMR (400 MHz, $CDCl_3$, 25°C) δ= 7.32 (m, 2H), 7.25 (m, 1H), 7.16 (m, 2H), 4.34 (dd, *J* = 6.9 Hz, 9.2 Hz, 1H), 4.04 (dd, *J* = 6.1 Hz, 9.2 Hz, 1H), 2.86 (m, 1H), 2.78 (dd, *J* = 3.2 Hz, 7.6 Hz, 2H), 2.61 (dd, *J* = 8.0 Hz, 17.5 Hz, 1H), 2.30 (dd, *J* = 7.0 Hz, 17.5 Hz, 1H).

^{13}C NMR (100 MHz, $CDCl_3$, 25°C) δ= 176.8, 138.2, 128.8, 128.6, 126.8, 72.6, 38.9, 37.2, 34.2.

MS (ESI): *m/z* (%): 199.6 (100) $[M+Na]^+$. M = 176.2 calcd for $C_{11}H_{12}O_2$.

CHN: Anal. Calcd for $C_{11}H_{12}O_2$: C 74.98; H 6.86; Found: C 74.82; H 7.13.

$[\alpha]_D^{20}$ = -8.1 (c = 1.0, $CHCl_3$, 97 % *ee*).

Analytical data are in agreement with the published data.[160,171]

The enantiomeric excess was determined by HPLC using a Chiracel AD-H column (*n*-hexane/*i*-PrOH 95:5, 25°C) at 0.5 mL/min, UV detection at 210 nm: t_R : (minor) = 33.1 min, (major) = 35.7 min.

(2*S*)-2-(Methylphenyl)-4-nitrobutanoic acid (88)

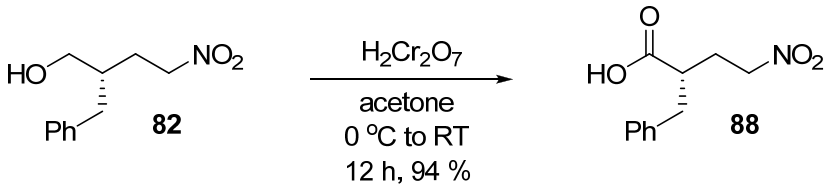

To a solution of 50 mg (2*S*)-2-benzyl-4-nitrobutan-1-ol **82** (50 mg, 239 µmol, 1 eq) dissolved in acetone (500 µL) at 0 °C was added a solution of Jones reagent[172-174] (750 µL, 375 µmol, 1.6 eq, prepared as a standard reagent, 8.0 M). The reaction mixture was allowed to warm to RT and stirring was continued for 12 h. The reaction was quenched with excess *i*-PrOH (100 µL) and the mixture stirred for 10 min, filtered, diluted with 2 M HCl (1.0 mL) and extracted with Et_2O (5 x 1.5 mL). Organic extracts were dried ($MgSO_4$), filtered, concentrated *in vacuo*, and purified by flash chromatography over silica gel (5 % v/v MeOH/CH_2Cl_2) affording the title compound **88** as a viscous colorless oil (50 mg, 94 %).

^{1}H NMR (400 MHz, $CDCl_3$, 25°C,) δ = 9.52 (bs, 1H), 7.32 (m, 2H), 7.26 (m, 1H), 7.18 (m, 2H), 4.43 (m, 2H), 3.12 (dd, *J* = 9.6, 16.7 Hz, 1H), 2.83 (m, 2H), 2.24 (m, 2H).

^{13}C NMR (100 MHz, $CDCl_3$, 25°C,) δ = 179.9, 137.5, 129.1, 128.9, 127.3, 73.3, 43.9, 38.1, 28.2.

MS (ESI): *m/z* (%): 246.8 (100) $[M+Na]^+$. M = 223.2 calcd for $C_{11}H_{13}NO_4$.

(2*S*)-2-(Methylphenyl)-4-aminobutanoic acid (89)

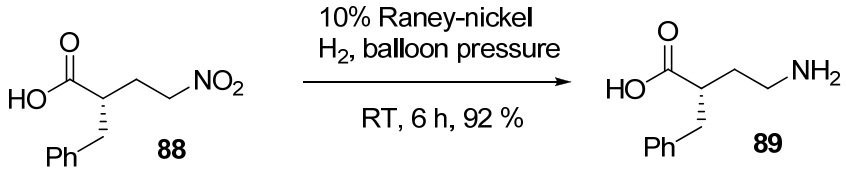

To a slurry of activated Raney-nickel catalyst (3.5 mg) in MeOH (1.0 mL) was added a solution of (*S*)-2-(methylphenyl)-4-nitrobutanoic acid **88** (35 mg, 157 μmol) in MeOH (1.0 mL) and the mixture was evacuated and purged with hydrogen gas (balloon pressure). The reaction was stirred under hydrogen at RT for 6 h then filtered through celite. Combined filtrates and MeOH washings were concentrated to dryness, and water (2.0 mL) was added. The aqueous solution was again concentrated to dryness, affording the title compound **89** as a fine white powder (28 mg, 92 %).

^{1}H NMR (400 MHz, D_2O, 25°C) δ = 7.22 (m, 2H), 7.14 (m, 3H), 2.81 (t, *J* = 8.0 Hz, 2H), 2.75 (dd, *J* = 8.6, 13.5 Hz, 1H), 2.63 (dd, *J* = 6.4, 13.5 Hz, 1H), 2.44 (m, 1H), 1.82-1.57 (m, 2H).

^{13}C NMR (100 MHz, D_2O, 25°C) δ = 182.9, 140.2, 129.3, 128.9, 126.8, 48.7, 38.9, 38.4, 30.0.

MS (ESI): *m/z* (%): 194.8 (100) $[M+H]^+$. M = 193.8 calcd for $C_{11}H_{15}NO_2$.

(2*S*)-4-(9-Fluorenylmethoxycarbonyl)-2-(methylphenyl)-butanoic acid (87)

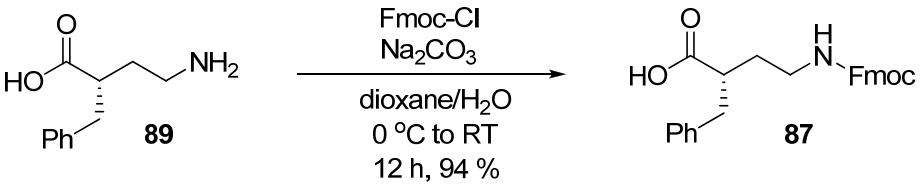

To a solution of (*S*)-2-(methylphenyl)-4-aminobutanoic acid **89** (25 mg, 129 μmol, 1.0 eq) in water (1.0 mL) was added anhydrous Na_2CO_3 (30 mg, 285 μmol, 2.2 eq) followed by a solution of 9-fluorenylmethoxycarbonyl chloride (37 mg, 142 μmol, 1.1 eq) in dioxane (1.0 mL). The reaction mixture was stirred at RT for 12 h then concentrated to remove dioxane (not to dryness). Water (2.0 mL) was added and the aqueous layer was washed with Et_2O (3 x 3.0 mL). The aqueous layer was then cooled with stirring and 2 M HCl was added dropwise to pH 2. The Fmoc-amino acid was extracted with $CHCl_3$ (4 x 1.5 mL) and combined extracts dried ($MgSO_4$) and concentrated *in vacuo*, affording the title compound **87** as a colourless oil which solidified upon standing (50 mg, 94 %).

^{1}H NMR (400 MHz, $CDCl_3$, 25°C) δ = 7.76 (d, *J* = 7.4 Hz, 2H), 7.57 (d, *J* = 7.4 Hz, 2H), 7.40 (t, *J* = 7.4 Hz, 2H), 7.30 (t, *J* = 7.4 Hz, 2H), 7.25 (d, *J* = 7.4 Hz, 1H), 7.21 (d, *J* = 7.4 Hz, 2H), 7.16 (d, *J* = 7.4 Hz, 2H), 4.92 (bs, 1H), 4.37 (m, 2H), 4.19 (m, 1H), 3.20 (m, 2H), 3.02 (m, 1H), 2.68 (m, 2H), 1.76 (m, 2H).

^{13}C NMR (100 MHz, $CDCl_3$, 25°C) δ = 180.0, 157.0, 144.3, 141.7, 139.0, 129.4, 128.9, 128.1, 127.5, 127.0, 125.5, 120.4, 47.7, 45.0, 39.4, 38.5, 32.1, 30.2.

MS (ESI): *m/z* (%): 438.3 (100) $[M+Na]^+$. M = 415.5 calcd for $C_{26}H_{25}NO_4$.

Enantiomeric excess determination of Fmoc-γ-amino acid (87) via formation of chiral amide (97)

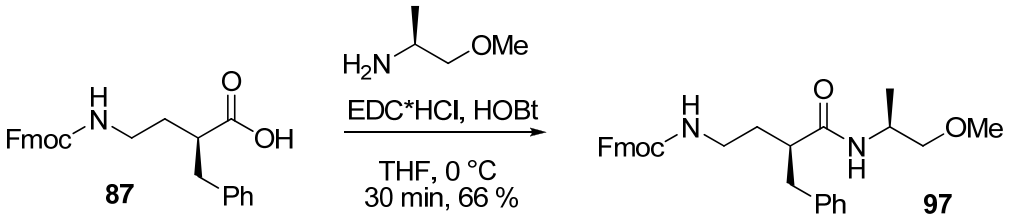

To a solution of (*S*)-4-(9-fluorenylmethoxycarbonyl)-2-(methylphenyl)-butanoic acid **87** (10 mg, 24 μmol) in dry CH_2Cl_2 (900 μL) and dry THF (100 μL) was added (*S*)-(+)-1-methoxy-2-propylamine (2 mg, 24 μmol, 1.0 eq) and the solution was cooled to 0 °C (ice bath) under nitrogen. HOBt (5.5 mg, 36 μmol, 1.5 eq) and EDC•HCl (7 mg, 36 μmol, 1.5 eq) was added in one portion and the reaction mixture was stirred for 30 min at 0 °C. The reaction mixture was concentrated to a small volume (~200 μL) and applied directly to a preparative silica TLC plate. The plate was eluted with EtOAc/*n*-hexanes 1:2 (v/v) and the product (R_f = 0.6) was extracted with EtOAc, filtered and concentrated, affording the title compound **97** as a fine white solid (8 mg, 16 μmol, 66 %).

The NMR spectra showed one major compound along with a minor compound that occurred to less than 2 %.

^{1}H NMR (400 MHz, CD_3OD, 25°C) δ = 7.72 (d, *J* = 7.4 Hz, 2H), 7.57 (d, *J* = 7.4 Hz, 2H), 7.31 (t, *J* = 7.4 Hz, 2H), 7.23 (t, *J* = 7.4 Hz, 2H), 7.16 (m, 2H), 7.07 (m, 3H), 4.28 (d, *J* = 6.6 Hz, 2H), 4.11 (t, *J* = 6.8 Hz, 1H), 3.88 (dd, *J* = 6.2, 12.4, 1H), 3.18 (s, 3H), 3.13 (d, *J* = 5.8 Hz, 2H), 3.03 (t, *J* = 7.7 Hz, 2H), 2.74 (dd, *J* = 10.0, 13.2 Hz, 1H), 2.61 (dd, *J* = 5.4, 13.2 Hz, 1H), 2.41 (ddd, *J* = 4.9, 9.7, 14.7, 1H), 1.72 (m, 1H), 1.58 (m, 1H), 0.74 (d, *J* = 6.8 Hz, 3H).

^{13}C NMR (100 MHz, CD_3OD, 25°C) δ = 144.4, 141.6, 139.8, 129.1, 128.3, 127.8, 127.1, 126.3, 125.1, 122.5, 119.9, 84.0, 82.3, 75.4, 66.5, 58.0, 47.1, 44.7, 39.0, 38.9, 33.0, 16.2.

MS (ESI): *m/z* (%): 509.6 (100) $[M+Na]^+$. M = 486.6 calcd for $C_{30}H_{34}N_2O_4$.

18. Conformational Studies

18.1 Calculations

Calculations of lowest energy structures were performed with MacroModel 8.0. The calculations used the OPLS-AA force field[121] and the GB/SA model for chloroform.[122] Searching was performed using the MCMM method in blocks of 20000 steps.

18.2 X-Ray Studies

Crystals of H-Pro-Pro-Asp-NH_2 **1**, H-D-Pro-Pro-Asp-NH_2 **21** and H-D-Pro-Pro-Glu-NH_2 **56**, suitable for x-ray single crystal structure analysis were obtained as follows: The peptides were desalted according to the general procedure (Protocol G) using VariPure™ IPE tubes. Desalted peptides (~10 mg) were transferred into small vials and dissolved in water (~1 drop) and MeOH (~3 drops). The open vials were kept in larger vials (closed) containing THF which was allowed to diffuse into the inner vials. Crystals were obtained within one day.

H-Pro-Pro-Asp-NH_2 (1)

Formula $C_{14}H_{22}N_4O_5$, M = 326.35, F(000) = 696, colorless plate, size 0.08 · 0.10 · 0.33 mm^3, orthorhombic, space group P 2_1 2_1 2_1 , Z = 4, a = 8.2586(3) Å, b = 12.7014(4) Å, c = 14.4787(4) Å, α = 90°, β = 90°, γ = 90°, V = 1518.75(8) $Å^3$, $D_{calc.}$ = 1.427 Mg · m^{-3}. The crystal was measured on a Nonius KappaCCD diffractometer at 173K using graphite-monochromated Mo K_α-radiation with λ = 0.71073 Å, Θ_{max} = 27.851°. Minimal/maximal transmission 0.99/0.99, μ = 0.109 mm^{-1}. The APEX2 software[175] has been used for datacollection and integration. From a total of 12460 reflections, 2067 were independent (merging r = 0.047). From these, 1674 were considered as observed (I>1.0σ(I)) and were used to refine 208 parameters. The structure was solved by direct methods using the program SIR92.[176] Least-squares refinement against F was carried out on all non-hydrogen atoms using the program CRYSTALS.[177] R = 0.0371 (observed data), wR = 0.0332 (all data), GOF

= 1.1648. Minimal/maximal residual electron density = -0.19/0.53 e $Å^{-3}$. Chebychev polynomial weights[178] were used to complete the refinement.

H-D-Pro-Pro-Asp-NH_2 (21)

Formula $C_{14}H_{24}N_4O_6$, M = 344.37, F(000) = 736, colorless block, size 0.18 · 0.19 · 0.24 mm^3, orthorhombic, space group P $2_12_12_1$, Z = 4, a = 7.28500(10) Å, b = 9.0911(2) Å, c = 24.9631(4) Å, α = 90°, β = 90°, γ = 90°, V = 1653.27(5) $Å^3$, $D_{calc.}$ = 1.383 Mg · m^{-3}. The crystal was measured on a Nonius KappaCCD diffractometer at 173K using graphite-monochromated Mo $K_α$-radiation with λ = 0.71073 Å, $Θ_{max}$ = 27.949°. Minimal/maximal transmission 0.98/0.98, μ = 0.109 mm^{-1}. The APEX2 software[175] has been used for datacollection and integration. From a total of 10845 reflections, 2289 were independent (merging r = 0.035). From these, 1849 were considered as observed (I>3.0σ(I)) and were used to refine 217 parameters. The structure was solved by direct methods using the program SIR92.[176] Least-squares refinement against F was carried out on all non-hydrogen atoms using the program CRYSTALS.[177] R = 0.0261 (observed data), wR = 0.0361 (all data), GOF = 1.1048. Minimal/maximal residual electron density = -0.15/0.16 e $Å^{-3}$. Chebychev polynomial weights[178] were used to complete the refinement.

H-D-Pro-Pro-Glu-NH_2 (56)

Formula $C_{15}H_{30}N_4O_{8.25}$, M = 398.43, F(000) = 428, colorless block, size 0.07 · 0.11 · 0.21 mm^3, monoclinic, space group P 2_1 , Z = 2, a = 7.7126(2) Å, b = 13.9556(3) Å, c = 9.3730(2) Å, α = 90°, β = 106.4510(10)°, γ = 90°, V = 967.55(4) $Å^3$, $D_{calc.}$ = 1.367 Mg · m^{-3}. The crystal was measured on a Nonius KappaCCD diffractometer at 173K using graphite-monochromated Mo $K_α$-radiation with λ = 0.71073 Å, $Θ_{max}$ = 34.721°. Minimal/maximal transmission 0.99/0.99, μ = 0.111 mm^{-1}. The APEX2 software[175] has been used for datacollection and integration. From a total of 21689 reflections, 4290 were independent (merging r = 0.035). From these, 3541 were considered as observed (I>3.0σ(I)) and were used to refine 262 parameters. The structure was solved by direct methods using the program SIR92.[176] Least-squares refinement against F was carried out on all non-hydrogen atoms using the program CRYSTALS.[177] R = 0.0518 (observed data), wR = 0.0413 (all data), GOF = 1.0765. Minimal/maximal residual electron density = -0.60/0.51 e $Å^{-3}$. Chebychev polynomial weights[178] were used to complete the refinement.

18.3 CD-Spectroscopy

CD spectra were recorded with a gap width of 1 nm, a time constant of 5 s and a resolution of 1 nm at 25 °C. CD data was stated in average molar ellipticity (Θ in deg cm1 $dmol^{-1}$). Thus, the obtained value in mdeg was divided by the concentration (in mol/L), by the number of amino acid moieties and by the thickness of the cuvette (in mm). Measurements were performed with a silica cuvette (Hellma) with a thickness of 2 mm. Solutions contained approximately 70 µg/mL ($6x10^{-4}$ M per amino acid moiety).

18.4 NMR Studies

All NMR experiments in chapter 9.2 were performed at 25 °C on a Bruker DRX-600 NMR spectrometer, equipped with a self-shielded *z*-axis field gradient, dual broadband and inverse probe-head. Chemical shifts were referenced to residual solvent peaks and the temperature was calibrated using a methanol sample.

18.4.1 H-D-Pro-Pro-Glu-NH_2 (56)

Samples in $CDCl_3$/CD_3OH/CD_3OD:

TOCSY and NOESY experiments were performed with 2048 time points in F2 and 1024 time increments in the indirect dimension F1, which corresponds to acquisition times of 155 ms in F2 and 77 ms in F1. Mixing times were 200 ms for the TOCSY and 1.0 s for the NOESY experiment. The total experiment times were 3.5 hours (TOCSY) and 6.5 h (NOESY).

^{1}H-NMR (600 MHz, $CDCl_3$/CD_3OD/CD_3OH, 23:1:1 v/v/v, 25°C): δ = 8.75 (d, $^3J_{H,H}$ = 7.3 Hz, 1H; Glu-H^N), 8.3 (br; D-Pro-NH_2), 6.89 (s, 1H; Glu-$CONH_2$), 6.38 (s, 1H; Glu-$CONH_2$), 4.66 (dd, $^3J_{H,H}$ = 8.3 Hz, 7.2 Hz, 1H; D-Pro-Hα), 4.39 (dd, $^3J_{H,H}$ = 7.3 Hz, 4.8 Hz, 1H; Pro-Hα), 4.31 (m, 1H; Glu-Hα), 3.81 (m, 1H; Pro-Hδ'), 3.47 (m, 1H; D-Pro-Hδ), 3.43 (m, 1H; Pro-Hδ), 3.33 (m, 1H; D-Pro-Hδ`), 2.45 (m, 2H; Glu-Hγ), 2.44 (m, 1H; D-Pro-Hβ), 2.16 (m, 2H; Pro-Hβ), 2.10 (m, 1H; D-Pro-Hγ), 2.07 (m, 1H: Glu-Hβ), 2.02 (m, 1H; D-Pro-Hγ`), 2.00 (m, 2H; Pro-Hγ), 1.89 (m, 1H; D-Pro-Hβ`), 1.88 (m, 1H; Glu-Hβ).

^{13}C-NMR (151 MHz, $CDCl_3/CD_3OD/CD_3OH$, 23:1:1 v/v/v, 25°C): δ = 177.5 (Glu-CO_2H), 173.4 (Glu-$CONH_2$), 169.9 (Pro-CO), 168.1 (D-Pro-CO), 60.8 (Pro-Cα), 58.0 (D-Pro-Cα), 52.0 (Glu-Cα), 46.5 (Pro-Cδ), 45.6 (D-Pro-Cδ), 29.1 (Glu-Cγ), 28.3 (Pro-Cβ), 27.8 (D-Pro-Cβ), 24.0 (Glu-Cβ), 23.8 (D-Pro-Cγ), 23.5 (Pro-Cγ).

Selected NOEs:

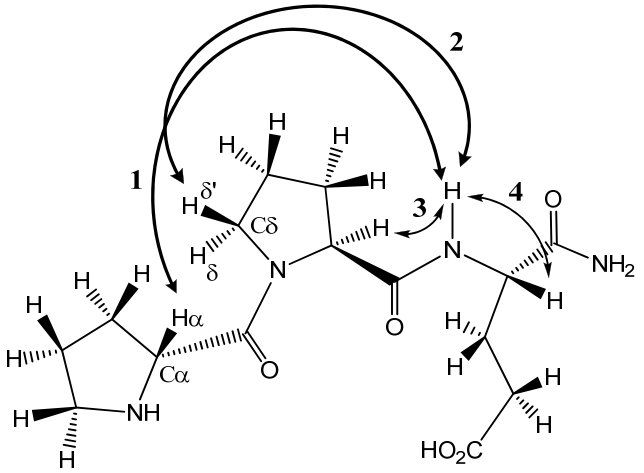

NOE:	*Normalized Intensities:*
D-Pro-Hα - Glu-H^N **(1)**	0.16 %
Pro-Hδ' - Glu-H^N **(2)**	0.49 %
Pro-Hα - Glu-H^N **(3)**	0.17 %
Glu-Hα - Glu-H^N **(4)**	0.33 %

Samples in d6-DMSO:

A ROESY experiment was performed with 2048 time points in F2 and 1024 time increments in the indirect dimension F1, which corresponds to acquisition times of 132 ms in F2 and 66 ms in F1. Mixing time was 550 ms for the ROESY experiment and the total experiment time was 18 hours.

^{1}H-NMR (600 MHz, d6-DMSO, 25°C): Major conformer (77.6%): δ = 12.19 (br, 1H; Glu-CO_2H), 9.57 (br, 1H; D-Pro-NH_2), 8.57 (br, 1H; D-Pro-NH_2), 8.13 (d, $^3J_{H,H}$ = 8.3 Hz, 1H; Glu-H^N), 7.22 (s, 1H; Glu-$CONH_2$), 7.05 (s, 1H; Glu-$CONH_2$), 4.50 (dd, $^3J_{H,H}$ = 7.3 Hz, 6.8 Hz, 1H; D-Pro-Hα), 4.38 (dd, $^3J_{H,H}$ = 8.8 Hz, 2.9 Hz, 1H; Pro-Hα), 4.16 (m, 1H; Glu-Hα), 3.67 (m, 1H; Pro-Hδ`), 3.17 (m, 1H, D-Pro-Hδ), 3.43 (m, 1H; Pro-Hδ), 3.25 (m, 1H; D-Pro-Hδ`), 2.26 (m, 1H, Glu-Hγ), 2.22 (m, 1H; Glu-Hγ), 2.40 (m, 1H; D-Pro-Hβ), 2.10 (m, 1H; Pro-Hβ), 1.93 (m, 1H; D-Pro-Hγ), 1.92 (m, 1H; Glu-Hβ), 1.86 (m, 1H; Pro-Hβ`), 1.86 (m, 1H; D-Pro-Hγ`), 1.91 (m, 2H; Pro-Hγ), 1.84 (m, 1H, D-Pro-Hβ`), 1.74 (m, 1H, Glu-Hβ).

^{13}C-NMR (151 MHz, d6-DMSO, 25°C): Major conformer (77.6%): δ = 59.7 (Pro-Cα), 58.2 (D-Pro-Cα), 51.6 (Glu-Cα), 46.6 (Pro-Cδ), 45.4 (D-Pro-Cδ), 30.1 (Glu-Cγ), 28.3 (Pro-Cβ), 27.8 (D-Pro-Cβ), 27.1 (Glu-Cβ), 23.3 (D-Pro-Cγ), 23.8 (Pro-Cγ).

^{1}H-NMR (600 MHz, d6-DMSO, 25°C): Minor conformer (22.4%): δ = 12.19 (br, 1H; Glu-CO_2H), 9.41 (br, 1H; D-Pro-NH_2), 8.57 (br, 1H; D-Pro-NH_2), 8.28 (d, $^{3}J_{H,H}$ = 8.0 Hz, 1H; Glu-H^N), 7.44 (s, 1H; Glu-$CONH_2$), 7.09 (s, 1H, Glu-$CONH_2$), 4.29 (dd, $^{3}J_{H,H}$ = 7.9 Hz, 7.8 Hz, 1H; D-Pro-Hα), 4.65 (dd, $^{3}J_{H,H}$ = 8.5 Hz, 1.3 Hz, 1H; Pro-Hα), 4.20 (m, 1H; Glu-Hα), 3.48 (m, 1H; Pro-Hδ`), 3.25 (m, 1H; D-Pro-Hδ), 3.48 (m, 1H; Pro-Hδ), 3.18 (m, 1H; D-Pro-Hδ`), 2.24 (m, 2H, Glu-Hγ), 2.06 (m, 1H; D-Pro-Hβ), 2.16 (m, 1H; Pro-Hβ), 1.88 (m, 1H, D-Pro Hγ), 1.92 (m, 1H; Glu-Hβ), 2.00 (m, 1H, Pro-Hβ`), 1.85 (m, 1H; D-Pro-Hγ`), 1.84 (m, 2H, Pro-Hγ), 1.72 (m, 1H, D-Pro-Hβ`), 1.80 (m, 1H, Glu-Hβ).

^{13}C-NMR (151 MHz, d6-DMSO, 25°C): Minor isomer (22.4%): δ = 59.0 (Pro-Cα), 57.9 (D-Pro-Cα), 51.6 (Glu-Cα), 46.9 (Pro-Cδ), 44.8 (D-Pro-Cδ), 27.1 (Glu-Cγ), 31.5 (Pro-Cβ), 28.1 (D-Pro-Cβ), 23.4 (Glu-Cβ), 21.4 (D-Pro-Cγ), 21.4 (Pro-Cγ).

Selected NOEs:

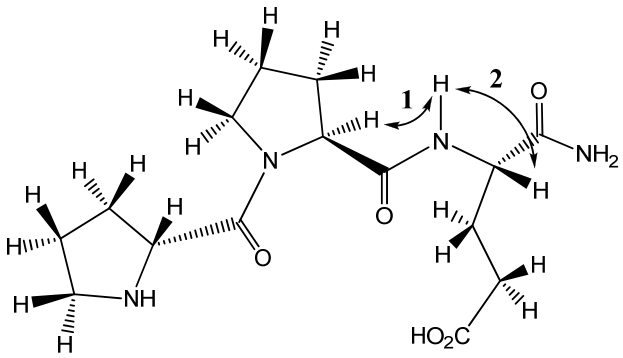

NOE:	*Normalised Intensities:*
Pro-Hα - Glu-H^N **(1)**	
major conformer	5.4 %
minor conformer	1.0 %
Glu-Hα - Glu-H^N **(2)**	5.0 %

18.4.2 Enamine Formation and Assignement

Desalted H-D-Pro-Pro-Glu-NH_2 **56** (14.4 mg, 42 µmol) was dissolved in CD_3OH (100 µL) and $CDCl_3$ (900 µL). $MgSO_4$ (~30 mg) was added to the solution. Molecular sieves (4Å, powder) was activated in the microwave (750 Watt, 3 min) and added to a NMR tube (one

spatula) which was then heated out by a Bunsen burner. After filtration, the peptide solution (~700 µL, ~30 µmol) was transferred into the NMR tube. Phenylacetaldehyde (2 µL, 18 µmol, freshly distilled and stored over $CaCl_2$) was added. The NMR tube was shaken and the first measurement occurred after approximately 30 min.

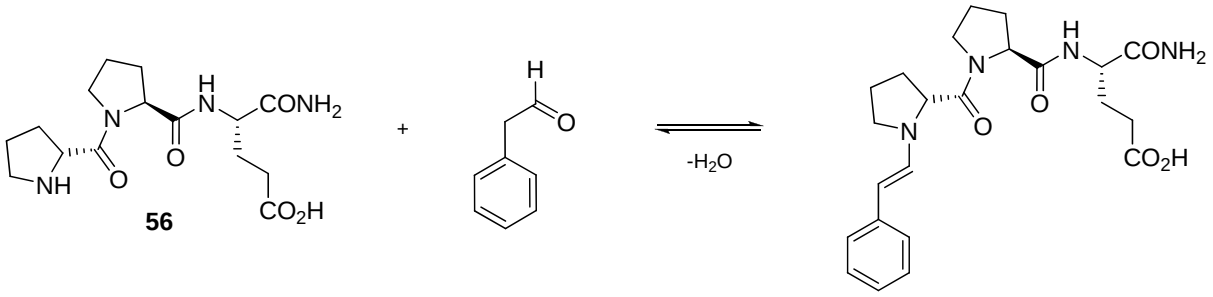

A NOESY experiment was performed with 2048 time points in F2 and 512 time increments in the indirect dimension F1, which corresponds to acquisition times of 143 ms in F2 and 71 ms in F1. Mixing time was 1.0 s, and the total experiment time was 1.5 hours. COSY, HMQC and HMBC experiments were performed in addition for assignment, using established pulse sequences.

Partial assignement of the enamine species:

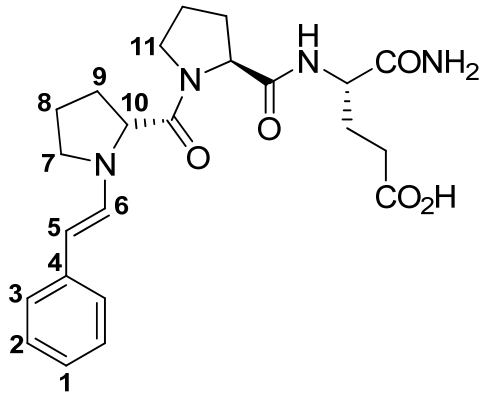

	Chemical Shifts (ppm)	
	C	**H**
1	127.6	7.25
2	127.5	7.09
3	122.6	7.06
4	138.6	-
5	98.4	5.09
6	124.1	6.92
7	47.8	3.22 and 3.40
8	31.7 (?)	2.00
9	31.0 or 28.9	2.25
10	63.2	4.34
11	-	3.88

19. Kinetic Studies on 1,4-Addition Reactions

In situ FT-IR spectroscopy was carried out on a ReactIR R4000 (SiComp probe connected to a MCT detector with K6 conduit) at normal resolution (every 8 wavenumber) with a spectral range of 4000 – 650 cm^{-1} and a normal (1x) gain adjustment. The apodization method was Happ-Genzel. All measurements were performed at RT, either collecting spectra every 2 min (256 scans) or every minute (154 scans).

Typical set up of an experiment at standard conditions:

Example calculated for the reaction between *n*-butanal (1 eq) and nitrostyrene (1 eq), catalysed by H-D-Pro-Pro-Glu-NH_2 **56** (1 mol %):

A volumetric flask (5 mL) was charged with TFA•H-D-Pro-Pro-Glu-NH_2 **56** (10 mg, 22 μmol, 4.4 mM related to the total volume of 5 mL). *n*-Butanal (200 μL, 2.2 mmol, 0.44 M), NMM (2.4 μL, 22 μmol, 4.4 mM) and $CHCl_3$/*i*-PrOH 9:1 (v/v) (approximately 1 mL) was added and the mixture was ultrasonicated until the catalyst was dissolved. Nitrostyrene was added from a stock solution (734 μL of a 3 M solution in $CHCl_3$/*i*-PrOH 9:1(v/v) = 2.2 mmol, 0.44 M) and $CHCl_3$/*i*-PrOH 9:1(v/v) was added until the total volume of 5 mL was reached. The clear solution was shortly shaken and immediately transferred into a round bottom flask (50 mL) containing the FT-IR probe and a small magnetic stirrer. The reaction mixture was gently stirred during the measurement.

Typical set up of an experiment at "dry conditions":

All glassware was previously heated out under N_2 flow. Solvents, aldehydes and stock-solutions were dried with molecular sieves (3Å). The reaction set up occurred in a similar way to the experiments under standard conditions.

V.
Appendix

20. References

[1] E. N. Jacobsen, A. Pfaltz, H. Yamamoto, *Comprehensive Asymmetric Catalysis*, Springer Verlag, Heidelberg, **1999**.
[2] D. W. C. MacMillan, *Nature* **2008**, *455*, 304.
[3] P. Melchiorre, M. Marigo, A. Carlone, G. Bartoli, *Angew. Chem. Int. Ed.* **2008**, *47*, 6138.
[4] J. Seayad, B. List, *Org. Biomol. Chem.* **2005**, *3*, 719.
[5] A. Dondoni, A. Massi, *Angew. Chem. Int. Ed.* **2008**, *47*, 4638.
[6] J. L. Vicario, D. Badia, L. Carrillo, *Synthesis* **2007**, 2065.
[7] A. Berkessel, H. Groerger, *Asymmetric Organocatalysis*, WILEY-VCH Verlag, Weinheim, **2005**.
[8] P. I. Dalko, L. Moisan, *Angew. Chem. Int. Ed.* **2004**, *43*, 5138.
[9] S. Mukherjee, J. W. Yang, S. Hoffmann, B. List, *Chem. Rev.* **2007**, *107*, 5471.
[10] G. Stork, J. Szmuszkovicz, R. Terrell, A. Brizzolara, H. Landesman, *J. Am. Chem. Soc.* **1963**, *85*, 207.
[11] Z. Rappoport, *The Chemistry of Enamines*, Wiley, New York, **1994**.
[12] Z. G. Hajos, D. R. Parrish, *J. Org. Chem.* **1974**, *39*, 1615.
[13] U. Eder, G. Sauer, R. Weichert, *Angew. Chem. Int. Ed.* **1971**, *10*, 496.
[14] B. List, R. A. Lerner, C. F. Barbas, *J. Am. Chem. Soc.* **2000**, *122*, 2395.
[15] K. A. Ahrendt, C. J. Borths, D. W. C. MacMillan, *J. Am. Chem. Soc.* **2000**, *122*, 4243.
[16] N. Mase, Y. Nakai, N. Ohara, H. Yoda, K. Takabe, F. Tanaka, C. F. Barbas, *J. Am. Chem. Soc.* **2006**, *128*, 734.
[17] W. Notz, F. Tanaka, S. Watanabe, N. S. Chowdari, J. M. Turner, R. Thayumanavan, C. F. Barbas, *J. Org. Chem.* **2003**, *68*, 9624.
[18] J. Franzen, M. Marigo, D. Fielenbach, T. C. Wabnitz, A. Kjaersgaard, K. A. Jorgensen, *J. Am. Chem. Soc.* **2005**, *127*, 18296.
[19] P. Perlmutter, *Conjugate Addition Reactions in Organic Synthesis*, Pergamon Press, Oxford, **1992**.
[20] B. List, P. Pojarliev, H. J. Martin, *Org. Lett.* **2001**, *3*, 2423.
[21] T. J. Peelen, Y. G. Chi, S. H. Gellman, *J. Am. Chem. Soc.* **2005**, *127*, 11598.
[22] S. Mosse, A. Alexakis, *Organic Letters* **2005**, *7*, 4361.
[23] J. M. Betancort, K. Sakthivel, R. Thayumanavan, F. Tanaka, C. F. Barbas, *Synthesis* **2004**, 1509.
[24] J. M. Betancort, C. F. Barbas, *Org. Lett.* **2001**, *3*, 3737.
[25] J. Wang, H. Li, B. S. Lou, L. S. Zu, H. Guo, W. Wang, *Chem. Eur. J.* **2006**, *12*, 4321.
[26] S. L. Zhu, S. Y. Yu, D. W. Ma, *Angew. Chem. Int. Ed.* **2008**, *47*, 545.
[27] N. Ruiz, E. Reyes, J. L. Vicario, D. Badia, L. Carrillo, U. Uria, *Chem. Eur. J.* **2008**, *14*, 9357.
[28] C. Palomo, S. Vera, A. Mielgo, E. Gomez-Bengoa, *Angew. Chem. Int. Ed.* **2006**, *45*, 5984.
[29] Y. Chi, L. Guo, N. A. Kopf, S. H. Gellman, *J. Am. Chem. Soc.* **2008**, *130*, 5608.
[30] S. Belot, A. Massaro, A. Tenti, A. Mordini, A. Alexakis, *Org. Lett.* **2008**, *10*, 4557.
[31] D. Enders, C. Wang, J. W. Bats, *Angew. Chem. Int. Ed.* **2008**, *47*, 7539.
[32] D. Enders, M. R. M. Huttl, G. Raabe, J. W. Bats, *Adv. Synth. Cat.* **2008**, *350*, 267.

[33] D. Enders, M. R. M. Huttl, J. Runsink, G. Raabe, B. Wendt, *Angew. Chem. Int. Ed.* **2007**, *46*, 467.
[34] Y. Hayashi, T. Okano, S. Aratake, D. Hazelard, *Angew. Chem. Int. Ed.* **2007**, *46*, 4922.
[35] D. Enders, M. R. M. Huttl, C. Grondal, G. Raabe, *Nature* **2006**, *441*, 861.
[36] P. Garcia-Garcia, A. Ladepeche, R. Halder, B. List, *Angew. Chem. Int. Ed.* **2008**, *47*, 4719.
[37] Y. Hayashi, T. Itoh, M. Ohkubo, H. Ishikawa, *Angew. Chem. Int. Ed.* **2008**, *47*, 4722.
[38] Q. Tao, G. Tang, K. Lin, Y. F. Zhao, *Chirality* **2008**, *20*, 833.
[39] T. Mandal, C. G. Zhao, *Angew. Chem. Int. Ed.* **2008**, *47*, 7714.
[40] X. J. Zhang, S. P. Liu, X. M. Li, M. Yan, A. S. C. Chan, *Chem. Comm.* **2009**, 833.
[41] S. H. McCooey, S. J. Connon, *Org. Lett.* **2007**, *9*, 599.
[42] S. Sulzer-Mosse, M. Tissot, A. Alexakis, *Org. Lett.* **2007**, *9*, 3749.
[43] M. T. Barros, A. M. F. Phillips, *Eur. J. Org. Chem.* **2007**, 178.
[44] H. B. Huang, E. N. Jacobsen, *J. Am. Chem. Soc.* **2006**, *128*, 7170.
[45] M. P. Lalonde, Y. G. Chen, E. N. Jacobsen, *Angew. Chem. Int. Ed.* **2006**, *45*, 6366.
[46] Y. W. Li, X. Y. Liu, G. Zhao, *Tetrahedron Asymm.* **2006**, *17*, 2034.
[47] C. L. Cao, M. C. Ye, X. L. Sun, Y. Tang, *Org. Lett.* **2006**, *8*, 2901.
[48] E. Reyes, J. L. Vicario, D. Badia, L. Carrillo, *Org. Lett.* **2006**, *8*, 6135.
[49] S. Mosse, M. Laars, K. Kriis, T. Kanger, A. Alexakis, *Org. Lett.* **2006**, *8*, 2559.
[50] N. Mase, K. Watanabe, H. Yoda, K. Takabe, F. Tanaka, C. F. Barbas, *J. Am. Chem. Soc.* **2006**, *128*, 4966.
[51] L. S. Zu, H. Li, J. Wang, X. H. Yu, W. Wang, *Tetrahedron Lett.* **2006**, *47*, 5131.
[52] S. Z. Luo, X. L. Mi, L. Zhang, S. Liu, H. Xu, J. P. Cheng, *Angew. Chem. Int. Ed.* **2006**, *45*, 3093.
[53] Y. Hayashi, H. Gotoh, T. Hayashi, M. Shoji, *Angew. Chem. Int. Ed.* **2005**, *44*, 4212.
[54] W. Wang, J. Wang, H. Li, *Angew. Chem. Int. Ed.* **2005**, *44*, 1369.
[55] T. Ishii, S. Fujioka, Y. Sekiguchi, H. Kotsuki, *J. Am. Chem. Soc.* **2004**, *126*, 9558.
[56] N. Mase, F. Tanaka, C. F. Barbas, *Angew. Chem. Int. Ed.* **2004**, *43*, 2420.
[57] D. Enders, A. Seki, *Synlett* **2002**, 26.
[58] K. Sakthivel, W. Notz, T. Bui, C. F. Barbas, *J. Am. Chem. Soc.* **2001**, *123*, 5260.
[59] O. Andrey, A. Vidonne, A. Alexakis, *Tetrahedron Lett.* **2003**, *44*, 7901.
[60] L. Planas, J. Perard-Viret, J. Royer, *Tetrahedron Asymm.* **2004**, *15*, 2399.
[61] N. Mase, R. Thayumanavan, F. Tanaka, C. F. Barbas, *Org. Lett.* **2004**, *6*, 2527.
[62] C. E. T. Mitchell, A. J. A. Cobb, S. V. Ley, *Synlett* **2005**, 611.
[63] L. S. Zu, J. Wang, H. Li, W. Wang, *Org. Lett.* **2006**, *8*, 3077.
[64] Z. X. Shen, Y. Q. Mang, C. J. Jiao, B. Li, J. Ding, Y. W. Zhang, *Chirality* **2007**, *19*, 307.
[65] B. K. Ni, Q. Y. Zhang, A. D. Headley, *Green Chem.* **2007**, *9*, 737.
[66] S. Sulzer-Mosse, M. Laars, K. Kriis, T. Kanger, A. Alexakis, *Synthesis* **2007**, 1729.
[67] Q. Y. Zhang, B. K. Ni, A. D. Headley, *Tetrahedron* **2008**, *64*, 5091.
[68] Z. Yacob, J. Shah, J. Leistner, J. Liebscher, *Synlett* **2008**, 2342.
[69] D. Q. Xu, H. D. Yue, S. P. Luo, A. B. Xia, S. Zhang, Z. Y. Xu, *Org. Biomol. Chem.* **2008**, *6*, 2054.
[70] D. Q. Xu, L. P. Wang, S. P. Luo, Y. F. Wang, S. Zhang, Z. Y. Xu, *Eur. J. Org. Chem.* **2008**, 1049.
[71] B. K. Ni, Q. Y. Zhang, A. D. Headley, *Tetrahedron Lett.* **2008**, *49*, 1249.
[72] A. Alexakis, O. Andrey, *Org. Lett.* **2002**, *4*, 3611.
[73] J. I. Oku, S. Inoue, *Chem. Commun.* **1981**, 229.
[74] S. Julia, J. Masana, J. C. Vega, *Angew. Chem. Int. Ed.* **1980**, *19*, 929.
[75] D. R. Kelly, S. M. Roberts, *Biopolymers* **2006**, *84*, 74.

[76] J. D. Revell, H. Wennemers, *Curr. Opin. Chem. Biol.* **2007**, *11*, 269.
[77] A. Berkessel, *Curr. Opin. Chem. Biol.* **2003**, *7*, 409.
[78] E. R. Jarvo, S. J. Miller, *Tetrahedron* **2002**, *58*, 2481.
[79] C. A. Lewis, S. J. Miller, *Angew. Chem. Int. Ed.* **2006**, *45*, 5616.
[80] C. A. Lewis, J. Merkel, S. J. Miller, *Bioorg. Med. Chem. Lett.* **2008**, *18*, 6007.
[81] C. A. Lewis, A. Chiu, M. Kubryk, J. Balsells, D. Pollard, C. K. Esser, J. Murry, R. A. Reamer, K. B. Hansen, S. J. Miller, *J. Am. Chem. Soc.* **2006**, *128*, 16454.
[82] S. M. Mennen, J. D. Gipson, Y. R. Kim, S. J. Miller, *J. Am. Chem. Soc.* **2005**, *127*, 1654.
[83] Y. Zhao, J. Rodrigo, A. H. Hoveyda, M. L. Snapper, *Nature* **2006**, *443*, 67.
[84] B. R. Sculimbrene, A. J. Morgan, S. J. Miller, *J. Am. Chem. Soc.* **2002**, *124*, 11653.
[85] P. Vachal, E. N. Jacobsen, *J. Am. Chem. Soc.* **2002**, *124*, 10012.
[86] M. S. Taylor, E. N. Jacobsen, *J. Am. Chem. Soc.* **2004**, *126*, 10558.
[87] E. Delort, T. Darbre, J. L. Reymond, *J. Am. Chem. Soc.* **2004**, *126*, 15642.
[88] S. B. Tsogoeva, S. B. Jagtap, Z. A. Ardemasova, V. N. Kalikhevich, *Eur. J. Org. Chem.* **2004**, 4014.
[89] S. B. Tsogoeva, S. B. Jagtap, *Synlett* **2004**, 2624.
[90] Z. Tang, Z. H. Yang, L. F. Cun, L. Z. Gong, A. Q. Mi, Y. Z. Jiang, *Org. Lett.* **2004**, *6*, 2285.
[91] J. Kofoed, J. Nielsen, J. L. Reymond, *Bioorg. Med. Chem. Lett.* **2003**, *13*, 2445.
[92] H. J. Martin, B. List, *Synlett* **2003**, 1901.
[93] P. Krattiger, R. Kovasy, J. D. Revell, S. Ivan, H. Wennemers, *Org. Lett.* **2005**, *7*, 1101.
[94] J. C. Yan, L. Wang, *Chirality* **2009**, *21*, 413.
[95] L. X. Shi, Q. Sun, Z. M. Ge, Y. Q. Zhu, T. M. Cheng, R. T. Li, *Synlett* **2004**, 2215.
[96] M. Lei, L. X. Shi, G. Li, S. Chen, W. H. Fang, Z. M. Ge, T. M. Cheng, R. T. Li, *Tetrahedron* **2007**, *63*, 7892.
[97] J. F. Zheng, Y. X. Li, S. Q. Zhang, S. T. Yang, X. M. Wang, Y. Z. Wang, J. Bai, F. A. Liu, *Tetrahedron Lett.* **2006**, *47*, 7793.
[98] G. Luppi, P. G. Cozzi, M. Monari, B. Kaptein, Q. B. Broxterman, C. Tomasini, *J. Org. Chem.* **2005**, *70*, 7418.
[99] W. B. Zou, I. Ibrahem, P. Dziedzic, H. Sunden, A. Cordova, *Chem. Commun.* **2005**, 4946.
[100] S. B. Tsogoeva, S. W. Wei, *Tetrahedron Asymm.* **2005**, *16*, 1947.
[101] A. Cordova, W. B. Zou, P. Dziedzic, I. Ibrahem, E. Reyes, Y. M. Xu, *Chem. Eur. J.* **2006**, *12*, 5383.
[102] J. D. Revell, H. Wennerners, *Creative Chemical Sensor Systems* **2007**, *277*, 251.
[103] M. H. Fonseca, B. List, *Curr. Opin. Chem. Biol.* **2004**, *8*, 319.
[104] W. C. Still, *Acc. Chem. Res.* **1996**, *29*, 155.
[105] H. Wennemers, *Combinatorial Chemistry & High Throughput Screening* **2001**, *4*, 273.
[106] A. Furka, F. Sebestyen, M. Asgedom, G. Dibo, *Int. J. Pept. Prot. Res.* **1991**, *37*, 487.
[107] K. S. Lam, S. E. Salmon, E. M. Hersh, V. J. Hruby, W. M. Kazmierski, R. J. Knapp, *Nature* **1991**, *354*, 82.
[108] C. Schmuck, H. Wennerners, *Highlights in Bioorganic Chemistry*, WILEY-VCH, Weinheim, **2004**.
[109] P. Krattiger, C. McCarthy, A. Pfaltz, H. Wennemers, *Angew. Chem. Int. Ed.* **2003**, *42*, 1722.
[110] J. D. Revell, H. Wennemers, *Tetrahedron* **2007**, *63*, 8420.
[111] F. R. Clemente, K. N. Houk, *Angew. Chem. Int. Ed.* **2004**, *43*, 5766.
[112] B. List, L. Hoang, H. J. Martin, *PNAS* **2004**, *101*, 5839.
[113] S. Bahmanyar, K. N. Houk, H. J. Martin, B. List, *J. Am. Chem. Soc.* **2003**, *125*, 2475.

[114] L. Hoang, S. Bahmanyar, K. N. Houk, B. List, *J. Am. Chem. Soc.* **2003**, *125*, 16.
[115] O. M. Berner, L. Tedeschi, D. Enders, *Eur. J. Org. Chem.* **2002**, 1877.
[116] S. B. Tsogoeva, *Eur. J. Org. Chem.* **2007**, 1701.
[117] S. Sulzer-Mosse, A. Alexakis, *Chem. Commun.* **2007**, 3123.
[118] D. Almasi, D. A. Alonso, C. Najera, *Tetrahedron Asymm.* **2007**, *18*, 299.
[119] M. Wiesner, Masterthesis, University of Basel **2005**.
[120] F. Mohamadi, N. G. J. Richards, W. C. Guida, R. Liskamp, M. Lipton, C. Caufield, G. Chang, T. Hendrickson, W. C. Still, *J. Comp. Chem.* **1990**, *11*, 440.
[121] W. L. Jorgensen, D. S. Maxwell, J. TiradoRives, *J. Am. Chem. Soc.* **1996**, *118*, 11225.
[122] D. Qiu, P. S. Shenkin, F. P. Hollinger, W. C. Still, *J. Phys. Chem. A* **1997**, *101*, 3005.
[123] D. Seebach, J. Golinski, *Helv. Chim. Ac.* **1981**, *64*, 1413.
[124] M. Favre, K. Moehle, L. Y. Jiang, B. Pfeiffer, J. A. Robinson, *J. Am. Chem. Soc.* **1999**, *121*, 2679.
[125] S. Hanessian, M. Angiolini, *Chem. Eur. J.* **2002**, *8*, 111.
[126] R. Rai, S. Aravinda, K. Kanagarajadurai, S. Raghothama, N. Shamala, P. Balaram, *J. Am. Chem. Soc.* **2006**, *128*, 7916.
[127] A. Aubry, B. Vitoux, M. Marraud, *Biopolymers* **1985**, *24*, 1089.
[128] R. Paulini, K. Muller, F. Diederich, *Angew. Chem. Int. Ed.* **2005**, *44*, 1788.
[129] A. F. Trindade, P. M. P. Gois, C. A. M. Afonso, *Chem. Rev.* **2009**, *109*, 418.
[130] J. D. Revell, D. Gantenbein, P. Krattiger, H. Wennemers, *Biopolymers* **2006**, *84*, 105.
[131] D. Polet, A. Alexakis, *Tetrahedron Lett.* **2005**, *46*, 1529.
[132] H. Choi, Z. H. Hua, I. Ojima, *Org. Lett.* **2004**, *6*, 2689.
[133] D. M. Mampreian, A. H. Hoveyda, *Org. Lett.* **2004**, *6*, 2829.
[134] A. Rimkus, N. Sewald, *Synthesis* **2004**, 135.
[135] A. Duursma, A. J. Minnaard, B. L. Feringa, *Tetrahedron* **2002**, *58*, 5773.
[136] O. Andrey, A. Alexakis, A. Tomassini, G. Bernardinelli, *Adv. Synth. Cat.* **2004**, *346*, 1147.
[137] A. Pintar, J. Batista, J. Levec, *Analyst* **2002**, *127*, 1535.
[138] D. G. Blackmond, *Angew. Chem. Int. Ed.* **2005**, *44*, 4302.
[139] C. Girard, H. B. Kagan, *Angew. Chem. Int. Ed.* **1998**, *37*, 2923.
[140] C. Puchot, O. Samuel, E. Dunach, S. Zhao, C. Agami, H. B. Kagan, *J. Am. Chem. Soc.* **1986**, *108*, 2353.
[141] J. P. Birk, *J. .Chem. Educ.* **1976**, *53*, 704.
[142] R. Cabot, A. Lledo, M. Reves, A. Riera, X. Verdaguer, *Organometallics* **2007**, *26*, 1134.
[143] C. M. Goodman, S. Choi, S. Shandler, W. F. DeGrado, *Nat. Chem. Biol.* **2007**, *3*, 252.
[144] D. Seebach, D. F. Hook, A. Glattli, *Biopolymers* **2006**, *84*, 23.
[145] S. H. Gellman, *Acc. Chem. Res.* **1998**, *31*, 173.
[146] D. Seebach, M. Brenner, M. Rueping, B. Jaun, *Chem. Eur. J.* **2002**, *8*, 573.
[147] M. G. Woll, J. R. Lai, I. A. Guzei, S. J. C. Taylor, M. E. B. Smith, S. H. Gellman, *J. Am. Chem. Soc.* **2001**, *123*, 11077.
[148] S. Hanessian, X. H. Luo, R. Schaum, S. Michnick, *J. Am. Chem. Soc.* **1998**, *120*, 8569.
[149] T. Ok, A. Jeon, J. Lee, J. H. Lim, C. S. Hong, H. S. Lee, *J. Org. Chem.* **2007**, *72*, 7390.
[150] D. Seebach, L. Schaeffer, M. Brenner, D. Hoyer, *Angew. Chem. Int. Ed.* **2003**, *42*, 776.
[151] M. Ordonez, C. Cativiela, *Tetrahedron Asymm.* **2007**, *18*, 3.
[152] P. Camps, D. Munoz-Torrero, L. Sanchez, *Tetrahedron Asymm.* **2004**, *15*, 2039.
[153] D. A. Evans, J. R. Gage, J. L. Leighton, A. S. Kim, *J. Org. Chem.* **1992**, *57*, 1961.
[154] R. A. Kunetsky, A. D. Dilman, M. I. Struchkova, V. A. Tartakovsky, S. L. Ioffe, *Tetrahedron Lett.* **2005**, *46*, 5203.

[155] S. Ranganathan, D. Ranganathan, S. K. Singh, *Tetrahedron Lett.* **1987**, *28*, 2893.
[156] G. D. Buckley, C. W. Scaife, *J. Chem. Soc.* **1947**, 1471.
[157] T. Possner, *Berichte der Deutschen Chemischen Gesellschaft* **1898**, *31*, 656
[158] Y. Chi, T. J. Peelen, S. H. Gellman, *Org. Lett.* **2005**, *7*, 3469.
[159] M. Sefkow, *Natural Products Synthesis I: Targets Methods Concepts* **2004**, *243*, 185.
[160] G. Hughes, M. Kimura, S. L. Buchwald, *J. Am. Chem. Soc.* **2003**, *125*, 11253.
[161] R. B. Merrifield, *J. Am. Chem. Soc.* **1963**, *85*, 2149.
[162] Novabiochem Catalog **2004**.
[163] T. Vojkovsky, *Pept. Res.* **1995**, *8*, 236.
[164] W. S. Hancock, J. E. Battersby, D. R. K. Harding, *Analyt. Biochem.* **1975**, *69*, 497.
[165] E. Kaiser, R. L. Colescot, C. D. Bossinge, P. I. Cook, *Analyt. Biochem.* **1970**, *34*, 595.
[166] M. J. Crossley, M. L. Fisher, J. J. Potter, P. W. Kuchel, M. J. York, *J. Chem. Soc.-Perkin Transactions 1* **1990**, 2363.
[167] L. Aurelio, J. S. Box, R. T. C. Brownlee, A. B. Hughes, M. M. Sleebs, *J. Org. Chem.* **2003**, *68*, 2652.
[168] D. Lucet, S. Sabelle, O. Kostelitz, T. Le Gall, C. Mioskowski, *Eur. J. Org. Chem.* **1999**, 2583.
[169] S. E. Denmark, L. R. Marcin, *J. Org. Chem.* **1993**, *58*, 3850.
[170] P. Kotrusz, S. Toma, H. G. Schmalz, A. Adler, *Eur. J. Org. Chem.* **2004**, 1577.
[171] Y. Caro, C. F. Masaguer, E. Ravina, *Tetrahedron Asymm.* **2001**, *12*, 1723.
[172] R. G. Curtis, I. Heilbron, E. R. H. Jones, G. F. Woods, *J. Chem. Soc.* **1953**, 457.
[173] A. Bowers, T. G. Halsall, E. R. H. Jones, A. J. Lemin, *J. Chem. Soc.* **1953**, 2548.
[174] C. Djerassi, R. R. Engle, A. Bowers, *J. Chem. Soc.* **1956**, *21*, 1547.
[175] Bruker AXS Inc., Madison **2006**.
[176] A. Altomare, G. Cascarano, C. Giacovazzo, A. Guagliardi, *J. Appl. Cryst.* **1994**, *27*, 1045.
[177] P. W. C. Betteridge, J. R..; Cooper, R. I.; Prout, K.; Watkin, D. J., *J. Appl. Cryst.* **2003**, *36*, 1487.
[178] J. R. Carruthers, D. J. Watkin, *Acta Cryst.* **1979**, *35*, 698.

21. Abbreviations

δ	chemical shift
$[\alpha]_D$	specific optical rotation
Aad	L-aminoadipic acid
Abu	aminobutyric acid
Ac	acetyl
Ala	L-alanin
Api	L-aminopimelic acid
aq	aqueous
Asn	L-asparagine
Asp	L-aspartic acid
Asu	L-aminosuberic acid
Ava	aminovaleric acid
Bn	benzyl
Boc	*tert*-butyl-oxycarbonyl
bp	boiling point
Bu	*n*-butyl
c / conc.	concentration / concentrated
calcd	calculated
Cbz / Z	carboxybenzyl
CD	circular dichroism
c-Hex	cyclohexyl
COSY	correlation spectroscopy
Cy	cyclohexyl
Cys	L-cysteine
d	days
DEPT	distortionless enhancement by polarization
DIC	diisopropylcarbodiimide
DMAP	4-(dimethylamino)-pyrindine
DMF	dimethylformamide
DMSO	dimethyl sulfoxide
dr	diastereomeric ratio
EDC	*N*-(3-dimethylaminopropyl)-*N*'-ethylcarbodiimide-hydrochloride
ee	enantiomeric excess
eq / equiv.	equivalents
ESI	electrospray ionisation
Et	ethyl
FAB	fast atom bomabardment
FID	flame ionisation detector
Fmoc	9-fluoromethoxycarbonyl
FT	Fourier transformation
GC	gas chromatography
Gln	L-glutamine
Glu	L-glutamic acid
Gly	glycine
h	hours
HCTU	O-(1H-6-chlorobenzotriazole-1-yl)-1,1,3,3-tetramethyluronium

	hexafluorophoshat
His	L-histidine
HMBC	heteronuclear multiple bond coherence
HMQC	heteronuclear multiple quantum coherence
HOBt	1-hydrobenzotriazole
HOMO	highest occupied molecular orbital
HPLC	high performance liquid chromatography
HRMS	high resolution mass spectroscopy
i-Pr	*iso*-propyl
IR	infrared (spectroscopy)
J	NMR coupling constant
Leu	L-leucine
M	molar
Me	methyl
min	minutes
MS	mass spectroscopy
MSNT	1-(2-mesitylenesulfonyl)-3-nitro-1H-1,2,4-triazole
NMM	*N*-methylmorpholine
NMP	*N*-methylpyrrolidone
NMR	nuclear magnetic resonance
NOE	nuclear Overhauser effect
NOESY	nuclear Overhauser effect spectroscopy
Ph	phenyl
Phe	L-phenylalanine
Pr	*n*-propyl
Pro	L-proline
R^2	square of the sample correlation coefficient
R_f	retention factor
ROESY	rotating frame Overhause effect spectroscopy
RT	room temperature
s	seconds
Ser	L-serine
t	time
TBSCl	*tert*-butyldimethylsilyl chloride
t-Bu / tBu	*tert*-butyl
TFA	trifluoroacetic acid
THF	tetrahydrofuran
THP	tetrahydropyran
TLC	thin layer chromatography
TMS	tetramethylsilane
TMSCl	trimethylsilyl chloride
TNBS	2,4,6-trinitrobenzenesulfonic acid
TOCSY	total correlated spectroscopy
t_R	retention time
Trt / trt	trityl
Ts / tosyl	*para*-toluene sulphonyl
TSP	2,2,3,3-d4-3-(trimethylsilyl)propionic acid sodium salt
Xaa	random amino acid

22. Kinetic Studies (Chapter 10): Detailed Information and Additional Experiments

According to Chapter 10.1.2 Investigation of Catalyst Instabilities (Page 68)

The experiment described in chapter 10.1.2 was repeated with different concentrations: [nitrostyrene] = 0.2 M / 0.17 M, 0.25 M excess of *n*-butanal. Both reactions overlay, underlining the absence of catalyst instabilities.

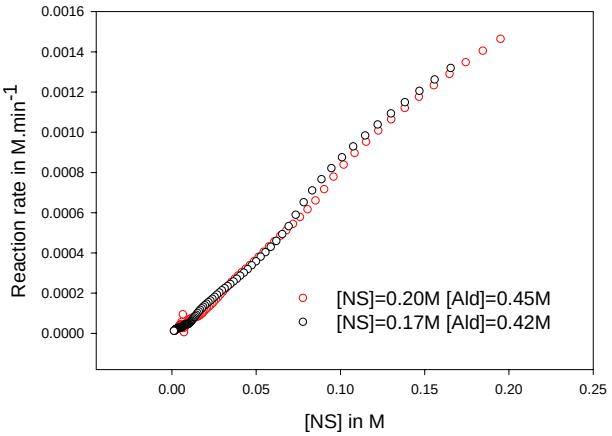

According to Chapter 10.2: Reaction Progress Kinetic Analysis (Page 71)[138]

Theoretical Considerations

For the studies of reaction progress kinetic analysis we assumed the mechanism and the corresponding rate equation shown in figure **A**.

a)

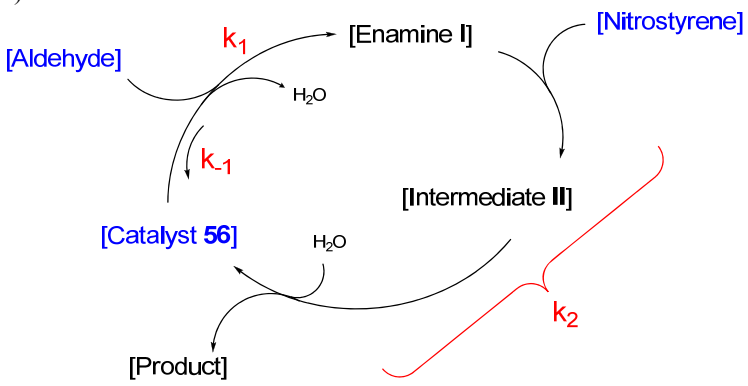

b)

$$v = \frac{k_1 k_2 [Ald][NS][cat]}{k_{-1} + k_1[Ald] + k_2[NS]}$$

$$v = \frac{a[Ald][NS][cat]}{1 + b[Ald] + c[NS]}$$

$$a = \frac{k_1}{k_{-1}} k_2 \quad b = \frac{k_1}{k_{-1}} \quad c = \frac{k_2}{k_{-1}}$$

b dominating: $v = k_2[NS][cat]$

c dominating: $v = k_1[Ald][cat]$

Figure A. a) *Proposed reaction mechanism. b) Corresponding rate equation. Note: If b is high, saturation kinetics in* ***I*** *is reached (Enamine* ***I*** *= resting state). If c is high,* ***I*** *does not built up, thus, formation of* ***I*** *is rate limiting (unbound catalyst* ***56*** *= resting state).*

Since the standard reaction proceeds without formation of any side product and since both [*n*-butanal] and [nitrostyrene] change with time, each time one molecule of *n*-butanal is converted into product, one molecule of nitrostyrene is converted as well. The introduction of a parameter [excess], which determines the differences in the initial concentrations of the two substrates leads to the following general relationship where [NS] = [nitrostyrene] and [Ald] = [aldehyde]:

$[NS] = [NS]_0 - [Ald]_0 + [Ald] \Rightarrow [NS] = [excess] + [Ald]$, while [excess] does not change as the reaction progresses.

Substituton of [excess] into the rate equation leads to:

$$v = a' \frac{[excess][Ald] + [Ald]^2}{1 + b'[Ald]} [cat], \qquad a' = \frac{k_1 k_2}{k_{-1} + k_2[excess]}, \; b' = \frac{k_1 + k_2}{k_{-1} + k_2[excess]}$$

[cat], [excess], k_1, k_{-1} and k_2 are constant, therefore [Ald] is the only variable. With the data pairs of ([NS], time), ([Ald], time) and (rate, time) it is possible to construct graphical rate equations for reactions with two substrates.

Construction of Graphical Rate Equations:

Experimental Set Up

Primary data for the experiment described above was obtained by the measurement of the absorbance (= [product **56**]) vs. time of three different reactions (Figure **B**), carried out at the same [excess] (red and blue curve) and at different [excess] (green curve) of *n*-butanal. Initial concentrations for the reactions at the same [excess] were [nitrostyrene] = 0.4 M and 0.35 M with [*n*-butanal] = 0.9 M and 0.85 M. The reaction at the different [excess] was performed with [nitrostyrene] = 0.4 M and [*n*-butanal] = 1.2 M. The catalyst loading was kept constant at [cat **56**] = 13 mM for each reaction.

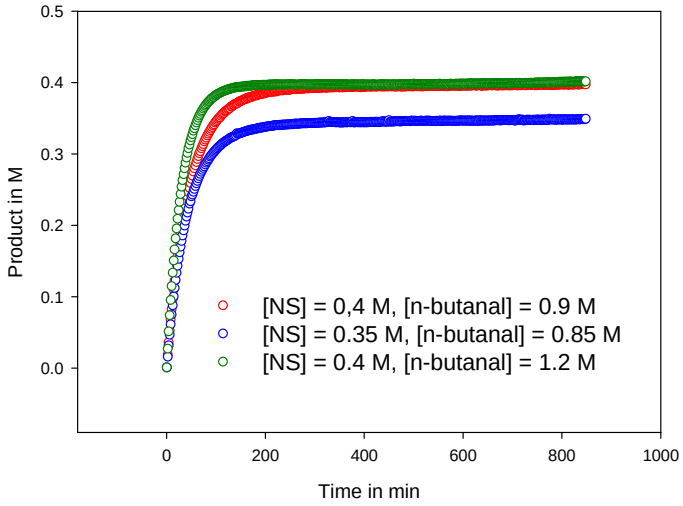

Figure B. *[Product **3**] vs. time of three experiments carried out at the same [excess] (red and blue curve) and at different [excess] (green curve) of n-butanal. [cat **56**] = 0.013 M.*

Plot of Graphical Rate Equations

Derived from the rate equations earlier discussed, different plots of the primary data would generate following information about integer reaction orders if curves overlay:

Reaction rate vs. [*n*-butanal]: Overlay = zero order in nitrostyrene.
Reaction rate/[*n*-butanal] vs. [nitrostyrene]: Overlay = first order in *n*-butanal.
Reaction rate/[nitrostyrene] vs. [*n*-butanal]: Overlay = first order in nitrostyrene.

The corresponding plots, calculated from the obtained primary data of the previous three reactions revealed that an overlay of all three curves was not observed (Figure C).

a)

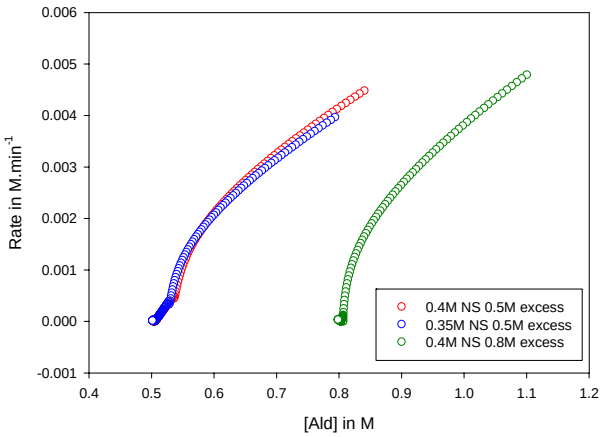

b)

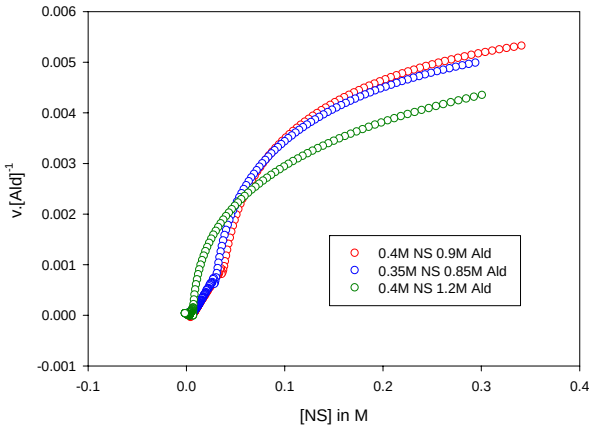

c)

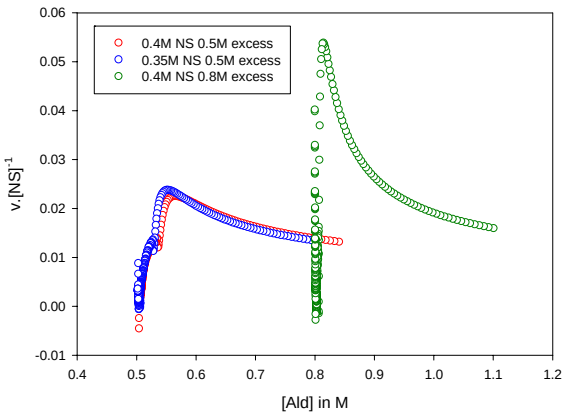

Figure C. *a) Plot of reaction rate vs. [n-butanal]. b) Plot of reaction rate/[n-butanal] vs. [nitrostyrene]. c) Plot of reaction rate/[nitrostyrene] vs. [n-butanal]. Since no overlay of all three curves was obtained, the reaction under the chosen conditions is neither zero order in nitrostyrene, nor first order in n-butanal or nitrostyrene.*

The missing overlay of the curves in figure C led us to the suggestion that no integer reaction orders are existent in this reaction of the peptide **56** catalysed conjugate addition reaction of *n*-butanal and nitrostyrene under the chosen conditions. This indicates that the reaction does not have only one rate limiting step, therefore the catalyst has no definitive "resting state".

However, the overlay of the curves with the same [excess] in each plot underlined the previously found result, that catalyst deactivation or product inhibition does not exist for this reaction.

According to Chapter 10.3.1
Reaction Order with Respect to the Catalyst (Page 72)

The reaction order with respect to catalyst **56** was studied with 6 different catalyst loadings [cat **56**] = 0.25 mol% = 1.1 mM, 0.5 mol% = 2.2 mM, 0.75 mol% = 3.3 mM, 1.0 mol% = 4.4 mM, 1.25 mol% = 5.5 mM and 1.5 mol% = 6.6 mM. Other concentrations were kept constant at [nitrostyrene] = 0.44 M and [*n*-butanal] = 0.44 M.

According to Chapter 10.3.2
Reaction Order with Respect to the Aldehyde (Page 73)

At 1 mol% Catalyst (56):
11 different reactions were performed, varying the aldehyde concentration [*n*-butanal] = 0.22 M, 0.33 M, 0.44 M, 0.55 M, 0.66 M, 0.77 M, 0.88 M, 0.99 M, 1.10 M, 1.21 M and 1.43 M at constant [cat **56**] = 4.4 mM and [nitrostyrene] = 0.44 M

At 2 mol% Catalyst (56):
The reactions were carried out with [cat **56**] = 8.8 mM, [nitrostyrene] = 0.44 M and 12 different concentrations of *n*-butanal **1**: [*n*-butanal] = 0.22 M, 0.33 M, 0.44 M, 0.55 M, 0.66 M, 0.77 M, 0.88 M, 1.10 M, 1.32 M, 1.43 M, 1.54 M and 1.65 M.

According to Chapter 10.3.3
Reaction Order with Respect to the Nitrostyrene (Page 75)

At Standard Conditions: 0.44 M *n*-Butanal, 4.4 mM Catalyst (56)
The nitrostyrene concentration was varied in 7 different experiments: [nitrostyrene] = 0.22 M, 0.44 M, 0.66 M, 0.88 M, 1.10 M, 1.27 M, 2.12 M at constant catalyst [cat **56**] = 4.4 mM and aldehyde concentration [*n*-butanal] = 0.44 M.

Increased Aldehyde Concentration: 0.88 M *n*-Butanal, 4.4 mM Catalyst (56)
The experiments were then repeated at a higher aldehyde concentration of [*n*-butanal] = 0.88 M and [nitrostyrene] = 0.22 M, 0.44 M, 0.66 M, 0.88 M and 1.10 M.

According to Chapter 10.3.5
Less Reactive Aldehyde: Addition of Isovaleraldehyde to Nitrostyrene (Page 78)

Different Isovaleraldehyde Concentrations
The influence of the aldehyde on the reaction rate was determined by performing 9 reactions at different [isovaleraldehyde] = 0.22 M, 0.44 M, 0.77 M, 0.88 M, 0.99 M, 1.10 M, 1.32 M, 1.54 M and 1.76 M at constant [cat **56**] = 8.8 mM (2 mol%) and [nitrostyrene] = 0.44 M.

Different Nitrostyrene Concentrations (Additional Experiment)

The reaction order with respect to nitrostyrene was determined with 5 experiments at constant [cat **56**] = 8.8 mM and at a very high aldehyde concentration of [isovaleraldehyde] = 1.54 M. According to the experiments described in chapter 10.3.5, this concentration is in the range of the observed 0 order plateau. The nitrostyrene concentration was varied with [nitrostyrene] = 0.22 M, 0.44 M, 0.66 M, 0.88 M and 1.10 M. The corresponding log-log plot showed a linear correlation (R^2 = 0.99) with a slope of 0.42 (Figure A). This value is a little lower compared to the standard reaction between *n*-butanal and nitrostyrene (slope = 0.53 at [cat **56**] = 8.8 mM). This result could indicate that the hydrolysis step in this case is slower in relation to the C-C bond formation step in the reaction. Therefore the bond formation is "less rate determining" and the order with respect of isovaleraldehyde is lower.

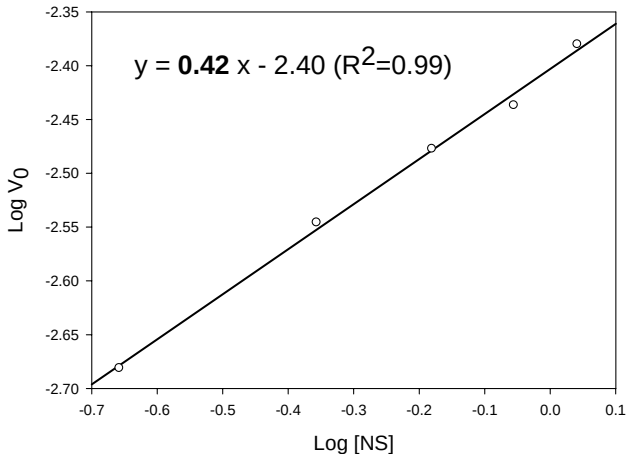

Figure A. *Plot of log (initial rate) vs. log [nitrostyrene] providing a slope of 0.42. Experiments were carried out with a constant [isovaleraldehyde] of 1.54 M.*

According to Chapter 10.3.6
Less Reactive Nitrostyrenes: Addition of *n*-Butanal to 4-Methoxy-nitrostyrene and 2,4-Dimethoxynitrostyrene (Page 80)

Different 4-Methoxynitrostyrene Concentrations

The reaction order with respect to 4-methoxynitrostyrene was determined with 5 experiments at constant [cat **56**] = 8.8 mM and at [*n*-butanal] = 0.44 M. The 4-methoxynitrostyrene concentration was varied with [4-MeO-NS] = 0.1 M, 0.3 M, 0.44 M, 0.66 M and 0.8 M.

4-Methoxynitrostyrene: Different *n*-Butanal Concentrations (Additional Experiment)

The influence of the *n*-butanal concentration in this reaction was investigated by performing 7 reactions at different [*n*-butanal] = 0.22 M, 0.33 M, 0.44 M, 0.67 M, 0.88 M, 1.10 M and 1.32 M at constant [cat **56**] = 8.8 mM (2 mol%) and 4-methoxynitrostyrene concentration = [4-MeO-NS] = 0.44 M (Figure A). A slope of 0.37 (R^2 = 0.95) was obtained and at a concentration of approximately [*n*-butanal] = 0.8 M the slope became flat (Figure A).

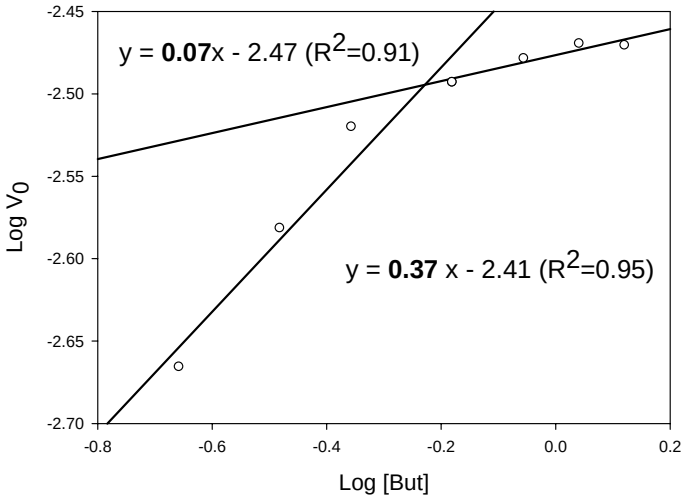

Figure A. *Plot of log (initial rate) vs. log [n-butanal] providing a slope of 0.37 for [n-butanal] 0.22 to 0.66 M and 0.07 for [n-butanal] 0.88 to 1.32 M.*

Reaction of *n*-Butanal to 2,4-Dimethoxynitrostyrene

After performing the reactions with different 2,4-dimethoxynitrostyrene concentrations at [*n*-butanal] = 0.44 M and [cat **56**] = 8.8 mM (2 mol%), we found that the reaction was very slow. Therefore the absorbance was low and the error for the corresponding derivatives was high. In order to obtain more accurate data we carried out the reactions of different 2,4-dimethoxy-nitrostyrene concentrations = [2,4-$(MeO)_2$-NS] = 0.17 M, 0.31 M, 0.44 M and 0.63 M at [*n*-butanal] = 0.44 M and [cat **56**] = 13.2 mM (3 mol%).

According to Chapter 10.3.7
Standard Reaction, Dry Conditions and Additional Water – Influence on Reaction Rates and Reaction Orders (Page 78)

Influence of Water in the Reaction Mixture (Additional Experiment)

The reaction of *n*-butanal and nitrostyrene with [cat **56**] = 4.4 mM, [nitrostyrene] = 0.44 M and [n-butanal] = 0.44 M was performed using TFA•H-D-Pro-Pro-Glu-NH_2 **56** under standard conditions (Figure A, blue curve) and under dry conditons (green curve, solvents and *n*-butanal dried over freshly activated molecular sives), to demonstrate the influence of moisture on the reaction progress.

Figure A

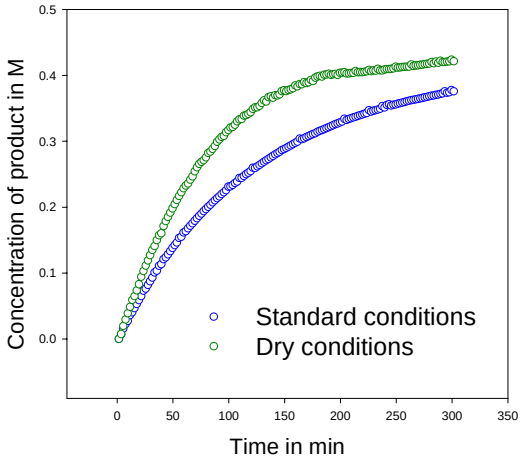

In comparison to the reaction under standard condition, the reaction under dry conditions proceeded significantly faster (>90 % conversion after five hours, determined by ^{1}H NMR with *i*-PrOH as an internal standard) indicating that moisture slows down the reaction. Besides, the diastereoselectivity was lower (*syn:anti* ≈ 25:1 under dry conditions vs. 50:1 at standard conditions) and the enantioselectivity was not influenced (97 % *ee* for both reactions).

To confirm the necessity of water the standard reaction ([cat **56**] = 4.4 mM, [*n*-butanal] = 0.44 M, [nitrostyrene] = 0.44 M) was carried out under dry conditions and in the presence of activated molecular sieves (4Å, powder). Under these conditions product formation was observed in the first few minutes before the reaction stopped.

To examine the influence of additional water in the reaction mixture we performed different experiments at constant [cat **56**] = 4.4 mM, [*n*-butanal] = 0.44 M and [nitrostyrene] = 0.44 M and added different amounts of water to the reaction mixture: 5 mol%, 10 mol%, 15 mol%, 20 mol%. These experiments demonstated that already 5 mol% of additional water slow down the reaction significantly (Figure B). Interestingly this decrease in reaction rate shows a linear behaviour in the corresponding log-log plot (slope of -0.33, $R^2 = 0.99$) as shown in figure C.

Figure B

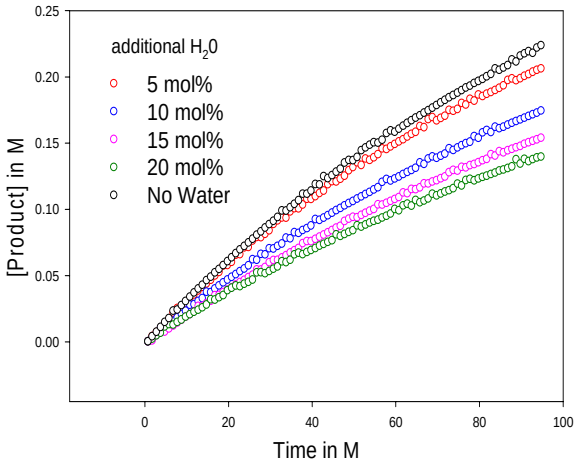

Figure C

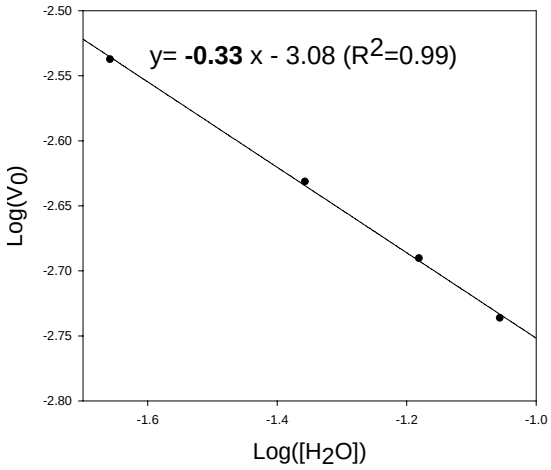

Additional Water: Reaction Order with Respect to *n*-Butanal and Nitrostyrene (Chapter 10.3.7.1)

Six different reaction of *n*-butanal ([*n*-butanal] = 0,55 M, 0.77 M, 0.88 M, 1.10 M, 1.32 M and 1.56 M) and [nitrostyrene] = 0.44 M at [cat **56**] = 4.4 mM with 10 mol% additional water [H_2O] = 44 mM were performed.

The influence of 10 mol% additional water on the reaction order with respect to nitrostyrene was tested with 5 different experiments: [*n*-butanal] = 0.44 M, [cat **56**] = 4.4 mM, [H_2O] = 44 mM and [nitrostyrene] = 0.22 M, 0.44 M, 0.66 M, 0.88 M, 1.10 M.

Dry Conditions: Reaction Order with Respect to *n*-Butanal and Nitrostyrene (Chapter 10.3.7.2)

Additional experiments concerning the water content were carried out under dry conditions. Therefore the solvent-mixture ($CHCl_3$/*i*-PrOH 9:1 v/v) and *n*-butanal were previously dried

over molecular sieves (3Å) and all glassware was heated out for each experiment. Six reactions were performed at [cat **56**] = 4.4 mM, [nitrostyrene] = 0.44 M and [*n*-butanal] = 0.22 M, 0.44 M, 0.55 M, 0.66 M, 0.77 M and 0.88 M.

Reactions of different nitrostyrene concentrations were performed with [nitrostyrene] = 0.22 M, 0.44 M, 0.66 M, 0.88 M and 1.10 M and [*n*-butanal] = 0.44 M at [cat **56**] = 4.4 mM under the dry conditions described above.

23. NMR Data of H-D-Pro-Pro-Glu-NH_2 (56)

^{1}H-NMR (600 MHz, $CDCl_3$/CD_3OD/CD_3OH, 23:1:1 v/v/v, 25°C)

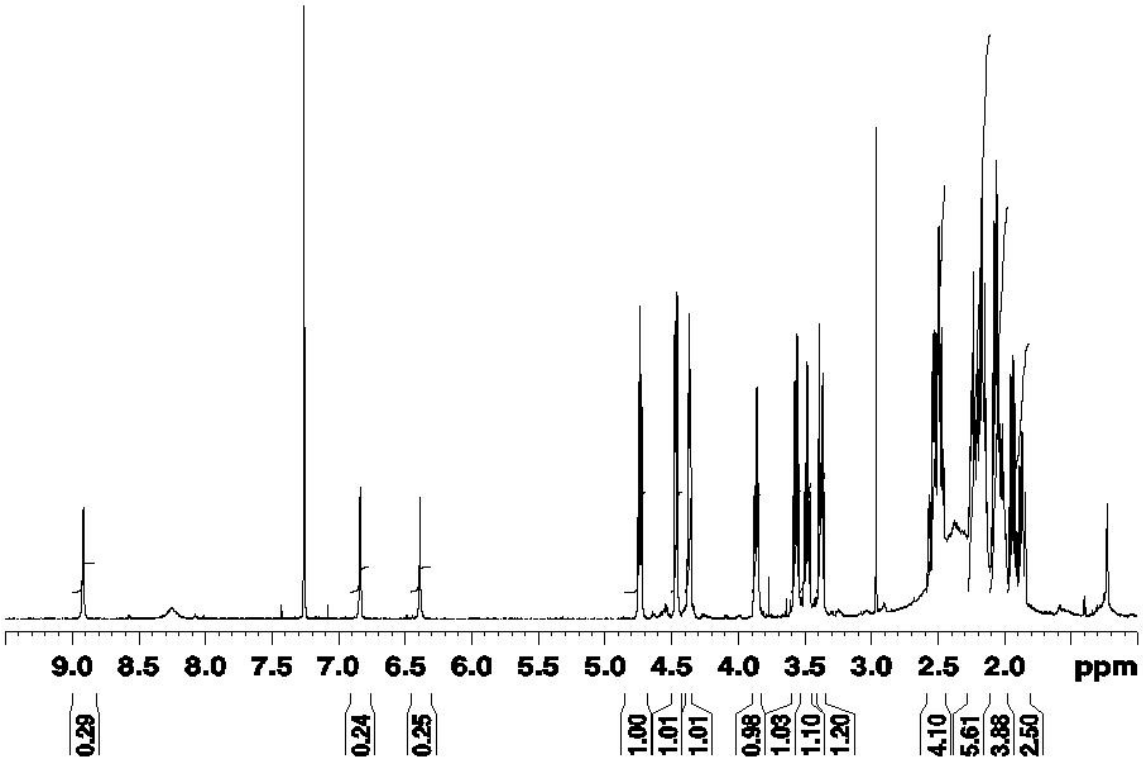

NOESY (600 MHz, $CDCl_3$/CD_3OD/CD_3OH, 23:1:1 v/v/v, 25°C)

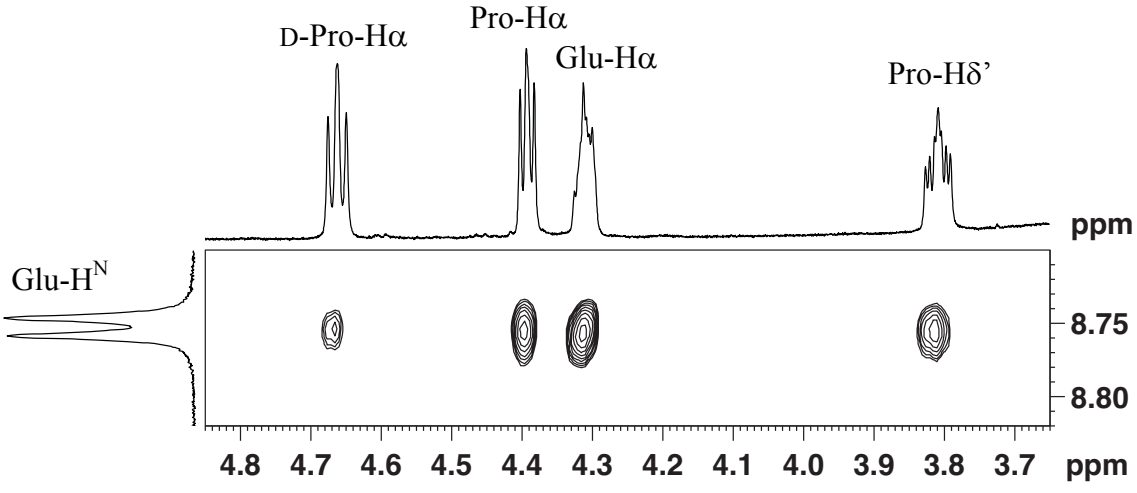

Eidesstattliche Erklärung

Ich erkläre, dass ich die Dissertation mit dem Titel „Peptides as Catalysts for Asymmetric 1,4-Addition Reactions of Aldehydes to Nitroolefins“ nur mit der darin angegebenen Hilfe verfasst und bei keiner anderen Universität und bei keiner anderen Fakultät der Universität Basel eingereicht habe.

Basel, den 03.08.2009

Markus Wiesner

An meiner Hochschulausbildung waren folgende Dozenten beteiligt:

Prof. Dr. E. Constable, Prof. Dr. P. Hauser, Prof. Dr. C. Housecroft, Prof. Dr. H. Huber, Prof. B. Giese, Prof. Dr. Th. Kaden, Prof. Dr. J. P. Maier, Prof. Dr. M. Mayor, Prof. Dr. W. Meier, Prof. Dr. M. Meuwly, Prof. Dr. M. Oehme, Prof. Dr. A. Pfaltz, Prof. Dr. U. Séquin, Prof. Dr. H. Sigel, Prof. Dr. E. Stulz, Prof. A. Vedani, Prof. Dr. H. Wennemers, Prof. Dr. J. Wirz, Prof. Dr. W-D. Woggon, Prof. Dr. A. Zuberbühler.

Lebenslauf

Markus Wiesner

Geboren am 07.10.1976

Ausbildung

ab Okt. 2009	Gruppenleiter in der Abteilung Biochemikalien und Prozessforschung der Firma Bachem AG in Bubendorf
April 2006 – Juni 2009	Doktorarbeit bei Prof. Dr. Helma Wennemers, Departement Chemie, Universität Basel *Peptides as Catalysts for Asymmetric 1,4-Addition Reactions of Aldehydes to Nitroolefins*
Okt. 2001 – Jan. 2006	Chemiestudium (Bachelor & Master) an der Universität Basel. Masterarbeit bei Prof. Dr. Helma Wennemers, Departement Chemie, Universität Basel *Peptide als Organokatalysatoren für asymmetrische Aldolreaktionen*
Aug. 1998 – Sept. 2001	Eidg. Maturität, Typus E (Wirtschaft) an der Minerva Schule in Basel
Aug. 1997 – Juni 1998	Technische Berufsmaturiät an der gewerblich-industriellen Berufsschule in Liestal
Aug. 1992 – Juli 1997	Berufslehre (Laborist & Chemielaborant) und anschliessende Anstellung als Chemielaborant bei Bachem AG in Bubendorf

Berufliche Tätigkeiten

Sept. 1996 – Juli 1997 Juli 1999 – Aug. 1999 Nov. 2004 – Jan. 2005 Feb. 2006 – März 2006	Anstellungen als Chemielaborant in den Abteilungen Biochemikalien, Produktionsanalytik und Wirkstoffe bei der Firma Bachem AG in Bubendorf
2007 – 2009	Assistent im Praktikum für organische Chemie (für Biologie- und Pharamziestudierende) und Betreuer mehrerer Diplom- und Masterarbeiten von Chemiestudierenden an der Universität Basel
1994 – 2003	Mitglied des Schweizerischen Nationalkaders Turnen / Trampolin. 1997 – 2003: Anstellung als Athlet beim Schweizerischen Turnverband (50%) 2000: Teilnahme an den Olympischen Spielen in Sydney